Prion-like mechanisms of TDP-43 in ALS

Phillip Smethurst

A thesis submitted as partial fulfilment for the degree of Doctor of Philosophy in the

Faculty of Brain sciences and the UCL Institute of Neurology

March 2014

Supervisors Dr Katie Sidle and Professor John Hardy

Declaration

'I, Phillip Smethurst confirm that the work presented in this thesis is my own. Where information has been derived from other sources, I confirm that this has been indicated in the thesis.'

Abstract

Mounting evidence now suggests that many neurodegenerative diseases behave in a similar manner to prion diseases. Although there is no demonstrable infectivity of these conditions, numerous biological studies show that aggregated proteins linked to each of these diseases can behave in a prion-like manner at the cellular level. One of the conditions shown to have prominent clinical and cellular prion-like behaviour, in terms of focal onset and spread of pathology, is amyotrophic lateral sclerosis (ALS). Indeed, it is now well recognised that TDP-43 is the main component of the ubiquitinated inclusions observed in the neurons of the brain and spinal cord in patients with ALS and frontotemporal lobar degeneration with ubiquitinated inclusions (FTLD-U). TDP-43 is deposited in more than 90% of sporadic ALS cases, and mutations in the TARDBP gene encoding for TDP-43 are found to cause ALS. In this thesis, we show that the levels of TDP-43 are significantly elevated in different regions of the CNS in ALS patients compared to controls. We also demonstrate that pathological TDP-43 has a degree of protease resistance, and can be seeded into cell culture directly from ALS CNS tissue to reproduce the characteristic TDP-43 pathology. In addition to this we demonstrate that pathologically aggregated and phosphorylated TDP-43 can propagate from cell to cell in a prion-like manner. We also investigated whether this TDP-43 pathology can be transmitted in vivo to wild type mice, and utilised a novel MRI imaging technology to attempt to non-invasively detect protein aggregation in the spinal cord of the well characterised SOD1 G93A ALS mouse model. In summary, we demonstrate that TDP-43 displays characteristic cellular prion-like behaviour, which could potentially explain some of the pathological mechanisms in ALS, and highlights potential mechanisms for therapeutic investigation.

Table of Contents

List of Figures

List of Tables

List of Abbreviations

AAV	Adeno-associated virus
AD	Alzheimer's disease
ALS	Amyotrophic lateral sclerosis
APT	Amide proton transfer
ANG	Angiogenin
APOA2	Apolipoprotein A2
ATXN2	Ataxin 2
BSE	Bovine spongiform encephalopathy
CDC7	Cell division cycle 7 kinase
CDK6	Cyclin dependent kinase 6
CK1	Casein kinase 1
CNS	Central nervous system
CBLM	Cerebellum
CSF	Cerebrospinal fluid
CV	Cervical
CHMP2B	Charged multivesicular modified protein 2B
C9orf72	Chromosome 9 open reading frame 72
CWD	Chronic wasting disease
CT	Chymotrypsin

CBD	Cortico-basal degeneration
CJD	Creutzfeld-Jakob disease
CFTR	Cystic fibrosis transmembrane conductance regulator
CDC7	Cell division cycle 7 protein kinase
CTF	C-terminal fragment
CDK6	Cyclin dependent kinase 6
DAO	D-Amino acid oxidase
DNA	Deoxyribonucleic acid
ER	Endoplasmic reticulum
ESCRT	Endosomal transporting complexes required for transport
ERK	Extracellular signal related kinase
EAAT2	Excitatory amino acid transporter 2
fALS	Familial ALS
FFI	Fatal familial insomnia
FCX	Frontal cortex
FTLD	Frontotemporal lobar degeneration
FTLD-U/TDP	FTLD with ubiquitinated inclusions/TDP-43 pathology
FTLD-Tau	FTLD with tau pathology
FUS/TLS	Fused in sarcoma/ Translated in liposarcoma
GABA	Gamma-amino-butyric acid

GSS   Gerstmann-Straussler-Scheinker syndrome

GPI   Glycophosphatidyl inositol

GSK-3   Glycogen synthase kinase 3

GRN   Granulin

HDAC6   Histone deacetylase 6

HSP70   Heat shock protein 70

hnRNP   Heterogeneous nuclear ribonucleoprotein

HITS-CLIP   High throughput sequencing of RNA isolated crosslinking immunoprecipitation

hNFL   Human low molecular weight neurofilament

HD   Huntington's disease

HCI   Hyaline Conglomerate inclusions

IBMPFTD   Inclusion body myositis with Paget's disease and FTD

IP3   Inositol 1,4,5 triphosphate

LBD   Lewy body disease#

LMN   Lower motor neuron

LU   Lumbar

mRNA   Messenger RNA

MALAT1   Metastasis associated lung adenocarcinoma transcript 1

miRNA   Micro RNA

MAP1B   Microtubule associated protein 1

MC	Motor cortex
MND	Motor neuron disease
mTDP-43	Monoclonal TDP-43 antibody
NSC-34	Neuroblastoma spinal cord -34
NC	Normal control
ncRNA	Non-coding RNA
NEAT1	Nuclear enriched abundant transcript 1
NES	Nuclear export sequence
NLS	Nuclear localization sequence
OPTN	Optineurin
PD	Parkinson's disease
PBS	Phosphate buffered saline
pTDP-43	Phosphorylated TDP-43
pS409/410	Phosphorylated at residues 409 and 410
PrP	Prion protein
PrP^{Sc}	Scrapie prion protein
PRNP	Prion protein gene
PFN1	Profilin 1
PMA	Progressive muscular atrophy
PK	Proteinase K

PLS	Primary lateral sclerosis
RNA	Ribonucleic acid
RRM	RNA recognition motif
ROS	Reactive oxygen species
SETX	Senataxin
SC35	Serine/arginine rich splicing factor 2
SIGMAR1	Sigma non-opioid intracellular receptor 1
Si-RNA	Small interfering RNA
SC	Spinal cord
SMA	Spinal muscular atrophy
sALS	Sporadic ALS
SOD1	Super oxide dismutase 1
SMN2	Survival of motor neuron 2 gene
TBPH	Drosophila homologue of TDP-43
TIA-1	T-Cell internal antigen 1
TCX	Temporal cortex
Th	Thoracic
TDP-43	Trans-active response DNA binding protein of 43 kDa
TARDBP	Trans-active response DNA binding protein gene
TSE	Transmissible spongiform encephalopathies

TGF-β   Transforming growth factor beta

T   Trypsin

UBI   Ubiquitinated inclusions

UBQLN2   Ubiquilin 2

UPS   Ubiquitin proteasome system

UPR   Unfolded protein response

UTR   Untranslated Region

UMN   Upper motor neuron

VAPB   Vesicle associated membrane protein B

VCP   Valosin containing protein

vCJD   Variant Creutzfeld-Jakob disease

Chapter 1

Introduction

1. Introduction

1.1. Protein folding, misfolding and aggregation

1.1.1. Protein folding

Protein folding is the process whereby the native post translationally produced unfolded polypeptide undergoes folding into its 3D biologically active state. This process is driven by the amino acid sequence and subsequently influenced by the cellular environment (Onuchic and Wolynes, 2004). The protein folding process can take place either before protein translation at the ribosome, in the cytosol or in specific cellular compartments such as the mitochondria and endoplasmic reticulum (ER) (Hardesty and Kramer, 2001; Harding, 1985). The folding process is largely controlled by molecular chaperones which act to increase the efficiency of the folding process by preventing competing factors such as aggregation (Hartl and Hayer-Hartl, 2002) (Figure 1). The gene sequence for the protein directs the inherent fluctuations within the polypeptide sequence, allowing the protein to form tertiary interactions and a more energetically favourable native state. In this process, certain specific sequences are sampled from the number of possible sequences to select the most suitable one for globular protein folding. The energetics of the folding process has been described as an 'energy landscape', where the free energy of each protein is depicted as a function of the conformation of the protein. The number of these potential folding conformations decreases as the protein reaches its native state (Dinner et al., 2000).

The folding process can be described as a 'nucleation-condensation' reaction whereby the residues in the unfolded polypeptide act as nuclei for the remaining residues to condense and stop the protein polymerization (Schiene and Fischer, 2000). Most proteins stay in this folded state by forming hydrophobic cores from side chain packing, and have charged polar side chains on the surface to interact with the surrounding environment. The folding process is thought to work by minimizing the number of hydrophobic side chains that are exposed to water, and by formation of hydrogen bonds between the carbonyl and amide groups in the peptide (Anfinsen, 1972; Dobson, 2003). However, the cellular milieu plays a large part in the type of folding that occurs. For example, even if the protein has the

same sequence topology, the location and cellular environment present will determine the resultant protein conformation (Alexander et al., 2007). The number of different folding states is also determined by the number of amino acid residues within the protein. For example, proteins consisting of 100 amino acids and lower only exist in the unfolded and folded functional states, where as proteins with more than 100 amino acids in size can form an intermediate called a 'molten globule'(Naeem et al., 2004, 2005). These molten globules are formed by hydrophobic side chains that fall inside the protein and clump together, a process termed 'hydrophobic collapse' (Rose et al., 2006). The molten globules are stable containing native secondary structure and fluctuating tertiary structure (Naeem et al., 2004, 2005). In vitro, these structures are collapsed and present usually at low pH, mild denaturing conditions and high temperature. These properties are largely present in most transient folding intermediates of globular proteins undergoing hydrophobic collapse. The difference between the native state of the protein and these molten globules is that they lack some of the close packing of the amino acid side chains present in the native state (Pande and Rokhsar, 1998).

The protein folding process has a number of quality control mechanisms to avoid protein misfolding, and the passage of the unfolded polypeptide through transitional states to the folded state can act as one of these control mechanisms (Soto, 2003). In addition to this, cells contain molecular chaperones and enzymes which help prevent misfolding of the protein. For example, when new polypeptides are synthesized, the molecular chaperone Heat shock protein 70 (Hsp70) binds to the extended and unstructured regions containing a high content of hydrophobic residues. This is thought to prevent incorrect association of residues whilst the protein is in the partially folded state, and as such prevents protein misfolding and aggregation (Flynn et al., 1991).

1.1.2 Protein misfolding

Misfolding of proteins can occur by proteins altering their native state or incorrect folding of newly manufactured polypeptides. A misfolded protein is the folding of a protein into a non-native folded state through the formation of abnormal interactions. This misfolding can occur either via a mutation, cellular stress event or post-translational

modification. Misfolded proteins can also be unfolded to break these abnormal interactions and produce the natively folded protein. However, sometimes a misfolded protein core can expose usually buried hydrophobic amino acid side chains; this can recruit additional monomers and can initiate the aggregation process. If the protein becomes trapped in the misfolded state, the population of these misfolded proteins can increase by a process known as 'self-seeded polymerization'. The misfolded states of these proteins become more loosely packed and expose the hydrophobic core residues at the surface, which facilitates the aggregation of these proteins (Dobson, 2003).

Protein conformational disorders are thought to arise through the accumulation of misfolded proteins and protein aggregation (Chiti and Dobson, 2006). As such, the characterisation of the misfolded intermediates have been the focus of much investigation as targets for therapeutic intervention (Aguzzi and O'Connor, 2010). However, protein folding is a highly complex and dynamic process and, as such, it can be difficult to determine what the partially folded stable intermediates are during this process (Naeem et al., 2005). In addition, the intermediate states can vary greatly in terms of the packing and secondary structure making them even more difficult to characterize.

1.1.3 Protein aggregation

The aggregation process starts with a conformational change of the protein into an unfolded or misfolded state. Exposed hydrophobic residues recruit the addition of monomers to form oligomers then fibrils and this eventually leads to aggregate assembly. It is the instability caused by low transition energy of the secondary intermediates in this process that allows them to escape the cells protein quality control system, and subsequently form pre-conditions required for aggregate formation (Amaral, 2004). When the protein quality control network becomes exhausted with the increasing population of misfolded conformers and the cell is no longer able to refold or degrade the proteins, this leads to abnormal protein aggregation. Indeed, this aggregation process can also be influenced by the amino acid sequence (i.e. mutation) or gene and protein expression levels (Naeem and Fazili, 2011).

The type of misfolding present in the intermediate forms will usually predict the type of aggregation produced. If most of the structure is lost this will lead to the formation of disordered amorphous aggregates, however if the intermediate is partially misfolded this can lead to the formation of cross β-sheet spine structures known as amyloid which can be deposited as intra or extracellular deposits (Sawaya et al., 2007) (Figure 1). These deposits have been detected in neurodegenerative disorders such as Parkinson's, Alzheimer's and prion disease, and non-neurodegenerative diseases such as systemic amyloidosis. As such, there has been a large focus on discovering the mechanisms of amyloid formation, how this could contribute to cellular toxicity and how it can be prevented (Chiti and Dobson, 2006). However, more recent evidence suggests that amyloid formation is not always toxic and can be a normal cellular process, such as the biogenesis of mammalian melanosomes (Berson et al., 2003). As such, the definition of amyloidosis is now being redefined to encompass various other aspects of disease (Westermark, 2005). Despite this the formation of amyloid is still a key important factor for investigation of neurodegenerative disorders. One of the first and most well characterized neurodegenerative disorders with prominent protein misfolding and amyloid formation was prion disease.
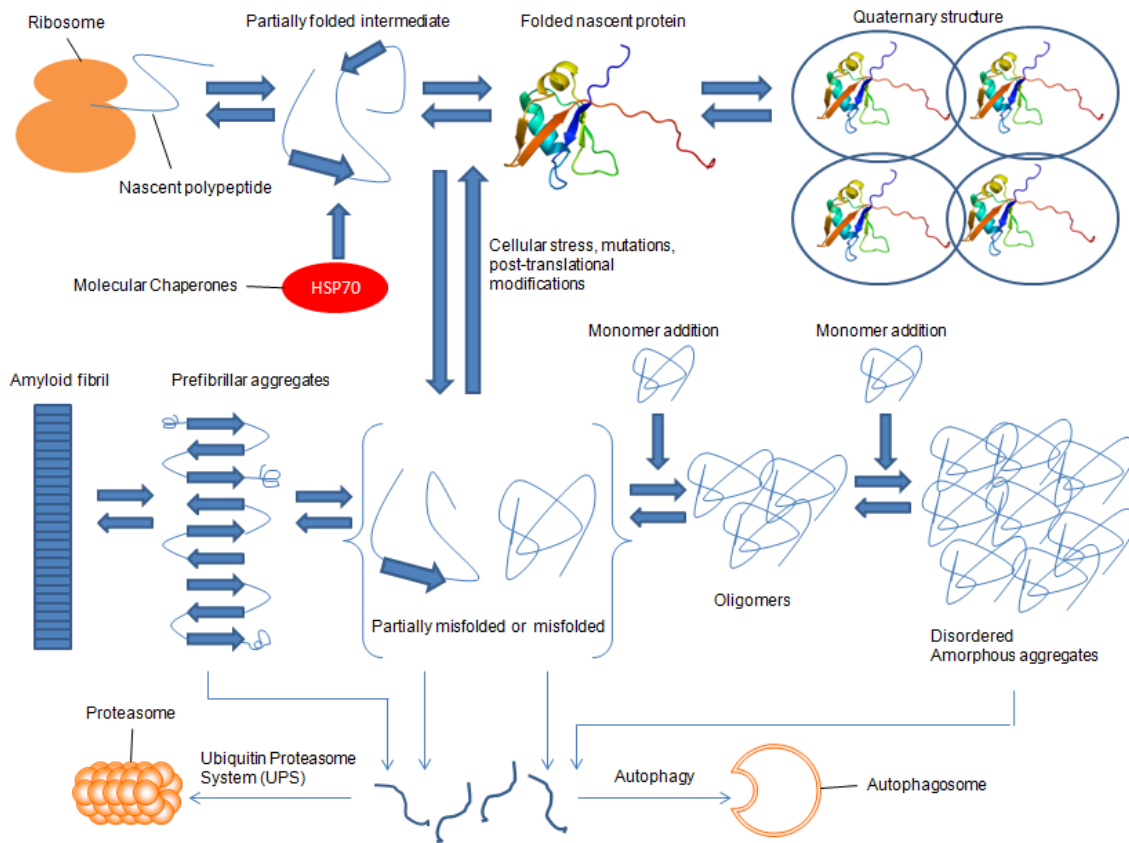
Figure 1. Protein folding, misfolding and aggregation process. Native protein folding occurs after the translation of the polypeptide on the ribosome where it goes through a partially folded intermediate states regulated via molecular chaperones (HSP70). These partialy folded intermediates then can become misfolded by cellular stress, mutations or post-translational modifications. These misfolded intermediates can then either be refolded to the native state or degraded. If the protein degradation system becomes dysfunctional these misfolded forms persist and can form aggregates. Misfolded forms of the protein can either become partially misfolded with intact β-sheets and polymerize to form pre-fibrillar aggregates and amyloid, or it can be highly misfolded and form oligomers, fibrils and then amorphous aggregates. These aggregates and misfolded intermediates can then be targeted for degradation by either the autophagy system or the ubiquitin proteasome system (UPS). Diagram adapted and modified from (Tyedmers et al., 2010).

1.2   Protein misfolding and neurodegenerative disease

1.2.1 Prion disease

The prototypical neurodegenerative protein misfolding disorders are the prion diseases where it is now widely accepted that, upon misfolding, the prion protein (PrP) is the sole cause of the condition. The prion diseases are the most well studied in terms of protein misfolding, and are the only known transmissible protein species that are responsible for neurodegeneration (Moore et al. 2009). Prion diseases are incurable, fatal, rapidly progressive dementias, often with ataxic and pyramidal signs. They are also known as transmissible spongiform encephalopathies (TSEs) and can manifest as scrapie in sheep, chronic wasting disease (CWD) in deer and elk, transmissible mink encephalopathy (TME) in mink and bovine spongiform encephalopathy (BSE) in cows. In humans there are three main forms including: Creutzfeldt-Jakob disease (CJD) which is sporadic, inherited forms from mutations in the PrP gene which cause fatal familial insomnia (FFI) and Gerstmann-Straussler-Scheinker syndrome (GSS), and thirdly from acquired infection with prion contaminated materials (Wadsworth, 2003). Some of these acquired prion infections can be iatrogenic from contaminated surgical materials, blood transfusions and organ transplantation (Barrenetxea, 2012); human ingestion of contaminated BSE meat in cows caused variant CJD (vCJD) (Collinge et al. 1996); and kuru which was a result of endocannibalistic rituals on the islands of Papa New Guinea (Zigas and Gajdusek, 1957).

The PrP protein is a ubiquitously expressed mammalian glycoprotein encoded for by 1 exon in the PRNP gene. The protein is linked at the cell surface with a glycophosphatidyl inositol (GPI) membrane anchor. After cleavage of the signal peptide and GPI anchor, the protein is approximately 208 amino acids in length (residues 23-231). The PrP protein is then processed through the secretory pathway where it is glycosylated at N-glycosylation sites and eventually becomes bound to the cell surface via the GPI anchor (Somerville, 2002). During the prion disease process, the protein misfolds from an alpha helical secondary structure which is protease sensitive, to a β-sheeted amyloid like structure which is protease resistant (Pan et al., 1993). Prion proteins are known for their infectious capability and are the only known proteins to be able to 'replicate' and transmit from different individuals, and

from cell to cell in a conformation dependent manner (Aguzzi and O'Connor, 2010; Fernandez-Funez et al., 2010). There are glutamine (Q) and asparganine (N) rich domains in the N-terminus of prion proteins that facilitate prion protein propagation of amyloid conformers produced from the aggregation process (Wickner et al., 2008). Evidence suggests that this propagation of distinct conformers starts with environmental stress in prions (Tyedmers et al., 2008), and that distinct folding variants in the aggregates can mediate phenotypic variability (Collinge et al., 1996; Parchi et al., 1996). Although the Q/N rich region may assist in this process, it is not a necessity for propagation of different prion-like protein conformations. When these proteins are overexpressed they can easily self-aggregate, indicating that they may be important for protein self-regulation (Alberti et al., 2009; Michelitsch and Weissman, 2000). Interestingly the mammalian genome has many proteins containing Q/N rich domains which use self-aggregation to control its own activity. An example is the prion related protein T-cell internal antigen 1 (TIA-1) found in stress granules, this Q/N rich domain allows it to form stress granules and protein aggregates (Gilks et al., 2004; Harrison and Gerstein, 2003).

Prions will become infective if they form strong intermolecular interactions, become irreversibly aggregated, avoid cell clearance machinery and propagate from cell to cell recruiting extra PrP monomers (Krammer et al., 2009). Prions will often form distinct conformations of amyloid cross β sheets which acts as a self-template, recruiting native monomers to misfold (Shorter and Lindquist, 2005). This is called a self templated seeding polymerization reaction and is the basis of the prion aggregation, propagation and infectivity. Evidence that prions are the disease causing protein was gained from manufacturing amyloid PrP conformers produced from recombinant protein which can induce a transmissible disease process in mice overexpressing PrP (Colby et al., 2009; Legname et al., 2004). Similar more effective disease production was achieved in wild type mice treated with a more potent recombinant prion generated by RNA and lipid mediating factors (Wang et al. 2010). Further evidence to support the 'protein-only' hypothesis came from exogenous seeding of prion disease into PrP knockout mice, which was unable to elicit a disease process as the endogenous PrP is required to propagate the seed (Büeler et al.,

1993). Likewise if PrP expressing neurons are grafted into PrP null mice, only the grafted neurons become infected and normal tissue remains unperturbed (Brandner et al. 1996).

One of the most interesting findings about prion amyloid conformations is that different conformations are capable of inducing a unique clinical phenotype which is known as a 'strain effect' (Collinge et al. 1996; Mahal et al. 2010; Colby et al. 2009). These prion strains have varying CNS regional tropisms which can lead to a variation in deposition of PrP^{Sc} pathology and regional toxicity. In addition they produce variable rates of disease progression, which may ultimately be due to the ability of the prion seed to propagate throughout the CNS. One study has demonstrated the more frangible the amyloid conformation, and the higher resistance it has to clearance by cellular machinery, the stronger the seeding reaction is and hence the more severe the disease phenotype will be (Tanaka et al., 2006). These key characteristics of prions and misfolding have led to the investigation of these characteristics on other proteins involved in neurodegenerative disorders.

1.2.2 Prions and neurodegenerative disease

Current evidence would suggest that other proteins involved in neurodegenerative disease pathology are also largely misfolded and have a prion-like characteristics (Brundin et al., 2010; Cushman et al., 2010; Frost and Diamond, 2010; Goedert et al., 2010). Among these conditions with deposited aggregated proteins are: Alzheimer's with β-amyloid (Aβ) deposits and tau neurofibrillary tangles, Parkinson's disease with accumulated α-synuclein, Huntington's with huntingtin, and prion disease with PrP protein deposits. They all share misfolded protein and self templating amyloid conformational characteristics. However, it appears mammalian prion proteins are more likely to become infectious, experimentally transmit and propagate because of their extracellular GPI membrane bound origins. Whereas other neurodegenerative proteins like tau, Aβ, α-synuclein and huntingtin are either nuclear or cytosolic, and could therefore require further transport mechanisms potentially abrogating their infective and propagative nature. A number of other reasons could account for the lack of their infectious capabilities such as lack of optimal strain fragility and auxiliary factors for survival in the extracellular space (Cushman et al., 2010).

While there is currently no evidence for naturally occurring horizontal transmissibility of these diseases (Jucker and Walker 2011), there is considerable data supporting the non-cell autonomous nature of these common neurodegenerative disorders (Goedert et al. 2010). The high degree of misfolding of these proteins in pathological conditions, and experimental evidence demonstrating their seeding characteristics suggests they have a great deal in common with prions. As a result, these proteins may share similar neurodegenerative mechanisms which has led to the terminology of 'prion-like' or 'prionoid' to distinguish between conditions with non-infectious characteristics, but similarities in prion-like cellular behaviours (Aguzzi, 2009). Evidence now suggests that one of the conditions most likely to have clinical prion-like characteristics involving aggregated proteins with cellular prion-like behaviour is amyotrophic lateral sclerosis (ALS) (Münch et al. 2011; Furukawa et al. 2011; Udan & Baloh 2011; Gitler & Shorter 2011; Polymenidou & Cleveland 2011). Indeed, this thesis aims to explore the prion-like mechanisms of one of the core proteins involved in ALS called 'TDP-43'.

1.3 Amyotrophic lateral sclerosis (ALS)

Motor neuron disease (MND) is a widely used umbrella term encompassing several cruel and complex motor neurodegenerative conditions. Amyotrophic lateral sclerosis (ALS) is the most common variant of MND and, although the condition had been described earlier, it was first scientifically described from an autopsy study by Jean Martin Charcot in 1874 (Charcot, 1874). ALS is a fatal progressive neurodegenerative disorder that causes muscle weakness, spasticity, paralysis and atrophy due to death of the motor neurons innervating the muscles. ALS affects both the upper motor neurons (UMN) in the brain and the lower motor neurons (LMN) in the brain stem and spinal cord which supply the muscles. Ultimately death is caused by destruction of the motor neurons which control breathing (Wijesekera and Leigh, 2009). ALS is the third most common neurodegenerative disease after Alzheimer's and Parkinson's disease and more commonly affects men than women. The incidence of ALS in Europe is 2-3 in 100,000 per year with a prevalence ranging between 2.7 to 7.4 in 100,000 and a lifetime risk of developing the condition of about 1 in 350 in men and 1 in 400 in women (Al-Chalabi and Hardiman, 2013). Cognitive impairment is now

increasingly recognised (~50%) (reviewed in Tsermentseli et al. 2011) but may still be infrequently recognised within an MND clinical setting. In about 15% of ALS patients cognitive impairment can manifest as a frank frontotemporal lobar degeneration (FTLD) which is the second most common form of dementia next to Alzheimer's and can adversely affect patient survival rates (Olney et al., 2005). There is now strong evidence to suggest a large clinical and pathological overlap between ALS and FTLD, where ALS and FTLD represent a spectrum disorder. This is supported by the more recent discovery of the C9orf72 gene intronic hexanucleotide repeat expansions as the most common cause of both FTLD and ALS (DeJesus-Hernandez et al., 2011; Renton et al., 2011). Indeed, one of the main pathological proteins deposited in ALS and FTLD is TDP-43 (Neumann et al. 2006), suggesting that similar pathological mechanisms may be involved in both conditions.

Currently, the diagnosis of ALS remains predominantly clinical and there are no reliable biomarkers for diagnosis or prognosis. Additionally, there remains no effective treatment or cure for the condition. The drug riluzole has been demonstrated to extend the life of ALS patients for 2-3 months (Miller et al. 2002). Many other clinical trials of drugs for ALS have been undertaken but have failed to demonstrate efficacy in slowing disease progression or ameliorating symptoms (Gibson and Bromberg, 2012). Fortunately, many animal and cellular models are beginning to reveal interesting new neuroprotective treatments targeting certain novel aspects of ALS pathobiology (Cozzolino et al., 2012). One of the key steps in forming these neuroprotective or disease altering treatments is gaining an effective understanding of the molecular and cellular mechanisms of ALS pathobiology.

1.3.1 ALS phenotypes

One of the distinguishing features of ALS is the heterogeneity of the observed clinical phenotypes which further add to the complexity of the condition. ALS is phenotypically and neuropathologically characterised by a degeneration of the upper motor neurons (UMN) in the brain and lower motor neurons (LMN) in the brain stem and spinal cord. There are many variable clinically different motor phenotypes observed in ALS which are due to four main factors: 1) region of onset 2) relative mix of UMN and LMN involvement 3) rate of progression 4) and involvement of other non-motor systems such as cognition. This UMN

and LMN division of the motor system is unique for its complex 3D anatomy which may explain its vulnerability to motor phenotype variation in ALS. The motor phenotypes observed in ALS are thought to be reflective of the underlying neuroanatomy from the superimposition of UMN and LMN degeneration occurring simultaneously (Ravits et al., 2007a). The clinical phenotypes are often distinguished by the anatomic location of neuropathology which can be observed clinically during the life of the patient. The clinical ALS phenotype that starts in the muscles that control speech, mastication and swallowing is called 'bulbar onset'. ALS that begins with symptoms in the limbs is termed 'limb onset' which is then divided into upper limb (i.e. arm or hand), lower limb (i.e. leg or foot) flail arm or flail leg onset; where just the muscles controlling the arms or legs are involved. This onset begins from a focal CNS site and slowly progresses over time and space and different onset sites tend to progress at different rates. Other subtypes of MND are generally much rarer than typical ALS and reflect a predominant UMN or LMN involvement. Primary lateral sclerosis (PLS) refers to a phenotype with predominant UMN degeneration, and progressive muscular atrophy (PMA) refers to a phenotype with predominant LMN degeneration. ALS involving non-motor regions is an additional phenotype that can involve cognitive impairment and development of frontotemporal dementia (FTD)(Strong and Yang, 2011), extrapyramidal motor signs (Pradat et al., 2002), autonomic nervous system (van der Graaff et al., 2009) and supranuclear gaze system involvement (Donaghy et al., 2011). It has now been established that cognitive impairment can have substantial negative effects on the phenotype and decrease survival rates in patients (Olney et al., 2005).

Even though many molecular neuropathological subtypes exist, these subtypes do not correlate with clinical ALS phenotypes (Ravits et al., 2013). Clinically sporadic ALS and familial ALS have been shown to be phenotypically indistinguishable from each other demonstrating that genetics alone is not enough to determine clinical phenotype. Additionally, many different gene mutations can have identical or highly similar phenotypes, indicating that multiple mechanisms can produce similar phenotypes. In addition, different mutations in the same gene can lead to multiple phenotypes (e.g. C9orf72 causes both ALS and FTLD) suggesting that single mechanisms can also lead to different phenotypes. This

suggests that ALS has both single and multiple molecular mechanisms that both converge and diverge to produce a heterogeneous mix of clinical phenotypes (Ravits et al., 2013). Here we attempt to explore a molecular basis of clinical ALS phenotypes by examining the TDP-43 protein. One of the other key characteristics of these clinical phenotypes is the rate of propagation of the pathology and degree of disease spread.

1.3.2 ALS spread and propagation

Once the focal onset in ALS occurs, the condition begins to spread contiguously in nearby anatomic regions on independent levels that correlate to symptom spread. A model of motor neuron degeneration and spread has been proposed to occur in four stages (Figure 2). Degeneration starts with a focal clinical onset at the UMN and LMN level innervating the same peripheral body region (Ravits et al., 2007a). Indeed, this is supported by a recent imaging study on ALS patients demonstrating that a lesion to the motor cortex could be capable of inducing the regional onset of ALS (Rosenbohm et al., 2013). This degeneration then spreads in a rostral to caudal direction neuroanatomically through the UMN and LMN levels. Eventually, the degeneration is thought to spread medially and laterally in the UMN level and eventual contralateral spread occurs in both the UMN and LMN levels. The final end stage appears as a diffuse symmetric summation of degeneration at both levels (Ravits and La Spada, 2009) (Figure 2). This has been verified by longitudinal and cross sectional studies (Brooks, 1991; Munsat et al., 1988; Pradas et al., 1993; Ravits et al., 2007a) and is strikingly similar to the clinical and pathological spread of degeneration in prion disease (Beekes and McBride, 2007). These studies indicate that as ALS spreads along the respective UMN and LMN areas, the degeneration summates within and between these regions that ultimately results in an array of complex motor phenotypes. The rate of propagation and disease progression will depend on the distribution of the disease burden between the UMN and LMN levels. For example limb onset and bulbar onset tend to have different distributions and burdens of pathology, and ALS and FTLD have different distributions and burdens of pathology, all of which have varying rates of progression. Indeed, a recent study suggests that the length of the interval period between symptom onset and spreading to

the next region is a strong predictor of survival in patients with sALS (Fujimura-Kiyono et al., 2011).

Evidence also suggests that this degeneration has a preferential directionality along these motor tracts. It appears that degeneration is more likely to spread rostral to caudal e.g. bulbar symptoms are more likely to spread to limb symptoms than *vice-versa* (Brooks, 1991; Ravits et al., 2007a). Therefore it can be speculated that this outward spread may reflect an underlying susceptibility of certain motor neurons to degeneration as previously postulated by Swash (Swash, 1980; Swash et al., 1986) and Brooks (Brooks, 1991). Susceptibility of motor neurons to degeneration may also be due to neuron size, axon length, dendritic arborisation, microenvironment or position in the gray matter (Ravits and La Spada, 2009). As well as neuroanatomic regional propagation it is thought that propagation could occur between distinct structural and functional networks called the 'connectome'. It appears that certain networks such as the motor network may be more vulnerable to degeneration than others through natural anatomical patterns, which could make them more susceptible to propagation (Seeley et al., 2009; Zhou et al., 2012). Advanced MRI data can now back up these ideas (Verstraete et al., 2011) and future molecular biological studies will be needed to confirm this.

Despite the complexity and variability of this degenerative spread there is an orderly active constant propagation which could have various causes. Some of these causes could include defective transmembrane signalling pathways, release of toxic factors from the neuron to the local neural microenvironment, growth factors, cytokine signalling, non-neuronal cell propagation e.g. glial cells, and protein misfolding (Ravits and La Spada, 2009). The immune system and neuroinflammation is also now thought to also act as a potential gateway to the propagation of ALS pathology (Zhao et al., 2013). From a clinicopathological perspective, the increasing microglial activation correlates directly with disease progression and UMN signs in ALS, suggesting that the immune system has a key role to play in mediating disease propagation (Brettschneider et al., 2012). However, most of the data available now on ALS spreading and propagation is emerging from the field of prion-like self templating of pathological proteins (Polymenidou and Cleveland, 2011). This data suggests

that a contiguous non-cell autonomous method of propagation could be a significant cause of disease progression in ALS. Hence we aim to explore this non cell autonomous mechanism of spread by attempting to demonstrate the spreading of pathological aggregates of TDP-43.
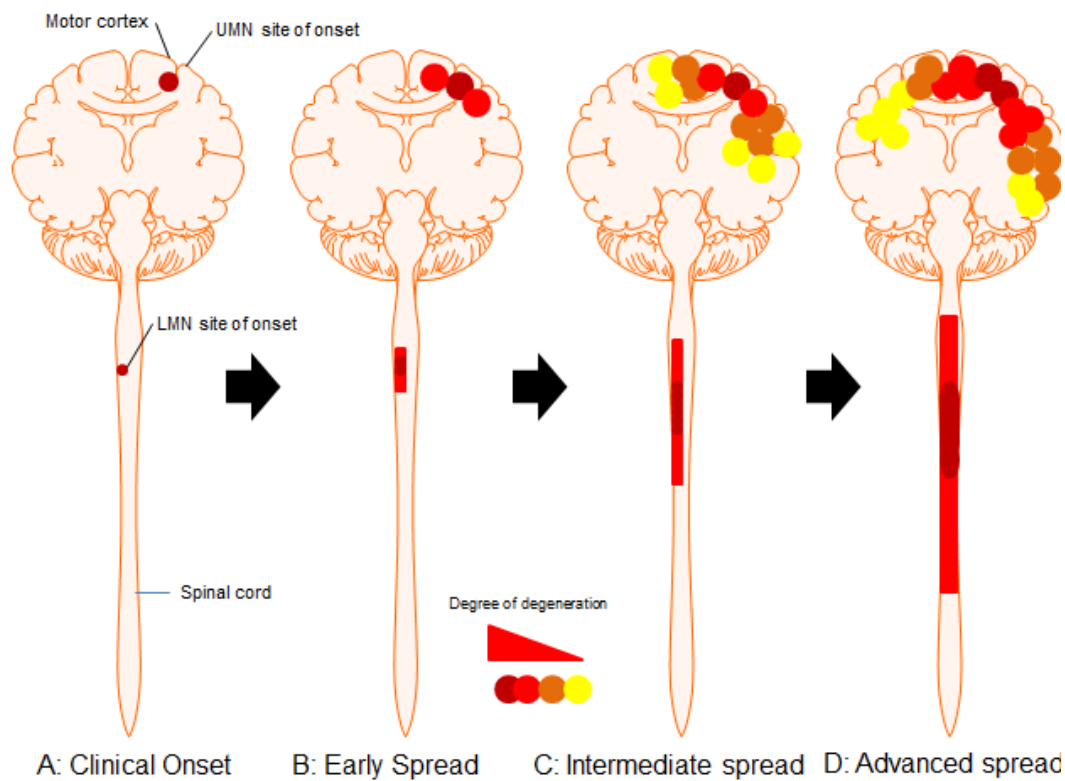
Figure 2. Proposed model of motor neuron degeneration spread and propagation in ALS. A) The clinical onset starts in focal regions simultaneously at both the UMN and LMN level that innervate the same region. B) The degeneration begins to spread neuroanatomically in the rostral caudal direction at the both the UMN and LMN levels. C) Intermediate spread occurs when the degeneration starts to spread medially and laterally at the UMN level and progresses to the contralateral side at both the UMN and LMN levels. D) Advanced spread is a diffuse symmetric summation of degeneration at both the UMN and LMN levels leading to severe paralysis and motor deficits. Diagram adapted from (Ravits and La Spada, 2009)

1.3.3 ALS pathology

The origin of the amyotrophic lateral sclerosis nomenclature refers back to the pathology of the condition, and a dissection of the individual terms indicates the type of clinical features and pathology observed. 'Myotrophy' means muscle support so therefore 'amyotrophy' is a lack of muscle support leading to muscle atrophy from subsequent denervation. The 'lateral' term refers to the lateral horn of the spinal cord and 'sclerosis' refers to the hardening and scarring over these regions caused by secondary reactive gliosis from the death of motor neurons in the corticospinal tracts (Wijesekera and Leigh, 2009). This degeneration in the upper and lower motor neurons is often accompanied by astrocytosis, microglial activation and intracellular neuronal inclusions. UMN pathology is predominantly atrophy of the motor cortex with a loss of layer V Betz cells, with variable degrees of astrocytosis affecting both grey matter and subcortical white matter in this region. Additionally, there is a degeneration of the descending pyramidal motor pathway indicated by shrinkage, astrocytosis and myelin pallor in the corticospinal tracts (Wharton S, 2003).

LMN pathology consists of degeneration of alpha motor neurons in the brain stem and Rexed Lamina IX in the anterior horn of the spinal cord. Motor neuron numbers in the spinal cord can be reduced by up to 50%, however, the degree of motor neuron loss varies between patients and can vary at different spinal levels (Ince, 2000). Additionally, axonal degeneration can be observed in the neural pathways projecting from the UMN in the corpus callosum, centrum semiovale, internal capsule, cerebral peduncle, basis pontis, medullary pyramids and lateral columns. Degeneration can also be seen in the projections from the LMN in the peripheral nerves and anterior roots which can subsequently lead to muscle denervation and wasting. The spongiosis, astrocytosis and activation of microglia observed are thought to be reactive secondary changes, although more recent research suggests these cells may play key role in the disease (Ince et al., 2011; Sloan and Barres, 2013).

The remaining neurons are atrophic and can contain different types of inclusion. These inclusions are usually either bunina bodies, hyaline conglomerate inclusions (HCIs) or

ubiquitinated inclusions (UBIs). Bunina bodies are small eosinophilic inclusions found in the cytoplasm of lower motor neurons which stain positive for cystatin C and transferrin. They are found in 70-100% of cases of ALS and are thought to be very specific as they are rarely seen in other conditions (Okamoto et al., 2008). More recently a small number of these inclusions were found to contain peripherin (Mizuno et al., 2011), but the remaining contents of these inclusions is still yet to be discovered. HCIs are agyrophillic inclusions of phosphorylated and non-phosphorylated neurofilaments found in the spinal cord motor neurons. These can be found in other neurodegenerative disorders and some control cases and therefore are not as specific as bunina bodies or UBIs (Leigh et al., 1989; Wharton S, 2003). Ubiquitinated inclusions (UBIs) have three different morphologies and can appear as either 'skein-like' (filamentous), spherical globular inclusions or dot like inclusions (Figure 3). These types of inclusions are particularly common in ALS and are observed ~95% of the time at autopsy (Leigh et al., 1988). Recent discoveries show that the major component of these inclusions is the RNA binding protein TDP-43 (Arai et al. 2006; Neumann et al. 2006). These inclusions can also contain other ALS associated proteins such as SOD1, FUS, Optineurin and Ubiquilin (Deng et al., 2010; Maruyama et al., 2010; Rosen, 1993; Williams et al., 2012) but the accumulation of these proteins is often co-observed with a mutation in the genes encoding these proteins. UBIs can also be present in glial cells, including astrocytes and oligodendrocytes highlighting the importance of glial cell involvement in ALS pathology (Ince et al., 2011; Sica, 2012).
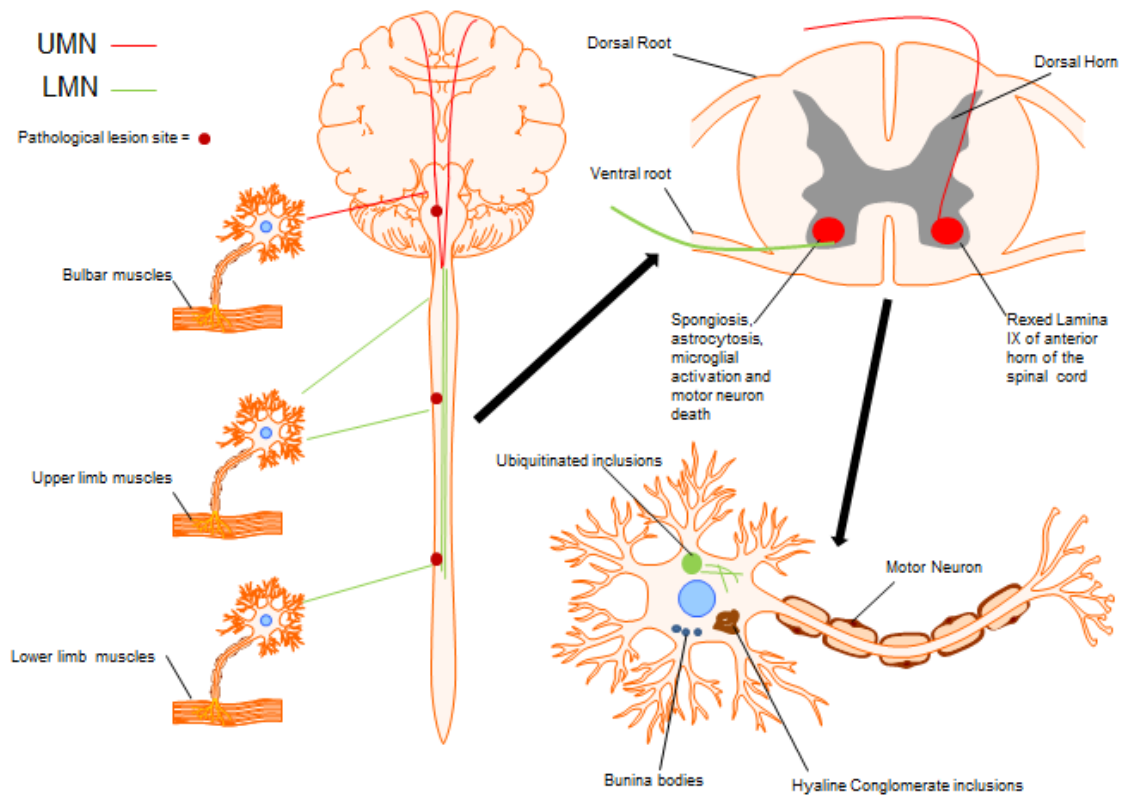
Figure 3. Central nervous system and the pathology of ALS. UMN are in the motor areas in the brain which can innervate bulbar muscles such as the oropharyngeal muscles used in speech, eating and swallowing. LMNs are in the spinal cord and brainstem and can innervate the upper and lower limb muscles. The UMNs decussate at the spinal cord and traverse down the anterior dorsal horn in the Rexed lamina IX corticospinal tracts. These UMNs then innervate the LMNs which exit through the ventral root of the cord and control upper and lower limb muscles. ALS that begins with an initiating pathological lesion in the UMNs affecting bulbar muscles is termed 'bulbar onset', and a lesion starting in the spinal cord affecting the LMNs is termed 'limb onset' which can either be upper or lower limb. At the level of the spinal cord motor neuron death occurs in the corticospinal tracts, which is accompanied by spongiosis, astrocytosis and microglial activation. At a cellular level the surviving motor neurons can contain ubiquitinated inclusions (UBIs), bunina bodies, or hyaline conglomerate inclusions (HCIs). UMN= upper motor neuron, LMN = lower motor neuron.

1.3.4 Toxic mechanisms in ALS

ALS is now considered a multisystem disorder with predominant motor neuron involvement, rather than a pure motor disorder, due to the involvement of sensory and spinocerebellar pathways, with pathology present in numerous brain regions including the hippocampal dentate granule layer and the substantia nigra (Wharton & Ince 2003). Most of the investigations into toxic mechanisms stem from the discovery of genetic mutations causing ALS (Table 1). As such, there is now a wide variety of heterogeneous potential pathological mechanisms involved in ALS. Due to indistinguishable clinical phenotypes between sporadic and familial cases, these mechanisms have been applied as potential mechanisms for sALS as well as fALS. Indeed, most of the cellular toxic mechanistic insights have spawned from the discovery of the mutations in the Cu/Zn superoxide dismutase 1 (SOD1) gene, which account for ~20% of fALS cases (Rosen, 1993). Since then, numerous investigators have developed SOD1 cellular and animal models to model the ALS disease process and investigate toxic mechanisms. Indeed, other ALS gene associated mutations have also been utilised to develop animal and cellular models of ALS (Bastow et al., 2011; Burkhardt et al., 2013; McGoldrick et al., 2013; Swarup and Julien, 2010). Some of the potential toxic mechanisms discovered using these animal and cellular models include: oxidative stress, mitochondrial dysfunction, excitotoxicity, dysregulation of endosomal trafficking, defective axonal transport, neuroinflammation, ER stress, dysfunctional transcription and RNA processing, non-neuronal cell mediated toxicity and protein misfolding and aggregation (Ferraiuolo et al. 2011). Many of these potential pathological mechanisms could potentially be involved simultaneously or be specific to a certain genetic mutation or from the initial toxic insult. The review of all these mechanisms is beyond the scope of this thesis and detailed reviews can be found elsewhere (reviewed by Ferraiuolo et al. 2011). Here we argue for the prominent involvement of protein misfolding as the main toxic mechanism and as a cause of the initial toxic insult in ALS.

Gene	Locus	Inheritance	ALS	FTLD	ALS-FTLD	PMA	PLS	Percentage of fALS
C9orf72	9p21.3–p13.3	Dominant	+	+	+	+	+	40-50%
SOD1	21q.22.1	Dominant	+	-	Rare	+	-	20%
TDP-43	1p36.2	Dominant	+	Rare	+	-	-	2-5%
FUS	16p11.2	Dominant	+	Rare	+	-	-	2-5%
Alsin	2q33.2	Recessive	+	-	-	-	-	<1%
ANG	14q11.2	Dominant	+	-	+	-	-	<1%
ATXN2	12q.24	Dominant	+	-	-	+	-	<1%
DAO	12q24	Dominant	+	-	-	-	-	<1%
OPTN	10p15-p14	Dominant	+	-	+	-	-	<1%
GRN	17q21	Dominant	Rare	+	Rare	-	-	<1%
PFN1	17p13.2	Dominant	+	-	-	-	-	<1%
SETX	9q34	Dominant	+	-	-	-	-	<1%
UBQLN2	Xp11	Dominant	+	+	+	-	-	<1%
VAPB	20q13.3	Dominant	+	-	-	+	+	<1%
VCP	9p13	Dominant	+	+	+	-	-	<1%

Table 1. Summary of all known ALS genes found so far in order of most common frequency in fALS patients. This includes the locus, nature of inheritance and presence of these mutations in different disease phenotypes including FTLD, ALS-FTLD, progressive muscular atrophy (PMA) and primary lateral sclerosis (PLS). (Adapted from Van Damme & Robberecht 2013)

1.2.1 *Prion disease and ALS*

The terms 'prionoid' and 'prion-like' were developed to distinguish between demonstrably transmissible prion diseases, and diseases that have pathological proteins with cellular prion-like behaviour (Aguzzi, 2009). Currently there is no evidence to demonstrate infectivity or transmissibility of ALS from human organ transplantation (Holmes and Diamond, 2012), unlike prion disease which can be iatrogenically transmitted in humans (Barrenetxea 2012; Brown et al. 1994). There is currently a large amount of experimental evidence for the transmission of prions, Aβ, tau and α-synuclein in vivo; however no data yet exists on the experimental transmission of key pathological ALS proteins in vivo.

The pathological prion protein can often appear to lay dormant for many years, but when disease is initiated, it spreads from focal propagation sites and causes relentlessly progressive dementia that can cause very short incubation periods before death (Brandner 2003). In a similar manner, ALS does not start until later on in life suggesting that ALS disease related proteins may lie dormant and become pathological due to ageing and cellular stress conditions. Prion protein conformations have been shown to change conformational status in environmental stress conditions which supports this idea (Tyedmers et al., 2008). However, ALS does not progress as rapidly as prion disease but progression can still be rapid from a focal symptom onset, and varies dependent upon the site of onset. Some of the reasons for a slower progression may include the cellular location of the pathological proteins and the complexity of ALS aggregated protein transport to the extracellular compartment. For example, prions are GPI membrane bound proteins (Hegde et al., 1998) which require no transport to the extracellular compartment, and could therefore account for the more effective propagation and transmission of prion disease throughout the CNS. Variability in seeding and propagative mechanisms of prions are also due to the variety of prion strains (Collinge and Clarke, 2007; Collinge et al., 1996). These prion strains have been shown to contain strong resistance to protease digestion, indicating that misfolded pathological prion protein is highly stable and can evade the cell defence mechanisms. It is also noted that these distinct prion strains have certain tropisms for

different brain regions and varying toxic properties. These distinct prion strains are responsible for a variety of different prion diseases with different ages of disease onset, different rates of progression, different regional patterns of pathology and differential toxicity (Collinge et al., 1996; Parchi et al., 1996; Tanaka et al., 2006). Although the clinical manifestations of prion disease are markedly different from ALS, the heterogeneity of clinical and pathological presentation bears resemblance to ALS (Ravits et al., 2013). The notable focal onset of the ALS at both the UMN and LMN level (Ravits et al., 2007a), and spreading of degeneration between body regions (Kanouchi et al., 2012), means that this prion-like disease spreading hypothesis can be easily assessed by quantification of the presence, severity and rate of progression of clinically apparent symptoms.

As previously mentioned prion disease is a protein misfolding disorder with the deposition of misfolded prion protein aggregates that can spread from cell to cell in the CNS. As it stands, there is strong evidence to support a prion-like non-cell autonomous protein misfolding hypothesis in many common neurodegenerative disorders including ALS (Brundin et al., 2010; Frost and Diamond, 2010; Goedert et al., 2010; Ilieva et al., 2009; Polymenidou and Cleveland, 2011, 2012). The main aggregated proteins in ALS thought to have prion-like characteristics are SOD1, FUS and TDP-43. So far the demonstration of the prion-like behaviour of FUS is in its infancy (Nomura et al., 2014), but SOD1 (Chia et al., 2010; Furukawa et al., 2013; Münch et al., 2011b; Pokrishevsky et al., 2012) and TDP-43 (Brettschneider et al., 2013; Furukawa et al., 2011; Nonaka et al., 2013; Tsuji et al., 2012; Udan-johns et al., 2013) have now been demonstrated to have cellular prion-like behaviour. In depth discussion of the prion-like mechanisms for SOD1 and FUS are beyond the scope of this thesis, and as such TDP-43 will be the main focus here.

1.4 TDP-43

One of the main characteristics of sporadic ALS cases is the presence of ubiquitinated immunoreactive inclusions (UBIs) in the upper and lower motor neurons of the brain and spinal cord. A ground-breaking discovery by two groups found that the major component of these inclusions was a protein called 'trans-active response DNA binding protein' with a molecular weight of 43kDa ('TDP-43'). These TDP-43 positive neuronal inclusions were also discovered in the brains of patients with frontotemporal lobar degeneration with ubiquitinated inclusions (FTLD-U) (Neumann et al. 2006; T. Arai et al. 2006). This discovery led to a heightened interest in the role of TDP-43 in ALS and FTLD, and defined a new era in ALS research. Despite this, TDP-43 pathology can also occur in other neurodegenerative diseases including: Alzheimer's disease (Amador-Ortiz et al., 2007; Higashi et al., 2007; Uryu et al., 2008), corticobasal degeneration (Uryu et al., 2008), parkinsonism dementia complex of Guam (Hasegawa et al., 2007), Lewy body disease (Higashi et al., 2007; Nakashima-Yasuda et al., 2007), Pick's disease (Arai et al. 2006), hippocampal sclerosis (Amador-Ortiz et al., 2007) and Perry syndrome (Wider et al., 2009). However, the degree of involvement is much smaller, and often restricted to the limbic system in most of these cases. A more recent study has also detected TDP-43 pathology in 29% of healthy control subjects over the age of 65 (Geser et al., 2010a) indicating that TDP-43 pathology can occur partially by the natural ageing process. Indeed, in cases of ALS heat mapping of TDP-43 pathology demonstrates the predominant presence of this pathology in motor regions, but also a widespread involvement of different CNS regions not affected in other diseases or controls (Geser et al., 2008). Although the presence or absence of this pathology may be non-specific, its regional presence in the motor system and the anterior frontal and temporal lobes seems to be essential for ALS and FTLD-U.

Shortly following the identification of TDP-43 as the major pathological substrate in ALS and FTLD, mutations in the TARDBP gene encoding for TDP-43 were identified in a number of sporadic and familial ALS cases suggesting a direct causal nature of this protein (Daoud et al., 2009; Kabashi et al., 2008; Rutherford et al., 2008; Sreedharan et al., 2008). The distinct role of this protein is supported by the fact that TDP-43 pathology is found in a majority of

sALS (<90%) cases. Interestingly, it does not coincide with SOD1 (Mackenzie et al. 2007), or Fused in Sarcoma (FUS) pathology (Kwiatkowski et al., 2009; Vance et al., 2009) suggesting that TDP-43 has a separate pathological mechanism from SOD1 and FUS. However, recent evidence may suggest that dysfunction of TDP-43 and FUS may lead to downstream SOD1 misfolding (Pokrishevsky et al., 2012). As mentioned earlier, ALS and FTLD can clinically overlap; they also share similar TDP-43 pathology, suggesting that as well as C9orf72 mutations, pathological TDP-43 may be one of the underlying causes of this ALS and FTLD-U disease continuum (Janssens and Van Broeckhoven, 2013). In order to thoroughly investigate the pathological importance of this protein, it is necessary to demonstrate its normal and pathological cellular function as described so far.

1.4.1 Normal function of TDP-43

The normal function of TDP-43 is still not completely understood but has been shown to be involved in a wide range of cellular processes and is essential for survival (Kraemer et al. 2010; Sephton et al. 2010; Wu et al. 2010). TDP-43 is encoded by the TARDBP gene on chromosome 1 and encodes a 414 amino acid protein that is ubiquitously expressed in all tissues and is well conserved in invertebrates and mammals. TDP-43 comprises an N-terminal domain, 2 RNA binding domains, a glycine rich C-terminal and bipartite nuclear export (NES) and localisation signals (NLS) (Figure 4). The TARDBP gene consists of 6 exons 5 of which are coding and 1 is non-coding. These exons can undergo alternative splicing to generate 11 different protein isoforms where the 43kDa isoform is the main isoform detected in human tissue (Wang et al. 2004). It was initially discovered by its ability to repress transcription of the HIV-1 virus by binding to the transactive response (TAR) DNA element (Ou et al., 1995), hence the name 'transactive response DNA binding protein'. The primary structure has similarities to the heterogeneous nuclear ribonucleoprotein (hnRNP) family which are complexes of RNA and protein in the nucleus involved in gene transcription and post-translational modification of pre-mRNA (Kreric and Swanson, 1999).

One of the main characteristics of TDP-43 is its RNA binding properties. The RNA recognition motif (RRM) domains are known to bind to nucleic acids including mRNA and DNA. As such,

TDP-43 is involved in regulating mRNA stability, splicing, transcription and translation (Ayala et al., 2005). It preferentially binds to RNAs via a dinucleotide GU repeat element rather than non-GU repeat elements (Buratti and Baralle, 2001). More recent evidence analysing global TDP-43 binding sites supports these findings by identifying a non-interrupted GU repeat element as the main RNA binding site of TDP-43 (Polymenidou et al., 2011; Sephton et al., 2010b). TDP-43 can bind to a large portion of the transcriptome as identified in recent studies using high throughput sequencing of RNA isolated crosslinking immunoprecipitation (HITS-CLIP), where it has been shown to bind more than 6,000 RNA's. It preferentially binds to long intronic sequences, 3' untranslated regions (UTR) and non-coding RNA's. Most of these TDP-43 bound transcripts are long transcripts for neuronal development and synaptic plasticity (Polymenidou et al., 2011; Tollervey et al., 2011), highlighting its significant role in these processes. As well as its sequence similarity to the hnRNP proteins, it can also bind to other hnRNP proteins such as hnRNP A2/B1, hnRNP A1, hnRNP A3 and hnRNP C1/C2 through its C-terminal glycine rich domain (Buratti et al., 2005; Freibaum et al., 2009; Ling et al., 2010).

One of the other main functions of TDP-43 as an hnRNP protein is to regulate splicing. As such, TDP-43 was found to promote the skipping of exon 9 of the cystic fibrosis transmembrane conductance regulator (CFTR) gene (Buratti and Baralle, 2001; Buratti et al., 2001), which has now been developed as one of the main criteria for functional testing of TDP-43. TDP-43 has also been shown to promote the inclusion of exon 7 in the Survival of motor neuron (SMN2) gene which is involved in spinal muscular atrophy (SMA)(Bose et al., 2008). Additionally, it can regulate the splicing of the apolipoprotein A2 (APOA2) (Mercado et al., 2005) and serine/arginine rich splicing factor 2 (SC35) (Dreumont et al., 2010). It is thought that some of this splicing activity occurs via the N-terminal domain of TDP-43 (Zhang et al., 2013).

TDP-43 is known to bind single stranded DNA, RNA and protein (Warraich et al., 2010). It has a major role in gene regulation via modification of mRNA levels. It can inhibit the expression of the mouse spermatid specific SP-10 gene (Acharya et al., 2006), testis mouse specific ACRV1 gene (Lalmansingh et al., 2011) and more interestingly, cyclin dependent

kinase 6 (cdk6) (Ayala et al., 2008a). It is capable of stabilising human low molecular weight neurofilament (hNFL) mRNA in spinal motor neurons (Strong et al., 2007), regulates mRNA levels of the Futsch protein (the Drosophila homologue of human microtubule associated protein 1B (MAP1B))(Godena et al., 2011), and regulates its own mRNA by binding to the TARDBP 3'UTR to produce a negative feedback mechanism (Ayala et al., 2010). TDP-43 knockdown in cells is known to decrease levels of histone deacetylase 6 (HDAC6) (Fiesel et al., 2010), which is further thought to decrease neurite outgrowth in neuronal cell lines (Fiesel et al., 2011). Indeed, TDP-43 and FUS have been shown to form a complex that co-regulates the HDAC6 mRNA, and this process requires the RNA binding and C-terminal protein interactions (Kim et al., 2010). TDP-43 has also been found localized to RNA granules and stress granules in neuronal processes where it is thought to be involved in RNA trafficking and stabilisation (Elvira et al., 2006; Liu-Yesucevitz et al., 2010; Wang et al., 2008). TDP-43 is also known to interact with the ALS and FTLD-U associated protein FUS (Freibaum et al., 2009; Ling et al., 2010), and involved in miRNA biogenesis where it binds to the primary miRNA processing Drosha complex in perichromatin fibres where miRNA biogenesis is thought to occur (Gregory et al., 2004). TDP-43 is now known to be involved in neuronal development via the stabilisation of the Drosha protein, and Drosha mediated regulation of the developmental factor Neurogenin 2 (Di Carlo et al., 2013). More recently TDP-43 has been shown to be heavily involved in fat metabolism and glucose homeostasis in vivo, which when depleted leads to muscle atrophy and early lethality in mice (Chiang et al., 2010; Stallings et al., 2013).

The various roles TDP-43 plays in micro RNA (mi-RNA) processing (Gregory et al., 2004), apoptosis (Sreedharan et al., 2008), cell division (Ayala et al., 2008a), mRNA stabilisation (Casafont et al., 2009), axonal transport (Alami et al., 2014; Fallini et al., 2012; Sato et al., 2009), neurite outgrowth (Fallini et al., 2012; Fiesel et al., 2011) and embryo development (Sephton et al. 2010) suggest an essential role of this protein in molecular and cellular processes. The roles described here could highlight a plausible reason why the disturbance of normal TDP-43 function could result in pathological consequences.
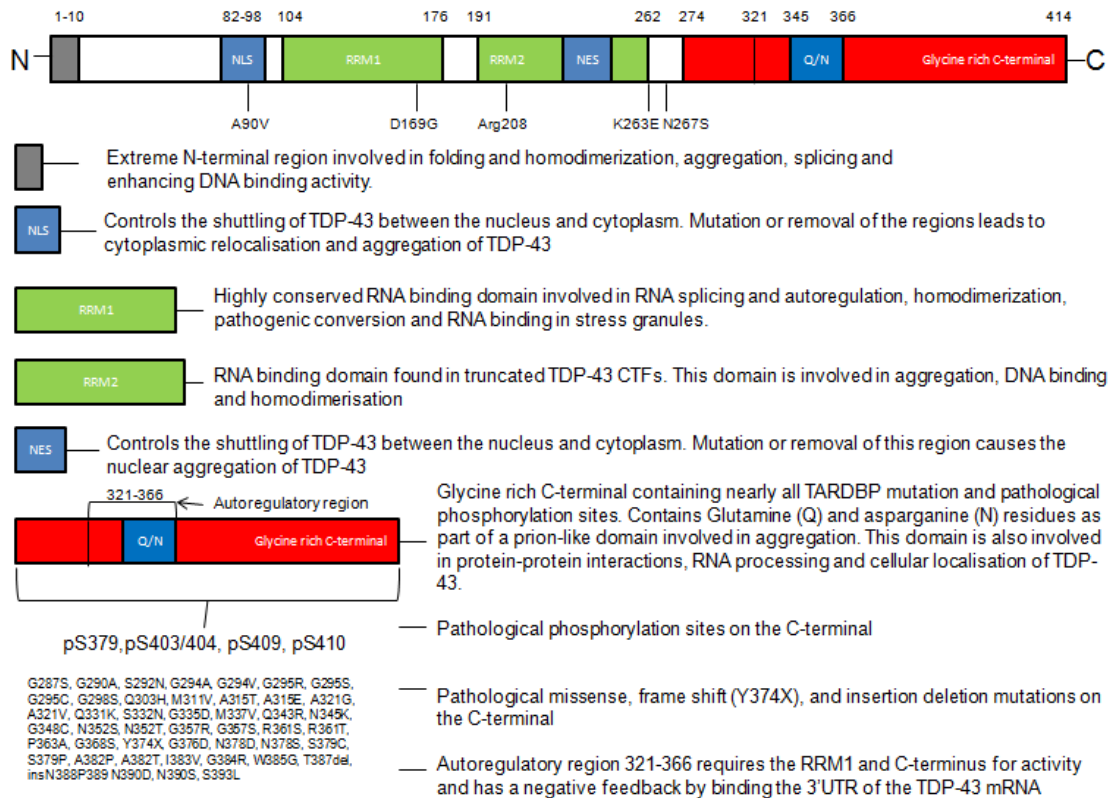
Figure 4. TDP-43 protein sequence with highlighted normal function and pathological alterations. Some of the normal and pathological functions and characteristics of the protein are highlighted through description of the different functional domains. NLS = Nuclear localization signal, NES = Nuclear export signal, RRM1 = RNA recognition motif 1, RRM2 = RNA recognition motif 2. Q=Glutamine, N= Asparganine. Diagram adapted from (Janssens and Van Broeckhoven, 2013)

1.4.2 Pathological function of TDP-43

In affected ALS or FTLD-U neurons, TDP-43 is often relocated from the nucleus to the cytoplasm and forms cytoplasmic inclusions. These cytoplasmic inclusions tend to be insoluble in sarkosyl, ubiquitinated, hyperphosphorylated and contain truncated 20-25kDa C-terminal fragments (CTF) of TDP-43 (Ayala, Zago, et al. 2008; Barmada et al. 2010; Neumann et al. 2006; Hasegawa et al. 2008; Arai et al. 2010). However, some TDP-43 animal and cellular models suggest that TDP-43 mediated neurodegeneration and cellular toxicity can develop without some of these pathological features (Arnold et al., 2013; Janssens et al., 2013). There is also some in vivo evidence in transgenic tau mice to demonstrate that tau pathology could potentially produce secondary TDP-43 pathology (Clippinger et al., 2013). However, there is yet no evidence to demonstrate this in human cases of FTLD-Tau. These apparent contradictions have raised questions about which TDP-43 pathological features are linked to TDP-43 induced neurodegeneration, and which features are epiphenomena of the disease process. There are currently three broad theories about how TDP-43 could account for cellular toxicity and pathology in ALS/FTLD. These include a potential 'loss of function', 'gain of toxic function' or both. Indeed, recent evidence investigating the loss and gain of function of the Drosophila homologue of TDP-43 (TBPH), suggests that both loss and gain of function of TBPH can lead to reduced life span, motor deficits and synaptic dysfunction (Diaper et al., 2013). Substantial progress has been made into investigating these potential mechanisms of neurotoxicity using the TDP-43 pathological hallmarks as a guide. The pathological hall marks of TDP-43 used to investigate its toxic mechanisms are the ubiquitination, phosphorylation, mislocalisation, nuclear clearance, autoregulation, truncation, insolubility and aggregation of the protein (Figure 5).
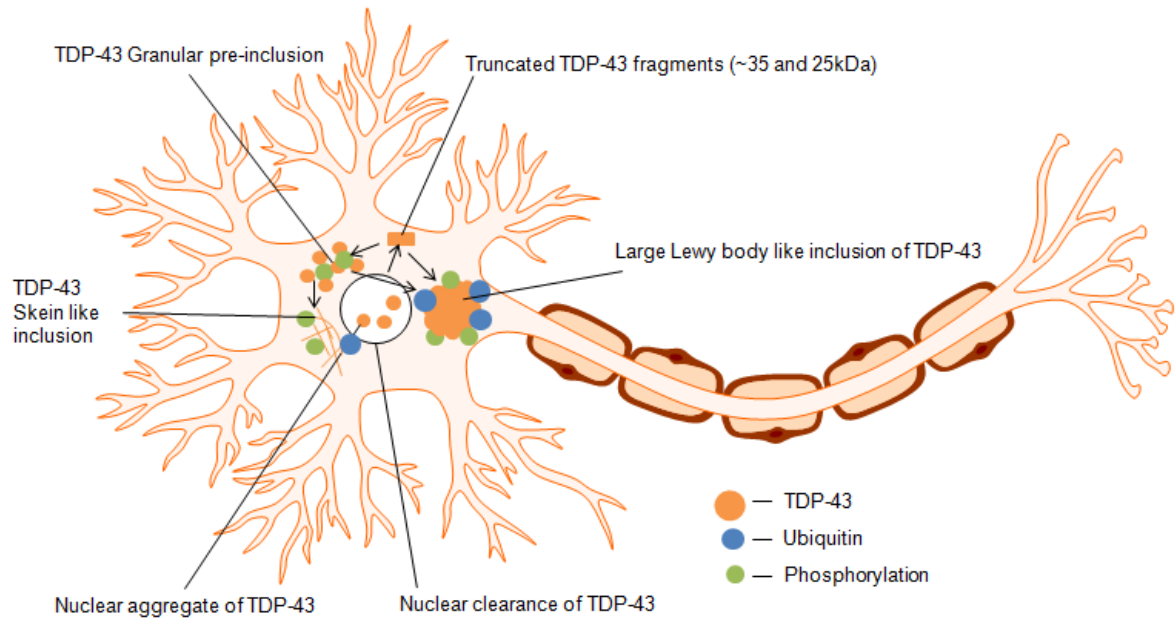
Figure 5. Diagram of pathological modifications of TDP-43 in a neuron. During cellular stress or pathological misfolding events, TDP-43 can relocate from the nucleus to the cytoplasm to form fine granular pre-inclusions, before the formation of larger aggregates. Additionally, the truncation of TDP-43 can also lead to inclusion formation. The types of mature inclusions of TDP-43 are skein-like, large round or dot inclusions. These inclusions are pathologically phosphorylated and commonly ubiquitinated; however granular pre-inclusions are often not ubiquitinated. TDP-43 can also be aggregated in the nucleus in cases of FTLD and especially with VCP mutations. However, during this aggregation process TDP-43 is commonly cleared from the nucleus in the ALS disease process.

1.4.2.1 TDP-43 ubiquitination

Ubiquitination of proteins in the cell indicates that the proteins are targeted for removal and degradation by the cells ubiquitin proteasome system (UPS). Evidence from immunohistochemistry on human ALS CNS tissue demonstrates that not all inclusions are ubiquitin positive. Indeed, the TDP-43 aggregates that are predominantly ubiquitin positive are the round dense lewy body like inclusions whereas the 'pre-inclusions' (granular less dense cytoplasmic inclusions) are not ubiquitinated. This suggests that ubiquitination is a late characteristic in the disease process when the cell targets the inclusions for degradation (Giordana et al., 2010; Strong et al., 2007). Phosphorylated TDP-43 antibodies that detect phosphorylation at serine residues 409 and 410 can detect all of the pathological inclusions including the truncated 25kDa CTFs and 'pre-inclusions' (Hasegawa et al., 2008; Neumann et al., 2010). This suggests that phosphorylation of TDP-43 occurs before ubiquitination, but says nothing about the toxicity of either of these post-translational modifications. Evidence to suggest that impairment of the UPS is linked to the formation of these inclusions comes from the discovery of rare dominant missense mutations in the ubiquilin 2 (UBQLN2) gene that causes X-linked ALS (Deng et al., 2011). The UBQLN2 disease associated mutations have been shown to inhibit the proteasome system in cell culture, and produce TDP-43 and UBQLN2 inclusions in human CNS tissue from patients with UBQLN2 mutations. Hence this protein is thought to have a significant role in protein degradation, including the degradation of TDP-43 aggregates. Other evidence to support that the disruption of the proteasome leads to the aggregation and ubiquitination of TDP-43 has been demonstrated by inhibiting the proteasome with MG-132 in a number of cell culture models (Winton, Igaz, et al. 2008; Wang et al. 2010; van Eersel et al. 2011). Additionally, the inhibition of autophagy, endosomes and the proteasome in TDP-43 expressing motor neurons in vitro and in vivo, all accelerate the formation of ubiquitinated TDP-43 aggregates and highlight the importance of the proteasome function in the development of TDP-43 pathology (Watabe et al., 2013). A more recent publication suggests that the UPS is involved with the clearance of soluble TDP-43 and the autophagy system is required to remove larger aggregates of insoluble oligomeric TDP-43 (Scotter et al., 2014). Interestingly, the full length TDP-43 has been demonstrated to have a long half-life of 12-34h whereas the CTFs have a

shorter half-life of ~4h (Ling et al., 2010; Pesiridis et al., 2011) and both ultimately become degraded by the UPS. Considering the lability of these CTFs, their accumulation and resistance to proteasomal degradation in ALS and FTLD-U is unique. Therefore, these CTFs may have different interactions with the proteasome due to their lack of NLS signals, increased cleavage and cytoplasmic localisation (Igaz et al., 2009; Winton et al., 2008a).

Autophagy mediated degradation is where cytoplasmic organelles and proteins are targeted to membrane bound vesicles for fusion with lysosomes and degradation by lysosomal enzymes. Evidence now suggests that this system also affects the turnover of TDP-43 as demonstrated by its interactions with various autophagy associated proteins (Urushitani et al., 2010; Wang et al., 2010b). The endosomal sorting complexes required for transport (ESCRT's) are involved in trafficking proteins to multivesicular bodies as part of the autophagy pathway. Experiments down regulating ESCRT's have been shown to inhibit autophagy and increase the amount of cytoplasmic and ubiquitinated TDP-43 (Filimonenko et al., 2007). However, even though mutations of one of the ESCRT subunits called charged multivesicular modified protein 2 B (CHMP2B) is a rare cause of FTLD, these cases produce no TDP-43 inclusions (Skibinski et al., 2005). Ubiquilin1 is an adaptor protein which functions to regulate autophagy and deliver ubiquitinated proteins to the proteasome. Overexpression of ubiquilin1 leads to a reduced number of TDP-43 aggregates in some studies (Kim et al. 2009), however, in another study it resulted in increased cellular toxicity and reduced Drosophila survival, despite the reduction in TDP-43 levels (Hanson et al., 2010). Finally, sequestosome 1 is also an adaptor protein which, upon overexpression in cell culture, led to the reduction of TDP-43 aggregation in a proteasome dependent manner (Brady et al., 2011). More recent studies on TDP-43 mouse models of FTLD-TDP suggest that the activation of autophagy can significantly rescue the disease phenotype and decrease aggregation and truncation of TDP-43 compared to controls (Wang et al. 2012). Together these data support the role of the UPS and autophagy mediated degradation of TDP-43, and that defects in these pathways caused by mutations in UBQLN2 may lead to TDP-43 mediated neurodegeneration. However, no evidence for proteasome or autophagy dysfunction outside of UBQLN2 mutations in familial and sporadic cases exists to date.

Additionally, both of these systems can affect the degradation and aggregation of many proteins in the CNS meaning that dysfunction of these systems may be non-specific.

1.4.2.2   TDP-43 phosphorylation

Full length TDP-43 phosphorylation results in a 45kDa band that is present in sarkosyl insoluble fractions in ALS/FTLD cases and not seen in controls (Neumann et al. 2006; Tetsuaki Arai et al. 2006). Several fragments (approximately 18–26 kDa) and indistinct high molecular weight smears have also been detected, and these fragment banding patterns differ among clinicopathological sub-types of TDP-43 proteinopathy (e.g. Type A, B C and D) (Hasegawa et al., 2008; Tsuji et al., 2012). Hasegawa and colleagues identified 36 of the 64 possible phosphorylation sites, and the ones that had the strongest co-immunoreactivity with the ubiquitinated inclusions where the pS379, pS403/404, pS409 and pS410 which are all located in the C-terminal (Hasegawa et al., 2008). This group, and a few others who used rat and mouse monoclonal antibodies, identified the pS409/410 sites to have the most significant immunoreactivity (Inukai et al., 2008; Neumann et al., 2010). The specific phosphorylation antibodies to pS409/410 were found to label all the inclusion variants including dystrophic neurites, neuronal cytoplasmic and glial cytoplasmic inclusions in various TDP-43 proteinopathies (Hasegawa et al., 2008; Neumann et al., 2010). Additionally, the use of phosphorylated antibodies have proved useful in more specific differentiation of FTLD-TDP subtypes at post mortem (Tan et al., 2013). These antibodies indicate that phosphorylation may be a disease specific process, as they do not detect normal nuclear TDP-43 and are specific in detection of the cytoplasmic C-terminal fragments (Dormann et al., 2009; Hasegawa et al., 2008; Igaz et al., 2009; Neumann et al., 2010; Zhang et al., 2009). This indicates that maybe the enhanced phosphorylation of cytoplasmic TDP-43 fragments may reflect a greater ability of kinases to access these fragments.

Different studies on this hypothesis are in contradiction with each other and whilst one study demonstrates increased phosphorylation of fragments from mutant TDP-43 lacking the NLS against wild type TDP-43 (Igaz et al., 2009), the other studies with mutants lacking part of the NLS showed no change in phosphorylation compared to full length wild type TDP-43 (Nonaka et al., 2009a; Zhang et al., 2009). Experiments have shown that TDP-43 is

phosphorylated by casein kinase 1 (CK1) and cell division cycle 7 kinase (CDC7) (Hasegawa et al., 2008; Liachko et al., 2013). Phosphorylation has been shown to enhance oligomerisation when recombinant human TDP-43 is phosphorylated by CK1. This also produces abundant 15nm filaments that are immunopositive for pS409/410, and have also been found in ALS motor neuron inclusions (Hasegawa et al., 2008). Specific enhanced TDP-43 phosphorylation with CK1ε in mutant TDP-43 Drosophila was found to promote TDP-43 oligomerisation and enhance neurotoxicity. Additionally, cell treatment of recombinant TDP-43 oligomers with rat CK1 enhanced cellular toxicity (Choksi et al., 2013). Therefore the formation of oligomers may represent a toxic intermediate stage that could be causing neural cell death, and this process may be mediated in turn by phosphorylation. In addition to this, the proteasome may play a significant role in phosphorylation of TDP-43 as inhibition of the proteasome in cells lacking part of the NLS increases the number of phosphorylated and ubiquitinated inclusions (Nonaka et al., 2009a).

Overexpression of TDP-43 CTFs or cytoplasmic TDP-43 in cell models often results in the formation of phosphorylated aggregates of TDP-43 (Igaz et al., 2009; Nonaka et al., 2009a, 2009b; Zhang et al., 2010). Indeed, overexpression of the full length TDP-43 in numerous transgenic TDP-43 models can also lead to the formation of phosphorylated TDP-43 aggregates (Igaz et al., 2011; Shan et al., 2010; Stallings et al., 2010; Wegorzewska et al., 2009; Wils et al., 2010; Xu et al., 2010). The phosphorylation of TDP-43 may contribute to the aggregation of the protein as the phosphorylated forms have a longer half-life than the non-phosphorylated forms, suggesting that the phosphorylation may inhibit UPS mediated degradation (Zhang et al., 2010). The detection of ubiquitin negative TDP-43 pS409/410 positive pre-inclusions may be an indicator that phosphorylation precedes ubiquitination (Neumann et al. 2010). However, phosphorylated TDP-43 is generated in the late stage of the conversion from soluble to insoluble TDP-43 suggesting that phosphorylation may not be required for aggregation but may just be a marker for aggregation (Dormann et al., 2009). Indeed, prolonged cellular stress can also cause abnormal phosphorylation of TDP-43, indicating that it could also be a cellular stress marker (Shindo et al., 2013).

ALS TDP-43 mutant transgenic *C.elegans* (G290A and M337V) with deleted phosphorylation sites have been shown to improve motor phenotype and ameliorate neurodegeneration (Liachko et al., 2010). This suggests that phosphorylation drives TDP-43 induced neurodegeneration in *C.elegans*. The same group also reported that the kinase CDC7 drives the phosphorylation of TDP-43, and that inhibition of CDC7 can block pathological phosphorylation and prevent TDP-43 induced neurodegeneration in *C.elegans* and HEK293 cells. This further suggests that phosphorylation could be a significant contributor to cellular toxicity (Liachko et al., 2013). In contrast to this, a non-human primate AAV transduced TDP-43 overexpression model of ALS demonstrated that phosphorylation occurred post neurodegeneration, indicating that phosphorylation may not be required for TDP-43 mediated toxicity (Uchida et al., 2012)

In summary, whilst TDP-43 phosphorylation has demonstrated neurotoxic properties, it is not essential for cleavage, aggregation and neurotoxicity (Dormann et al., 2009; Zhang et al., 2009). Contrasting evidence from these studies has made it difficult to ascertain if phosphorylation occurs before or after the aggregation of TDP-43. Additionally, the effects of phosphorylation on the normal function of TDP-43 are unknown, and disease associated mutations have shown no effect on phosphorylation. Future experiments investigating these aspects will provide more clarity on these issues.

1.4.2.3   TDP-43 mislocalisation

TDP-43 is a predominantly nuclear protein but is often present at low levels in the cytoplasm. Interspecies heterokaryon assays can measure the transfer of nuclear proteins between nuclei of different species and, as such, can measure the degree of nucleo-cytoplasmic shuttling ability of a specific protein. Using this assay it has been demonstrated that TDP-43 can readily shuttle between the nucleus and cytoplasm (Ayala et al., 2005, 2008b; Ou et al., 1995; Wang et al., 2004). Part of the main pathological characteristics of TDP-43 pathology is the re-localisation of TDP-43 from the nucleus to the cytoplasm in the form of aggregates (Neumann et al. 2006). It is now known that a variety of genetic and environmental cellular stresses can contribute to this mislocalisation of TDP-43. TDP-43 is normally localised to the euchromatin regions of the nucleoplasm, this includes sites of

transcription and co-transcriptional splicing such as the nuclear speckles and perichromatin fibrils (Casafont et al., 2009; Thorpe et al., 2008). Therefore mislocalisation does not always mean that TDP-43 is redistributed to the cytoplasm, as in some cases of FTLD the TDP-43 aggregates can be intranuclear and have a lenticular or 'cat-eye' morphology (Mackenzie et al., 2006, 2011; Sampathu et al., 2006). Four subtypes of FTLD-TDP from A-D have been described for different FTLD phenotypes and these intranuclear inclusions are predominantly present in FTLD-TDP Type D associated with mutations in the Valosin containing protein (VCP) (Mackenzie et al., 2006, 2011; Sampathu et al., 2006). However, it is still not understood why these VCP mutations lead to increased intranuclear inclusions.

In order to control its cellular location, TDP-43 has a nuclear localisation sequence (NLS) motif between the RRM1 (residues 82-98) domain and the N-terminus and one nuclear export sequence (NES) motif in the RRM2 domain (residues 239-250) (Ayala et al., 2008b). The pathogenic A90V mutation subsequently causes the cytoplasmic redistribution of TDP-43 to the cytoplasm due to the location of the mutation within the NLS region (Winton et al., 2008b). Mutations in the 3'UTR of the sigma non-opioid intracellular receptor 1 (SIGMAR1) are a rare cause of FTLD-TDP, and through unknown mechanisms, can increase the ratio of cytoplasmic to nuclear TDP-43 (Luty et al., 2010). Similar cytoplasmic redistribution of TDP-43 has also been observed in a VCP mutant Drosophila fly model (Ritson et al., 2010).

Cellular stress related events are also able to induce neuronal TDP-43 mislocalisation. Axotomy and chronic cerebral ischemia in mice, for example, can cause time dependent redistribution of TDP-43 to the cytoplasm (Moisse et al., 2008, 2009; Sato et al., 2009; Shindo et al., 2013), and a variety of cellular stressors can cause TDP-43 and its CTFs to localise in the cytoplasm with stress granules (Colombrita et al., 2009; Dewey et al., 2010; Volkening et al., 2009; Walker et al., 2013). Induction of the unfolded protein response (UPR) with Tunicamycin in organotypic brain slices caused the formation of cytoplasmic TDP-43 inclusions in neurons and astrocytes. Interestingly, similar effects were not seen with apoptosis induction or chronic glutamate excitotoxicity, suggesting the UPR is a specific cellular response for TDP-43 re-localisation (Leggett et al., 2012).

It is still unclear whether cytoplasmic redistribution of TDP-43 causes neurodegeneration as this tends to occur secondary to disease mutations, and can be found in other neurodegenerative disorders. A number of studies have investigated TDP-43 cytoplasmic redistribution using cell and animal models. A study in primary rat neurons demonstrated that the degree of cytoplasmic TDP-43 expression with overexpression of wild type and mutant TDP-43 correlated with neurotoxicity (Barmada et al., 2010). Additionally, expression of a mutated NLS motif in a developing Drosophila enhanced neurotoxicity in the development of the eye compared to wild type TDP-43. However, further study by the same group in adult flies demonstrated that the wild type overexpression caused more neurotoxicity in comparison to a mutated NLS or NES motif (Miguel et al., 2010). One study identified the type 1 inositol 1,4,5-triphosphate (IP3) receptor (ITPR1) as a significant modulator of TDP-43 localisation, and inhibition of this receptor can rescue the lethality and motor phenotype in Drosophila (Kim et al., 2012). A mislocalisation of TDP-43 with a mutant NLS in differentiated cortical neurons induced aberrant neurite morphology and decreased cell survival, which was unaffected by the addition of a mutation (Han et al., 2013). This suggests that mislocalisation alone is enough to cause cellular toxicity.

The overexpression of mutant NLS and wild type TDP-43 in transgenic mice resulted in the expression of cytoplasmic TDP-43 with a few rare inclusions. However, the degree of toxicity and neurodegeneration observed in each was very similar (Igaz et al., 2011). Indeed, this neuronal overexpression of TDP-43 has been shown to be sensitive to the timing of induction of overexpression, with later expression reducing lethality but still causing neurodegeneration and the formation of TDP-43 pathology (Cannon et al., 2012). In addition to this, mutant TDP-43 has been shown to have a longer half-life than the wild type, and has been linked to an accelerated disease onset. As such, the chronic stabilisation of the human TDP-43 in cells has been shown to cause toxicity through impairment of proteostasis (Watanabe et al., 2012). Indeed, stabilisation of human wild type and mutant TDP-43 in mouse motor neuron like NSC-34 cells caused a significantly higher rate of apoptotic cell death (Wu et al., 2013). One of the key pieces of evidence for TDP-43 overexpression as a causal nature of ALS comes from a study overexpressing wild type TDP-43 in a non-human

primate. Here they over expressed wild type TDP-43 in the cervical spinal cord using AAV transduction. This reproduced many of the clinical features of ALS including progressive motor weakness, muscle atrophy and fasciculations in the distal hand. This degenerative phenotype correlated with the degree of cytoplasmic mislocalisation of TDP-43, and was present before disease onset and in the neurons responsible for weakness in the distal hand (Uchida et al., 2012). In contrast to this, overexpression of pathogenic mutants in mice compared to wild type mice produced an adult onset motor disease phenotype without the mislocalisation, nuclear clearance, aggregation or insolubility of TDP-43. These defects in this study were associated with splicing defects suggesting that the development of characteristic TDP-43 pathology was not necessary for neurodegeneration, therefore this highlights the importance of altered splicing as a potential gain or loss of TDP-43 mediated toxicity (Arnold et al., 2013)

Overall, it has been demonstrated that, although the overexpression of cytoplasmic TDP-43 is neurotoxic; it is not a prerequisite for TDP-43 mediated toxicity. Despite this, it may still be a valuable contributor to cellular toxicity and exhibiting a toxic gain of function by retaining its functional binding capacity for RNA and protein but in an abnormal location. However, the results on this are still mixed and further investigation is required to clarify the importance of mislocalisation of TDP-43.

1.4.2.4   TDP-43 nuclear clearance and autoregulation

One of the main intriguing aspects of TDP-43 pathology in ALS and FTLD-U is its early clearance from neuronal nuclei which can occur even in cells with pre-inclusions and ubiquitin negative inclusions (Neumann et al. 2006; Giordana et al. 2010; Mori et al. 2008). Distinctively, this represents a decrease of the protein from its normal nuclear localisation rather than a mislocalisation, and therefore is thought to act as a loss of function toxic mechanism in the disease state. Loss of function mechanisms are illustrated by determining the normal function of the protein. As described above, TDP-43 has a wide range of normal functions and can regulate many genes and transcripts making it difficult to identify which normal function loss is contributing to cellular toxicity.

One of the key characteristics of RNA binding proteins is the ability of the protein to autoregulate its own mRNA transcripts. TDP-43 has been shown to downregulate the expression of endogenous TDP-43 mRNA and protein by binding to its own mRNA 3'UTR region when exogenously overexpressed in cell culture and transgenic mice (Ayala et al., 2010; Igaz et al., 2011; Winton et al., 2008a). It is still unclear as to whether this binding of its own mRNA leads to non-sense mediated decay or exosome mediated decay, or if this mechanism leads to nuclear clearance of TDP-43 (Ayala et al., 2010; Polymenidou et al., 2011). It has been suggested that increased TDP-43 levels in inclusion bearing neurons could lead to autoregulation of the protein and lead to nuclear clearance. This is supported by the strong correlation of neurodegeneration in transgenic mice with decreased expression of endogenous TDP-43 compared to other aspects of TDP-43 pathology (Igaz et al., 2011). Other evidence to support a loss of function of TDP-43 in the neurodegenerative process comes from various cellular and animal studies. Knockdown of endogenous TDP-43 in mice causes early embryonic lethality by disrupting the formation of the inner cell mass (Kraemer et al., 2010; Sephton et al., 2010a; Wu et al., 2010). The post natal tamoxifen inducible knockout of TDP-43 causes altered fat metabolism and rapid lethality in mice, and knockout of TDP-43 in embryonic stem cells inhibits stem cell proliferation (Chiang et al., 2010). Specific inducible spinal cord motor neuron TDP-43 depletion in mice has also been shown to produce a range of ALS like phenotypes and ubiquitinated inclusions in the spinal cord neurons depleted of TDP-43 (Wu et al., 2012). Again, a more recent study demonstrates that specific motor neuron depletion of TDP-43 in postnatal mice induced an age dependent progressive motor dysfunction reminiscent of ALS (Iguchi et al., 2013). However, another study suggests that down regulation of mouse TDP-43 does not cause toxicity or disease phenotypes, indicating a potential gain of toxic function of the overexpressed human TDP-43 (Xu et al., 2013).

On a cellular level it has been shown that reduced TDP-43 expression in Neuro-2a cells causes reduced neurite outgrowth and cell viability via dysregulation of the Rho family GTPases (Iguchi et al., 2009). Similarly a reduction of TDP-43 by si-RNA in primary differentiated cortical neurons also induced abnormal neurite morphology and decreased

cell survival (Han et al., 2013). Knockdown of TDP-43 in U2OS and HeLa cells causes apoptosis via the CDK6-retinoblastoma pathway (Ayala et al., 2008a). TDP-43 knockdown in Drosophila has been shown to result in early lethality or reduced lifespan, locomotor defects, reduced dendritic branching and malformed neuromuscular junctions (Feiguin et al., 2009; Fiesel et al., 2010). In zebrafish the overexpression of human TDP-43 and knockdown of zebrafish TDP-43 resulted in impaired motor activity, short motor axons and excessive branching suggesting that either up or down regulation can result in motor deficits (Kabashi et al., 2010). Taken together, these data suggest that the loss of TDP-43 function can potentially be toxic and may be an important pathogenic mechanism contributing to neurodegeneration.

1.4.2.5   TDP-43 aggregation and insolubility

Currently it is still unclear if TDP-43 aggregation and insolubility is toxic, an inert by-product of disease, or a protective event in the pathology of ALS and FTLD-TDP. Due to the strong correlation with other pathogenic events such as ubiquitination, phosphorylation, truncation, nuclear clearance and mislocalisation, the aggregation process can go hand in hand with these processes. As such, it makes it even more difficult to ascertain the toxic potential of TDP-43 aggregation.

The aggregation of TDP-43 has been characterised by pathological and experimental observation. Early on in the aggregation process TDP-43 can form pre-inclusions which appear as either diffuse granular, or wispy and straight filamentous cytoplasmic inclusions with the nuclear clearance of TDP-43 (Dickson et al., 2007; Giordana et al., 2010; Mori et al., 2008). In ALS, mature aggregates in the affected lower motor neurons form as large dense round inclusions, dot inclusions or filamentous skein-like inclusions. However in FTLD-TDP they form a variety of morphologically diverse intranuclear, cytoplasmic or neuritic inclusions in the forebrain neurons. These TDP-43 inclusions in FTLD-TDP have been classified into different subtypes (A-D) dependent upon the type of inclusions present in these cases (Mackenzie et al., 2006, 2011; Sampathu et al., 2006). Type A TDP-43 pathology is characterised by numerous short dystrophic neurites with crescent like or oval cytoplasmic inclusions, which is consistent with FTLD with a GRN mutation. Type B has

moderate numbers of cytoplasmic inclusions with very few dystrophic neurites throughout all the layers of the cortex. Type C has very few cytoplasmic inclusions and predominantly long dystrophic neurites in the upper cortical layers. Type D pathology has numerous short dystrophic neurites with frequent lentiform intranuclear inclusions, which is associated with Inclusion body myopathy with Pagets disease and FTD (IBMPFTD) with mutations in the VCP gene (Mackenzie et al., 2006; Thorpe and Cairns, 2009). Preliminary studies on patients with IBMPFD demonstrated UBIs of TDP-43 in muscle cytoplasm which also includes sporadic Inclusion body myositis (sIBM) (Weihl et al., 2008). However, another study revealed that TDP-43 pathology was not detected in the muscle of sporadic ALS patients (Sorarú et al., 2010), suggesting that TDP-43 pathology in the muscle may be restricted to patients with VCP mutations causing IBMPFD and patients with sIBM.

As well as being deposited in a majority of sALS cases, TDP-43 pathology can also occur in ALS patients with a TARDBP mutation (mostly ALS patients and very rare in FTLD patients) (Kabashi et al., 2008; Sreedharan et al., 2008). It can also occur in patients with a GRN mutation (Baker et al., 2006) and patients with a C9ORF72 mutation (DeJesus-Hernandez et al., 2011; Renton et al., 2011). In C9ORF72 patients the pathology occurs as an overlap between type A and type B pathology (Murray et al., 2011). This morphological diversity of inclusions is still not yet understood but may be of potential pathological importance. Recent biochemical evidence suggest that FTLD-TDP cases contain a unique 43kDa aggregated species which is only present at low levels in controls, suggesting that further aggregated species of TDP-43 may still yet go undetected (Bosque et al., 2013)

TDP-43 is an inherently aggregation prone protein in vitro (Johnson et al., 2009) and has been shown to form similar ultrastructural aggregates in cell culture as seen in ALS and FTLD-TDP inclusions (Igaz et al., 2009; Nonaka et al., 2009a, 2009b, 2013; Winton et al., 2008a). However, full length TDP-43 overexpression does not readily lead to TDP-43 aggregation, whereas expression of the CTFs or deletion/mutation of the NLS motif can readily form aggregates in cell culture (Che et al., 2011; Igaz et al., 2009; Nonaka et al., 2009a, 2009b; Wang et al., 2013; Zhang et al., 2009). Recent evidence highlights the importance of molecular chaperone binding and availability for the aggregation of TDP-43

which can be induced by the heat shock response (Udan-johns et al., 2013). Additionally, cysteine oxidation of the RRM1 domain has been demonstrated to induce conformational change leading to the loss of DNA binding function and aggregation of TDP-43 (Chang et al. 2013). Indeed, the transduction of recombinant TDP-43 fibrils into overexpressing TDP-43 cells causes the formation of inclusions reminiscent of a seeding reaction (Furukawa et al., 2011). Various predictive algorithms have delineated a prion-like domain in the C terminal, suggesting that this region is highly involved in TDP-43 aggregation (Couthouis et al., 2011). In vitro evidence now highlights the essential core aggregation sequences of TDP-43 in this C-terminal prion-like domain (Saini and Chauhan, 2011). Subsequently, experiments introducing Q/N repeat expansions in the 331-339 region of TDP-43 in neuronal and non-neuronal cells have been found to induce TDP-43 aggregation, ubiquitination and phosphorylation (Budini et al., 2012), indicating the importance of this region in the formation of TDP-43 pathology. A more recent study locates an amyloidogenic core on the C-terminal region of TDP-43 which undertakes a structural shift from the α-helix to the β-sheet to initiate the aggregation process (Jiang et al., 2013). This data is in support of numerous structural and behavioural studies confirming the prion-like nature of TDP-43, which will be discussed in more detail later.

Biochemical detection of TDP-43 insolubility involves the use of the sarkosyl detergent to reveal various sarkosyl resistant species of TDP-43. Normal TDP-43 is also sarkosyl insoluble but the phosphorylated 45kDa, 20-25kDa CTFs and high molecular weight ubiquitinated forms are specifically resistant in ALS and FTLD-TDP (Neumann et al. 2006). It appears that an early appearance of TDP-43 inclusions could make neurons more susceptible to neurodegeneration, as patients with sALS with an unusually long disease duration periods (10-20 years) had fewer inclusions compared to the average sALS patient (Nishihira et al., 2009). As TDP-43 aggregation in the anterior horn of the spinal cord is found in the centre of all neuronophagic cell clusters, it would indicate that TDP-43 aggregation is closely linked to neurodegeneration and does not protect motor neurons (Pamphlett and Kum, 2008). Unfortunately this still does not indicate the toxicity of these aggregates in the disease process, and they may well be a response to injury or part of a

toxic process. Indeed, a recent publication suggests that a reduction of TDP-43 aggregation using specific peptides in mutant or arsenite induced TDP-43 aggregation in HeLa cells does not prevent cytotoxicity (Liu et al. 2013). However, the major pitfall of this study is the use of HeLa cells rather than neurons which may be less susceptible to TDP-43 mediated toxicity.

Cellular studies indicate that cytoplasmic accumulation and aggregation of TDP-43 can be rescued by TGF-β stimulation (Nakamura et al., 2012), Methylene blue and Dimebon (Yamashita et al., 2009), maintenance of the cognate single stranded DNA and RNA capacity (Huang et al. 2013), and by modulation of specific neuronal kinase activity such as ERK phosphorylation, CDK6 and GSK3 (Moujalled et al., 2013; Parker et al., 2012). Recently, a *C.elegans* model which expressed WT and mutant TDP-43 and FUS in the GABAergic motor neurons developed an age dependent loss of motility, paralysis and motor neuron degeneration associated with an increase in insoluble TDP-43 and FUS. This indicates that increasing insolubility may be correlated with neurotoxicity (Vaccaro et al., 2012a). The same group subsequently demonstrated that the TDP-43 aggregation inhibitor Methylene blue could suppress this neurotoxicity in zebrafish and *C.elegans* expressing mutant TDP-43, again, suggesting that inhibition of aggregation has a potential therapeutic use and that the aggregation of TDP-43 is highly involved in TDP-43 induced neurotoxicity (Vaccaro et al., 2012b).

TDP-43 inclusions in transgenic mice overexpressing the full length human TDP-43 only show rare TDP-43 positive inclusions and the number of inclusions do not correlate with neurodegeneration (Igaz et al., 2011; Shan et al., 2010; Stallings et al., 2010; Wegorzewska et al., 2009; Wils et al., 2010; Xu et al., 2010). This suggests that TDP-43 inclusions are not necessary for TDP-43 mediated neurodegeneration in vivo, but still leaves open the question of whether they are sufficient to induce neural cell death. Some studies suggest that TDP-43 aggregation may cause pathological alteration of metabolic pathways due to the formation of mitochondrial Gemini coiled bodies in some transgenic mice (Shan et al., 2010), and dependence on mitochondria and oxidative stress for TDP-43 toxicity in yeast (Braun et al., 2011). However, this has not been detected in human ALS cases so the

relevance of this is unclear. Studies do suggest that TDP-43 aggregates may be capable of inducing neuronal death, but other studies also indicate that aggregation is not a pre-requisite for this toxicity.

So far it has not been demonstrated how the aggregation of TDP-43 affects a living neuron, as in most studies the other post translational modifications such as phosphorylation, ubiquitination and truncation also appear alongside aggregation, therefore making it difficult to dissect out the toxic capacity of each modification.

1.4.2.6 TDP-43 truncation

Evidence suggests that there are a number of different truncated isoforms of TDP-43 present in ubiquitinated inclusions. In pathological circumstances, TDP-43 is often cleaved into 20-25kDa forms detected in sarkosyl insoluble brain fractions from ALS/FTLD patients (Neuman et al. 2006; T. Arai et al. 2006). There is a large variation in the number of CTFs in different cases of ALS and FTLD-TDP. Indeed, large numbers of C-terminal fragments have been found in the hippocampus and cortex in FTLD-U and ALS cases where as the full length form is mainly present in motor neuron lesions in the spinal cord of ALS patients. This suggests that cleavage of TDP-43 subsequently leads to the deposition of truncation products which may be toxic and form in specific CNS regions (Igaz et al., 2008). Also this regional specificity suggests that this cleavage may not be essential for toxicity. Lymphoblastoid cell lines from ALS patients with TDP-43 mutations are capable of forming a ~35kDa fragment (Kabashi et al., 2008; Rutherford et al., 2008) which have also been detected in sarkosyl enriched human brain or spinal cord extracts (Neumann et al., 2006; Zhang et al., 2007). These 35 and 25 kDa fragments could potentially be due to proteolytic cleavage, alternative splice variants or in-frame translation sites downstream from the TARDBP natural initiation codon (Nishimoto et al., 2010). It is clear that there are many C-terminal fragments present in FTLD cases (Igaz et al., 2009; Nonaka et al., 2009b). Due to the heterogeneity and pathological overlap between ALS and FTLD-TDP, it is plausible to suggest that there may be many pathological fragments generated in both. Identifying these fragments and products may generate new insight into the pathological mechanics of TDP-43.

Caspase 3 is an enzyme involved in apoptosis and has shown to be activated in ALS and FTLD (Martin, 1999; Su et al., 2000). Indeed, caspase 3 was subsequently shown to cleave TDP-43 and is responsible for a majority of the TDP-43 cleaved fragments demonstrated in cell culture (Nishimoto et al. 2010; Dormann et al. 2009; Zhang et al. 2009; Zhang et al. 2007). TDP-43 has been shown to have 3 putative caspase cleavage sites which produce fragments of ~42, 35 and 25 kDa by incubation with caspase 3 and 7. This cleavage may account for at least three varieties of C- terminal fragments detected in TDP-43 proteinopathies (Zhang et al., 2007). Protein kinase inhibition with staurosporine was found to reduce the nuclear TDP-43 and increase the production of insoluble 35 and 25 KDa fragments in cell culture (Dormann et al. 2009). More recent studies have shown how the 35kDa form, compared to the full length and 25kDa form, is more likely to be responsible for aggregate formation and defects in regulating pre-mRNA and alternative splicing (Che et al., 2011). This could indicate that other regions other than the C-terminal may play a role in the formation of TDP-43 aggregates.

Various cell models with TDP-43 constructs containing a mutated NLS, or expressing C-terminal fragments lacking the NLS, causes TDP-43 to aggregate in the cytoplasm (Igaz et al., 2009; Johnson et al., 2008; Nonaka et al., 2009b; Winton et al., 2008a; Zhang et al., 2009). In turn, these aggregates may sequester full length TDP-43 and deplete the nucleus of TDP-43, the ability of which may be determined by the types of TDP-43 present in the aggregates (Igaz et al., 2009; Winton et al., 2008a). This suggests that mechanistically, TDP-43 may be cleaved to a C-terminal fragment that lacks an NLS during its shuttling between the nucleus and cytoplasm. This could result in an inability of the protein to regain access to the nucleus and cause subsequent aggregation. However, one study associated these aggregates with cytotoxicity which did not markedly alter the endogenous full length TDP-43, or TDP-43 nuclear function (Zhang et al., 2009). This suggests a toxic gain in function of the aggregates independent of the effects on endogenous TDP-43 and its nuclear function. However, human ALS and FTLD-U cases predominantly show a loss of neuronal nuclear TDP-43 that is not seen in these cell models, indicating that these cell models may not accurately represent the human disease state. Further, addition of pathogenic TDP-43 mutations in these CTF

expressing cells further increased the aggregation propensity of TDP-43 (Arai et al., 2010), which suggests that combining truncation and mutation of the protein can rapidly reproduce TDP-43 pathology. Similarly, the de novo intranuclear truncation of TDP-43 led to the production of CTFs which were translocated to the cytoplasm and rapidly degraded. As with the addition of a mutation, this system required a 'second hit' (such as the introduction of misfolded CTFs) to promote further aggregation (Pesiridis et al., 2011). Interestingly, the compounds methylene blue and dimebon were subsequently shown to reduce the amount of aggregation in these C-terminal induced aggregation models (Yamashita et al., 2009) suggesting that TDP-43 aggregation may be manipulated as a potential therapy.

Caspase cleaved fragment constructs expressed in HEK293 cells developed C-terminal fragments at 35kDa and 25kDa. These fragments are present in the both the cytoplasm and the nucleus whereas the full length TDP-43 is localised in the nucleus (Zhang et al., 2009). Despite the lack of biological activity of the 25kDa fragment, it was found to be cytotoxic in cell culture, potentially via a gain of function as it's exogenous expression was not detrimental to its normal splicing function or ability to sequester full length TDP-43 (Zhang et al., 2009). However, the overexpression of CTFs identified in FTLD-U brains were able to form ubiquitinated, phosphorylated TDP-43 aggregates and altered the CFTR exon 9 splicing activity, indicating a potential loss of TDP-43 function mechanism. Despite the clear ability of some C-terminal fragments to sequester endogenous nuclear TDP-43, the cleavage of TDP-43 is most likely to result in loss of its functional domains (Buratti and Baralle, 2001). In addition to sequestering nuclear TDP-43, the C-terminal fragments have also thought to interact with hnRNP A/B proteins as they shuttle between the nucleus and the cytoplasm decreasing the availability and equilibrium of hnRNP proteins. However, even though CTFs have been shown to bind to hnRNPA2 (Zhang et al., 2009), the other hnRNP A1, A2/B1, and C1/C2 have not been found in FTLD TDP-43 positive inclusions (Neumann et al., 2007a).

It has been suggested that these CTFs can act in a dominant negative mechanism, as they inhibit neurite outgrowth in the development of differentiated primary rat neurons, which can be rescued with full length TDP-43 (Yang et al., 2010). In contrast to this, the expression of CTFs in Drosophila models did not produce neurotoxicity in comparison to the

expression of the full length wild type TDP-43, which was toxic to a variety of cell types (Li et al. 2010). However, another more recent study demonstrates that either the full length or the aggregated 25kDa TDP-43 fragment is toxic when expressed in Drosophila. This toxicity can be ameliorated partially by inhibition of the full length TDP-43 aggregation, and completely abolished upon inhibition of aggregation of the 25kDa fragment (Gregory et al., 2012). This suggests that the 25kDa fragment is highly involved in TDP-43 mediated neurodegeneration. Importantly, in their experiments this toxicity in Drosophila and chick motor neurons required the TDP-43 RNA binding capacity (Voigt et al., 2010). When natively folded, the C-terminus is thought to act as a potential guardian of pathogenesis by inhibiting cleavage and maintaining its CFTR exon 9 skipping activity and subcellular localisation. Indeed, the self-interaction of the C-terminal appears to inhibit the degradation of the TDP-43 aggregates and leads to loss of function toxicity (Wang et al. 2012). A removal of the N-terminal by truncation of the protein may decrease its oligomerisation properties and reduce the DNA binding affinity of the protein (Chang et al., 2012), but the relevance this has for toxicity is unclear. Interestingly, the N-terminal has been shown to be essential for the aggregation of the full length TDP-43, suggesting that a removal of the N-terminus may not produce an accurate aggregate representation of disease associated TDP-43 (Zhang et al., 2013)(Figure 4). Together, this data indicates that the site of cleavage and remaining functional domains of the protein are essential for the degree of TDP-43 mediated neurotoxicity.

Several rodent models of TDP-43 proteinopathy have detected the development of TDP-43 CTFs (Medina et al., 2013; Stallings et al., 2010; Tsai et al., 2010; Wegorzewska et al., 2009; Wils et al., 2010; Xu et al., 2010). Indeed, the development of these CTFs can form before the onset of motor deficits and toxicity, and were found to increase in correlation with disease progression (Wegorzewska et al., 2009). Other groups also report the correlation of CTFs with disease progression and neurodegeneration (Stallings et al., 2010; Wils et al., 2010). However, compared to human brains, the mice brains have higher levels of the 35kDa fragment (Stallings et al., 2010; Wegorzewska et al., 2009; Wils et al., 2010), more soluble fragments (Tsai et al., 2010; Wegorzewska et al., 2009; Wils et al., 2010; Xu et

al., 2010) and the fragments are contained mostly in the nuclear fraction rather than the cytoplasmic fraction (Wils et al., 2010). Some of the TDP-43 transgenic mice do not develop TDP-43 CTFs but do develop motor degenerative phenotypes indicating that the development of CTFs may not be essential for TDP-43 mediated toxicity in mice (Igaz et al., 2011; Janssens et al., 2013; Shan et al., 2010). In accordance with this, the non-human primate TDP-43 overexpression model demonstrated that truncation of TDP-43 was not a pre-requisite for motor neuron degeneration (Uchida et al., 2012). Expression of the TDP-25 fragment in the brain and spinal cord of rats induced a non-lethal disease phenotype with motor deficits and a prominent forelimb impairment which was comparable to the expression of the mutated TDP-NLS. This suggests that in accordance with previous data, the TDP-25 fragment plays a significant role in disease pathogenesis (Dayton et al., 2013). More recently, In utero electroporation of TDP-43 CTFs (wild type and mutant M337V) into the brains of embryonic mice produced ubiquitinated and phosphorylated TDP-43 cytoplasmic inclusions with diffuse distribution of TDP-43 in the nucleus and cytoplasm (Akamatsu et al., 2013). These findings again suggest that these fragments are highly relevant for the development of TDP-43 pathology in vivo. The development of these CTFs have also shown to lead to synaptic loss and cognitive deficits as well as typical motor deficits (Medina et al., 2013).

Taken together, this data clearly demonstrates a significant role for the truncation of TDP-43 in the development of the disease process and formation of TDP-43 pathology. However, due to conflicting results, it is still not clear exactly if these CTFs are toxic and if so what the exact toxic mechanisms of these fragments are.

1.4.2.7   *TDP-43 RNA mediated toxicity*

As discussed previously, TDP-43 may be contributing to toxicity via loss or gain of function. In the case of RNA binding, either a loss of RNA binding function or a toxic gain of RNA function via abnormal RNA interactions may mediate this process. Alternatively, both of these mechanisms may be involved in TDP-43 mediated toxicity simultaneously. TDP-43 is known to be a member of the hnRNP protein family which are proteins prominently involved in RNA binding. As such, a number of groups have attempted to find the RNA

targets of TDP-43 in cell culture, mouse brain, human brain and from ALS and FTLD-TDP patients (Polymenidou et al., 2011; Sephton et al., 2010b; Tollervey et al., 2011; Xiao et al., 2011). These results revealed a very large and diverse number of RNA targets (>6000 mRNAs) with important functions in the brain. This large number of RNA targets makes it difficult to identify the key RNA targets altered by pathological TDP-43 in ALS and FTLD-TDP, but do strongly suggest that altered TDP-43 RNA metabolism could have a significant role in the pathogenesis of these conditions. Interestingly, TDP-43 was found to bind to many RNA's at the 3'UTRs which is subsequently linked to crucial neuronal integrity processes such as RNA stability or local translation transport (Dahm et al., 2007; Kindler et al., 2005). TDP-43 has also been found located in RNA granules which are translocated to dendritic spines upon numerous different neuronal stimuli (Wang et al., 2008). Additionally, a loss of TDP-43 can reduce synapse formation and dendritic branching in Drosophila neurons (Feiguin et al., 2009; Lu et al., 2009). The 3'UTR binding capacity of TDP-43 in neurons suggests that pathological TDP-43 can alter neuronal plasticity by modulating mRNA transport and local translation through loss of or abnormal binding to 3'UTRs of specific mRNAs in neurons. Indeed, TDP-43 has been found to bind the 3'UTR of certain ALS related genes such as FUS, light chain of neurofilament (NFL) and the glutamate transporter EAAT2 (Polymenidou et al., 2011). Depletion of TDP-43 in mice led to the alteration of 601 mRNA levels and 965 altered splicing events. Upon TDP-43 depletion, many of the down regulated genes contained numerous TDP-43 binding sites and exceptionally long introns enriched in the brain. This is indicative of a highly significant involvement of TDP-43, particularly in RNA metabolism which more severely affects neurons (Polymenidou et al., 2011). TDP-43 also interacts with and regulates long non coding RNAs (ncRNAs) such as MALAT1 and NEAT1 (Polymenidou et al., 2011; Tollervey et al., 2011). In addition, NEAT1 levels were found to be significantly increased in brains with FTLD-TDP pathology (Tollervey et al., 2011). The RNA binding behaviour on small non coding RNAs (sncRNAs) and micro-RNAs (miRNAs) however is still uncertain.

As discussed previously, TDP-43 is involved in miRNA biogenesis and maturation through association with proteins such as Drosha (Gregory et al., 2004), argonaute-2 and DDX-17

(Freibaum et al., 2009). The miRNAs let-7b and miR-663 have been shown to bind to TDP-43 and are up and down regulated respectively upon TDP-43 depletion in cell culture (Buratti et al., 2010). MicroRNAs are involved in pre and post transcriptional regulation of gene expression and often work to reduce transcription of non-essential genes during cellular stress. Therefore alteration of these miRNAs could lead to altered gene expression which could produce adverse effects leading to cell death. Evidence now suggests that TDP-43, along with FUS and SOD1, helps to maintain the spliceosome machinery (Tsuiji et al., 2012), which if defective, could lead to altered RNA metabolism and toxicity. Further studies in Drosophila indicate that RNA binding is crucial for TDP-43 mediated toxicity as toxicity is dependent on the RNA binding domain (Ihara et al., 2013). Recent evidence also demonstrates that inhibition of the RNA lariat debranching enzyme can suppress TDP-43 induced toxicity in yeast and primary neurons (Armakola et al., 2012), further supporting the fact that TDP-43-RNA interactions can be responsible for TDP-43 mediated toxicity.

Ultimately these deficits in RNA metabolism associated with TDP-43 dysfunction could also arise due to a significant alteration of the structure of the TDP-43 protein through misfolding. We therefore speculate that either gain or loss of function of TDP-43 could both be explained by the misfolding of the protein.

1.4.2.8   Prion-like mechanisms in TDP-43 pathology

Behavioural similarities between the prion protein and TDP-43 were demonstrated in a recent study where synthetic TDP-43 C-terminal fragments flanking the 315 residue were able to produce detergent and heat resistant high molecular weight aberrant TDP-43 species, and partially protease resistant low molecular weight species in primary neurons. These low molecular weight species were able to form β-sheeted amyloid fibrils that produced subsequent neural toxicity in primary neurons (Guo et al. 2011). However, in pathological studies TDP-43 is found in non-amyloid forms (Kwong et al., 2008; Neumann et al., 2007b), but TDP-43 positive skein-like inclusions with amyloid characteristics have now been demonstrated in a subset of ALS spinal cord samples (Robinson et al., 2012). A more stringent pre-treatment of CNS tissue from ALS and FTLD-U patients increased the frequency and strength of detection of amyloid TDP-43 positive inclusions (Bigio et al.,

2013). Misfolded TDP-43 has also been detected with a specific misfolded TDP-43 antibody in spinal cord inclusions of patients with ALS. This antibody recognised only cytoplasmic mislocalised TDP-43 in cell culture and not nuclear or wild type TDP-43 (Shodai et al., 2012). The same group showed that this misfolding of TDP-43 may be mediated via cysteine modulation of the RRM1 domain which may be the key region for pathogenic conversion and misfolding of TDP-43 (Shodai et al., 2013).

The prion-like behaviour of TDP-43 was identified by the detection of a prion related Q/N rich domain in the C-terminal of the protein. Indeed, this was noted when polyglutamine proteins in yeast culture were used to induce the localisation of TDP-43 into insoluble inclusions. This process required a Q/N rich stretch of residues which incorporated the Q/N domain with the β-fibrillar structure of the polyglutamine inclusion (Fuentealba et al., 2010). In addition to this we know that the C-terminal region of TDP-43 is highly prone to self-association and aggregation in cell culture (Budini et al., 2012; Igaz et al., 2009; Johnson et al., 2008; Zhang et al., 2009), and this is highly characteristic of prion related Q/N domain containing proteins. Last of all, bioinformatics studies using protein structure prediction algorithms have predicted prion related domain containing proteins, in yeast and human genomes (Alberti et al., 2009; Harrison and Gerstein, 2003; Michelitsch and Weissman, 2000). In the human genome TDP-43 and FUS proteins were identified as the 69th and 15th most likely to contain a prion related domain out of 27,879 proteins (Alberti et al., 2009). The prion domain predicted is analogous to the Sup35 yeast prion domain, which can change from a natively unfolded to an aggregated structure capable of inducing its conformation to the native form (Cushman et al., 2010; Fuentealba et al., 2010). This prion-like domain in TDP-43 is thought to be located from residues 274-414 in the C-terminal (Cushman et al., 2010), and potentially capable of inducing an aberrant conformation on to native TDP-43 isoforms and form a seeding reaction.

1.4.2.8.1 TDP-43 seeding

Recently Furukawa et al demonstrated the seeding capacity of recombinant wild type and mutant sarkosyl insoluble TDP-43 aggregates into HEK293 cells. These aggregates were shown to seed the fibrillisation of TDP-43 and contain protease resistant cores of CTFs within full length TDP-43 aggregates (Furukawa et al., 2011). The most convincing evidence for the prion-like behaviour of TDP-43 comes from Nonaka and colleagues. This group were able to transfect human ALS TDP-43 pathological brain extracts in to cells with and without overexpressing a full length wild type TDP-43 construct. These cells subsequently formed ubiquitinated, phosphorylated insoluble TDP-43 inclusions in the cytoplasm of cells. Indeed, this induced TDP-43 pathology was specific to TDP-43 and accumulated over time, which is a strong indication of a TDP-43 seeding reaction. Further still, they were able to show that the TDP-43 aggregates present in these cells were protease and heat resistant, and that the seeding reaction could be stopped by digesting the samples in formic acid indicating that TDP-43 seeds consist of β-sheeted fibrils. They also demonstrated that these inclusions could propagate between cells, and serial propagation from cells could seed this reaction further. Increased cellular toxicity and impairment of the proteasome was also reported to correlate with the presence of TDP-43 pathology, indicating this is a highly disease relevant model of TDP-43 proteinopathy (Nonaka et al., 2013). Not only does this model provide the most substantial evidence for the prion-like activity of pathological TDP-43, but it also suggests this could be the most accurate ALS in vitro model yet for further therapeutic drug screening.

Therefore we postulate a proposed pathological TDP-43 seeding process which is as follows: TDP-43 becomes pathologically misfolded from a mutation or post translational modification. This could happen either in the nucleus or after the cytoplasmic mislocalisation of TDP-43. This misfolding of TDP-43 is thought to occur in the C-terminal domain where most of the pathological mutations reside, where the prion-like domain is located and where the protein-protein interactions occur (Figure 4). The misfolding of TDP-43 about the C-terminal could recruit the normal endogenous TDP-43 monomers and induce a pathological misfolding event on the endogenous form. This could then nucleate a

pathological seeding reaction and the formation of aggregates with β-sheeted amyloid structure, these aggregates can then break apart at the ends and release monomers or oligomers of misfolded TDP-43, which could then be released into the neighbouring environment. Once this occurs the nearby cells can take up these seeds through various mechanisms and this seeding reaction can continue in the next cell (Figure 6). This model could not only account for the formation of TDP-43 aggregates but also has implications for the pathological spreading of the condition.

The implications this seeding ability has for the normal function TDP-43 however, are still unknown. The C-terminal domain of TDP-43 is also known for its ability to form protein to protein interactions with various mRNA splicing components (D'Ambrogio et al., 2009). It is therefore plausible that an abnormal folding variant of this C-terminal Q/N rich domain may interrupt the normal TDP-43 mRNA splicing component interaction. Evidence supporting this comes from a recent study of heat shock induced aggregation of TDP-43 which decreased the binding of hnRNPA1, suggesting that the misfolding of TDP-43 leads to a loss of protein binding function (Udan-johns et al., 2013). Alternatively, as these cytoplasmic ubiquitinated TDP-43 inclusions are seen in some controls or other neurodegenerative disorders, the aggregates formed may well not be toxic or protective, but a response to cellular stress which could be mediated by this prion related domain.

The C-terminal region turns out to be the key pathogenic area for study in TDP-43, as not only is this the site of a putative prion domain, but nearly all mutations and pathological phosphorylation of TDP-43 occur within this C-terminal (Hasegawa et al., 2008). In addition, recent proteomic studies have shown this region to be capable of forming β-sheets which is in turn increased by the A315T mutation (Guo et al 2011a). These β-sheets are thought to form the amyloid fibrils that start the seeding reaction, and more recent in vitro evidence demonstrates an amyloidogenic core that undergoes a structural change to initiate this aggregation (Jiang et al., 2013). Additionally, TDP-43 aggregation models have been made by introducing 331-339 Q/N repeat expansions in the prion-like domain of the C-terminal region to induce aggregation, phosphorylation and ubiquitination (Budini et al., 2012). The aggregation propensity of TDP-43 may be dependent on the region of the C-terminal

altered, as the core aggregation sequences are in specific locations of the C-terminus (Saini and Chauhan, 2011). Using a number of recombinant TDP-43 CTF peptides of the core aggregation sequence, one group were able to induce the formation of TDP-43 positive amyloid fibrils and seeding reactions in vitro and cell culture. However, truncation beyond residues 317 were not able to induce amyloid fibrils and formed amorphous aggregates (Liu et al. 2013). Therefore residue specific post translational modifications to this region may be the pathogenic event leading to a pathological TDP-43 amyloid formation and templated seeding reaction. This seeding reaction may be further enhanced by the autoregulation region of TDP-43 which could in turn enhance further protein synthesis and recruitment of TDP-43 monomers to the aggregates (Budini and Buratti, 2011; Buratti and Baralle, 2011). Evidence to support this demonstrates that the C-terminal of TDP-43 physically interacts with itself and the yeast prion domain Sup35 to form pathological aggregates. Indeed, mutants of this prion-like domain inhibit its self-interaction and subsequently form ~24 kDa CTFs which lead to a loss of CFTR exon 9 skipping function and mislocalisation. This suggests that alteration of this prion-like domain either by mutation or misfolding can cause a loss of TDP-43 function (Wang et al. 2012). Additionally, the CTFs of TDP-43 that form amyloid fibrils, are more aggregation prone than the full length protein, and potentially more toxic in cell culture (Chen et al., 2010; Igaz et al., 2009; Jiang et al., 2013; Johnson et al., 2009; Yang et al., 2010).

1.4.2.8.2   TDP-43 propagation

Unlike the evidence for the propagation of prions (Beekes and McBride, 2007), and of many other prion-like neurodegenerative disease related proteins (Guo and Lee, 2014; Hallbeck et al., 2013), there is only one cellular study demonstrating the propagation of TDP-43 pathology (Nonaka et al., 2013). However, a recent pathological staging study using the phosphorylated TDP-43 (pTDP-43) pathology demonstrates that TDP-43 pathology does appear to be spreading in a four stage process starting from the agranular frontal neocortex and somatomotor neurons of the spinal cord and lower brain stem, and eventually spreading to the medial temporal lobe and hippocampus by stage four (Brettschneider et al., 2013). Indeed, this staging of pTDP-43 pathology bears remarkable resemblances to the

four stage model of neuronal degeneration proposed by Ravits and La Spada (Ravits and La Spada, 2009). However, the staging of pTDP-43 observed here did not correlate with any clinical features of ALS including site of onset, age of onset, disease duration or the ALS functional rating score – revised (ALSFRS-R). Therefore the differential deposition of pTDP-43 in these cases cannot be correlated with different disease stages. Nevertheless, from this data the same group go on to speculate that the pTDP-43 pathology could be propagating transynaptically via corticofugal axonal projections using anterograde axonal transport (Braak et al., 2013). Indeed, the spread of other neurodegenerative disease associated proteins such as tau (Ahmed et al., 2014; de Calignon et al., 2012; Kfoury et al., 2012; Liu et al., 2012; Mohamed et al., 2013) and α-synuclein (Bétemps et al., 2014; Danzer et al., 2009; Desplats et al., 2009; Li et al., 2008; Ulusoy et al., 2013), are also thought to propagate transynaptically via axonal pathways.

The cellular mechanisms for pathological protein spread includes the method of the protein seed release from the cell, transport to the neighbouring cells, and uptake and release of the seed within the cell. Prions are thought to propagate via exosomes (Fevrier et al., 2004) and tunnelling nanotubes (Gousset et al., 2009). The exact mechanism for TDP-43 propagation is still not known, but Nonaka et al have demonstrated that this happens partially via exosomes (Nonaka et al., 2013). Exosome mediated transfer to the recipient cell usually occurs by direct fusion of the exosome with the plasma membrane to release the seed. Once the seed is inside the recipient cell it is thought that it nucleates the seeding of the soluble endogenous protein in a self-perpetuating aggregate formation (Guo and Lee, 2014). However, this may not be the only mechanism of TDP-43 propagation and it may also propagate via the release of 'naked' seeds or nanotubule transmission. Indeed, free floating seeds may be broken off from aggregates and released into the cellular environment by cell death or other transport mechanisms from the initial cell. These could then enter the recipient cell either by direct penetration of the plasma membrane, fluid phase endocytosis, or receptor mediated endocytosis. Uptake could also occur via various other protein dependent uptake mechanisms such as clathrin, calveolin and dynamin mediated endocytosis. Indeed, SOD1 has recently been shown to propagate and taken up by lipid raft

macropinocytosis (Münch et al., 2011a). More recently, this misfolded human SOD1 was found to be propagated via two mechanisms: release of protein aggregates from cells which are taken up by endocytosis, and exosomes secreted from the cells (Grad et al., 2014). Therefore the investigation of the exact mechanisms of this propagation will provide essential clues to target these propagation mechanisms in an attempt to arrest TDP-43 propagation.

1.4.2.8.3 TDP-43 strains

As with prion strain typing, the presence of a wide variety of different clinical ALS phenotypes could suggest that different conformations or 'strains' of misfolded TDP-43 may be responsible. Indeed, other neurodegenerative disease related proteins are now also revealing characteristic strains including α-synuclein (Bousset et al., 2013; Guo et al., 2013) and Aβ (Heilbronner et al., 2013). Different regional mutations or post translational modifications may cause variations in TDP-43 folding; this in turn could expose different hydrophobic residues and lead to varying misfolded conformers and pathogenic templates. These various pathogenic templates may have varying neural cellular or regional tropisms. In addition, they could form differential strengths of monomer recruitment for a seeding reaction, and possess varying levels of toxicity. There is a wide variation in site of onset in the spinal cord in patients with ALS, where autopsy studies have demonstrated that degeneration diminishes in a gradient like fashion from the site of onset. Theoretically, the site of onset may indicate the production of a unique folding variant of TDP-43 which specifically affects these regions. For example, when ALS is clinically limited to lower motor neurons in progressive muscular atrophy (PMA) it is a diffuse TDP-43 proteinopathy (Geser et al., 2011), therefore this folding variant of TDP-43 may have widespread deposition and cause LMN specific neurotoxicity. Alternatively, different folding variants may also produce specific UMN phenotypes such as PLS or bulbar or limb predominant phenotypes (Figure 7).

Evidence to support varying structural conformations or 'strains' of pathological TDP-43 came from Hasegawa and colleagues, as they demonstrated that sarkosyl insoluble TDP-43 from cortex and spinal cord of sALS patients produced distinct phosphorylated TDP-43 16-26kDa fragments with trypsin and chymotrypsin digestion (Hasegawa et al., 2011).

Moreover, the same group were able to demonstrate that the 203-209 residues form these protease resistant TDP-43 fragment (Tsuji et al. 2011). These patterns were the same between brain and spinal cord suggesting that the same modification most likely occurred in different regions simultaneously. The distinct banding patterns were specific for different TDP-43 proteinopathy subtypes A-D, suggesting that different conformational changes to the misfolded TDP-43 causes different patterns of pathology and disease phenotypes. The unique banding patterns formed here suggest that different conformations or 'strains' of TDP-43 could exist (Tsuji et al., 2012). However, this was only demonstrated in TDP-43 proteinopathy subtypes and not within ALS phenotypes. Therefore future investigation into a TDP-43 mediated molecular subtypes as a marker for clinical ALS phenotypes should be investigated, and may well provide interesting insights into ALS phenotype variability.
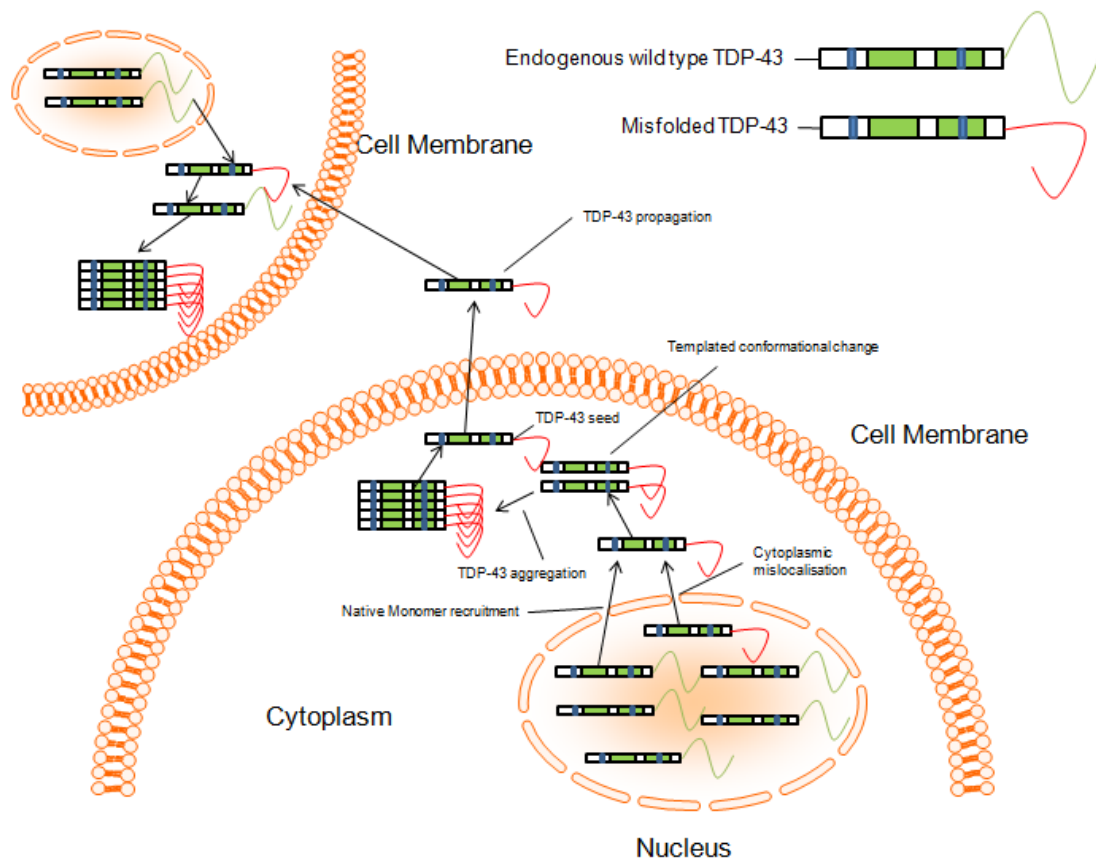
Figure 6. Proposed model of pathological TDP-43 seeding and propagation. Endogenous wild type TDP-43 is present in the nucleus and can either become pathologically misfolded in the nucleus, or be re-localised to the cytoplasm due to mutations or cellular stress (e.g. in stress granules) and then become misfolded. This misfolded conformation then recruits native monomers of TDP-43 to induce pathological misfolding on to the native form in what is known as 'templated conformational change'. This proceeds as a seeded polymerization reaction to form aggregates of TDP-43. This pathology may subsequently propagate in the form of seeds of TDP-43. TDP-43 aggregates may be frangible and can break off the aggregate to be released to the extracellular environment. These seeds can then be taken up by neighbouring cells where the templated conformational change can occur again on the endogenous TDP-43 in that cell. Therefore the reaction could continue in this process and account for the formation and spread of TDP-43 pathology.
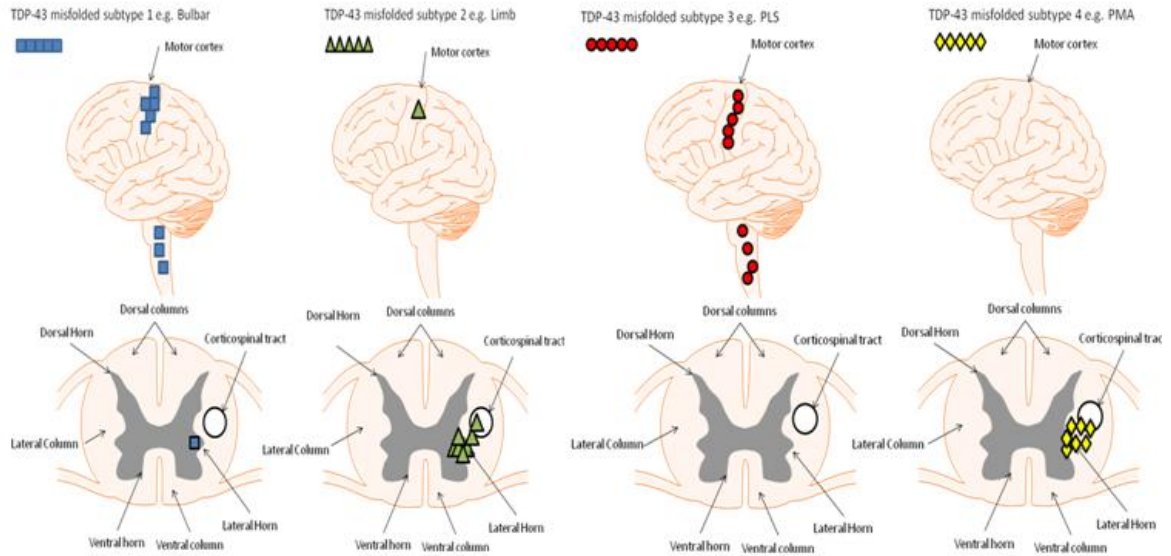
Figure 7. TDP-43 'strains' model of phenotypic variation in ALS and MND. As in prion disease different conformations or strains of the Prp^{Sc} protein could lead to CNS regional tropisms for pathology and varying disease phenotypes. We propose that TDP-43 may also have conformational variants or strains that lead to a diversity of clinical ALS phenotypes. For example, one conformational variant of TDP-43 could have a regional tropism and generate more adverse pathological effects for UMNs in the brain which result in a bulbar (subtype 1) or PLS phenotype (subtype 3). In a similar manner, a different misfolded subtype of TDP-43 may have a tropism for the LMNs in the spinal cord leading to a limb phenotype (subtype 2) or PMA (subtype 4). These regional tropisms may influence the site of onset and subsequent disease duration of each condition. PLS = primary lateral sclerosis, PMA = progressive muscular atrophy.

1.5   Aims of the project

Due to the recent discoveries about the prion-like nature of TDP-43 and its involvement in ALS, this thesis aims to further investigate and expand on some of the prion-like molecular and biochemical characteristics. In order to do this, the project aims to investigate the following:

1. Molecular characterisation of TDP-43 in ALS - The distribution of TDP-43 protein levels, banding ratios and protease resistant fragments in a range of relevant CNS regions of ALS patients compared to controls.

2. Prion-like mechanisms of TDP-43 in vitro – Investigate whether TDP-43 pathology from CNS tissue of sALS patients can form a seeding reaction in vitro. If so investigate whether TDP-43 can propagate between cells and asses what effects mutations inside and outside the prion-like domain have on this seeding reaction.

3. Prion-like mechanisms of TDP-43 in vivo – Investigate whether TDP-43 pathology from sALS patients can be transmitted to wild type mice, and if this can demonstrate any neurodegeneration or ALS like phenotype.

4. Finally, we will take part in a collaboration project that is ongoing at the institute to investigate in vivo protein aggregation using a new imaging method called amide proton transfer (APT). This project will investigate the non-invasive quantification of protein aggregation using the APT signal in SOD1 G93A ALS mouse model.

Chapter 2

Molecular characterisation of TDP-43 in ALS

2. Molecular characterisation of TDP-43 in ALS

2.1. Introduction

Part of the pathological process in ALS and FTLD is the aggregation of TDP-43 and its relocalisation from the nucleus to the cytoplasm. As such this aggregated TDP-43, like many neurodegenerative disease related proteins, becomes insoluble. In 2006, Manuela Neumann and colleagues reported that pathological TDP-43 in patients with ALS and FTLD-U is resistant to the detergent sarkosyl and that this resistance reveals the presence of pathological 25kDa fragments (Neumann et al., 2006). Insolubility of protein to detergents such as sarkosyl are key markers of protein aggregation, and therefore this discovery was an intriguing step forward in the understanding of TDP-43 in ALS and FTLD pathogenesis. One key factor not yet examined, in terms of TDP-43 insolubility, is the levels of this insoluble TDP-43 in different CNS regions in patients with ALS. Previous publications have reported increased levels of the TDP-43 protein in CSF, skin and plasma of patients with ALS and FTLD (Kasai et al., 2009; Noto et al., 2011; Suzuki et al., 2010). However, these studies are aimed at finding a biomarker of disease rather than characterizing the TDP-43 pathology in these patients. Neuropathological studies have also revealed that there is multiple CNS region involvement of TDP-43 pathology in ALS patients compared to controls (Geser et al., 2008). In addition to this the same group compared patients with FTLD, ALS and FTLD, and patients with ALS with cognitive impairment. As a result of this study they found the frequency and morphology of TDP-43 pathology to vary within all these patients and many of the clinical manifestations (e.g. motor neuron signs, extrapyramidal symptoms, cognitive impairments, neuropsychiatric features) were reflective of the presence and burden of TDP-43 pathology (Geser et al., 2009). However, no studies have yet examined the levels of insoluble TDP-43 protein in different CNS regions in neurologically normal controls and patients with ALS. Therefore in this study we investigated whether the levels of insoluble TDP-43 and the different isoforms detected here were altered between controls and ALS patients in different regions of the CNS.

As previously mentioned, ALS has clinically distinct phenotypes of which there is yet no molecular basis for understanding. To further investigate the molecular biochemical basis of ALS phenotypes we also used some of the well-established experimental features of prion phenotype classification including banding ratios and protease resistance. To investigate this we examined whether the ratios of isoforms detected here correlated with any ALS phenotype criteria. We also examined whether TDP-43 has a degree of protease resistance, and if so, to assess if the formation of novel protease resistant fragments also correlated with ALS phenotypes.

2.2. Results

2.2.1. TDP protein levels in control and ALS patients

In order to examine the levels of TDP-43 protein and its isoforms throughout the CNS, we used 8 different CNS regions in 8 neurologically normal controls and 13 ALS patients. The brain regions were first made into 10% homogenates in PBS and then subsequently extracted in a series of buffers containing detergents including sarkosyl, and the pellets were solubilised in urea (See methods). The urea soluble fraction was then immunoblotted and probed with the polyclonal TDP-43 antibody and β-actin. The blot was then developed using the Odyssey image scanner and densitometry was performed using Image J.

Figure 8 demonstrates representative western blots of normal control and ALS patient samples highlighting the 43, 40 and 35 kDa species or isoforms we consistently detected in both control and ALS patients. The levels of TDP-43, TDP-40, and TDP-35 proteins were measured by densitometry and normalized with β-actin as the loading and total protein control. The levels of TDP-43 were measured as ratios of β-actin and corrected levels were then compared within each region between the control and ALS patients using an unpaired two tailed student's t-test where significance was measured with a p value lower than 0.05 (*$p < 0.05$).

Full length TDP-43 measurement in each of these regions revealed significant increases in the motor cortex (***$p < 0.001$), cerebellum (***$p < 0.001$) and the pons (*$p < 0.05$) in the

ALS samples compared to the controls (Figure 9A). Whilst the levels in the frontal and temporal cortices are slightly raised they do not reach significance. Levels in the spinal cord remain unchanged between control and ALS patients. Analysis of the levels of the smaller TDP-40 fragment revealed a trend of increase in the motor, frontal and temporal cortex and the cerebellum however the only statistically significant increases were in the frontal cortex (*p<0.05) and cerebellum (*p<0.05) between control and ALS samples. No differences in TDP-40 levels were detected in the pons and spinal cord regions between control and ALS samples (Figure 9B). Interestingly, the TDP-35 levels are similar in all of the brain regions between control and ALS samples but were decreased in the spinal cord regions and statistically significant decreases were detected in the thoracic (*p<0.05) and lumbar (*p<0.05) regions (Figure 9C).
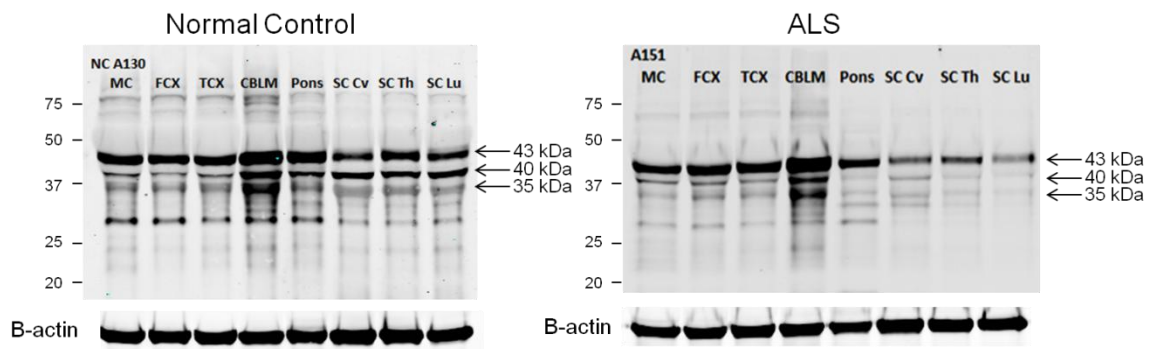
Figure 8. Representative western blots of different CNS regions in normal control and ALS patients probed with polyclonal TDP-43 and monoclonal β-actin antibodies. Arrows indicate TDP 43, 40 and 35 kDa bands used for measurement to correct with β-actin. MC= motor cortex, FCX = frontal cortex, TCX = temporal cortex, CBLM = cerebellum, SC Cv = spinal cord cervical, SC Th = spinal cord thoracic, SC Lu= spinal cord lumbar.
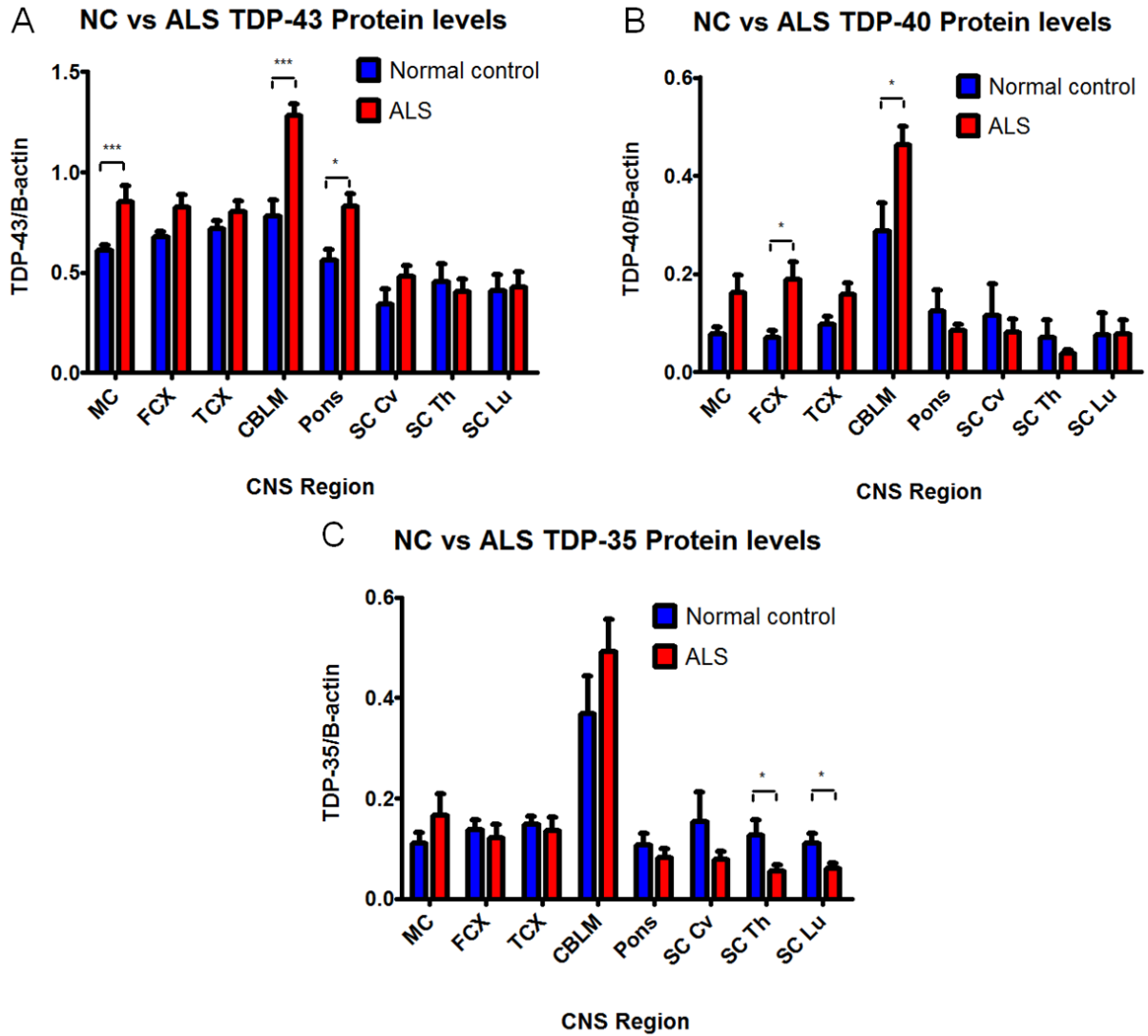
Figure 9. TDP-43, 40 and 35 protein levels in CNS regions of control and ALS patients. A) TDP-43 protein levels in the CNS of control (n=8) and ALS (n=13) patients in different CNS regions. B) TDP-40 isoform protein levels in the CNS of control and ALS patients in different CNS regions. C) TDP-35 isoform protein levels in the CNS of control and ALS patients in different CNS regions. All protein levels were corrected for with β-actin and statistical significance was compared with each region with a two tailed unpaired student's t-test. Statistically significant p values are as follows: * $p<0.05$, **$p<0.01$, ***$p<0.001$.

2.2.2 TDP protein levels and ALS phenotypes

Currently there is no molecular or biochemical basis known for varying ALS clinical phenotypes. Essentially sALS and fALS are phenotypically indistinguishable and although there are distinctive molecular neuropathological subtypes of ALS (Al-Chalabi et al., 2012), so far these subtypes do not appear to definitively correlate with ALS clinical phenotype (Ravits et al., 2013). Many different ALS associated gene mutations including *TARDBP* gene mutations, can produce similar clinical and neuropathological phenotypes whilst, conversely, a single genotype can produce different phenotypes. This essentially means pathological mechanisms in ALS may both diverge and converge (Ravits et al., 2013). To investigate a molecular and biochemical basis for differing ALS phenotypes, we hypothesized that differences in the insoluble TDP protein levels in various regions of the CNS and/or isoform ratios might act as a biochemical marker for clinical phenotype variability. Such markers have been previously used for the molecular and biochemical basis for phenotype distinction in prion diseases (Collinge et al., 1996; Parchi et al., 1996). In order to investigate this hypothesis we examined the insoluble levels of TDP isoforms by correcting for β-actin, and compared them to different aspects of clinical phenotype in ALS. Although ALS phenotype is clearly more complicated than this, but for simplicity of analysis, the four phenotype criteria selected were bulbar or limb onset, male or female sex, disease duration and age of disease onset.

2.2.2.1 Bulbar vs limb

Firstly, we separated the bulbar (n=5) and limb onset (n=8) ALS cases and compared their TDP western blot profile in identical regions of the CNS. Results reveal that most of the insoluble TDP-43 protein levels are similar in all brain and spinal cord regions except for a statistically significant increase in the lumbar spinal cord of bulbar patients compared to the limb onset (Figure 10A) (*$p < 0.05$). However, upon examination of the insoluble TDP-40 and TDP-35 levels no significant changes were observed between limb or bulbar onset ALS cases (Figure 10B and C).

2.2.2.2   Male vs female

The insoluble levels of TDP-43 were then compared between normal control male (n=4) and female (n=4), and ALS male (n=7) and female patients (n=6). There was a significant increase in insoluble TDP-43 levels in the ALS male patients in the motor cortex ($*p<0.05$) between the control males and females, which was not significant when compared with the ALS female motor cortex samples (Figure 11A). Although the female ALS cerebellum insoluble TDP-43 levels are increased compared to the male and female controls, statistical analysis reveals that significant increase was only observed in ALS male cerebellum samples compared to control male ($***p<0.001$) and female ($**p<0.01$) patients (Figure 11A). Finally, the significant increase in the insoluble TDP-43 levels observed in the ALS male pons region, compared to the control male ($**p<0.01$) and control female ($*p<0.05$) patients, was not detected in the ALS female pons samples (Figure 11A). Interestingly, the significant increases in insoluble TDP-43 levels in the motor cortex, cerebellum and pons in ALS patients observed in Figure 9A were observed to be predominantly due to increases in the insoluble TDP-43 levels from the male ALS patients. There was a significant increase in the insoluble TDP-40 fraction in frontal cortex of ALS females compared to controls ($*p<0.05$). There was also a significant increase in the insoluble TDP-40 levels in the temporal cortex of ALS females compared to both control and male ALS patients. (Figure 11B). Overall, the significant increase in insoluble TDP-40 levels detected (Figure 9B) between control and ALS samples in the frontal and temporal cortex were found to be due to the female ALS patients. The insoluble levels of TDP-35 were decreased overall in all regions of the spinal cord. However, statistically significant decreased TDP-35 levels were observed in the thoracic spinal cord (Figure 11C) ($*p<0.05$) between female controls and females with ALS.

2.2.2.3   Disease duration and age of onset

Analysis of the length of disease duration in all the ALS patients compared to the insoluble TDP protein levels revealed no significant linear correlation for any isoform in any CNS region of all the patients. Figure 12 demonstrates the motor cortex chosen as a representative region in the analysis. However, all the other CNS regions were analysed and reported similar non-significant findings (data not shown). In addition, the insoluble TDP protein levels did not correlate with age of onset of each of the patients in any of the CNS regions (Figure 13), indicating that levels of the TDP protein or its isoforms may not be markers for the length of disease duration or the age of onset of each ALS patient.
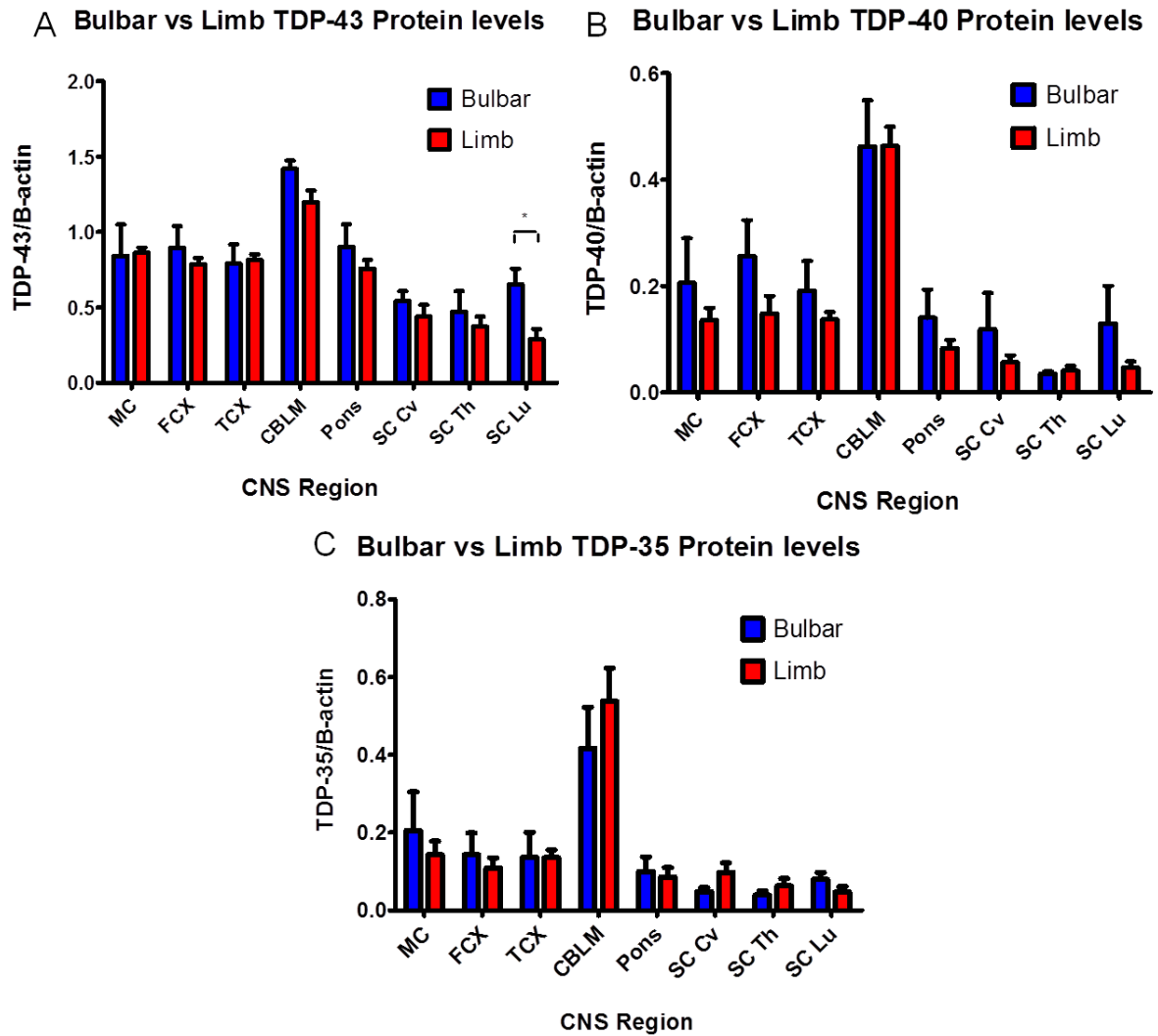
Figure 10. Insoluble TDP protein levels in bulbar vs limb onset ALS in different CNS regions. A) Insoluble TDP-43 protein levels in bulbar (n=5) vs limb onset (n=8) ALS in different CNS regions. B) Insoluble TDP-40 protein levels in bulbar vs limb onset ALS in different CNS regions. C) Insoluble TDP-35 protein levels in bulbar vs limb onset ALS in different CNS regions. All protein levels were corrected for with β-actin and statistical significance was compared with each region with a two tailed unpaired student's t-test. Statistically significant p values are as follows: * $p<0.05$, **$p<0.01$, ***$p<0.001$.
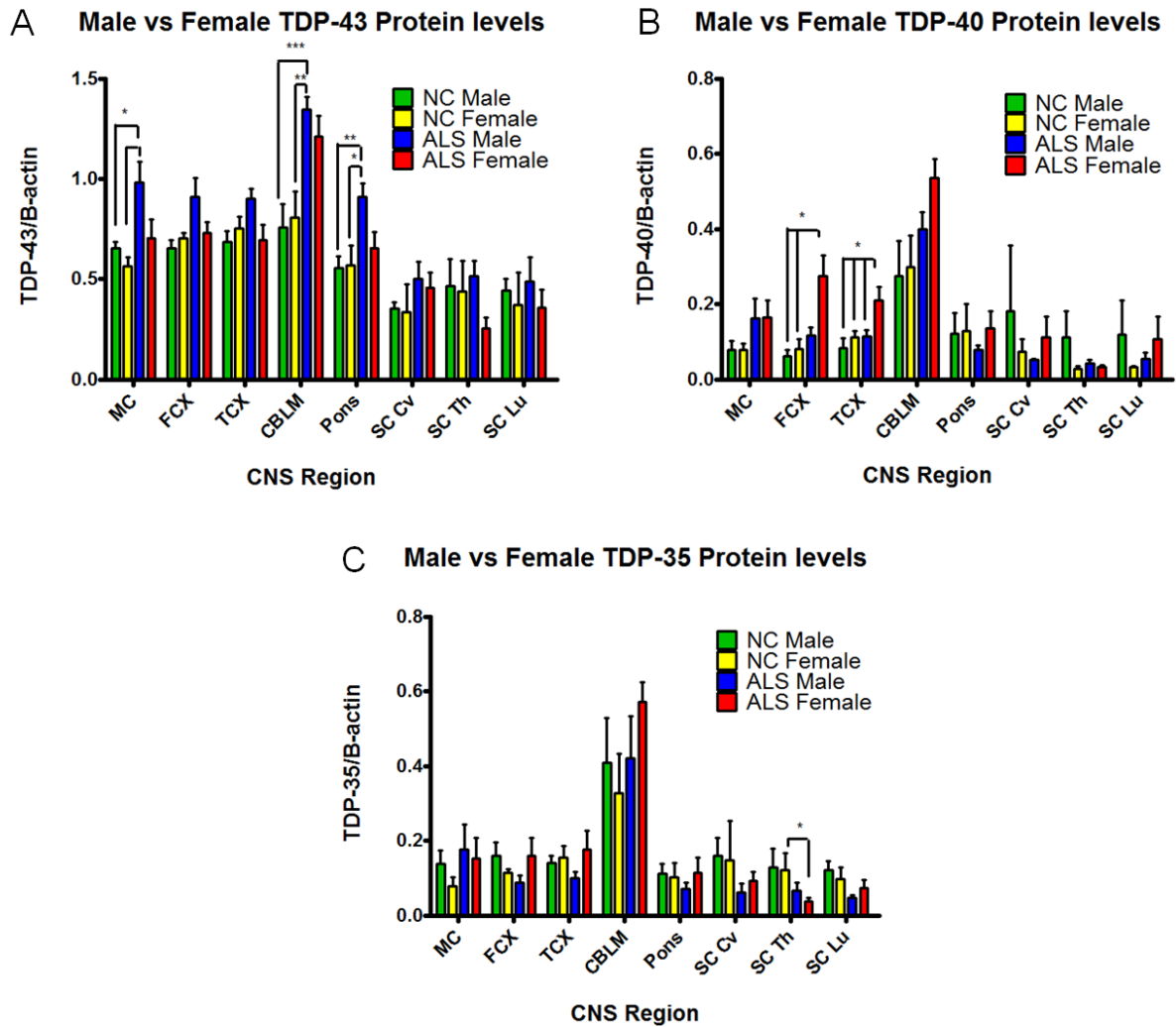
Figure 11. Insoluble TDP protein levels in control and ALS male and female patients in different CNS regions. A) Male and female insoluble TDP-43 protein levels in control and ALS patients in different CNS regions. B) Male and female insoluble TDP-40 protein levels in control and ALS patients in different CNS regions. C) Male and female insoluble TDP-35 protein levels in control and ALS patients. All protein levels were corrected for with β-actin and statistical significance was compared with each region with a two tailed unpaired student's t-test. Control male (n=4), control female (n=4), ALS male (n=7) ALS female (n=6). Statistically significant p values are as follows: * $p<0.05$, **$p<0.01$, ***$p<0.001$.

A MC TDP-43 protein levels vs Disease duration   B MC TDP-40 Protein levels vs Disease duration
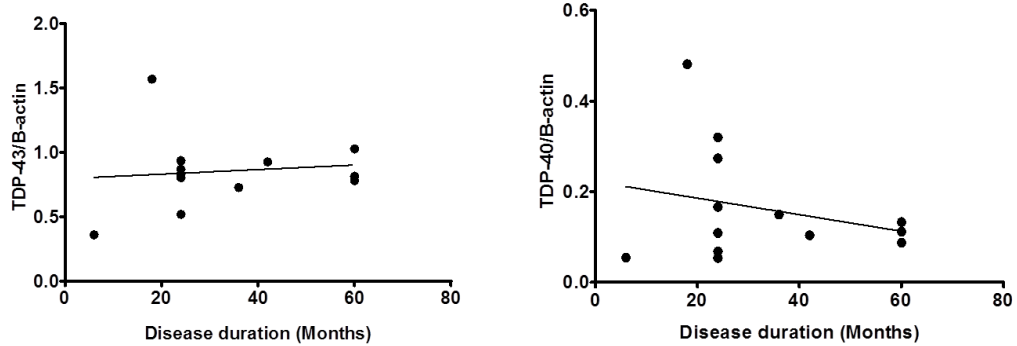
C MC TDP-35 protein levels vs Disease duration
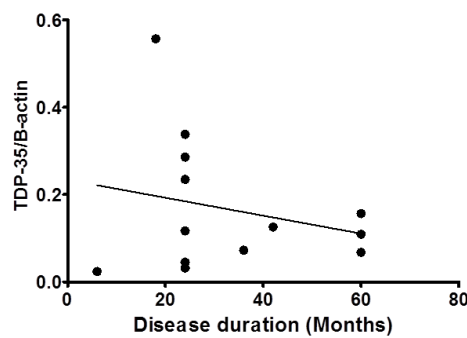
Figure 12. Representative insoluble TDP protein isoform levels in the motor cortex of ALS patients compared to disease duration. A) ALS insoluble TDP-43 protein levels in the motor cortex compared with disease duration of each patient. B) ALS insoluble TDP-40 protein levels in the motor cortex compared with disease duration of each patient. C) ALS insoluble TDP-35 protein levels in the motor cortex compared with disease duration of each patient. MC = motor cortex. Other CNS regions analysed were frontal cortex, temporal cortex, cerebellum, pons, cervical, thoracic and lumbar spinal cord, again showing no correlation (data not shown).
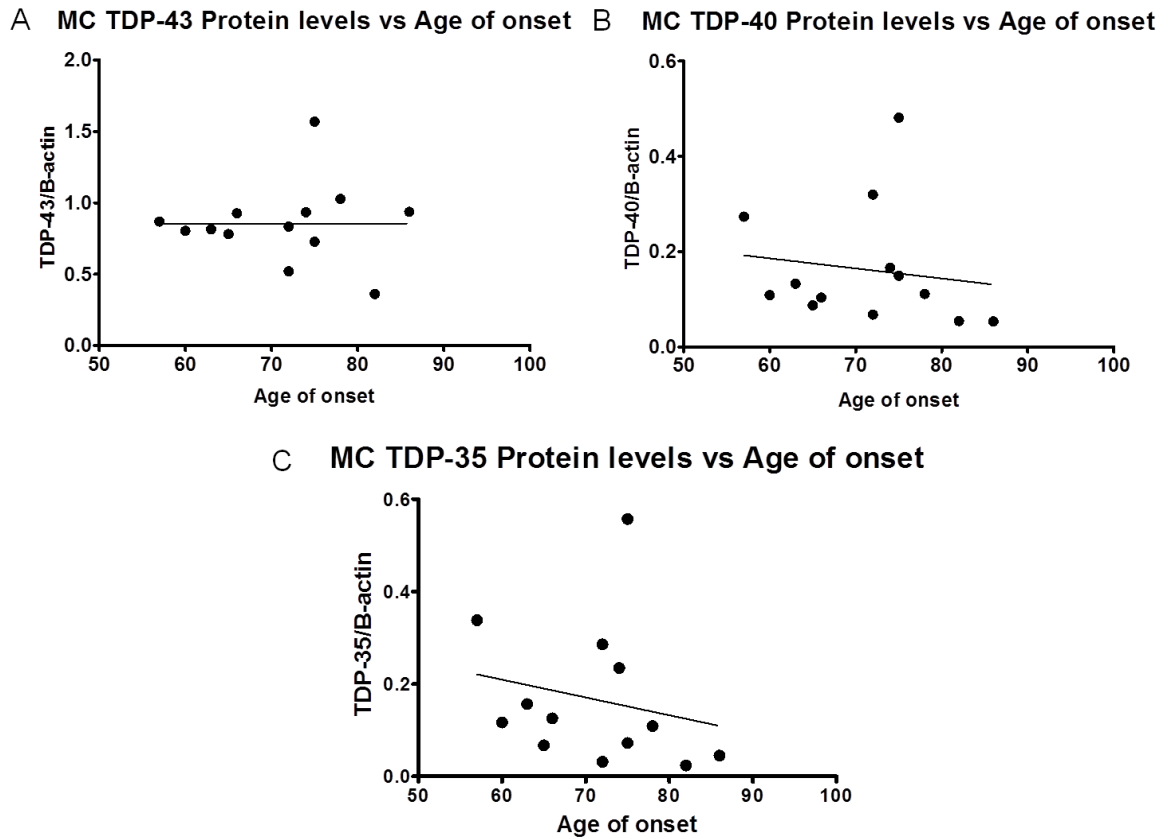
Figure 13. Representative insoluble TDP protein levels in the motor cortex of ALS patients compared to age of disease onset. A) ALS insoluble TDP-43 protein levels in the motor cortex compared with age of onset of each patient. B) ALS insoluble TDP-40 protein levels in the motor cortex compared with age of onset of each patient. C) ALS insoluble TDP-35 protein levels in the motor cortex compared with the age of onset of each patient. MC=motor cortex. All graphs show no significant positive or negative correlation.

2.2.3 TDP isoform ratios and ALS disease phenotype

Studies from the prion field found that the different types of prion disease are related to structural variations of the pathological prion protein (PrP^{Sc}), which were termed strain variants or 'strains'. These variations in the structural differences can alter the exposure of hydrophobic residues and enzyme cleavage sites within the protein. Therefore the structural differences between these pathological proteins could be detected by digestion of the PrP^{Sc} protein by proteinase K (PK) and visualized by western blot. Strains of PrP^{Sc} could be distinguished by their differing ratios of glycosylated PrP isoforms post PK digestion, which form a robust molecular marker for strain type (Collinge et al., 1996; Parchi et al., 1996). Recent evidence now suggests that strain variants may also be appearing with other pathological misfolded proteins in other neurodegenerative conditions (Guo et al., 2013; Heilbronner et al., 2013). Therefore we speculated that misfolded TDP-43 may also be able to form strain variants which could potentially lead to different ALS disease phenotypes.

Firstly, we examined the 3 characteristic bands seen across all control (n=8) and ALS (n=13) CNS sample regions pre-protease digestion (Figure 8). This includes the full length 43 kDa isoform and an observed 40 and 35 kDa isoform detected on our western blots. In order to process this information we performed densitometry on all of these isoforms in the insoluble fraction of each CNS region, and then added up the sum total of these values to calculate a ratio of each isoform, and plotted these values to detect any significant differences between control and ALS samples (Figure 14A and C) and between ALS phenotypes (Figure 14B-I).

Figure 12, Figure 13, and Figure 14 are all representative graphs using the motor cortex as a representative region for analysis. All other regions were examined but the data is not shown here. The analysis of the TDP banding ratios revealed that there was no significant difference between control and ALS patients, and no correlation of these ratios with the ALS clinical phenotype.
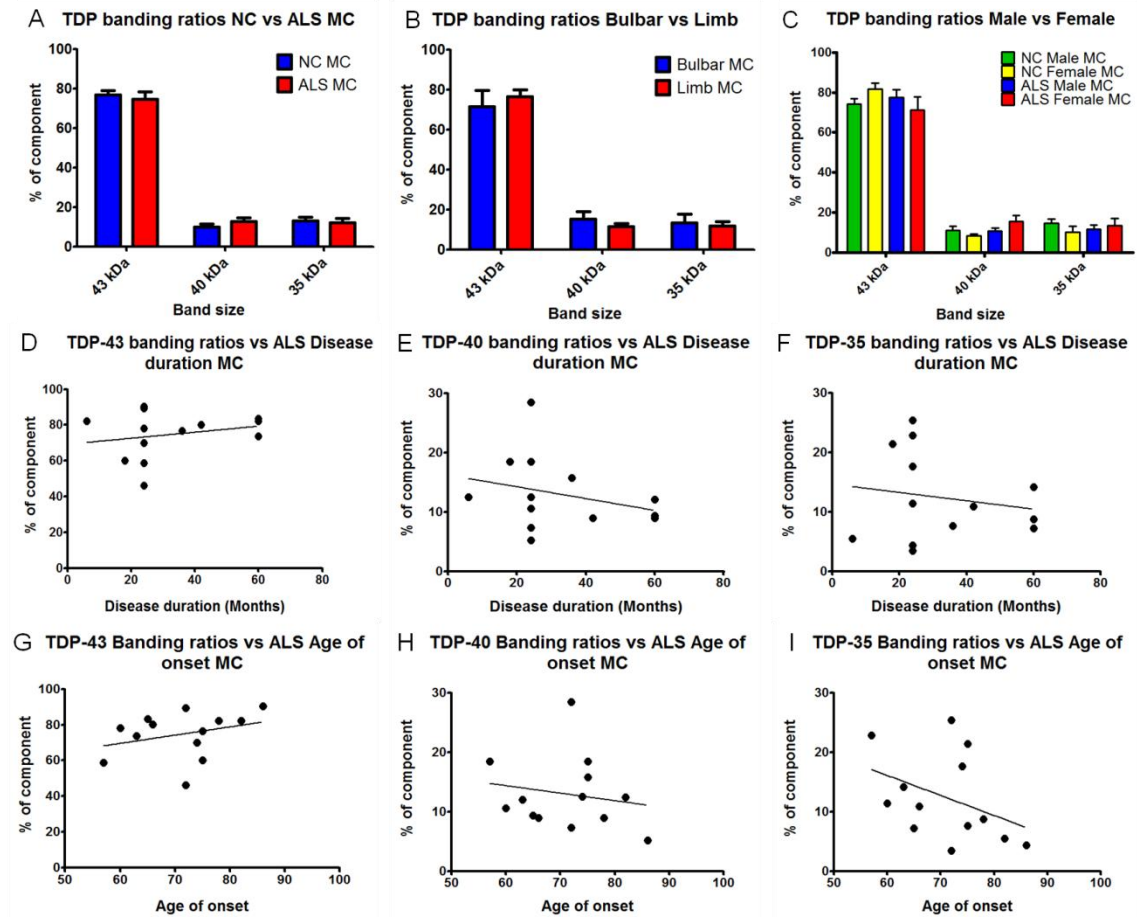
Figure 14. Representative graphs of TDP banding ratios from the insoluble fraction of the motor cortex in control vs ALS samples and within ALS phenotypes. A) Representative control and ALS banding ratios. B) Representative graph of banding ratios comparing bulbar and limb onset ALS. C) Representative graph of TDP banding ratios comparing control and ALS male and females. D) Representative scatter diagram of the 43 kDa fragment ratio values compared with disease duration. E) Representative scatter diagram of the 40 kDa fragment ratio values compared with disease duration. F) Representative scatter diagram of the 35 kDa fragment ratio values compared with ALS disease duration. G) Representative scatter diagram of 43 kDa fragment ratio values compared with ALS age of onset. H) Representative scatter diagram of 40 kDa fragment ratio values compared with ALS age of onset. I) Representative scatter diagram of 35 kDa fragment ratio values compared with ALS age of onset. MC = motor cortex.

2.2.4 Protease sensitivity of TDP-43 in ALS

One of the main pathological characteristics of the prion diseases is the resistance of the pathogenic misfolded prion protein (PrP^{Sc}) to protease digestion. This protease resistance may contribute to the proteins pathogenicity including its evasion of the cellular clearance machinery which allows the protein to survive and propagate in the cellular environment (Aguzzi, 2009). Resistance to protease digestion is an indicator of buried protease cleavage sites due to altered protein structure and conformation from protein misfolding. This phenomenon is well characterized in the prion disease field where the misfolded form of the normal PrP protein, termed PrP Scrapie (PrP^{Sc}), was shown to be resistant to PK digestion. This is a key characteristic of the protein that was critical in the determination of strain phenotyping in prion disease and the discovery of 'new variant CJD' (Collinge et al. 1996).

Here, we attempted to investigate the protease sensitivity of TDP-43 and to explore if there are any novel TDP-43 protease resistant fragments after digestion with proteases. In order to do this, we first used whole brain homogenates from the motor cortex and lumbar spinal cord of control and ALS patients and digested these samples with increasing concentrations of PK. We used whole brain homogenates to avoid any potential protein conformational changes that can occur with detergent extractions. These samples were then immunoblotted and probed with the monoclonal and polyclonal TDP-43 antibody. In addition we also probed with the phosphorylated pS409/410 antibody but no positive staining could be detected with this antibody on whole brain and spinal cord homogenates (data not shown). From these blots we found the minimum concentrations required to remove the full length TDP-43 protein was 2µg/ml in the motor cortex and 1µg/ml in the spinal cord. However there was no difference between control and ALS samples after digestion and no novel TDP-43 fragments were formed. The only minor difference was an increase in TDP-43 protein levels in the ALS samples, which meant that the digestion products remained after digestion at higher concentrations of PK. However, upon correction of TDP-43 levels no difference between control or ALS samples could be observed (data not shown). In order to confirm a lack of PK resistance of TDP-43 in whole brain homogenates

we digested all the other control and ALS motor cortex and spinal cord samples with the appropriate PK concentrations and found no resistant TDP-43 fragments in any of the samples.

We repeated this process with different enzymes including trypsin, chymotrypsin and pronase. Trypsin and chymotrypsin are serine protease digestive enzymes called endopeptidases and were chosen for their ability to digest mainly C-terminal arginine and lysines residues and aromatic amino acids respectively (Huber and Bode, 1978; Wilcox, 1970). Trypsin and chymotrypsin were useful in this instance as they are relatively weak enzymes which can target the misfolded C-terminal domain containing the prion-like domain. Therefore this region could be an effective target for enzymes to demonstrate protease resistance. Pronase is a mixture of enzymes which can completely digest the protein into individual substituent amino acids making it useful as a non-specific powerful enzyme to highlight any potential resistance across the protein (Sweeney and Walker, 1993). Upon digestion of the CNS tissue homogenates with each of these enzymes we found that none of these enzymes revealed any novel TDP-43 protease resistant fragments in the ALS samples compared to controls, and that enzyme digestion abolished all TDP-43 immunoreactivity (data not shown).

The next step was then to enrich the amount of insoluble TDP-43 in these samples and purify the insoluble pathological forms by performing detergent extractions (see methods). Sarkosyl insoluble fractions were prepared which have previously been demonstrated to be enriched for the pathological phosphorylated TDP-43. In order to find the minimum concentrations of each of the enzymes to digest out the full length form of TDP-43 we digested extracted control and ALS motor cortex samples with increasing concentrations of PK, trypsin and chymotrypsin at 37°C for 30 minutes (Figure 15). The samples were then immunoblotted and probed with mTDP-43 and pS409/410 antibodies. Digestion with increasing concentrations of PK revealed that the minimum concentration to remove the full length TDP-43 in the control was 5µg/ml. This revealed some digestion product bands at ~37 kDa which were more intense in the ALS samples compared to controls. However, upon correction with β-actin these higher intensity products were found to be caused by

increased levels of TDP-43 in the ALS sample starting material as previously observed (Figure 9). Less intense bands were also revealed at ~30kDa (molecular weight of PK) and doublet bands at 11 and 12 kDa were present in both control and ALS motor cortex samples (A). As such, these bands were discounted from the analysis here as being non disease specific. The same blots were also co-probed with pS409/410 and samples pre digestion showed no positive phosphorylated TDP-43 (pTDP-43) bands in the control but the characteristic phosphorylated 45 and 25 kDa bands in the ALS motor cortex sample, indicating that the antibody was working and able to detect phosphorylated TDP-43 pathology. However, after digestion with increasing concentrations of PK the blot revealed no bands in the control and some incomplete digestion products at 5µg/ml but no remaining bands at higher concentrations. This indicates that we could not detect phosphorylated TDP-43 resistant bands after digestion with PK (Figure 15B).

When blotted and probed with mTDP-43, digestion with increasing concentrations of trypsin in control and ALS MC samples revealed no resistant bands after 10µg/ml of trypsin in the control sample, and a resistant doublet forming ~20kDa in the ALS MC sample (Figure 15C). When the same blot was probed with pS409/410 a resistant pTDP-43 band formed at ~18kDa indicating that some novel lower molecular weight resistant products are forming after digestion with trypsin (Figure 15D).

Next the samples were digested with increasing concentrations of chymotrypsin, immunoblotted and probed with mTDP-43 and pS409/410 antibodies. Increasing concentrations of chymotrypsin revealed that full length TDP-43 was completely digested at 5µg/ml in the control and a number of TDP-43 resistant bands were formed in the ALS MC sample at 43, 40, 35, 30 and 25 kDa that remain resistant up to 15µg/ml of chymotrypsin (Figure 15F). When the same blot was probed with pS409/410 no resistant pTDP-43 bands could be observed after digestion with chymotrypsin (Figure 15F). Faint bands are detected at ~25kDa after digestion with chymotrypsin. However, the molecular weight of chymotrypsin is 25 kDa and the same band appears in the secondary antibody staining alone indicating that this band is non-specific and most likely to be chymotrypsin (Figure 16).

To confirm the specificity of these resistant bands, a panel of 4 control and 8 ALS MC samples were digested with 10µg/ml of trypsin and 10µg/ml of chymotrypsin for 30 minutes at 37°C, then immunoblotted and probed with mTDP-43 and pS409/410 (Figure 16). Control samples showed no TDP-43 or pS409/410 protease resistance with either trypsin or chymotrypsin at 10µg/ml (Figure 16A and B). However, the ALS MC samples demonstrated variable protease resistance between each sample. For example, it seems that the novel phosphorylated 18kDa band formed only if the pS409/410 staining before digestion had clear 25kDa bands, as seen in patients A381, A203 (Figure 16F) and A148 (Figure 16D). However, the TDP-43 chymotrypsin resistant bands seen in Figure 15E could not be observed in any of the other ALS samples. These data suggest that TDP-43 protease resistance is variable within ALS patients and use of the protease resistant properties may give unreliable results. Despite the promising nature of the resistant bands present in Figure 15, the same bands could not be observed in all of the ALS MC samples for each patient meaning that any potential strain type analysis could not be performed.

In order to confirm the pathological phosphorylation variability between ALS patients and within CNS regions, all the CNS regions from each patient were extracted in sarkosyl and resolubilised in urea to immunoblot for pS409/410. These results indicated that some of the ALS patients had no positive pTDP-43 bands in any of the CNS regions (Figure 17 A, F, L and M) and other patients had characteristic pTDP-43 bands in some regions and not others (Figure 17 B, C, D, E, G, H, I, J and K). Comparison of the pTDP-43 bands across each CNS region in each patient to the ALS phenotype revealed no significant correlation to any of the four phenotype criteria examined previously. Unfortunately no phosphorylated staining was conducted on the tissue acquired for this study; however the TDP-43 staining does appear to correlate with the presence of pTDP-43 bands in each patient. This further suggests that TDP-43 pathology is variable between ALS patients and CNS regions. Additionally, the examination of each phenotype and the presence of pTDP-43 pathology revealed no correlation (data not shown), suggesting that the presence and distribution of pTDP-43 pathology may not be directly related to ALS phenotype.
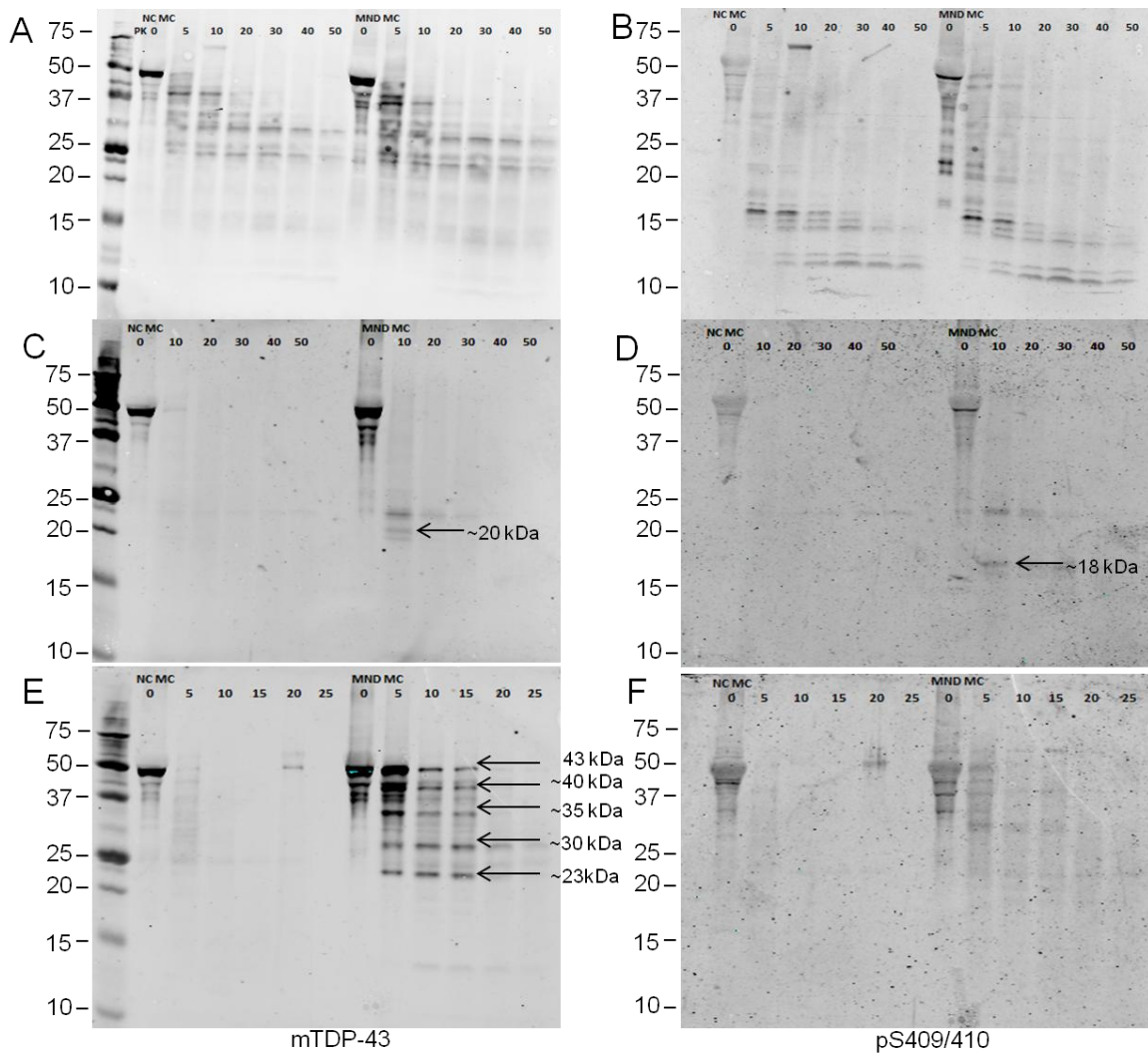
Figure 15. Western blots of protease titration digestion in control and ALS samples. A) Proteinase K (PK) treatment of insoluble control and ALS MC samples with increasing concentrations of PK probed with monoclonal TDP-43 (mTDP-43) (A) and polyclonal pS409/410 (B) antibodies, demonstrating no novel PK resistant bands in the ALS MC. Increasing concentrations of trypsin digested control and ALS MC samples probed with mTDP-43 (C) and pS409/410 (D). Arrows demonstrate novel ALS MC trypsin resistant ~20kDa doublet bands at 10μg/ml with mTDP-43 (C) and novel ~18kDa trypsin resistant band with pS409/410 (D). E) and F) show control and ALS MC samples digested with increasing concentrations of chymotrypsin probed with mTDP-43 (E) and pS409/410 (F). Arrows demonstrate novel ALS MC chymotrypsin resistant bands of ~40, ~35, ~30 and ~23kDa at 10 and 15μg/ml of chymotrypsin probed with mTDP-43 (E), and no chymotrypsin resistant bands when probed with pS409/410 (F). All enzyme concentrations are in μg/ml and digested for 30 minutes at 37°C. pTDP-43 = phosphorylated TDP-43, mTDP-43= monoclonal TDP-43 antibody.
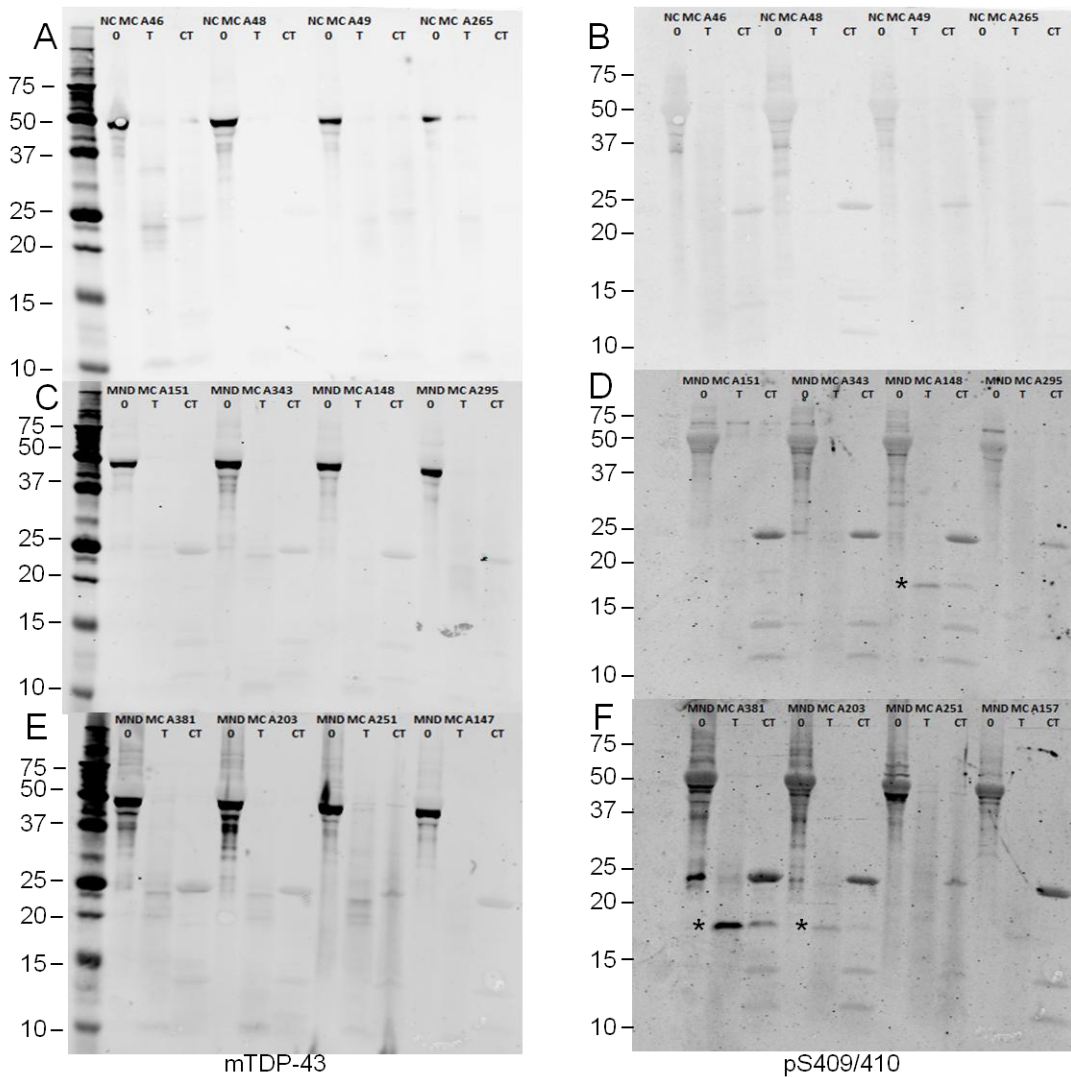
Figure 16. Insoluble control and ALS motor cortex samples digested with trypsin and chymotrypsin. A) Four control motor cortex samples pre and post digestion with 10μg/ml of trypsin and chymotrypsin revealing no remaining TDP-43 (A) or pTDP-43 bands (B). C) and D) are four motor cortex (MC) samples from different ALS patients pre and post trypsin and chymotrypsin digestion at 10μg/ml probed with mTDP-43 (C) and pS409/410 (D) antibodies. E) and F) are 4 motor cortex samples from different ALS patients pre and post digestion with trypsin and chymotrypsin at 10μg/ml probed with mTDP-43 (E) and pS409/410 (F) antibodies. * indicate novel pTDP-43 trypsin resistant bands formed after digestion. pTDP-43 = phosphorylated TDP-43, mTDP-43= monoclonal TDP-43 antibody
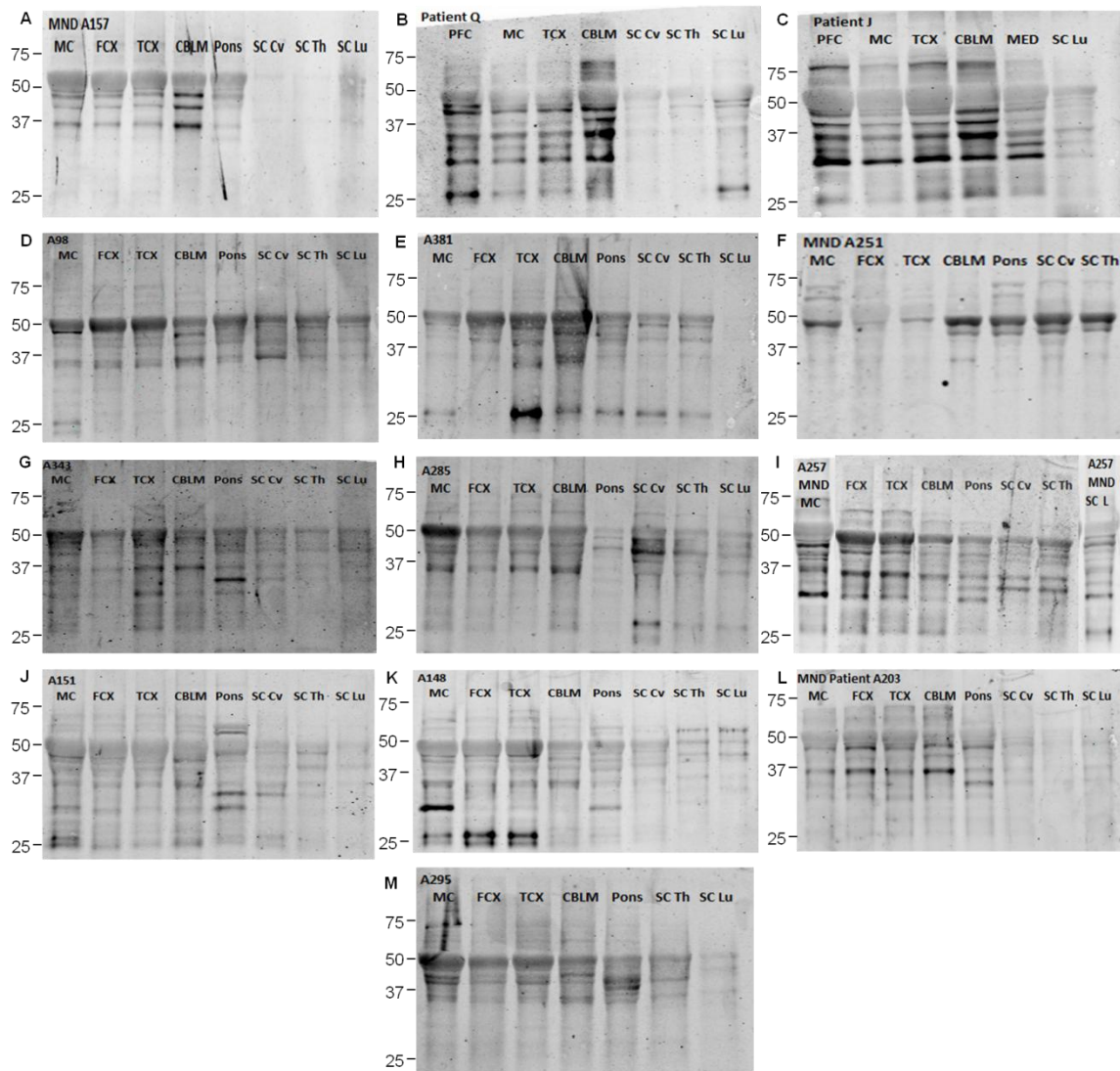
Figure 17. Phosphorylated (pS409/410) TDP-43 status of all ALS patients in the insoluble fractions of different CNS regions. No pTDP-43 bands can be seen in patient A157 (A), A251 (F), A203 (L) and A295 (M) in any of the CNS regions examined. Patient Q has 45 and 25kDa positive bands in the PFC, FCX, TCX, CBLM and SC Lu (B). Patient J has characteristic 45 and 25 kDa pS409/410 bands PFC, TCX, CBLM and MED (C). Patient A98 has faint 45 and 25 kDa pS409/410 positive bands in the MC only (D). Patient A381 has pTDP-43 bands in the MC, TCX, CBLM, Pons, SC Cv, and SC Th (E). A343 has some faint 45 and 25 kDa pTDP-43 bands in the MC and TCX (G). Patient A285 has positive 45 and 25 kDa pTDP-43 bands in the SC Cv, Th and Lu regions (H). Patient A257 has pTDP-43 positive bands in the FCX, TCX, and CBLM (I). Patient A151 has pTDP-43 positive bands in the MC, FCX, TCX CBLM and SC Cv (J). Patient A148 has 45 and 25kDa pTDP-43 bands in the MC, FCX and TCX (K). MC = motor cortex, FCX = frontal cortex, PFC = prefrontal cortex, TCX = temporal cortex, CBLM = cerebellum, SC = spinal cord, CV = cervical, Th = thoracic, Lu = lumbar, pTDP-43 = phosphorylated TDP-43.

2.3   *Discussion*

To date, studies looking at TDP-43 protein levels have looked only in CSF and skin for use as a potential diagnostic and prognostic marker (Noto et al., 2011; Suzuki et al., 2010; Tortelli et al., 2012). Whilst this information is useful in biomarker detection it does not provide information about actual CNS TDP-43 protein levels. Currently, no data exists on the protein levels of TDP-43 in different CNS regions comparing controls and ALS patients, and within ALS phenotypes. Indeed, little knowledge exists on the molecular pathological basis behind ALS phenotypes. Although the analysis of TDP-43 levels in the CNS regions will not be useful as a biomarker, it could tell us more about the pathological nature of TDP-43 in the CNS.

Here, we demonstrate that the levels of full length TDP-43 and other isoforms are altered and predominantly elevated in ALS in different CNS regions. We have demonstrated that TDP-43 levels are significantly raised in the motor cortex, cerebellum and pons in ALS patients compared to controls (Figure 9A). The TARDBP gene expression throughout different regions of the CNS is fairly uniform (Su et al., 2004), therefore altered levels of TDP-43 protein are most likely to be due to post translational modifications such as aggregation. These significant increases in the motor cortex and pons regions could reflect the regions of the CNS that are predominantly affected in ALS due to the location of the descending pyramidal motor tracts. The significant increases in the cerebellum were surprising given the lack of clinical cerebellar signs in ALS and frequent TDP-43 negative p62 positive inclusions in the cerebellum. However, more recent studies have provided strong evidence for the cerebellar involvement in ALS (reviewed in (Prell and Grosskreutz, 2013)). Even though no typical TDP-43 pathology is observed in the cerebellum, it does contain ubiquitinated forms of TDP-43 co-localized with p62 (Arai et al., 2006; Geser et al., 2009; Neumann et al., 2006). However, there are many more p62 inclusions in the cerebellum most of which are negative for TDP-43 (King et al. 2010; Troakes et al. 2012). In cases of ALS or FTLD caused by hexanucleotide expansions in the C9orf72 gene, there is usually a deposition of non ATG dependent translated dipeptide repeats proteins deposited in the frontal cortex, hippocampus and cerebellum (Ash et al., 2013). These cases are often

positive for prominent p62 inclusions in each of these regions and especially the cerebellum (Murray et al., 2011). Biochemically there are increased levels of the oxidative damage response DNA repair enzyme Poly (ADP-Ribose) polymerase (PARP) in the motor cortex, parietal cortex and cerebellum in patients with ALS (Kim et al., 2004). Additionally, the SOD1 G93A mouse was found to have increased phosphorylated extracellular regulated kinase (pERK) staining and altered tau expression in the cerebellum (Barańczyk-Kuźma et al., 2007; Chung et al., 2005), indicating that there is indeed pathological changes in the cerebellum during ALS. Finally, a heat mapping topographical study of TDP-43 pathology also shows mild TDP-43 pathology in the cerebellum (Geser et al., 2008).

Advanced MRI imaging studies on ALS patients demonstrate that the cerebellum along with a number of other brain regions is recruited in order to compensate for functional motor impairment (Schoenfeld et al., 2005). Furthermore, pathological changes in the cerebellum could also be explained by the recent discoveries about the involvement of the cerebellum in emotional and higher cognitive functions (Ito, 2008), and the frequent impairment of these faculties in patients with ALS and FTLD (Tsermentseli et al., 2011). If neurodegenerative diseases do indeed propagate via neural networks and tracts, then the reciprocal neural fibre tracts and connections between the frontal cortex and the cerebellum could be a reason for the presence of cerebellar TDP-43 pathology (Ramnani, 2012). The involvement of the cerebellum in ALS is an interesting phenomenon and requires further investigation. Our findings here have further added to this growing body of knowledge about the cerebellum, TDP-43 and ALS, and the relationship between them will be a potential future line of enquiry.

These results suggest, so far, that the most important CNS regions for TDP-43 over expression in ALS are the motor cortex, cerebellum and pons. However, there are increases in TDP-43 in other brain regions suggesting that there may be a global increase in TDP-43 levels in ALS affected brain tissue. This may be reflected in the increased levels in the CSF and skin of ALS patients (Kasai et al., 2009; Noto et al., 2011; Suzuki et al., 2010). However, a more recent study could not find significant differences between control and ALS and FTLD patient CSF TDP-43 levels. In addition they suggest that most of the TDP-43 detected in CSF

originates from the blood and therefore may have a limited role as a diagnostic tool in TDP-43 proteinopathies. However, the CSF TDP-43 levels may still be of importance in monitoring TDP-43 modifying therapies (Feneberg et al., 2014). The regional specificity of TDP-43, with higher levels in some regions compared to others, may suggest that certain cell populations are more vulnerable to TDP-43 associated pathogenic mechanisms. These anatomical areas are non-contiguous and these findings may therefore suggest that there may be a specific cellular tropism for TDP-43 mediated pathological mechanisms with enhanced toxicity in the motor system. The TDP-43 and TDP-40 isoforms remain similar between controls and ALS patients in the spinal cord regions, and only a reduction in the TDP-35 levels occurs in ALS samples compared to controls. This reduction is specific to the spinal cord, suggesting that there is either selective regional cell vulnerability in those sub population of cells expressing this isoform, or there is a disease specific down regulation. To rule out the potential influence of post mortem delay on the levels of these TDP isoforms, the levels were compared to the post mortem delay for each patient and found to have no correlation (data not shown). Therefore to confirm the specificity of these altered TDP isoform levels, further work would need to include neurodegenerative disease controls to ensure secondary disease processes are not the cause, and that these observations are specific to ALS.

Analysis of this data with the stratification by clinical ALS phenotype revealed significantly decreased TDP-43 levels in the limb onset compared to bulbar onset ALS patients in the lumbar spinal cord (Figure 10A). These changes could be explained by an increased amount of cell death in patients that have disease onset within the spinal cord, and if this is the case it would further suggest that the lumbar region of the spinal cord is also the most heavily affected in patients with ALS. In order to confirm this hypothesis, cell death should be corrected for by quantification of the Bax protein which is known to be up-regulated during cell death in ALS spinal cords (Ekegren et al. 1999). Alternatively, these changes could potentially be disease specific and suggest that either, a lower level of expression of TDP-43 in the lumbar spinal region could predispose the patient to developing limb onset ALS, or, that downregulation of the TDP-43 protein levels occurs in the lumbar

spinal cord as part of a pathogenic or neuroprotective response. Low TDP-43 protein levels, as a result of low intrinsic levels in ALS affected individuals or through altered TDP-43 regulation, could be linked to a loss of TDP-43 function in the lumbar spinal cord. Hence this could suggest a potential cellular mechanistic basis for the development of limb onset ALS. However, such down regulation may also occur as a neuroprotective response to prevent the production of toxic TDP-43 species. To test this hypothesis, a rodent model of CNS regional specific overexpression or knockout of wild type and mutant TDP-43 would help to delineate the emergence of an ALS phenotype. This may suggest that the phenotype could be dependent upon a regional variance in TDP-43 protein levels, and would highlight the role of TDP-43 regulation in the pathogenic process.

When the regional increases in TDP-43 levels in control and ALS patients were separated based on sex of the patient, the significant changes in TDP-43 levels revealed in the motor cortex, cerebellum and pons were found to be predominantly due to increases of TDP-43 levels in the male patients (Figure 11A). Unfortunately due to the lack of female bulbar cases, a cross comparison of male or female bulbar patients with male or female limb patients could not be made, but a future increase in patient numbers analysed will allow for this analysis in the future. However, ALS more commonly affects males than females (Manjaly et al., 2010), and these results appear to reflect this disease bias. Additionally these results may also reflect an underlying genetic susceptibility for ALS in males, or a greater male predisposition for TDP-43 overexpression and susceptibility to TDP-43 mediated toxicity. However, a recent study also suggests that age and sex play a combined role in determination of the risk of getting ALS, as the male to female ratio decreases after the age of 55 (Manjaly et al., 2010). Therefore using the sex of the patient alone may be insufficient to determine disease risk without using age as a co-variable.

In contrast to this, the observed significant increases in TDP-40 levels in the frontal and temporal cortex were predominantly due to the female ALS patients (Figure 11B). The TDP-40 levels were still raised in the motor cortex, but there was no different between male and female ALS patients, and again increases were observed in the female cerebellum TDP-40 levels but were of no significance. Although the overall TDP-35 levels are decreased in male

and female ALS patients (Figure 11C), the only significance detected was in the thoracic spinal cord. However, the remaining regions may reach significance with an increase in sample numbers. These unique differences may suggest a specific increase in TDP isoform levels that varies with sex differences in ALS patients. Unfortunately due to the low numbers of patients and samples available in this study, a study with a greater cohort and sample number would be required for greater statistical power.

When the TDP protein levels were compared with the age of onset (Figure 13) and disease duration (Figure 12) of all the ALS patients, no significant correlations could be found. These results suggest that the levels of TDP-43 protein may not influence the progression or the age of disease onset. However, these results are preliminary and a larger sample cohort will be required to confirm these observations. Alternatively, one study links accelerated disease onset to the increased stability and longer half-lives of the TDP-43 mutant proteins (Watanabe et al., 2012). This could indicate that the levels of the protein may not be essential, but the ability of the toxic mutant protein to survive and promote toxicity in the CNS may influence the onset and progression of the disease.

Measurements of the ratios of each of the TDP isoform bands in all CNS regions between control and ALS patients (Figure 14A), and for all four ALS phenotypes (Figure 14B-I) revealed no significant differences or correlations in any of the parameters. This indicates that the ratios of these bands may not be useful in distinguishing ALS phenotypes. However, the exploration of TDP isoform protein levels in the CNS could still yield further interesting results about the molecular properties underlying ALS, and therefore requires further exploration with larger numbers of patients and brain regions. Additionally, neurodegenerative disease controls including FTLD, PD and AD samples will be required to measure the specificity of any significant changes observed.

During this research, published data on the molecular characterisation of TDP-43 proteinopathies, including ALS, FTLD and different FTLD subtypes, became available (Tsuji et al., 2012). Tsuji et al. 2012 reported that phosphorylated TDP-43 demonstrated unique banding patterns between four different TDP-43 proteinopathies (A-D) which were

indistinguishable between brain regions. This suggests that the different TDP-43 proteinopathies are either a result of, or correlated with, different molecular conformations of the protein. They also reported the formation of unique TDP-43 and phosphorylated TDP-43 protease resistant bands which are also unique to each TDP-43 subtype, potentially introducing a new clinicopathological classification of TDP-43 proteinopathies. More importantly, here it would suggest pathological protein misfolding of TDP-43 potentially underlies each unique FTLD-TDP disease subtype.

In parallel to this work, we were also looking at protease sensitivity of TDP-43. However, in our study, we were looking at the protease sensitivity of TDP-43 within ALS patients and comparing within ALS phenotypes, rather than within all the TDP-43 proteinopathies. Tsuji et al did not mention any PK sensitivity of TDP-43 but a previous smaller publication from the same group did mention that PK digestion abolished all TDP-43 immunoreactivity (Hasegawa et al., 2011). Our results also demonstrated a lack of TDP-43 immunoreactivity after PK digestion in both control and ALS samples with the monoclonal TDP-43 antibody (Figure 15A) and the pS409/410 antibody (Figure 15B). Tsuji et al also noted a TDP-43 resistance to trypsin at a final concentration of 100µg/ml for 30 minutes at 37°C which formed a pTDP-43 doublet band at ~16kDa and minor 23-24kDa bands. We also tried trypsin digests, although using a much lower concentration of 10µg/ml, and found a resistant doublet band at ~20kDa with the monoclonal TDP-43 antibody (Figure 15C) and a single pTDP-43 resistant band at ~18kDa (Figure 15D). The discrepancies in molecular weight of the digestion products between the two studies may be due to different molecular markers used, different blotting techniques, or may be different TDP-43 protease resistant species in the patients we studied. However, the remarkably different concentrations of trypsin from 100µg/ml in the Tsuji et al study to 10µg/ml in this study are unusual and may be explained by human error or different blotting techniques. In our study any concentration above 10µg/ml here was shown to completely remove TDP-43 immunoreactivity with the monoclonal TDP-43 (Figure 15A) and with the pS409/410 antibody (Figure 15).

In order to confirm the sensitivity and specificity of these post enzyme digestion bands, we repeated the digestions in 4 more controls and 8 ALS motor cortex samples. However,

we found that there was significant variability in the presence of TDP-43 protease resistant bands formed from these samples using the monoclonal TDP-43 antibody. The ~18kDa pS409/410 resistant band was detected in 3 ALS patients (indicated by * in Figure 16D and F) which appeared to be dependent on the amount of pS409/410 staining before digestion. The fact that only one resistant band is formed post digestion, and is dependent on the degree of pS409/410 staining prior to digestion, suggests that these pTDP-43 trypsin resistant fragments are not robust enough to distinguish between ALS phenotypes.

We repeated this process using chymotrypsin and report the formation of the 43, 40, 35, 30 and 25 kDa resistant fragments after digestion (Figure 15E) with the monoclonal TDP-43 antibody. Tsuji et al also report protease resistant bands using chymotrypsin comparing differing TDP-43 proteinopathies, and not comparing different ALS phenotypes. However, they report formation of prominent ~23 and ~18 kDa bands with the monoclonal antibody which may be due to similar differences seen in the trypsin digests. Further chymotrypsin digestion in 4 controls and 8 ALS motor cortex samples found these fragments to be variably reproduced, suggesting that the protease sensitivity of TDP-43 is variable both between patients, and with repeated testing of patient samples. Therefore the digestion of brain or spinal cord with trypsin is not likely to be a reliable disease or phenotype marker (Figure 16C and E). In contrast, Tsuji et al demonstrated the formation of pTDP-43 resistant bands and found triplet bands at 21, 22 and 23kDa which were equal in intensity throughout each ALS patient but varied about the 16 and 15 kDa bands. Here we found no pTDP-43 resistant bands in any of our ALS samples (Figure 15F and Figure 16D and F) with chymotrypsin digestion, again suggesting that variations in pTDP-43 pathology and experimental techniques can make these studies unreliable to identify specific banding patterns in ALS phenotypes.

To determine if the pattern of TDP-43 phosphorylation differed throughout each region in the CNS of our ALS patients samples, we immunoblotted all the sarkosyl insoluble urea soluble fractions from each of these regions and probed with the pS409/410 antibody to detect pTDP-43 (Figure 17). We found that the degree of pTDP-43 pathology varied greatly from patient to patient and region to region. Some ALS patients contained no pTDP-43

bands (Figure 17 A, F, L and M) whereas others had bands in limited regions (Figure 17 B, C, D, E, G, H, I, J and K). Additionally, some patients had strong positive pTDP-43 in some regions and weaker staining in other regions. For example, Patient A381 has intense 25kDa pTDP-43 bands in the temporal cortex, and weaker bands in the motor cortex, cerebellum, pons and spinal cord regions (Figure 17E). Upon examination of the ALS phenotypes and the presence of pTDP-43 pathology, no correlation could be found in any of the clinical phenotype criteria (data not shown). This indicates that the pattern or degree of pTDP-43 present in each CNS region may not be reflective of the site of disease onset, age of disease onset, duration of illness or the sex of each patient. Rather that it may reflect the presence of the underlying TDP-43 pathology in each patient. Tsuji et al demonstrated pTDP-43 C-terminal fragments in a number of CNS regions but the intensity of this staining varied between each region. However, they only examined 3 cases and concluded that the fragment pattern was the same between all regions. Here we report that the presence of pTDP-43 bands is not consistently present in all regions of all 13 ALS patients, but also found that the intensity of the pTDP-43 bands varies significantly between each region. The discrepancies between our study and theirs may lie in experimental techniques and immunoblotting developing methods. However, our data does suggest, at least, that TDP-43 has a degree of protease resistance in patients with ALS, but this resistance can vary between each patient and potentially between each region.

2.4 Future work

In order to progress this work forward the quantification of TDP-43 levels should be repeated with a larger ALS patient cohort and more CNS regions. This will allow us to gain greater statistical power and more detailed information on the regional variance of TDP-43 levels in the CNS. Disease controls with prominent neuronal death such as Parkinson's and Alzheimer's disease, should also be used to control for secondary disease processes and confirm the specificity of these changes to ALS. FTLD patient equivalent CNS regions should also be used to include the broad spectrum of TDP-43 proteinopathies. This data set can then be used to assess any further significant differences in the ALS phenotype criteria measured here. Indeed, the ALS phenotype criteria should be expanded to include degree of

cognitive impairment including any development of FTLD signs. This type of data will be more readily available in the future with more abundant and thorough cognitive assessments in ALS clinics. The emerging pathological relevance of the cerebellum in ALS and its involvement in emotion and cognition, suggests that a more comprehensive molecular study of pathological changes in the cerebellum should be conducted to correlate this with the degree of cognitive impairment. Future work should also include patients with C9orf72 expansions and patients with TARDBP mutations to include the full spectrum of ALS patients with TDP-43 pathology.

In terms of assessing the protease sensitivity of TDP-43 future work should involve using a larger panel of enzymes for TDP-43 digestion. This may reveal some interesting protease resistant products which could help further elucidate the structure of pathological misfolded TDP-43. In turn more knowledge about its structure and protease resistant properties will be useful for future therapeutic design when targeting TDP-43 misfolding.

2.5   Conclusion

In summary, the increased levels of TDP-43 present in various regions of the CNS seem to be an important factor in ALS which correlates with various in vivo and in vitro studies of TDP-43 mediated neurodegeneration (reviewed in Janssens & Van Broeckhoven 2013). Indeed, it could be speculated that variations in the levels of TDP-43 may lead to a toxic gain/loss of function or both dependent upon the regional variance in TDP-43 levels. It also appears that sex differences may influence the alteration of TDP-43 levels, and variations of TDP-43 levels in the lumbar spinal cord could also influence the development of a bulbar or limb ALS phenotype. However, the levels of different TDP isoforms detected here appear not to be influenced by the age of onset or duration of disease. Similarly ratios of all these isoforms do not seem to act as a disease or clinical phenotype marker in each of the criteria measured here. Our data also suggests that TDP-43 does indeed have a degree of protease resistance, but this can be highly variable between patients and depend upon the degree of pTDP-43 pathology present in that particular CNS region. The development of a single protease resistant band and variable presence of pTDP-43 pathology in each region make the enzymatic digestion of TDP-43 an unreliable phenotype marker in ALS.

Chapter 3

'Prion-like' mechanisms of TDP-43 in vitro

3. 'Prion-like' mechanisms of TDP-43 in vitro

3.1. Introduction

Part of the pathological process driving the deposition of prion protein aggregates in prion disease is called a 'seeded templating polymerization reaction', whereby the misfolded PrP^{Sc} protein can induce its pathological structural conformation on to the endogenous wild type PrP protein. This serves as a nucleation reaction to recruit prion monomers and form prion aggregates (Aguzzi, 2009). This self templated seeding principle has now been demonstrated in Alzheimer's disease with β-amyloid and tau (Bolmont et al., 2007; Eisele et al., 2009; Guo and Lee, 2011; Hamaguchi et al., 2012; Hu et al., 2009; Langer et al., 2011; Meyer-Luehmann et al., 2006; Walker et al., 2002), Parkinson's disease with alpha synuclein (Danzer et al., 2009; Desplats et al., 2009; Hansen et al., 2011; Luk et al., 2009, 2012a, 2012b; Nonoka et al., 2010; Volpicelli-Daley et al., 2011), and a number of other neurodegenerative disorders (reviewed in (Walker, 2012)) as the mechanism for driving protein aggregation.

Aggregation in many neurodegenerative disorders commonly follows a nucleation-growth mechanism. This nucleation phase is considered to be thermodynamically unfavourable, which results in a long lag phase period (Chiti and Dobson, 2006). Indeed, this lag phase combined with efficient cellular clearance mechanisms could potentially be responsible for the late onset of neurodegenerative disorders. Once the aggregation nucleus has formed, the recruitment of soluble monomers and oligomers leads to the formation of aggregates. Experimentally, this lag phase is commonly removed by the addition of pre-formed seeds to initiate a templated seeding reaction. This templated seeding reaction may lead to the formation of fibrils with a β-sheeted structure of the aggregated protein called 'amyloid'. Amyloid is a major component of many protein aggregates in a number of neurodegenerative diseases and other systemic conditions such as systemic amyloidosis (Chiti and Dobson, 2006). Although the formation of amyloid is a common finding in these seeding reactions, studies on prions suggests that they need not polymerize to form amyloid but they can also propagate as oligomers (Alper et al., 1966; Bellinger-Kawahara et al., 1988;

McKinley et al., 1986; Silveira et al., 2005). Indeed, recently tau was found to be one of these prion-like proteins that can propagate via the formation of oligomers (Lasagna-Reeves et al., 2012). As a result of a lack of β-sheeted structure, the deposits may form disordered amorphous aggregates and these amorphous aggregates may also be seeded as well as amyloid.

One of the more recent proteins involved in the pathogenesis of ALS and FTLD thought to have prion-like characteristics is TDP-43 (Furukawa et al., 2011; Nonaka et al., 2013; Tsuji et al., 2012). Initial histopathological analysis of ALS and FTLD patients found TDP-43 aggregates to be disordered and amorphous in nature and did not reveal any amyloid characteristics (Kerman et al., 2010; Kwong et al., 2008; Neumann et al., 2007b). However, more recent discoveries suggest that a subset of TDP-43 skein-like inclusions do have amyloid properties (Robinson et al., 2012), and subsequent improvement in antigen retrieval techniques has improved the detection of these amyloid characteristics (Bigio et al., 2013). Indeed, in vitro induction of C-terminal fragments (CTFs) of TDP-43 can cause the formation of amyloid fibrils (Chen et al., 2010), and structurally TDP-43 contains amyloidogenic core regions (Jiang et al., 2013). Therefore it is likely that TDP-43 does indeed form amyloid, but the formation of amorphous aggregates could be suggestive of the formation of different structural species of TDP-43. Current evidence also demonstrates that recombinant TDP-43 can form aggregates via a templated seeding reaction in cell culture (Furukawa et al., 2011), and TDP-43 aggregates from diseased ALS and FTLD brains can also reproduce characteristic TDP-43 pathology in cell culture (Nonaka et al., 2013). Together this data suggests that TDP-43 can seed the formation of TDP-43 aggregates in vitro.

The early stages of many neurodegenerative diseases are marked by neuronal dysfunction and protein aggregation which appears to start focally in a specific CNS region, and then becomes more diffuse as the disease progresses. This would indicate that the disease is spreading and propagating through the CNS. Indeed, many of the neurodegenerative disease have been demonstrated to spread throughout the CNS from a focal onset including prion disease (Aguzzi and Rajendran, 2009), Alzheimer's disease (AD) (Braak and Braak, 1991), Parkinson's disease (PD) (Braak et al., 2003), Huntington's (HD)

(Deng et al., 2004), FTLD (Kril and Halliday, 2011) and ALS (Ravits et al., 2007b). In vitro some neurodegenerative disease proteins have also been discovered to propagate between cells, which could potentially account for this pathological disease spread. These proteins include prions (Aguzzi and Rajendran, 2009), α-synuclein (Danzer et al., 2009; Desplats et al., 2009; Hansen et al., 2011; Li et al., 2008), tau (de Calignon et al., 2012; Frost et al., 2009; Kfoury et al., 2012; Liu et al., 2012) and SOD1 (Münch et al., 2011a). More recently TDP-43 has also been demonstrated to propagate in an SHSY5Y neuroblastoma cell line (Nonaka et al., 2013).

To probe further the existing body of knowledge on TDP-43 seeding and propagation, we investigated whether pathological TDP-43 could form a seeding reaction directly from TDP-43 positive ALS brain and spinal cord samples into cells. We also wanted to investigate if these TDP-43 aggregates could then propagate from cell to cell in a prion-like manner. Our findings here demonstrate that TDP-43 can seed the formation of TDP-43 aggregates in vitro directly from ALS brain and spinal cord extracts. The morphology of the pathological TDP-43 inclusions is highly reminiscent of the TDP-43 pathology seen in the ALS patients, and all different morphologies of inclusions can be replicated. We also propose that mutations in the prion-like domain act as a more permissive template for TDP-43 seeding compared to a mutation outside this domain. Finally, we have also demonstrated that TDP-43 can propagate from cell to cell in co-culture experiments. This data further supports the prion-like nature of TDP-43, and if TDP-43 is actually the toxic entity in ALS, then this could be a potential explanation for the spreading and propagative nature of this condition. Indeed, future examination into this phenomenon could use this model to screen for therapies to inhibit this seeding and propagation and potentially disrupt the disease process.

3.2. Results

3.2.1. Seeding and aggregation of TDP-43 from ALS CNS tissue

Previous studies have demonstrated that protein aggregates can be taken up directly from the cell culture medium (Cronier et al., 2004; Ren et al., 2009). Therefore the initial investigations began with the application of crude brain homogenates directly to cell culture. The numerous variables in these experiments including the dilution factor, cell type, incubation period, sonication of the homogenate and removal of cell debris were undertaken (Table 2). Initially, 10% homogenates of control and ALS motor cortex and spinal cord were added to SHSY5Y and HEK293 cells at 1 in 100 and 1 in 1000 dilution for 3 days. This was done to observe for any cytoplasmic mislocalisation and aggregation of TDP-43 using immunofluorescent (IF) staining with the polyclonal TDP-43 antibody. However, this method produced large amounts of non-specific secondary background staining caused by cell debris from the brain homogenate adhering to the cell surface (data not shown). This meant it was difficult to assess for positive cytoplasmic mislocalisation of TDP-43. This non-specific background staining was confirmed with the secondary antibody alone demonstrating nonspecific binding of the secondary antibody to the cell debris resulting in false positive signal (data not shown). To overcome this, the cells were trypsinised after treatment to remove the excess homogenate and re-plated overnight for staining the next day. This successfully removed the background but did not reveal any TDP-43 positive cytoplasmic inclusions. We therefore increased the concentration of brain homogenate applied to a maximum of a 1 in 10 dilution (due to the scarcity of the available ALS tissue) which still did not reveal the formation of any TDP-43 inclusions formed after 3 days of incubation. We also tried longer incubation periods of up to a week with SHSY5Y and HEK293 cells, and up to two weeks with primary cell lines (Table 2). However, again, no TDP-43 pathology formed after treatment as observed with IF staining.

Western blots were then performed on sarkosyl extracted cell lysates to analyse insoluble fractions of these treated cells and blots were then probed for TDP-43 and phosphorylated TDP-43 (pS409/410 antibody or pTDP-43). These blots confirmed the lack of formation of pTDP-43 bands and a lack of 25kDa fragments, which was also observed with IF staining. We

were also unable to observe any increase in insoluble TDP-43 suggesting that TDP-43 was not aggregating (data not shown). Together this data suggests that TDP-43 aggregation cannot be efficiently seeded from unenriched 10% brain homogenates.

To continue these experiments we aimed to enrich for TDP-43 seeds from our brain homogenates in order to produce a seeding reaction. Due to the resistance of TDP-43 aggregates to the detergent sarkosyl, we then purified the brain extracts as done previously in chapter 2 to reveal the pathological forms of TDP-43 (See methods), and resuspended the pellets in sterile PBS. We then used 10µg of protein from these brain extracts and added them to both HEK and SHSY5Y cells and incubated for 3 days. However, upon IF staining or western blotting analysis, no cytoplasmic TDP-43 aggregation or pTDP-43 bands could be observed (data not shown) (Table 2).

In order to distinguish between insoluble TDP-43 seeds inoculated and genuine de novo aggregation, we transiently expressed a full length wild type (FL WT) human TDP-43 construct with an N-terminal FLAG tag on a pCMV2 promoter to overexpress the human TDP-43. Additionally, the overexpression of the disease related protein is commonly used in in vivo transmission studies of other neurodegenerative disease related proteins to reduce incubation periods (Clavaguera et al., 2010; Kane et al., 2000; Luk et al., 2012a). This overexpression is thought to reduce incubation times for seeding reactions by increasing the amount of templating substrate required for seeding. However, even with this FLAG tagged overexpressing human TDP-43 in the cells and addition of brain extracts or homogenates, no TDP-43 pathology could be observed in these cells with IF and western blotting (data not shown).

Cell type	Number of experiments	TDP-43 ALS seed type and amount	Transfection	Incubation period	Sonication	Cell mounting method	Blotted	TDP-43 pathology
SHSY5Y	20	10% - 1/100, 1/10	No	1, 2, 3, 7, 14 days	No	C-slip x10 Tryp x10	x 6	X
SHSY5Y	3	Sarkosyl insoluble-10ug	Yes	3 days	Yes	C-slips		
HEK	5	10% - 1/100, 1/10	No	1, 2, 3, 7, 14 days	No	C-slip x2 Tryp x3	x 8	X
HEK	3	Sarkosyl insoluble - 10ug	Yes	3 days	Yes	C-slips		
Primary rat cortical neurons	2	10% - 1/100	No	0, 7, 14 days	Yes	C-slips	No	X
Primary Mouse motor neurons	1	10% -1/100	No	3 days	Yes + filtration	C-slips	No	X

Table 2. Matrix of experimental variables in initial attempts to seed TDP-43 in vitro to different cell types using control and ALS brain homogenates. This includes the type of TDP-43 seed, incubation periods, sonication, method of cell mounting and the formation of TDP-43 pathology. C-slips = coverslips, 5Y = SHSY5Y, HEK = HEK293, X= No TDP-43 pathology.

More recent publications suggest that cationic lipid transfection reagents can be used for the delivery of protein to cells (Nonaka and Hasegawa, 2011; Nonoka et al., 2010; Weill et al., 2008; Zelphati et al., 2001). Therefore we attempted to use the Lipofectamine 2000 reagent (as previously used by Nonoka et al. 2010) to transfect cells with the ALS motor cortex and spinal cord extracted homogenates using 10µg of protein in cells with and without the FL TDP-43 construct. However, we still could not see any TDP-43 accumulation or phosphorylation by IF and western blotting in cells with or without the construct, suggesting that a seeding reaction did not occur (data not shown).

Whilst conducting this work, Nonaka and colleagues demonstrated a TDP-43 seeding reaction in SHSY5Y and HEK293 cells directly from ALS and FTLD diseased brains (Nonaka et al., 2013). In order to optimise our protocol and verify their observations, we adopted their method of brain extraction which involved a series of smaller spinning steps with only sarkosyl as the detergent in a different homogenization buffer (See Methods). We attempted this extraction method on 4 ALS brain samples and 2 ALS spinal cord samples (Figure 18A). These samples were chosen due to the amount of pathological phosphorylated TDP-43 (pS409/410 or pTDP-43) staining present in each of these cases (A). These sample 10% homogenates underwent the new extraction protocol, and 10µg of insoluble protein from each of these samples were transfected in to HEK293 cells with either no construct, or expressing the FL WT TDP-43 FLAG tagged construct (FL WT). The results were then analysed either with IF staining or western blot analysis comparing sarkosyl soluble (SS) and insoluble (SI) cell fractions. To adequately control for these experiments we used control brain, control spinal cord and Parkinson's disease brain sarkosyl extracted samples (Figure 18). Here we show that transfection of TDP-43 seeds from ALS brain and spinal cord alone into HEK cells did not reveal any SI pTDP-43 pathology after 3 days of incubation on a western blot (Figure 18B). However, IF staining of cells transfected with ALS brain and spinal cord revealed the formation of very small quantities of cytoplasmic pTDP-43 pathology after 3 days incubation, which was not present in controls (Figure 18E). In contrast, transfection of HEK cells with the additional FL WT TDP-43 construct and ALS seeds from brain and spinal cord, revealed pathological pTDP-43 bands in the SI fraction (Figure 18C). Some bands were

appearing in the soluble fractions of the cell lysates with the pS409/410 antibody, but these were found to be non-specific when probed with the secondary antibody alone (Figure 18B). The seeds transfected from the ALS brains more commonly formed the 25kDa pTDP-43 bands compared to the spinal cord samples which only formed the 45kDa pTDP-43 band (appears as ~48kDa due to the added 1kDa FLAG on the construct), which is in agreement with previous observations of enrichment of the 25kDa CTFs in ALS brain rather than spinal cord (Igaz et al., 2008). These pTDP-43 bands in the insoluble fractions of the cell lysates were not present when the cells were transfected with the FL WT TDP-43 alone, or with the control brain or spinal cord and disease controls (Figure 18C, E and F). IF staining of cells transfected with both the FL WT TDP-43 and ALS MC or SC seeds demonstrated the formation of numerous pTDP-43 positive cytoplasmic aggregates, these aggregates co-localised with the FLAG tagged FL WT TDP-43 after 3 days of incubation (Figure 18E). Again, these inclusions were not present in cells transfected with the FL WT TDP-43 alone, control brain or spinal cord tissue (Figure 18C and E) and FL WT plus the Parkinson's disease control (PDC) (Figure 18F).

The fact that this TDP-43 seeding reaction is more efficient in cells expressing the FL WT construct suggested that TDP-43 is overexpressed in these cells. In order to test this we measured the levels of SS and SI TDP-43 on blots with densitometry and corrected for β-actin. D shows the significantly increased expression of endogenous TDP-43 in both the SS and SI fractions in cells expressing the FL WT construct compared to the cells without the construct (***$p<0.001$). This suggests that the reason for the enhanced TDP-43 seeding reaction in cells expressing this construct, is that the increased protein levels of TDP-43 act as an increase in the template substrate for this reaction (Figure 18D). In these experiments we could not detect the ubiquitination of these pTDP-43 aggregates. This may due to a number of reasons including technical difficulties with the ubiquitin antibody, a lack of a positive control to test this antibody or that HEK cells do not readily ubiquitinate aggregates in the same way as neural cell lines. Unfortunately this TDP-43 seeding reaction could not be observed with SHSY5Y cell lines due to the poor transfection efficiency of these cells (data not shown). As a result all further experiments were conducted in HEK293 cells.
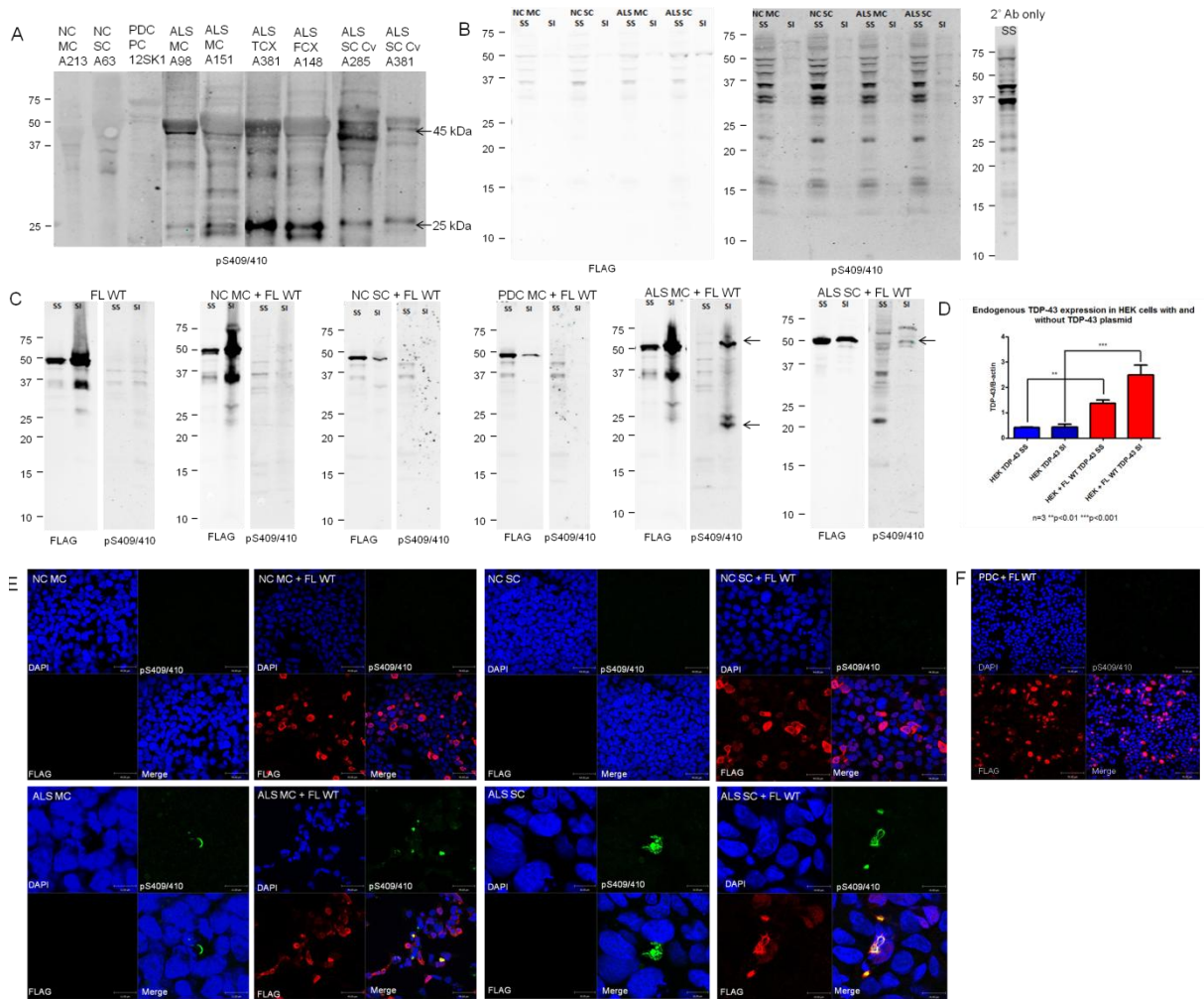
Figure 18. Seeding of TDP-43 from ALS brain and spinal cord to HEK cells. A) Sarkosyl insoluble urea soluble control and ALS patient samples blotted for pS409/410 and used as TDP-43 seeds. B) Sarkosyl soluble (SS) and insoluble (SI) fractions of HEK cells expressing no construct and transfected with 10μg of normal control (NC) and ALS motor cortex (MC) and spinal cord (SC) samples stained with FLAG and pS409/410. C) Sarkosyl soluble (SS) and insoluble (SI) fractions of HEK cells transfected with the FL WT alone and FL WT + 10μg of control and ALS TDP-43 seeds stained with FLAG and pS409/410 antibodies. The pTDP-43 bands are indicated with arrows. D) Quantification of endogenous TDP-43 levels from SS and SI fractions of HEK cells expressing no construct (blue) and expressing the FL WT construct (red). E) IF staining of HEK cells transfected with 10μg control or ALS TDP-43 MC and SC seeds with or without a FL WT construct. F) IF staining of HEK cells transfected with 10μg of Parkinson's disease control (PDC) brain with the FL WT construct. NC = normal control, MC = motor cortex, PDC = Parkinson's disease control, SS = sarkosyl soluble, SI = sarkosyl insoluble, FL WT = full length wild type TDP-43 plasmid. All blots and IF images are representative images of n=3.

121

To ensure that the formation of pTDP-43 pathology seen in Figure 18 was a result of genuine de novo aggregation, and not just the pTDP-43 from the inocula, a time course seeding experiment was conducted over 3 days (Figure 19). The cells were extracted on each day with triton-X (TX) and sarkosyl to produce soluble (SS) and insoluble (SI) fractions. This data shows the formation of the pTDP-43 bands in the sarkosyl insoluble (SI) fraction is not present on day 1 and only occurs after a minimum of 2 days. We therefore concluded that the pTDP-43 bands observed in Figure 18 were not a result of addition of the pTDP-43 positive inocula, and the reaction is a result of genuine de novo aggregation. In addition the ALS SC seeds only formed the 45kDa pTDP-43 band after 2-3 days (Figure 19B), whereas the ALS MC sample formed both the 45 and 25kDa pTDP-43 bands after 3 days (Figure 19A). In the ALS MC treated cells the 45kDa band forms before the 25kDa band from day 2 to 3 suggesting that the cleavage of TDP-43 occurs post phosphorylation (Figure 19A).
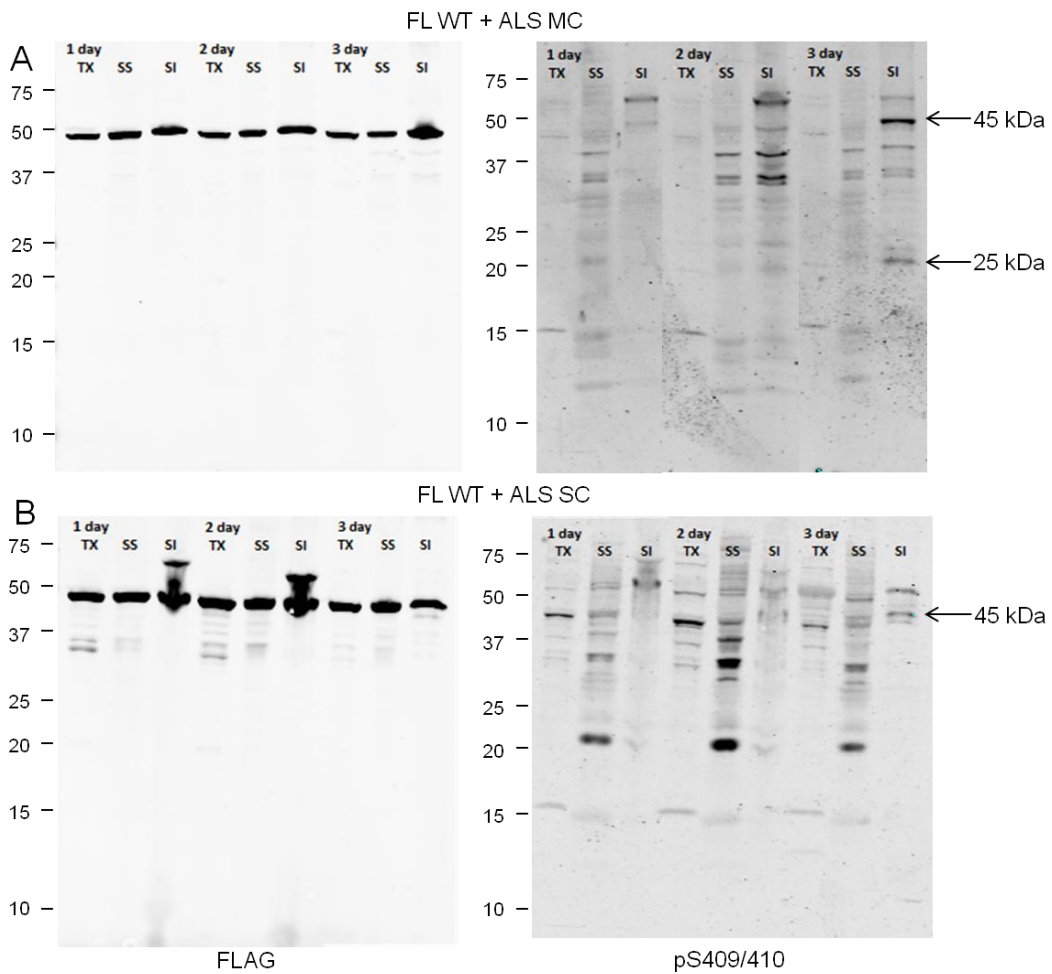
Figure 19. Time course seeding of TDP-43 in HEK293 cells. A) Triton X (TX) and sarkosyl extracted fractions of HEK cells transfected with the FL WT and ALS MC samples over 1, 2 and 3 days stained with FLAG and pS409/410 (pTDP-43). pTDP-43 45 and 25kDa bands (indicated by arrows) appear after 3 days treatment in the insoluble fraction (SI) which are absent on day 1 and 25kDa bands form only on day 3. B) Triton X (TX) and sarkosyl extracted fractions of HEK cells transfected with the FL WT and ALS SC sample over 1, 2 and 3 days stained with FLAG and pS409/410. Only the 45 kDa pTDP-43 band appears after 3 days in the insoluble fraction (SI). TX= triton X, SS= sarkosyl soluble, SI= sarkosyl insoluble.

3.2.2.   *Morphological diversity of seeded TDP-43 inclusions*

TDP-43 inclusions in the brains and spinal cords of patients with ALS can have varying morphologies including pre-inclusions, skein, dot, and round inclusions (Mori et al., 2008). From our IF staining experiments of cells seeded with TDP-43 from ALS brains and spinal cords we found that all these different morphological types of inclusions are directly reproduced in the cells which co-localise with FLAG and endogenous TDP-43 (Figure 20). The co-localisation of the FLAG TDP-43 in the aggregates is highly suggestive of a de novo seeded aggregation reaction. Recruitment of the endogenous TDP-43 in these aggregates suggests that the endogenous TDP-43 is also being used as an additional seeding template alongside the FLAG tagged construct (Figure 20N). These cells also demonstrate the characteristic relocalisation of TDP-43 (FLAG tagged and endogenous) from the nucleus to the cytoplasm (Figure 20 B, C, D, G, H, I, J, K, M, N, O and P) as seen in patients with ALS and FTLD. However, some inclusions are also formed with the FL WT FLAG tagged TDP-43 still present in the nucleus (Figure 20A, F and L), suggestive of an incomplete aggregation process. Additionally, the presence of diffuse cytoplasmic staining in the form of granular 'pre-inclusions' (Figure 20P) suggests that some of these aggregates may still be in the maturation stage (Mori et al., 2008). There are two different types of this diffuse cytoplasmic staining: linear wisps and punctuate granules. Here we demonstrate the formation of both linear wisps (Figure 20O) and punctuate granules (Figure 20P) in cells treated with the FL WT and ALS TDP-43 seeds. Additionally, some round pTDP-43 inclusions can contain radiating spiculae in their margin, or fringes of thread like structures (Lowe et al., 1988; Murayama et al., 1990; Sasaki and Maruyama, 1991). These particular morphological characteristics can also be observed in the pTDP-43 inclusions formed here (Figure 20A, B, F and G), further adding to the reproducible characteristics of the TDP-43 inclusions seen in ALS and FTLD.

Due to the distinct morphological characteristics of these pTDP-43 inclusions, we aimed to observe if they recapitulate the morphological aspects of the pathology seen in each of these ALS patients at post mortem. Table 3 demonstrates the identity of ALS samples, the number of times the reaction was repeated, the types and degree of morphological

inclusions present and whether these inclusions are present in the original pathology. By comparing the morphology of these TDP-43 inclusions to the neuropathology reports, we observed that all ALS seeded samples were able to reproduce the original morphology of TDP-43 inclusions seen in each of the ALS patient samples (Table 3). We also noted that there was a predominance of different types of pTDP-43 inclusion observed in each case. These were given an observed rating (+++ = large number of inclusions, ++ = medium number of inclusions, + = low number of inclusions) to identify the degree of the types of inclusions present. One of the most striking differences we observed was the predominance of the skein inclusions in the ALS A148 FCX treated cells and the predominance of round and dot inclusions in the ALS A381 TCX treated cells. However, ratings of morphological types of pTDP-43 inclusions were not detailed in the neuropathology reports, so no quantitative comparison could be made. Interestingly, the pTDP-43 blots of each of these samples used for seeding demonstrate different 25kDa pTDP-43 bands; the ALS FCX A148 sample had a doublet band where as the ALS TCX A381 has a single pTDP-43 25 kDa band (Figure 18A). This could potentially be a molecular signature for the different morphologies of pTDP-43 pathology present in each case. However, this is only one example and further experiments are required to confirm this. Finally, C9orf72 positive cases of ALS and FTLD commonly have characteristic TDP-43 pathology; therefore we aimed to investigate if TDP-43 inclusions can be seeded from C9orf72 positive cases. In this case we have observed inclusions from this sample (data not shown) (Table 3), however the aggregate numbers were low and this requires further repetition.
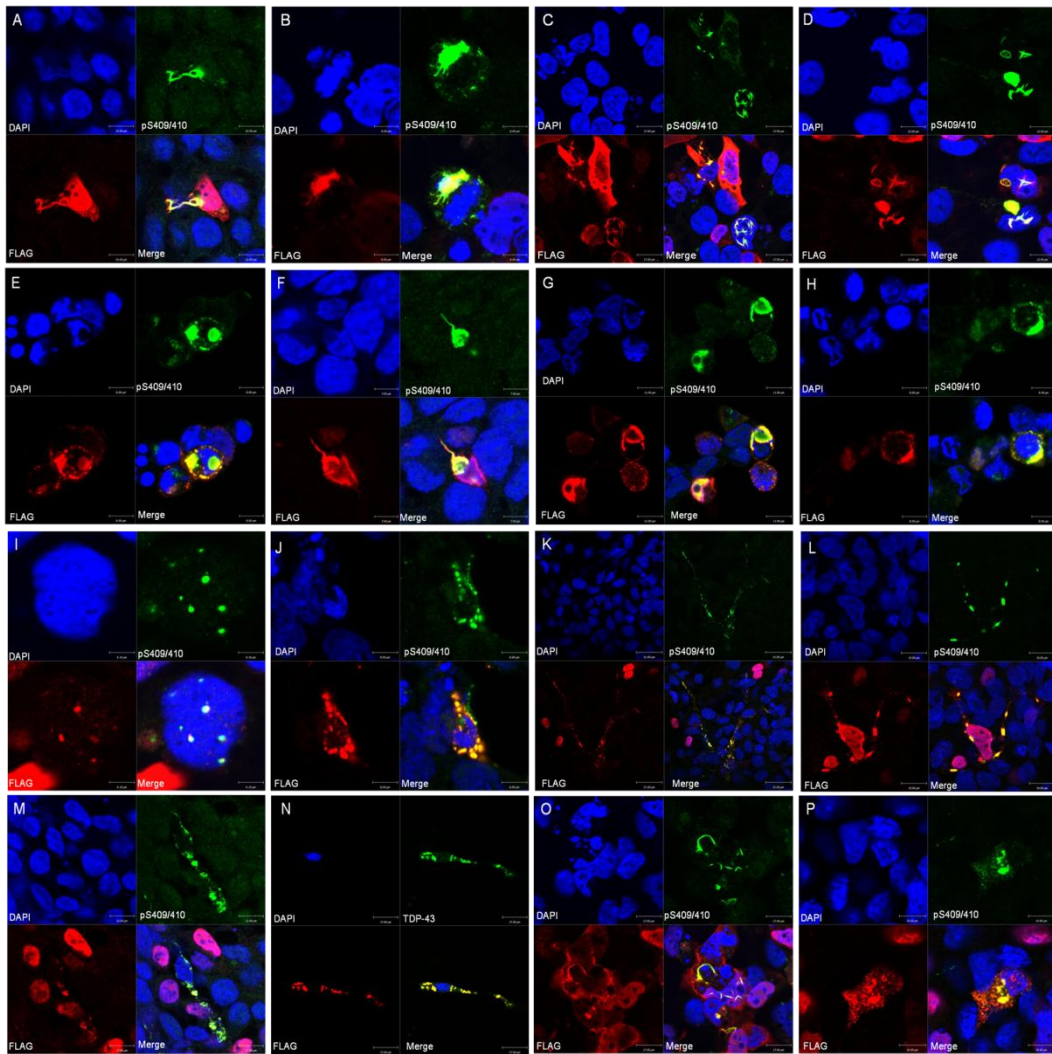
Figure 20. Morphological diversity of pTDP-43 inclusions seeded into HEK cells. A) and B) are skein-like pTDP-43 and FLAG positive inclusions. C) Mixtures of cytoplasmic pTDP-43 and FLAG positive dot and skein-like dash inclusions. D) Mixtures of dash, dense compact and ring inclusions positive for pTDP-43 and FLAG. E) Round pTDP-43 and FLAG positive inclusions. F) Round inclusion with radiating spiculae (racket shaped) positive for pTDP-43 and FLAG. G) Round pTDP-43 and FLAG positive inclusions with radiating spiculae. H) Circular pTDP-43 and FLAG positive inclusion. I) Dot like inclusions positive for FLAG and pTDP-43. J) Numerous dot inclusions positive for pTDP-43 and FLAG. K) Widespread dot inclusions throughout the cell positive for pTDP-43 and FLAG. L) Widespread dot inclusions positive for pTDP-43 and FLAG. M) Large dot inclusions positive for pTDP-43 and FLAG. N) Dot inclusions positive for TDP-43 and FLAG. O) Pre-inclusion with a mix of wispy straight and wavy filaments positive for pTDP-43 and FLAG. P) Diffuse granular pre-inclusion positive for pTDP-43 and FLAG with early coalescence into round inclusions. All images are representative images for the types of inclusions observed in each ALS sample used. Cells were stained for DAPI (DNA/nuclear marker) in blue, pS409/410 (pTDP-43) in green, FLAG in red and all are images merged.

Sample	Number of trials	Skein	Round	Dot	Pre inclusion Filaments	Pre inclusion Granular	TDP-43 inclusion morphology present in original histology
ALS MC A98	3	+++	++	+	+	+	Yes
ALS FCX A148	3	+++	+	+	+	-	Yes
ALS MC A151	1	+	++	++	-	-	Yes
ALS TCX A381	3	+	++	+++	-	+	Yes
ALS SC Cv A285	2	+	+	+	-	-	N/A
ALS SC Cv A381	1	-	+	+	-	-	N/A
ALS SC Th C9orf72 case	1	-	+	+	-	-	N/A
NC MC	13	-	-	-	-	-	-
Disease Control	3	-	-	-	-	-	-

Table 3. Morphological characteristics of seeded pTDP-43 inclusions from ALS patient samples. Table includes the patient samples used, types of inclusions appearing, the numbers of times this was replicated and whether this pathology replicates the original TDP-43 pathology observed in each patient. MC = motor cortex, FCX = frontal cortex, TCX = temporal cortex, SC = Spinal cord, Cv = cervical, Th = thoracic, NC = normal control. +++ = large number of inclusions, ++ = mild number of inclusions, + = low number of inclusions.

3.2.3. *Prion-like domain and TDP-43 seeding*

To further dissect some of the mechanisms that affect the seeding of pathological TDP-43, we generated different mutant constructs of TDP-43 (Figure 21) in order to explore the importance of the prion-like domain between residues 274-414 (Alberti et al., 2009). Using the FL construct and site directed mutagenesis we introduced two known ALS causing mutations D169G and M337V. The M337V mutation is a well-known pathogenic ALS causing mutation that lies within the 'prion-like' domain (residues 274-414), and the D169G mutation is also an ALS causing pathogenic mutation that lies outside the prion-like domain in the RRM1 domain involved in DNA and RNA binding.

First of all we aimed to observe if these constructs alone were capable of inducing spontaneous aggregation and phosphorylation of TDP-43 (pTDP-43). Blotting of these transiently expressing FL WT, FL D169G and FL M337V transfected cells only shows formation of the pTDP-43 pathology (45kDa band) in the sarkosyl insoluble (SI) fractions of the M337V mutation, but not the SI fraction of the FL WT or FL D169G transfected cells (Figure 21B). The reliability of the pTDP-43 staining on a western blot was poor (most likely due to levels of pTDP-43 being at the limits of sensitivity) and therefore we used the more sensitive IF staining to assess the quantity of pTDP-43 inclusions. Using IF staining we found that, in agreement with the western blotting results, the FL WT demonstrated no pTDP-43 inclusions after 3 days of incubation (Figure 21B, D and E). However, transient expression of the FL D169G and M337V mutated constructs resulted in the formation of a small number of cytoplasmic pTDP-43 inclusions after 3 days of incubation (Figure 21D and E). The FL M337V construct demonstrates significantly more pTDP-43 inclusions per FLAG positive cells compared to the FL D169G mutation (***$p<0.001$). This is in agreement with the development of the 45kDa pTDP-43 on the western blots (Figure 21B). Together this suggests that the M337V mutation in the prion-like domain can more readily produce pTDP-43 aggregation than the mutation outside the domain. Blotting of all these constructs revealed a statistically significant increase in the levels of TDP-43 in the SS and SI fractions compared to cells expressing no construct (*** $p<0.001$)(Figure 21C). The insoluble levels of TDP-43 are the most significantly raised (***$p<0.001$) compared to the cells expressing no

construct, but there was no significant difference in the SS or SI fraction levels between any of the constructs (Figure 21C). Figure 21E demonstrates representative images of the pTDP-43 inclusions formed with each construct alone which are present in the mutants but not in the wild type (Figure 21E).
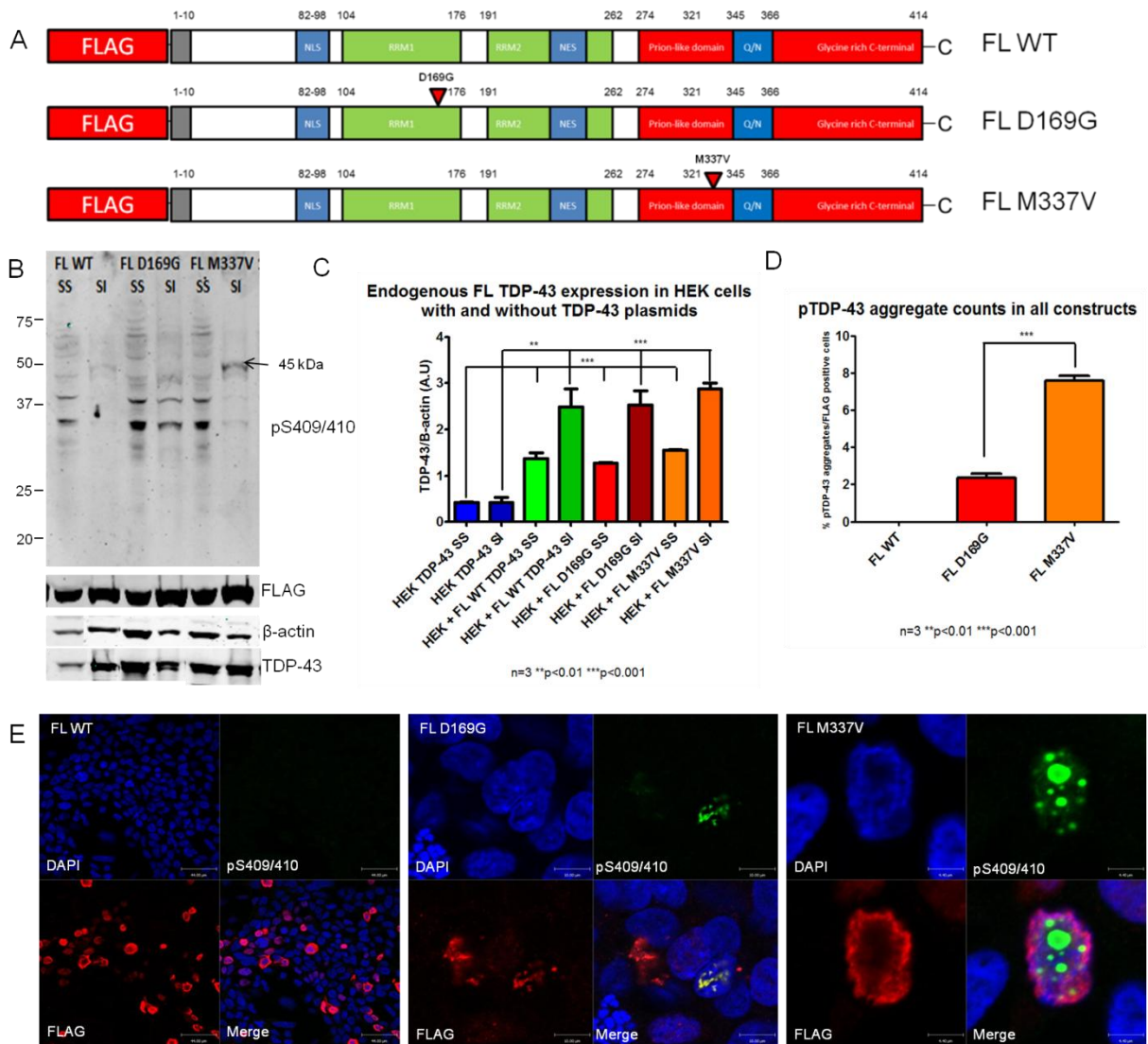
Figure 21. TDP-43 constructs used to assess the effects on mutations on the prion-like domain on TDP-43 seeding in cells. A) Diagrammatic representation of TDP-43 constructs used with mutations outside (D169G) and inside (M337V) the prion-like domain (274-414). B) Blotting demonstrates the presence of a pTDP-43 band in the SI fraction of cells expressing the M337V construct after 3 days. C) Graph of the levels of endogenous TDP-43 in sarkosyl soluble (SS) and insoluble (SI) fractions of cell lysates expressing these constructs after 3 days. D) Graph of pTDP-43 aggregate counts from 10 random fields at 40X magnification with each construct. Results were corrected for the number of FLAG positive cells in each field. E) Image representations of pTDP-43 aggregates found in cells transfected with each construct after 3 days. Cells were stained for DAPI (DNA/nuclear marker) in blue, pS409/410 (pTDP-43) in green, FLAG in red and all images are merged. All results are from 3 independent experiments. Error bars are +/-SEM and statistical analysis was done with an unpaired two-tailed student's t-test with a p value below 0.05 (*p<0.05) considered statistically significant.

After the characterisation of these constructs, we next attempted to investigate any differences these mutations may have on the seeding capacity of TDP-43 in the HEK cells. To do this, we quantified the amount of pTDP-43 protein levels from the SI fractions of cells after 3 days of incubation (Figure 22A and B). This revealed increases in the amount of pTDP-43 protein levels in both the FL D169G and FL M337V compared to the FL WT, with the most substantial increase in the FL M337V mutant (Figure 22B). In addition, we quantified the number of pTDP-43 aggregates induced in cells transiently expressing all constructs and treated with an ALS TDP-43 seed after 3 days. As all the inclusions co-localised with FLAG we corrected the number of inclusions for the number of FLAG positive cells per field of view. This revealed increases in pTDP-43 aggregates in the FL M337V (34%) compared to the FL WT (21%) and FL D169G (18%), but a slight unexpected decrease in the number of pTDP-43 aggregates in the FL D169G (18%) mutant compared to the FL WT (21%) (Figure 22C). Representative IF images of each construct taken at 40X magnification are shown to demonstrate the number of aggregates per field of view (Figure 22D). Indeed, the number of pTDP-43 inclusions observed in the ALS TDP-43 seeded cells were much higher in the FL WT + ALS seed (21%) compared to FL WT alone (0%), in the FL D169G + ALS seed (18%) compared to FL D169G alone (2.35% +/- 0.24%), and in the FL M337V + ALS seed (34%) compared to the FL M337V alone (7.59% +/- 2.48%). Statistical analysis could not be performed on the ALS treated cells here because of the limited number of experimental repeats to date. Therefore these experiments need to be repeated in the future to effectively quantify these effects. Together this initial data suggests that the M337V mutation in the prion-like domain enhances the formation of pTDP-43 pathology compared to the WT and D169G mutation.
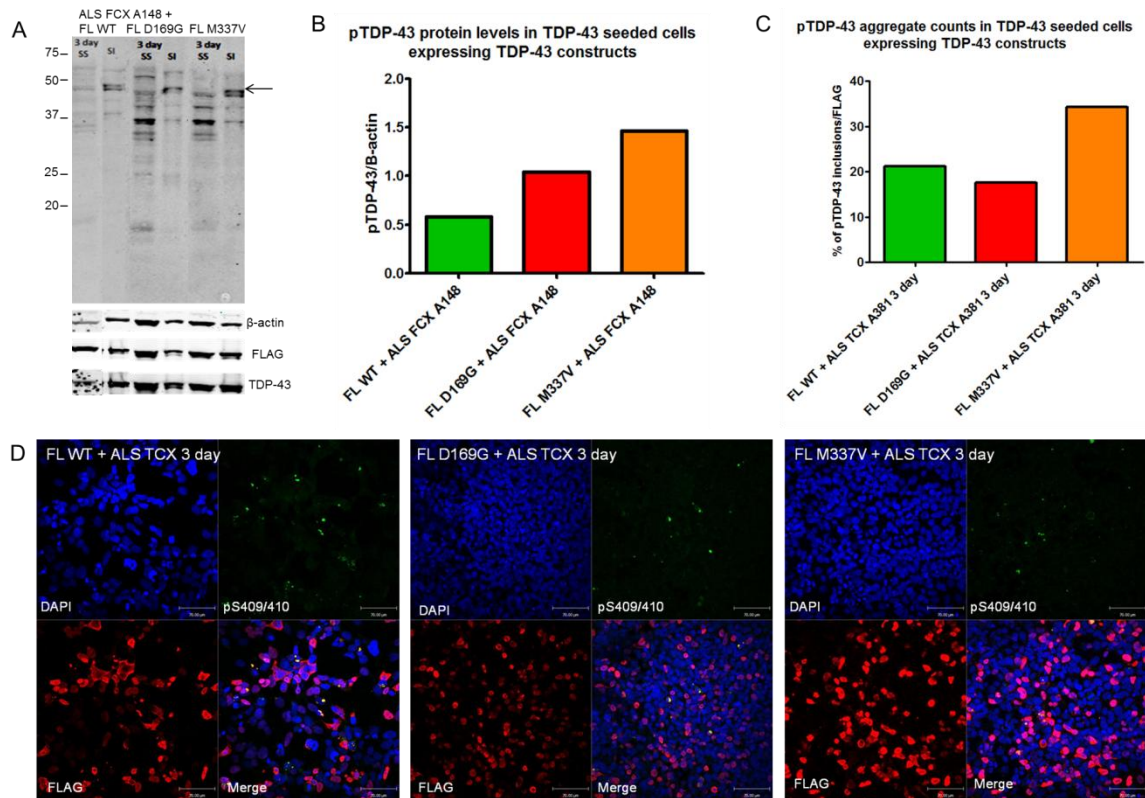
Figure 22. All TDP-43 constructs seeded with ALS TDP-43 seed. A) Blot of sarkosyl soluble (SS) and insoluble (SI) fractions of HEK cells transiently expressing all TDP-43 constructs after 3 days of incubation. Blot was probed for pTDP-43 (pS409/410), β-actin, FLAG and TDP-43. B) Quantification of pTDP-43 levels after 3 days of incubation in the sarkosyl insoluble (SI) fractions of cells expressing constructs and treated with ALS FCX A148 seeds. All pTDP-43 levels are corrected for β-actin. C) pTDP-43 aggregate counts in cells expressing all TDP-43 constructs and treated with ALS TCX A381 seeds after 3 days of incubation. Cell counts are from 10 random fields of view at 40X magnification and corrected for by the number of FLAG positive cells in each field of view. D) Representative IF images of cells treated with all TDP-43 constructs and treated with ALS TCX A381 for 3 days. Cells were stained for DAPI (DNA/nuclear marker) in blue, pS409/410 (pTDP-43) in green, FLAG in red and all images are merged.

3.2.4. *TDP-43 propagation*

In order to assess whether TDP-43 inclusions can spread from cell to cell in a prion-like manner, we co-cultured cells containing pTDP-43 inclusions and mixed them in a 1:1 ratio with cells expressing GFP. The cells expressing GFP were used as markers of 'acceptor cells' or naïve cells for the potential uptake of aggregates in the propagation process. These cells were then further cultured for 3 days and immunostained for pTDP-43 (pS409/410) and analysed for the presence of pTDP-43 aggregates within cells expressing GFP. Figure 23A and B are representative images of cells containing pathological cytoplasmic pTDP-43 inclusions which also express GFP. The 3D reconstruction of these images show the presence of the cytoplasmic inclusion in all XYZ axes (Figure 23A and B), and the intensity distribution profiles show the presence of the pTDP-43 inclusion (red line) with GFP (green line) and its cytoplasmic localization (nucleus is the blue line) (Figure 23C and D). This indicates that the inclusions of pTDP-43 from the original seeded cells are now present in the acceptor cells, which is further suggestive of pTDP-43 aggregate propagation from cell to cell. After 3 days the number of cells expressing GFP and pTDP-43 inclusions was very low and deemed unquantifiable, indicating that aggregate spreading may be a slow process. As an additional method of exploring pTDP-43 aggregate propagation we also attempted to use conditioned media from cells treated with ALS seeds and incubate this conditioned media on fresh naïve cells for 3 days. In this case we were unable to observe the formation of any pTDP-43 inclusions in cells treated with the conditioned media (data not shown).
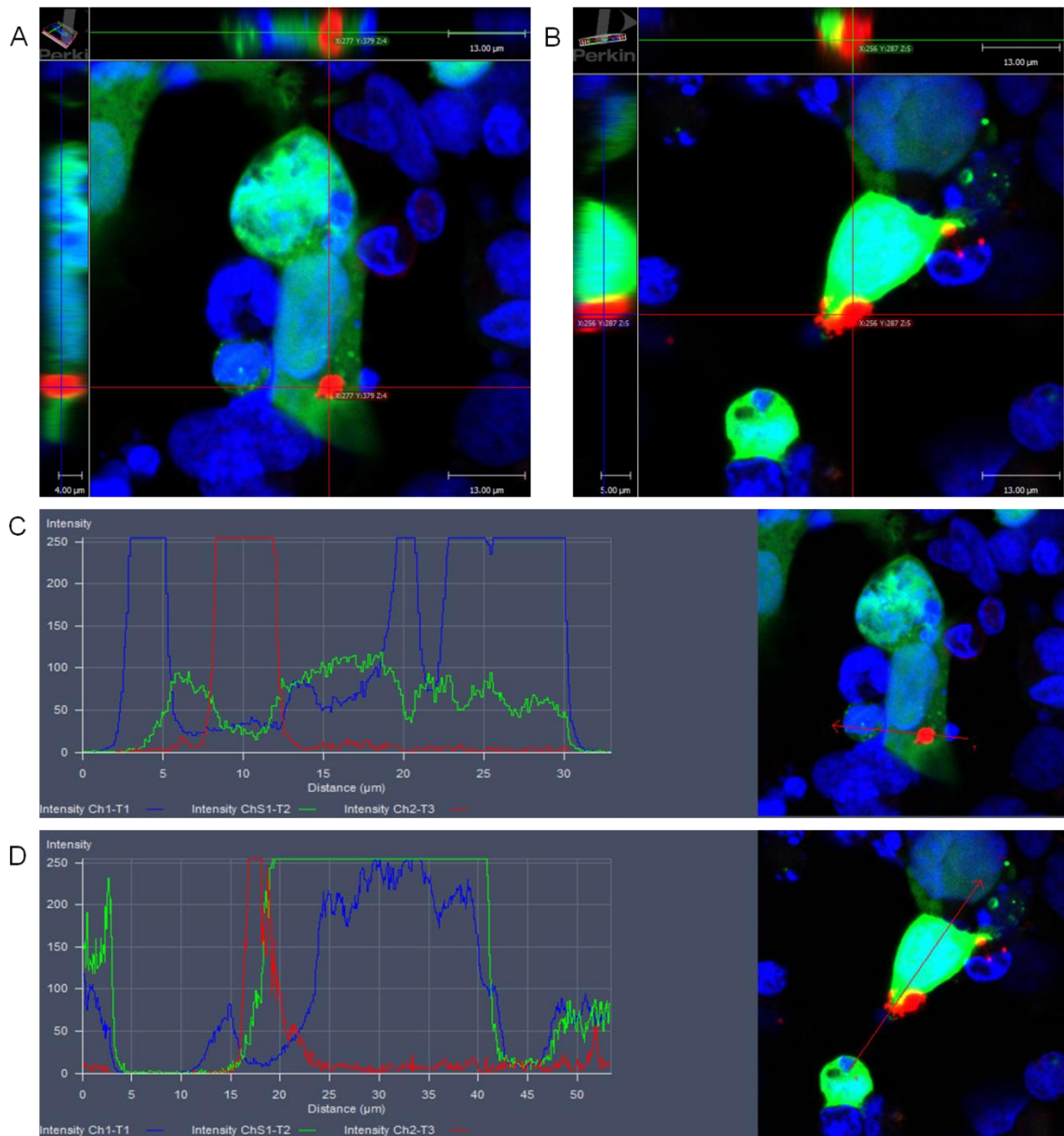
Figure 23. Propagation of pTDP-43 aggregates to naïve cells expressing GFP. Co-culture of cells containing pTDP-43 aggregates and cells expressing GFP in a 1:1 ratio. After 3 days of incubation the cells were stained with pS409/410 (pTDP-43) (Red) and DAPI (Blue). Images (A) and (B) are 3D reconstructions of cells with pTDP-43 aggregates (Red). The red lines represent the X-Y axis, the green line represents the X-Z axes and blue line represents the Y-Z axes. Images (C) and (D) are intensity distribution profiles of images (A) and (B) respectively, with blue lines representing DAPI, green lines representing GFP and red line representing pTDP-43 in a merged image. All images are representative of 3 independent experiments.

3.3. *Discussion*

Developing cellular models of TDP-43 protein aggregation has been the focus of many studies in order to understand the protein aggregation process and some of the molecular mechanisms underlying the disease process in ALS or FTLD (Dewey et al., 2012). To date most studies have utilised the overexpression of mutant, expanded, deleted or truncated constructs and chemical modification to induce the aggregation of TDP-43 (van Eersel et al., 2011; Johnson et al., 2009; Nonaka et al., 2009a, 2009b; Wang et al., 2013). Here however we have developed a TDP-43 aggregation model that can be reproduced directly from the CNS of patients with ALS. As well as the development of this aggregation model, the means of its production involved the demonstration of a key prion-like characteristic of TDP-43. Indeed, the demonstration of the prion-like seeding of TDP-43 was a long and difficult process with the testing of a number of different methods and variables in order to reproduce this reaction in cells (Table 2). The main issues in getting the reaction to work included the correct extraction and purification of the TDP-43 seeds from the CNS, the correct choice of ALS sample with sufficient pTDP-43 pathology and the method of introduction of these seeds into the cells. Indeed, the crucial factor appeared to be the extraction of the CNS tissue in sarkosyl alone which may have allowed for the liberation of the seeds of TDP-43. Once this had been optimised we also discovered that this reaction did not work in SHSY5Y neuroblastoma cells as they do not transfect well. Therefore the choice of cell line also proved crucial, and as such we used HEK cells due to their high transfection efficiency.

Once the protocol was established we demonstrated the formation of pTDP-43 aggregates in cells from ALS brain and spinal cord tissue with and without an overexpressed FL WT TDP-43 construct (Figure 18C and E). However, the FLAG TDP-43 construct expressing cells developed significantly more inclusions than without the construct as detected by blotting and IF staining (Figure 18B, C and E). In addition the levels of endogenous TDP-43 in cells with the FL WT construct were significantly higher in the cells transiently expressing the FL WT construct (***p<0.001) (Figure 18D). Together this suggests that the seeding reaction was enhanced in cells expressing the construct, and the elevated levels of endogenous TDP-

43 in the FL WT expressing cells may be enhancing aggregation by acting as an increased templating substrate for the seeding reaction (Figure 18D). In order to assess the specificity of this reaction to ALS CNS tissue we used normal control motor cortex (NC MC), spinal cord (NC SC) and Parkinson's disease (PD) CNS tissue extracts to ensure the lack of formation of pTDP-43 aggregates with any of these samples (Figure 18C and E), and we also used the construct alone to ensure that the expression of the construct was not the cause of aggregation (Figure 18C).

To ensure that this pTDP-43 pathology observed was not due to the initial inocula added to these cells, we performed a time course seeded experiments over 1, 2 and 3 days using both ALS MC and SC (Figure 19). The formation of pTDP-43 bands in the ALS MC and SC treated cells in the SI fractions of cells formed at 2 days which increased at 3 days, this indicates that this reaction takes place over time and is not due to the presence of the pTDP-43 in the inocula. Interestingly, the pathological pTDP-43 bands observed after 3 days of incubation included the 45kDa and 25kDa doublet in the ALS MC treated cells and the 45kDa band in the ALS SC treated cells. This supports previous findings that the 25kDa pTDP-43 bands are preferentially enriched in the brain and not the spinal cord (Igaz et al., 2008). Indeed, these C-terminal fragments may develop over longer periods of time and therefore longer incubation periods may demonstrate the formation of these 25kDa C-terminal fragments. This finding is supported by the Nonaka et al study who demonstrated that the 25kDa fragments form post pathological phosphorylation of TDP-43 (Nonaka et al., 2013). If these C-terminal fragments are more prone to develop in the brain it would suggest that the pathogenic TDP-43 in the spinal cord of ALS patients may not be cleaved by caspases which could reflect some of the differential toxicities of the protein in different regions of the CNS. To assess any toxic effects of this induced pTDP-43 seeding and aggregation on the HEK cells we conducted an MTT assay on these cells and did not observe any toxicity (data not shown). The lack of toxicity observed may be due to the assay method, the cell type, the high degree of cell proliferation which exceeds the aggregation kinetics, or that the TDP-43 aggregation process is not toxic. As Nonaka et al noted that the presence of pTDP-43 pathology correlated with an increase in cellular toxicity in the neuroblastoma SHSY5Y cell

line with an LDH assay (Nonaka et al., 2013), we suspect that the human embryonic kidney cell line is not as susceptible to TDP-43 mediated toxicity as a neural cell line. This could be due to the efficient clearance mechanisms (UPS and autophagy etc) observed in HEK cells, or other specific physiological properties of neural cells that make them more receptive to TDP-43 mediated neurotoxicity.

Our next observation was the development of morphological characteristics of pTDP-43 pathology developed in our cells. TDP-43 inclusions take on the form of either skein, round, dot or granular 'pre-inclusions' (Mori et al., 2008). The presence of 'pre-inclusions' in these cells indicates that some pTDP-43 aggregates are still immature, suggesting that with longer incubation periods they will mature into larger inclusions. It is thought that fine pTDP-43 positive filaments and wisp inclusions eventually mature into coarse thick skein inclusions, and round inclusions arise from the maturation of punctate granules (Mori et al., 2008). However, this hypothesis is difficult to test due to the need to focus on individual cells and long observation periods needed. All of these inclusions were detected in our cells in different samples and the images represented here are characteristic of the typical appearance within the cells (Figure 20). Interestingly, morphological strain types have now been characterised in Aβ transmission experiments in APP transgenic mice (Heilbronner et al., 2013), and the different morphologies of pTDP-43 pathology present here appear to match the type and proportion of pTDP-43 inclusions in each patient (Table 3). From the samples used for seeding here, there was a significant contrast in the morphological type of pTDP-43 inclusion produced between the ALS FCX A148 sample, which consistently reproduced a predominance of skein inclusions, and the ALS TCX A381 sample, which consistently reproduced round and dot inclusions. Intriguingly, the sarkosyl insoluble and urea soluble fractions of these samples have different pTDP-43 25kDa bands. The ALS FCX A148 sample has a doublet 25 kDa band and the ALS TCX A381 sample had a single pTDP-43 band (Figure 18A). Therefore, this different morphology of pTDP-43 inclusions may be reminiscent of morphological strain types, which could have a molecular signature in terms of the presence of a single or doublet pTDP-43 band on a blot. However, this is a first observation and more experimental repeats will be needed to confirm these observations.

The morphological appearance of pTDP-43 inclusions here do not correlate to any particular ALS phenotype criteria based on available information (data not shown), but this may become more apparent with a further characterisation of these inclusions. Indeed, the presence of amyloid positive skeins in a subset of patients with ALS suggest that different structural types of TDP-43 inclusions may exist (Robinson et al., 2012). Therefore staining the inclusions observed here with ThT, ThS or Congo red for amyloid may help characterise this further. Also for clinical phenotype comparison we will require more detailed clinical and pathological reports with distinct characterisation of these TDP-43 inclusions.

To probe this cellular model further we investigated the importance of the prion-like domain. To do this we utilised TDP-43 constructs containing pathogenic ALS causing mutations. One construct contained a pathogenic mutation outside the prion-like domain (D169G) and one construct has a mutation inside the prion-like domain (M337V) (Figure 21A). Using both western blotting and aggregate counts in cells, we noted that the FL M337V was more prone to producing pTDP-43 pathology (Figure 21B and D). In addition to this, the levels of sarkosyl insoluble endogenous TDP-43 measured did not significantly differ between each mutant and wild type construct (Figure 21C), suggesting that the insoluble levels of TDP-43 are not responsible for increased pTDP-43 pathology observed in these constructs and that this is due to the presence of the pathogenic mutation.

Once these constructs were characterized, we then quantified the levels of pTDP-43 and number of pTDP-43 aggregates formed after a 3 day treatment with an ALS TDP-43 seed in HEK cells expressing the FL WT, FL D169G and FL M337V constructs (Figure 22). However, the results are only from 1 experiment to date and must therefore be interpreted with caution, in this case we found that the M337V mutation produced higher levels of pTDP-43 45 kDa as determined by western blotting, and a significant increase in aggregate numbers on IF analysis (Figure 22). This could suggest that the M337V mutation is producing greater pTDP-43 pathology with the addition of the TDP-43 seed, or that the M337V mutation enhances the formation of pTDP-43 pathology by acting as a more permissive template for the TDP-43 seeding reaction (Figure 22). To further add to this, the results should be repeated and additional time points of 1 and 2 days should be added to investigate whether

these mutations can accelerate the formation of pTDP-43 pathology upon the addition of a TDP-43 seed. Therefore a mutation in the prion-like domain, such as the M337V mutation, may make the protein more prone to misfolding and aggregation and a mutation in this domain may act as a more efficient template to increase the levels of pTDP-43 pathology. However, further analysis should be conducted on the effects of this mutation including examining the rate of pathology development and the toxicity of each construct alone, and upon the addition of the ALS CNS extracted seeds. To thoroughly investigate the effects of this prion-like domain on the seeding activity of TDP-43, it will be a useful to examine a number of other pathogenic mutations in this domain, and also develop a prion-like domain deletion construct of TDP-43. Ultimately this will give us a unique insight into the seeding process and if this domain is essential for a TDP-43 seeding reaction. It will also be useful to develop an array of constructs with various deleted domains to investigate what the exact essential seeding domains are. In addition these experiments should preferably be carried out in a neuronal cell line, which may be more appropriate to accurately assess the physiological characteristics associated with these seeding reactions.

Finally, we investigated whether pTDP-43 aggregates could propagate from cell to cell in a prion-like manner. After co-culturing cells containing pTDP-43 aggregates with 'acceptor' cells expressing GFP in a 1:1 ratio for 3 days, numerous aggregates were formed and survived the co-culture. Most cells containing aggregates in this co-culture were not expressing GFP which suggests that they were the original 'donor' cells. However, a small number of cells did express both GFP and contained cytoplasmic pTDP-43 aggregates suggesting that these aggregates are indeed propagating to new cells (Figure 23). The low incidence of propagation is most likely due to the short incubation times. Therefore longer co-culture incubation periods with stable GFP expressing HEKs could yield a higher propagation rate. However, from our results it does suggest that the pTDP-43 aggregates do propagate from cell to cell in a prion-like manner. To investigate this further we attempted to use conditioned media experiments from cells containing pTDP-43 aggregates after 3 days. However, we were not able to observe the development of pTDP-43 pathology on these conditioned media treated cells (data not shown). This could be due to the short

incubation times or sub optimal experimental conditions. Alternatively the cells may require closer contact for signalling mechanisms required in this propagation process.

Nonaka et al have demonstrated the presence of TDP-43 in the exosomal fractions of cells expressing TDP-43 and treated with the ALS extract, which suggests that TDP-43 pathology is propagated at least partly via exosomes (Nonaka et al., 2013). Additionally, recent studies utilising the staging of pTDP-43 pathology in the brain (Brettschneider et al., 2013), and the spinal cord (Brettschneider et al., 2014), suggest that pTDP-43 pathology may propagate transynaptically in an anterograde fashion along corticofugal axonal projections (Braak et al., 2013). Indeed, this is supported by data from the same group showing significant diffusion tensor imaging (DTI) changes along the selected regions originally measured from the pathological staging (Kassubek et al., 2014). However, as mentioned earlier the staging of pTDP-43 observed here did not correlate with any clinical features of ALS including site of onset, age of onset, disease duration or the ALS Functional rating score – revised (ALSFRS-R) (Brettschneider et al., 2013, 2014). In contrast to this, the changes in DTI signal measured by Kassubek et al demonstrated a significant correlation between disease duration and the ALSFRS-R. The discrepancy between these two findings may be that TDP-43 deposition does not correlate with ALS phenotype, but other intermediates of TDP-43 aggregation may be toxic to the cells, and the TDP-43 deposited may be the remnants of this toxic spread of pathology. This again supports our data from chapter 2 (Figure 17) that the differential deposition of pTDP-43 may not be correlated with different disease stages. More importantly the same group followed up their pathology pTDP-43 staging study in the brain, with a similar staging study in the spinal cord (Brettschneider et al., 2014). This study revealed that the most significant pTDP-43 pathology occurred in lamina IX of the cervical and lumbar segments of the cord, but pTDP-43 deposition was also detected outside these motor regions in some cases. Although neuronal loss and pTDP-43 deposition correlated with disease duration in extremity onset cases, stages of pTDP-43 did not correlate with the ALSFRS-R (Brettschneider et al., 2014). This backs up their previous findings on pTDP-43 deposition and clinical phenotype correlation (Brettschneider et al., 2013). Interestingly the same group report that gray matter oligodendrocytes may act as

harbingers of pTDP-43 pathology, as pTDP-43 oligodendroglial inclusions are frequently found in areas devoid of neuronal loss and neuronal and white matter pTDP-43 pathology (Brettschneider et al., 2014). The collective data here supports our findings of a cell to cell spreading of pTDP-43 pathology.

The exact cellular mechanisms for pathological TDP-43 spread still remain elusive. Asides from exosome propagation of pTDP-43, other mechanisms of potential aggregate spread include free floating aggregates or seeds, or nanotubule transmission as seen previously with prions (Gousset et al., 2009) still remain a possibility. Additionally, the method of seed uptake by the recipient cell has still yet to be discovered. These potential methods of uptake could include direct penetration of the plasma membrane, fluid phase endocytosis, or receptor mediated endocytosis. Indeed, SOD1 has recently been shown to propagate via exosomes and free floating aggregates and seeds which are taken up by lipid raft macropinocytosis (Grad et al., 2014; Münch et al., 2011a). Uptake of TDP-43 could also potentially occur via various other protein dependent uptake mechanisms such as clathrin, calveolin and dynamin mediated endocytosis. Therefore the investigation of the exact mechanisms of this propagation will provide essential clues to target these mechanisms in an attempt to arrest TDP-43 propagation.

3.4. Future Work

Now that TDP-43 seeding and propagation has been effectively demonstrated, this marks the starting point for a further detailed investigation of this phenomenon, and how it can be used to model ALS and FTLD effectively in vitro and in vivo. First of all, the seeding of TDP-43 should be reproduced in an appropriate neuronal cell model. This could include primary cortical neurons, primary motor neurons, mouse motor neuron like hybridoma cell lines (e.g. NSC-34) and human iPS cell lines. Indeed, seeding in each of these cell lines will need to be tested with and without the human TDP-43 construct overexpression to ensure that this reaction can work effectively as demonstrated here and in Nonaka et al. 2013. Some of these cell lines like primary motor neurons and human iPS cells will not tolerate the standard transfection reagents such as Lipofectamine. Therefore other transfection methods such as magnetofection and electroporation may be more appropriate for gene

and protein delivery to these cells. These cell types will be more useful in the assessment of TDP-43 pathology development, cellular toxicity induced by this TDP-43 seeding reaction, and other physiological consequences of this seeding reaction. In addition, this seeding reaction could be continued for longer time periods and sequential imaging of the seeded cells could allow us to monitor the maturation and movement of the aggregates, and track the spreading and propagation process. Due to the mainly selective degeneration of motor neurons in ALS, we predict that certain cell types may be more susceptible than others to this seeding and propagation of TDP-43. Therefore the selective culture of astrocytes, microglia, oligodendrocytes, motor neurons and mixed co-cultures could indicate which kind of cell type the TDP-43 seeding reaction prefers, and which cell type is more vulnerable to TDP-43 mediated toxicity.

Recent reports suggest that certain regions of the TDP-43 protein are essential for seeding, aggregation and propagation (Liu et al. 2013; Saini & Chauhan 2011). We therefore hypothesize that certain regions of TDP-43 may be required for this TDP-43 seeding reaction to occur, and in particular the core aggregation sequence and prion-like domain. To investigate this further, a number of other mutants and truncated TDP-43 constructs in critical regions of the protein would help to elucidate the involvement of each region of the protein in the seeding reaction and propagation. Indeed, if an essential region could be highlighted within the protein then it could be possible to target these regions for therapy with antisense oligonucleotides (ASOs) or antibodies to halt this seeding and propagation reaction. Providing this TDP-43 seeding reaction is a prominent cause of cellular toxicity, this targeted reduction of misfolded TDP-43 seeding and inhibition of propagation may halt disease progression and spread.

One of the key findings in current TDP-43 research is to identify if there is a specific cellular toxic species. Previous studies on prions, Aβ, tau and α-synuclein (Benilova et al., 2012; Kalia et al., 2013; Simoneau et al., 2007; Ward et al., 2012) have shown that the toxic species of each of the proteins are thought to be intermediate soluble oligomeric species. Therefore, due to the similar aggregation and seeding properties of these proteins, we predict that the oligomeric species of TDP-43 may also be the toxic species for TDP-43

induced neurodegeneration. To test this hypothesis, a number of different aggregated forms of synthetic wild type and mutant TDP-43 including monomers, oligomers and fibrils could be added to an appropriate neuronal cell type to assess for cellular toxicity with the use of MTT, LDH and propidium iodide and TUNEL staining.

Finally, to assess the mechanisms for TDP-43 propagation it will be useful to verify the exosome mediated transport mechanism described in the Nonaka study (Nonaka et al., 2013), but also to fully explore all the other mechanisms of propagation. These mechanisms include free floating seeds that can directly penetrate the plasma membrane of the recipient cells, or uptake via endocytosis or nanotubules. Indeed, if the process is thought to occur by endocytosis, it will be useful to investigate whether this endocytosis is clathrin dependent mediated or clathrin independent mediated endocytosis such as calveolae mediated uptake, macropinocytosis, or phagocytosis (Marsh, 1999). Further repetition of the conditioned media experiments will help to determine if these seeds are secreted to the medium and will indicate whether propagation of pTDP-43 pathology require cell to cell contact, or if it can occur in a non-cell autonomous manner. Highlighting the role of all of these pathways in the transfer of TDP-43 aggregates, will increase the number of potential therapeutic targets for inhibiting this propagation and potentially disease spread.

3.5. Conclusion

Here we have demonstrated that TDP-43 has a cellular prion-like behaviour. This behaviour includes the time dependent seeded aggregation of TDP-43 aggregates directly from ALS CNS tissue, directly reproducible morphologically diverse TDP-43 aggregates, a mutated prion-like domain which enhances the seeded aggregation of TDP-43 and the cell to cell propagation of TDP-43 with co-culture. Some of these findings including the seeded aggregation and propagation of TDP-43 from diseased ALS brains are backed up by parallel studies from Nonaka and colleagues (Nonaka et al. 2013). These findings have now established a foundation for further investigation in to this cellular model. Compared to other cellular models of TDP-43 aggregation, this cellular model circumvents the need for expansions, mutants, truncations or chemical modifications. In addition to this, our model is a more accurate representative of disease related TDP-43 aggregation due to the reproduction of this pathology directly from diseased ALS brain and spinal cord. Once this model has been further developed, the potential of this method of disease modelling is enormous and will most likely prove to be the most accurate in vitro model of TDP-43 mediated toxicity in neurodegenerative disorders such as ALS and FTLD. Ultimately the goal is to investigate the mechanisms of TDP-43 aggregate spread and toxicity using this novel cellular model in an attempt to highlight potential neuroprotective targets for inhibiting disease spread and ameliorating toxicity in these devastating disorders.

Chapter 4

Prion-like transmission of TDP-43 in vivo

4. Prion-like transmission of TDP-43 in vivo

4.1.   Introduction

One of the defining characteristic of prion diseases is their infectivity. Infectivity is the capacity to cause disease by transferring the infective agent from one individual to another (Prusiner, 1998). Indeed, a key aspect in demonstrating the prion-like nature of proteins is to be able to transmit the protein pathology into mammalian species using misfolded protein seeds taken from various sources. This was first successfully demonstrated in the prion diseases, and has now been demonstrated with various other neurodegenerative disease related proteins (Jucker and Walker, 2013). The main criteria for the prion-like behaviour of a disease related protein is for it form a seeded templating reaction with the host endogenous protein, to spread from cell to cell and to have different structural conformations or 'strains'. This set of criteria was initially founded by prion studies and was extrapolated to investigations into other neurodegenerative disease related proteins.

4.1.1. Prions

The transmissibility of prion disease was first experimentally demonstrated back in 1966 from transmission of a kuru-like syndrome to chimpanzees (Gajdusek et al., 1966). These experiments were conducted based on the pandemic outbreak of kuru in the islands of Papa New Guinea. From these experiments, it was shown that kuru could be transmitted between human hosts as a result of endocannabilistic rituals within this population (Gajdusek and Zigas, 1957; Zigas and Gajdusek, 1957). These observations led to the 'protein-only' hypothesis (Griffith, 1967), which states that the infectious agent in these conditions is a misfolded protein. The hypothesis also states that this misfolded protein can then subsequently induce its abnormal conformation on to the normal host protein, and be replicated in the absence of nucleic acids. This seeded templating of pathological proteins is then thought to aggregate in the form of β-sheet rich structures called 'amyloid'(Griffith, 1967). This hypothesis is now widely accepted with the premise being that the infectious agent in these conditions is indeed a misfolded form of the normal prion (PrP^C) protein ('PrP^{Sc}') (Prusiner, 1982). The evidence to further support this hypothesis comes from

numerous transmission studies of prions into various animal hosts and humans (Brown et al., 1994). In mammals, prion diseases are often referred to as transmissible spongiform encephalopathies (TSEs) which include bovine spongiform encephalopathy (BSE), transmissible mink encephalopathy (TME) and chronic wasting disease (CWD) in deer and elk. Variants of prion diseases in humans occur as Creutzfeld-Jakob disease (CJD), variant CJD (vCJD), fatal familial insomnia (FFI), Gerstmann-Straussler-Scheinker syndrome (GSS) and kuru (Prusiner, 1998). Prion diseases have also been shown to be iatrogenically transmitted to humans, where the protein can be passed via blood transfusions, tissue grafts, organ and hormone transplantation and infected surgical equipment (Barrenetxea, 2012). In addition to infectious prions, some prion diseases can be genetic or sporadic. Genetic or sporadic prion diseases occur with an age related stochastic misfolding and nucleation of PrP into PrP^{Sc}, which takes the form of a self-propagating seed. Once this prion infection occurs the prions grow, fragment and spread throughout the CNS ultimately leading to dysfunction of the nervous system and death of the infected cells. Pathologically this appears as a loss of neurons, gliosis, spongiform vacuolation and accumulation of aggregated prion protein (DeArmond and Prusiner, 1995). There are a large number of different sized prions, but the most effective prions used as seeds were found to be the small soluble species (Silveira et al., 2005). Indeed, more recent evidence suggests that the oligomeric forms are more toxic to the CNS, in comparison to prion monomers and fibrils (Simoneau et al., 2007).

One of the issues with transmitting prion-like proteins in vivo is known as the 'species barrier'. Some prion transmission studies with hamster PrP in mouse show that non transgenic wild type mice are not susceptible to hamster Sc237 prions, unlike transgenic mice expressing hamster PrP which are very susceptible to hamster prions (Prusiner et al., 1990). Therefore the primary structure of the endogenous prion protein in the host is thought be of significant importance in facilitating a seeded templating reaction of prions. This is also seen in human prion cases, as sporadic and acquired CJD occurs mainly in individuals who are homozygous at the polymorphic residue 129 of PrP. This suggests that the interaction of PrP^{Sc} seeds and host PrP^{C} for the propagation of pathology requires

similar sequences (Collinge, 2001; Collinge et al., 1991; Palmer et al., 1991). However, prion disease can behave differently and have varying pathologies within and amongst species. Indeed, vCJD was found to be more permissive to wild type mice expressing no human PrP transgene than mice expressing the human PrP transgene, suggesting that prion transmission may not have a 'species barrier' as such, but a 'transmission barrier' instead dependent on protein sequence homology (Hill et al., 1997).

One of the key aspects of prion propagation is the development of structurally unique 'strains'. The identification of strains of prions came from immunoblotting sporadic, iatrogenic, and variant CJD brain samples from patients. Sporadic, iatrogenic and vCJD were found to contain varying amounts of glycosylated and unglycosylated isoforms of the prion protein after proteinase K digestion. Each prion phenotype was found to contain a unique ratio combination of these glycosylated and unglycosylated PrP isoforms (Collinge et al., 1996). These samples were then experimentally transmitted in mice and found to produce similar PK resistant fragments and ratios of glycosylated prions in the infected mouse brain homogenates. These banding ratios were demonstrated to breed true after serial propagation to new mice, suggesting that these are structurally unique conformations or strains of PrP^{Sc} for each phenotype (Collinge et al., 1996). Additionally, polymorphisms of methionine (M) and valine (V) around codon 129 of the PRNP gene also produce distinct variations of protease resistant prion proteins (Collinge et al., 1996; Parchi et al., 1996). These strains have distinct properties such as varying degrees of seeding and propagation abilities, and this subsequently causes varying disease incubation periods, patterns of prion pathology and disease phenotypes (Aguzzi et al., 2007; Collinge and Clarke, 2007; Collinge et al., 1996; Parchi et al., 1996).

The 'protein-only' hypothesis developed in prion disease has now been extended to include various other neurodegenerative diseases with prominent protein misfolding. The experimental transmission of these proteins to live animal hosts so far has been very successful. The neurodegenerative disease associated proteins with demonstrable in vivo transmissibility are β-amyloid (Aβ), tau and α-synuclein. However, the only transmissible protein that has been demonstrated to produce neurotoxicity and a neurodegenerative

phenotype is α-synuclein (Luk et al., 2012a; Mougenot et al., 2011), which has still not been consistent among studies (Masuda-Suzukake et al., 2013).

4.1.2. Beta-amyloid (Aβ)

Aβ is the natural cleavage product of the amyloid precursor protein (APP) which has a key role in Alzheimer's disease (AD), the most common form of dementia (Holtzman et al., 2011). In vitro studies first predicted the potential prion-like nature of Aβ (Jarrett and Lansbury, 1993), and the transmissibility of Aβ pathology was demonstrated by Aβ plaque formation in primates, after the injection of human brain extracts from patients with AD (Baker et al., 1994). This work was expanded on by Jucker and Walker using human APP transgenic mice intracerebrally injected with brain homogenates, either from human Alzheimer's patients or aged Alzheimer's disease model (APP23) mice with high load of Aβ plaques. The pre-formed fibrils of Aβ in this case were found to act as seeds to enhance the aggregation of Aβ independent of age (Hamaguchi et al., 2012; Kane et al., 2000; Meyer-Luehmann et al., 2006; Walker et al., 2002). The production of Aβ plaques in the host depends upon the concentration of Aβ seeds in the inocula, and production of the human Aβ sequence in the host brain. Indeed, either the denaturation of the proteins, removal of Aβ and passive immunization of the host with Aβ antibodies can all inhibit this Aβ seeding reaction and the formation of Aβ plaques (Meyer-Luehmann et al., 2006). Further investigation into the Aβ seeds demonstrate that, like prions, they can be either small, soluble and protease sensitive, or large insoluble amyloid protease resistant fibrils. Again like prions (Silveira et al., 2005), the mainly soluble, partially protease resistant smaller monomers are more prone to induce seeding and aggregation of Aβ (Langer et al., 2011). In addition to this Walker and colleagues were able to demonstrate that Aβ brain extracts can also induce tau pathology in APP and tau double transgenic mice, suggesting that the seeding process can initiate a more widespread disease process (Bolmont et al., 2007). Finally, synthetic Aβ as well as Aβ purified from human brains, can induce Aβ aggregation and can self-propagate in bigenic mice which can subsequently be tracked with bioluminescence imaging to trace the spreading of this aggregation (Stohr et al., 2012).

Like prion disease, the formation of this Aβ pathology starts focally within the brain and then begins to spread via axonally connected regions. Eventually this pathology becomes more widespread and affects neocortical and subcortical regions as seen in patients with AD (Hamaguchi et al., 2012). Even an intraperitoneal cavity injection of Aβ seeds is enough to initiate Aβ plaque formation within the brain of transgenic APP mice (Eisele et al., 2010). More recently, morphological strain types of Aβ were found from Aβ laden brain extracts of different APP transgenic mice (Heilbronner et al., 2013). Suggesting that like prions, Aβ could also have strain variants responsible for different pathological deposition of Aβ. Together this data demonstrates the in vivo transmissibility and prion-like behaviour of the Aβ protein.

4.1.3. Tau

Tau is a cytoplasmic microtubule stabilizing protein which is often found hyperphosphorylated, aggregated and deposited in the form of tangles in the brains of patients with AD, FTLD, progressive supra nuclear palsy (PSP), cortico-basal degeneration (CBD), MSA, chronic traumatic encephalopathy (CTE) and others (Lee et al., 2001). Tau brain extracts can also seed human tau inclusion formation and spreading in human tau transgenic mice that do not normally develop inclusions (Clavaguera et al., 2010). Unlike Aβ, tau oligomers from AD brains can be transmitted to non-transgenic (wild type) mice (Lasagna-Reeves et al., 2012), suggesting that there is no transmission barrier and the murine tau itself maybe amyloidogenic. This also suggests that the seeds need not be amyloid to transmit a seeding reaction but can propagate in the form of oligomers.

Overexpression of the human tau in transgenic mice produced five times the number of inclusions than injection to wild type mice, suggesting that increasing the tau substrate concentration increased the efficiency of the seeding reaction. Synthetic tau has also been found to seed neurofibrillary tangles of tau in transgenic mice expressing human tau (Iba et al., 2013). In a similar manner to prions and Aβ (Langer et al., 2011; Silveira et al., 2005), the tau seeds are variable in size with the most effective seeds being the small soluble species, and the most toxic species are thought to be oligomers (Lasagna-Reeves et al., 2012).

Subsequent in vivo studies have also demonstrated the ability of tau to propagate in neural networks via trans synaptic spread (de Calignon et al., 2012; Liu et al., 2012). More recently tau pathology from human brain extracts with various tauopathies, were also able to induce tau pathology in human wild type tau transgenic mice (Clavaguera et al., 2013). These mice developed similar tau lesions as observed in the human samples injected, suggesting that tau may also have varying conformations or strains that give rise to clinically distinct tauopathies. Indeed, a more recent study created distinct prion strains that recreate distinct amyloid morphological tau conformations that can propagate in a clonal fashion in cell culture and mice through 3 generations. In addition, they were able to isolate strains of tau from 5 distinct tauopathies from 29 different patients using a cell system (Sanders et al., 2014). Altogether this data makes tau a strong candidate as a misfolded protein with prion-like behaviour.

4.1.4. Alpha-synuclein

Strong evidence also supports the prion-like characteristics of the Parkinson's disease (PD), Lewy Body dementia (LBD) and multiple system atrophy (MSA) associated protein α-synuclein. Misfolded α-synuclein often deposits as Lewy body inclusions and Lewy neurites in the brains of patients with PD, LBD and MSA (Goedert et al., 2013). The transmission of Lewy body pathology was first observed from treatment of stem cell tissue grafts into patients with PD. After long incubation periods, these new tissue grafts developed Lewy body inclusions, suggesting that α-synuclein was able to propagate from cell to cell (Li et al., 2008). Since then these findings have been replicated in mice and cell culture using brain extracts, synthetic α-synuclein and neuron grafts to rodents (Danzer et al., 2009; Hansen et al., 2011; Luk et al., 2009, 2012a, 2012b; Mougenot et al., 2011; Nonoka et al., 2010). Importantly, injection of aged α-synuclein mutant mice brain extracts into mutant α-synuclein mice accelerated α-synuclein aggregation and disease severity and onset (Mougenot et al. 2011; Luk et al. 2012). This suggests that seeds from these extracts are involved in a seeding reaction to enhance aggregation, disease progression and neurotoxicity in murine models of PD. However, there is evidence now to suggest that α-synuclein transmission can occur in non-transgenic wild type mice with synthetic α-

synuclein, leading to neurodegeneration and motor deficits. This suggests that there is not a 'transmission barrier' between endogenous mouse and human α-synuclein, and transmission does not require a human α-synuclein transgene as a substrate for propagation (Luk et al., 2012b). In addition to this, transmission of α-synuclein has now also been demonstrated from the brains of patients with MSA in transgenic A53T mutant α-synuclein mice (Watts et al., 2013). Reminiscent of prion cell to cell spreading, α-synuclein has been shown to propagate from cell to cell in vitro via endocytosis (Desplats et al., 2009; Hansen et al., 2011), and transmission of α-synuclein into mice demonstrated the transmission of α-synuclein pathology to interconnected brain regions (Luk et al. 2012). In addition the transmission of human α-synuclein monomers and oligomers in to mice, has shown spread from a focal onset in the olfactory bulb to interconnected brain regions (Rey et al., 2013). This is not only reminiscent of the Braak staging hypothesis in PD (Braak et al., 2003), but also of the characteristic prion-like cell to cell transmission of protein aggregates. Evidence also suggests that α-synuclein could promote the formation of tau inclusions via a cross seeding mechanism. Different proposed 'strains' of α-synuclein were also found to promote varying degrees of tau pathology (Guo et al., 2013). These different conformations or 'strains' are additional evidence to support a prion-like behaviour of α-synuclein.

4.1.5. TDP-43

As discussed previously, TDP-43 has well characterized prion-like properties and behaviour in vitro (Furukawa et al., 2011; Nonaka et al., 2013; Tsuji et al., 2011, 2012). However, there is no evidence to currently suggest that this prion-like behaviour is maintained in vivo. Due to the observed prion-like behaviour of TDP-43, and a high human and murine TDP-43 amino acid sequence similarity (96%), we hypothesise that pathologically misfolded TDP-43 will be able to seed the misfolding of endogenous mouse TDP-43 in vivo, without the need for a human TDP-43 transgene.

4.2.   Results

In order to investigate if endogenous mouse TDP-43 can seed TDP-43 pathology from human ALS brains, we took pathological TDP-43 positive brain and spinal cord homogenates from 2 ALS patients and 1 control patient, and intracerebrally injected these into non-transgenic wild type C57BL mice. The main reason for using this mouse strain is that they are congenic which minimizes genetic heterogeneity amongst the mice. In addition they are widely used in modelling human disease due to their availability, robustness and easy breeding. We monitored these mice for any neurodegenerative phenotypes or motor deficits that may accompany this pathology with a standard SHIRPA protocol (see methods). The ALS samples were chosen to be of similar age and disease duration but with different sites of disease onset (i.e. bulbar and limb). Additionally these patients were male and female respectively, to assess if either of these aspects affected the outcome of pathology or any observable disease phenotype.

Firstly, in order to assess whether control and ALS brain extracts contained TDP-43 pathology these samples were extracted in triton-X, sarkosyl and CHAPS and then resuspended in urea (See Methods) to purify the insoluble pathological TDP-43 from the tissue. These samples were then run on a western blot and probed for TDP-43 and phosphorylated TDP-43 (pS409/410) to detect the pathological 25kDa fragments, and phosphorylated 45 and 25kDa fragments. Figure 24A demonstrates that the ALS samples contained these pathological 25kDa TDP-43 fragments which were absent in the controls. The 25kDa bands detected in ALS were found to be more prominent in ALS brain samples rather than spinal cords, which is in line with previous findings (Igaz et al., 2008).

For these studies we used 1% w/v whole tissue homogenates in sterile PBS from the control, and the two TDP-43 positive ALS brain and spinal cord samples (Table 4). 30ul of each sample was intracerebrally injected into the right parietal lobe of 5 groups of 11 female C57BL/6OlaHsd mice at ~6 weeks of age. These mice were then culled at planned time points of 7, 90 and 180 days post injection. Later time points of 360 and 720 days were also included for future analysis (Figure 24B). The left side of the brain was assessed for any gross abnormal pathology and neurodegeneration using H&E, GFAP (marker for

astrocytosis) and Iba-1 (microglial activation marker) stains. In addition, antibodies for p62, ubiquitin and phosphorylated TDP-43 (pTDP-43) were used on immunohistochemistry (IHC) to detect any induction of autophagy, ubiquitination and phosphorylated TDP-43 pathology. The other half of the brain was frozen for use in western blotting for TDP-43 pathology. The spinal cord was also removed from each mouse and fixed for similar IHC and motor neuron count staining, to assess for any spinal pathology and reduction in motor neuron numbers.

Patient	Diagnosis	Tissue	Phenotype	Sex	Age	Age of onset	Disease duration
A213	Neurologically normal	MC	N/A	M	78	N/A	N/A
A213	Neurologically normal	SC Lu	N/A	M	78	N/A	N/A
A381	ALS	MC	Limb onset	F	86	84	24 months
A381	ALS	SC Lu	Limb Onset	F	86	84	24 months
A257	ALS	MC	Bulbar Onset	M	75	74	18 months
A257	ALS	SC Lu	Bulbar Onset	M	75	74	18 months

Table 4. TDP-43 transmission samples. Table of all normal control and ALS CNS tissue used for transmission to wild type mice including the phenotype, sex, age, age of disease onset and disease duration of each patient.
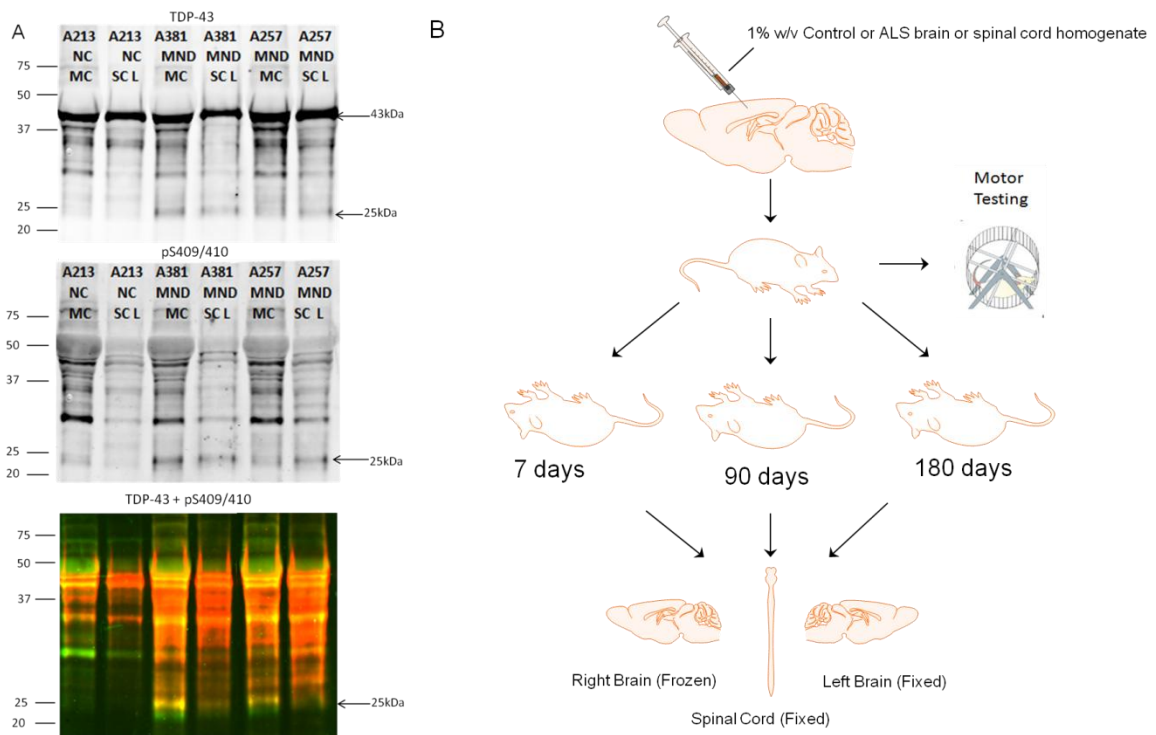
Figure 24. TDP-43 transmission protocol and pathological verification of samples used.
A) Western blots of sarkosyl insoluble urea soluble pellets of regions used for transmission probed with TDP-43 and pS409/410. Blots show the presence of pathological 25kDa bands and phosphorylated 25kDa bands in ALS samples which are absent in controls. B) Diagrammatic representation of TDP-43 transmission protocol. All inoculations and SHIRPA monitoring were conducted by Mike Brown and Anthony White at the MRC prion unit.

In order to demonstrate the presence of TDP-43 pathology, all mice brain and spinal cord sections were stained with the pS409/410 phosphorylated TDP-43 antibody (pTDP-43) which can detect all pathological forms of TDP-43 including pre-inclusions and ubiquitinated cytoplasmic aggregates containing the truncated 25kDa forms. In these experiments all the 7, 90 and 180 day post injection incubation periods demonstrated no observable pTDP-43 pathology in any regions of the CNS (data not shown). As TDP-43 pathology occurs predominantly in the frontal and motor cortices, representative images were taken from these regions in each of these mice at the final 180 day post injection time point to demonstrate that lack of formation of any noticeable pTDP-43 pathology (Figure 25). In addition to this, western blotting of sarkosyl extracted brain fractions also revealed no observable TDP-43 pathology (data not shown). Ubiquitin and p62 antibodies were used on each of these sections to determine if any aggregating proteins were targeted for degradation or removal by the autophagy-lysosome system. These two features are characteristic of neurodegenerative diseases including ALS, Alzheimer's and Parkinson's disease. Here we demonstrate that the degrees of expression of these two proteins were at a baseline level for each of the post injection time points (Figure 25), suggesting that no pathological neurodegenerative disease process has taken place to date. However, in each of the control and ALS injected mice there was a small number of observable p62 inclusions which are shown in a high 40X magnification in the frontal cortex regions of each of these mice (Figure 25). However, due to the presence of these inclusions in both the control and ALS sample treated mice, these inclusions are thought to be due to the ageing process rather than a protein aggregation disease related process.

The two most reliable markers of neurodegeneration in the CNS are glial fibrillary acidic protein (GFAP) (marker for astrocytes) and ionized calcium binding adaptor molecule (Iba-1) (microglial activation marker). GFAP has a mild background staining of astrocytes in normal conditions but under neurodegenerative and inflammatory conditions astrocytes become reactive to repair the damaged and dying tissue. Therefore if neurodegeneration is present then the number of reactive astrocytes increase and cluster around the area of damage and degeneration. In addition, when an infection, cell death or neuroinflammation is present,

microglia become activated in that region. This can be detected with an upregulation of the Iba-1 protein. However, in all our post injection time points we demonstrate that no reactive astrocytosis or microglial activation could be detected with GFAP or Iba-1 in the frontal cortex or spinal cord of each mouse (spinal cord images not shown) (Figure 26). Indeed, no observable neurodegenerative phenotype or motor deficits were observed in any of these mice as assessed by the standard SHIRPA protocol.
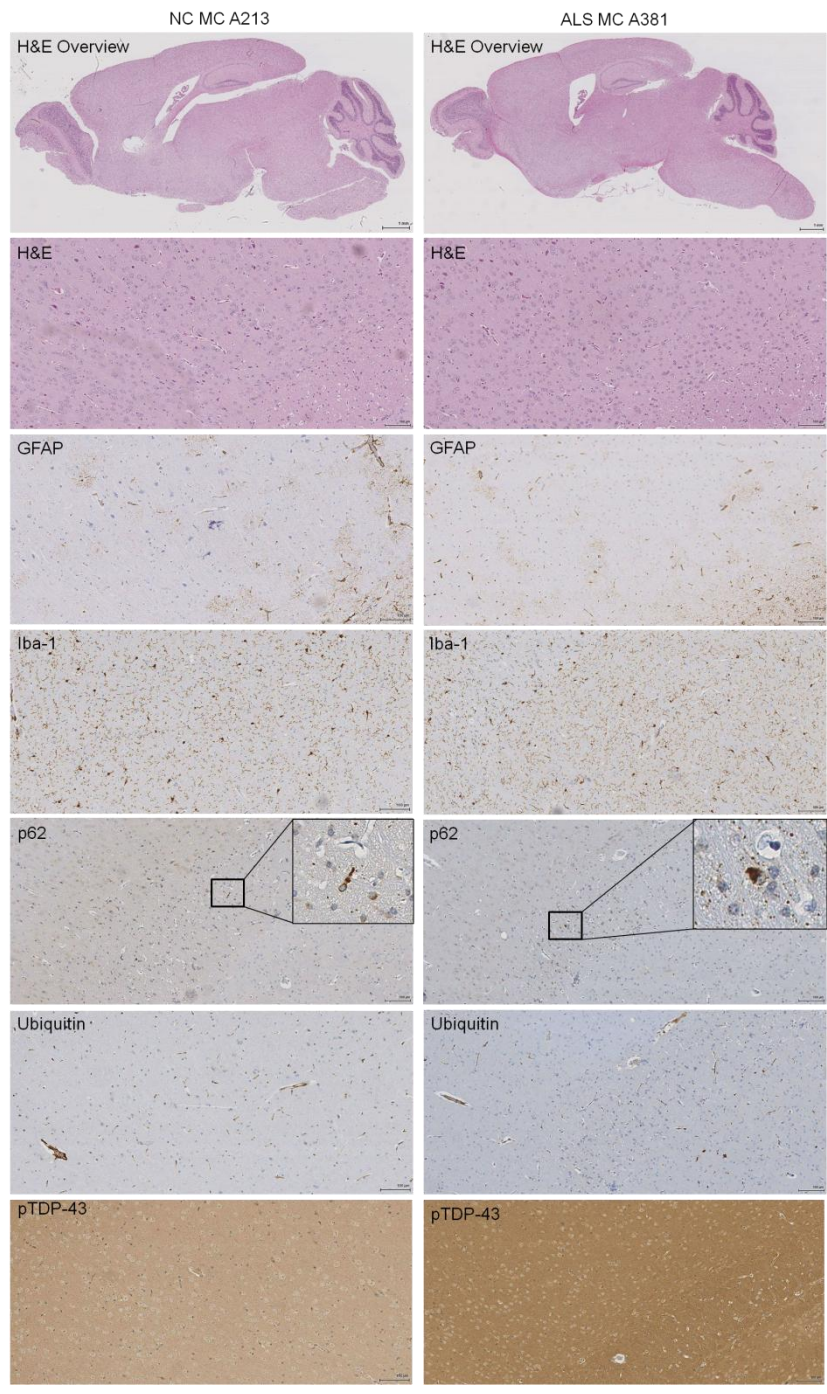
Figure 25. Representative frontal cortex images of 180 day post injection mice injected with normal control and ALS motor cortex brain homogenates. Stains include: H&E for morphological analysis, GFAP for astrocytosis, Iba-1 for microglial activation, p62 for autophagy induction, ubiquitin to detect ubiquitinated aggregates and phosphorylated TDP-43 (pTDP-43) to detect for the formation of TDP-43 pathology. The p62 inclusions are magnified at 40X demonstrating p62 deposition in enlarged boxes. Images are representative of all mice in each group (n=11). All images were captured at 10X magnification and scale bars are 100µm.
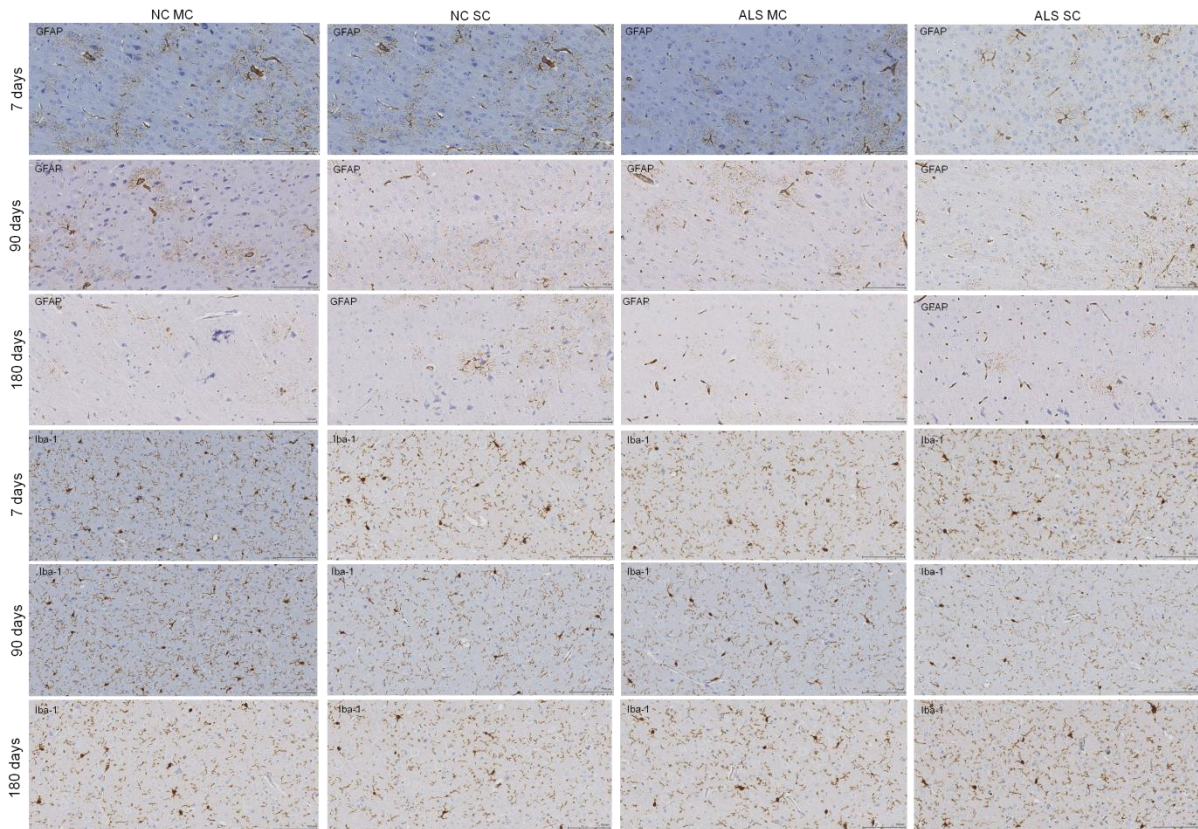
Figure 26. Representative images of the frontal cortex of inoculated mice stained GFAP and Iba-1 at cull time points of 7, 90 and 180 days. GFAP was used to detect the induction of astrocytosis as a marker of cell repair, and Iba-1 for the activation of microglial cells which mark the presence of the neuroinflammatory process accompanying neurodegeneration. All images are representative of all mice (n=11), were captured at 40X magnification and scale bars represent 100μm.

4.3.   *Discussion*

The transmission of protein aggregation pathology, observed in many neurodegenerative diseases, has now been observed on a number of occasions in mice and non-human primates (Jucker and Walker, 2011). Therefore the transmission of pathological TDP-43 to mice was the next logical step in providing evidence for the prion-like cellular mechanisms of TDP-43 pathology. However, this attempt at pathological transmission of TDP-43 from human ALS CNS tissue to wild type mice has not yet yielded positive results, although longer incubations remain ongoing. The unsuccessful transmission of TDP-43 at these time points may be due to a number of reasons.

First of all, the preparation of the brain homogenates from human samples was diluted to a 1% solution in PBS according to the prion transmission protocol. This may well be sufficient for the transmission of PrP^{Sc}, where even a small number of misfolded PrP^{Sc} seeds are present in diluted extracts. However, the dilution of the brain homogenate to 1% may have diluted out any misfolded seeds of TDP-43 in the inocula. Indeed, immunoblotting of 10% ALS brain homogenates (not enriched for TDP-43 via sarkosyl extraction) did not show pathological 25kDa fragments or phosphorylated TDP-43 pathology (45 and 25kDa bands). However, the extraction of ALS brain samples in sarkosyl, which purified and enriched the insoluble pathological TDP-43, enabled the visualisation of these pathological bands. Therefore any misfolded seeds of TDP-43 are likely to be diluted out in a 1% homogenate compared to a sarkosyl detergent enriched sample. Previous studies of Aβ, tau and α-synuclein have used sonicated 10-20% homogenates which may increase the yield and solubilisation of the seeds in these experiments (Clavaguera et al., 2013; Kane et al., 2000; Luk et al., 2012a). However, the TDP-43 pathology in ALS CNS tissue is only observed after stringent detergent extraction, suggesting that the number of TDP-43 seeds in a brain homogenate may still be very low.

Secondly, the injection site was in the right parietal lobe and immunohistochemistry was performed in the left side of the brain. So if TDP-43 pathology propagates through the CNS like prion disease, any development of TDP-43 pathology may not have spread to the contralateral side of the injection site in the incubation times observed. Indeed, this has

been the case for the transmission of α-synuclein (Masuda-Suzukake et al., 2013), where even with bilateral injection, the pathology seems to initiate from the injection site and spread in a time dependent manner. The blots of the right hand sides of the brain do not show any TDP-43 pathology (data not shown) although small amounts of pathology are not always detectable by western blot as the technique is not as sensitive. Therefore a bilateral injection of TDP-43 seeds to the CNS may prove useful in the future to initiate the formation of TDP-43 pathology. Also a parietal lobe injection may not spread the TDP-43 seeds to TDP-43 pathology susceptible regions such the motor cortex and frontal cortex.

Thirdly, in some cases there appears to be a 'transmission barrier' for the transmission of prions. In prion disease, this transmission barrier is dependent on the primary structure and sequence homology between the inoculated pathological prion protein, and the host endogenous prion (Collinge, 2001). Indeed, a number of other studies using Aβ (Kane et al., 2000; Walker et al., 2002), tau (Clavaguera et al., 2010, 2013; de Calignon et al., 2012) and α-synuclein (Luk et al. 2012; Masuda-Suzukake et al. 2013; Mougenot et al. 2011) have noted that a human transgene with similar sequence identity to the pathological form of the protein, is required as a substrate for the seeding and transmission of pathology to occur. Together this data suggests that there may be a 'transmission barrier' related to structural and sequence based properties of the endogenous protein in the host (Prusiner et al., 1990). Therefore, the fact that the wild type C57BL mice in this study expressed no human TARDBP gene means that a lack of sequence homology could have impeded the formation of an in vivo seeding reaction. However, the counter argument for this comes from studies on variant CJD (vCJD). Unlike classical CJD prions, which do not transmit to wild type mice, the vCJD prions (with similar primary structure to PrP) are able to more readily transmit to wild type mice than mice expressing human PrP (Hill et al., 1997). Indeed, other studies on α-synuclein (Luk et al., 2012b), and tau (Lasagna-Reeves et al., 2012) demonstrate that seeding and transmission of both of these proteins can occur from human samples without an endogenous human template. Bearing this in mind and considering the 96% sequence homology of human and murine TDP-43, it still remains possible that human pathological TDP-43 could still potentially transmit to wild type mice. This also suggests that other factors

may be contributing to the negative results observed here. A primary structural sequence difference between the mouse and human TDP-43 may still be plausible but, in a similar manner to vCJD, a different strain variant of TDP-43 could still potentially induce a TDP-43 seeding reaction on murine TDP-43 in vivo. The main variable at play may be the post inoculation incubation times. A previous study with synthetic prions indicated that prion transmission was not successful until between 380 and 660 days post inoculation in human PrP transgenic mice (Legname et al., 2004). Indeed, initial studies of Aβ transmission into non-human primates exceed 3.5 years (Baker et al., 1994; Ridley et al., 2006). Therefore, a longer incubation period (due to be processed later at 360 and 720 days) may reveal the age related induction of TDP-43 pathology from these ALS CNS samples.

Due to the pre-existing knowledge of TDP-43 pathology to seed in vitro from our studies in chapter 3, and from Nonaka and colleagues (Nonaka et al., 2013), the prion-like behaviour and transmission of TDP-43 is still a realistic notion. Therefore, the combination of a non-enriched TDP-43 inoculum for injection, unilateral injection sites, mice lacking a human TADRBP transgene, and short incubation periods seem to be the combined factors for the negative results observed here. However, there are currently no commercially available human TARDBP transgenic mice to use for these studies, and the preparation of such an animal requires additional time, money and research. Even though the sequence homology of the human TARDBP and murine TARDBP is 96%, the 4% sequence difference could also be responsible for a transmission barrier. This transmission barrier was also seen with the transmission of Aβ, in that seeding did not occur in non-transgenic mice due to 3 amino acid differences in the human Aβ sequence (Kane et al., 2000). Indeed, a mutation in a single tryptophan residue at codon 32 in the human SOD1 gene was enough to inhibit an in vitro seeded misfolding reaction of SOD1 (Grad et al., 2011). Therefore it seems that the primary sequence of the host and inoculated protein is of significant importance. Indeed, the overexpression of a transgene in mice can sometimes lead to the age related pathological deposition of the overexpressed protein, and the inoculation of pre formed seeds from various sources just accelerates the formation of this pathology. It is thought that the overexpression of this protein acts as an increased concentration of the templating

substrate, which ultimately incites a more rapid onset and increased deposition of the pathological protein. This is in line with our findings from our in vitro seeding model in chapter 3. The seeding of the endogenous human TDP-43 present in the HEK cells expressing no TDP-43 construct was very minimal on ICC and not detectable on western blot. However, the addition of a FLAG tagged human TDP-43 construct resulted in the significantly increased overexpression of human TDP-43, and accelerated the formation of TDP-43 pathology in cells. Despite the identical sequence similarity in the human HEK cells, an overexpression of the TDP-43 protein is required to induce any noticeable formation of TDP-43 pathology. However, these in vitro experiments were only conducted over short periods of time due to the rapid rate of cell division of the HEK cells. Therefore longer incubation periods without the overexpression of a FLAG tagged TDP-43 may result in an efficient seeding reaction of TDP-43.

4.4. Future work

To conclude this work it will be necessary to evaluate the remaining time points of 360 and 720 days for neurodegeneration and pTDP-43 pathology. However, as our modified TDP-43 seeding reaction is now effective in vitro, we propose that the method of extraction of the initial homogenate was the main impeding problem. The sarkosyl extraction method is thought to help to purify and enrich these TDP-43 seeds which can facilitate the seeding and aggregation of TDP-43. Indeed, a similar sarkosyl extraction protocol for α-synuclein transmission from human brains was recently conducted to produce the effective seeding of α-synuclein in mice (Masuda-Suzukake et al., 2013). Even with this extraction method our in vitro results only demonstrate minimal seeding activity on HEK cells lacking the overexpression of human TDP-43. So far we have no evidence to demonstrate that this reaction could occur with endogenous mouse TDP-43, and that there may still be a transmission barrier. As previously demonstrated, this TDP-43 seeding reaction does not occur readily without the expression of a human TARDBP gene, presumably there will be an identical sequence and primary structure, and an increased substrate available for the seeding reaction to occur. Therefore the mice injected with TDP-43 seeds from human brain may need to either be transgenic mice overexpressing human TARDBP gene, or mice

expressing AAV induced human TARDBP gene for seeding to occur in a reasonable time frame. In addition, using transgenic mice or AAV induced expression of a TDP-43 construct with a deleted C-terminal containing the prion-like domain would give insight into the value of the prion-like domain in the seeding of TDP-43 and mechanistic insight into TDP-43 mediated toxicity. Indeed, if this region proves to be essential for the reaction to occur then it could be targeted for therapeutic intervention in the future.

4.5.   Conclusion

Here we have attempted to seed the transmission of TDP-43 from 1% ALS brain and spinal cords of TDP-43 positive ALS patients to wild type mice. Unfortunately no transmitted TDP-43 pathology could be observed in any of these mice up to the 180 day incubation time point. However, future experimental modifications and longer incubation time periods may well produce TDP-43 seeding in vivo in a similar manner seen in the in vitro experiments in chapter 3. If this in vivo transmission of TDP-43 pathology is effective at producing a neurodegenerative phenotype reminiscent of ALS, it could potentially be the most accurate model of TDP-43 mediated toxicity produced so far. The next logical step will be to generate synthetic TDP-43 seeds for use in the transmission to mice. If these mice were to develop TDP-43 pathology and a neurodegenerative phenotype, then this would add to the growing evidence that misfolded TDP-43 can exert neural toxicity in vivo. The successful development of these models would enable their future use in therapeutic screening, with the target being misfolded TDP-43.

Chapter 5

Non-invasive imaging of protein aggregation in vivo with APT imaging

5. Non-invasive Imaging of protein aggregation in vivo with APT imaging

5.1. Introduction

Currently there is no reliable biomarker for disease onset, progression or treatment response in ALS. A key biomarker for this and other neurodegenerative conditions is the cellular aggregation of proteins involved in the condition. Often in neurodegenerative disease a persistent increase in insoluble pathogenic protein levels tend to correlate with disease progression and severity (Ross and Poirier, 2004). Recently a novel MRI spectroscopy imaging technique call amide proton transfer (APT) (Zhou et al., 2003a) has been developed for detecting protein accumulation, and therefore has the potential to non-invasively measure protein aggregation as a potential biomarker of disease progression. Additionally, if the approach to treating neurodegeneration might be to reduce the amount of protein aggregation, then this technique would benefit future in vivo therapeutic studies. Here we explore the use of this technique on the well-established mutant SOD1 G93A mouse model of ALS, to determine if changes in APT signal correlate with increase protein concentrations detected in the spinal cord of wild type and end stage mutant SOD1 G93A mice.

5.1.1. SOD1

From the 10% of fALS cases, about 20% of these familial cases are due to over 150 mutations in the copper/zinc superoxide dismutase 1 (SOD1) gene (Andersen, 2006). The discovery of these mutations subsequently led to the development of some of the first ALS mouse models with overexpressed mutant SOD1 protein, and therefore significantly furthered our knowledge of the condition. Despite 20 years of research into SOD1 ALS cell and animal models the knowledge of how exactly SOD1 causes cellular toxicity remains elusive.

SOD1 is a ubiquitously expressed cytoplasmic and mitochondrial enzyme that functions as a dimer to catalyze the breakdown of reactive oxygen species (ROS) and prevent

oxidative stress (Rosen, 1993). It was originally proposed that SOD1 may cause neurodegeneration by a loss of enzymatic function (Rosen, 1993). However, SOD1 transgenic knockout mouse models did not develop motor neuron disease (Reaume et al., 1996), and mutant SOD1 activity did not correlate with cell death and toxicity (Borchelt et al., 1995). Therefore the main hypothesis was a toxic gain of function for SOD1, which has been the focus of investigation using transgenic overexpressing mutant SOD1 animals. The most well established SOD1 mouse model is the SOD1 G93A mouse which develops a progressive age related motor disorder that is strikingly similar to patients with ALS (Gurney et al., 1994). Since then over 20 other SOD1 models have been generated and are now the predominant rodent model to study ALS. As well as a progressive age related motor phenotype, these mice also display a number of other disease characteristics observed in ALS. This includes axonal and mitochondrial dysfunction, progressive neuromuscular dysfunction, gliosis and motor neuron loss (Bruijn et al., 1997; Dal Canto and Gurney, 1997; Gurney et al., 1994; Ripps et al., 1995). One of the key features of the SOD1 transgenic model used in this study, is the characteristic accumulation and aggregation of the SOD1 protein in the spinal cord as visualized by immunoblotting and immunohistochemistry (Karch et al., 2009; Prudencio et al., 2009). Studies also demonstrate that as the age related motor degeneration progresses, SOD1 becomes more insoluble as it becomes aggregated making this feature useful for tracking disease progression and neurodegeneration (Johnston et al. 2000; Wang et al. 2003). In contrast to other rodent ALS models, including FUS and TDP-43, this particular SOD1 model has a well characterised robust formation of insoluble SOD1 aggregates in the spinal cord which are not as well characterized in other rodent models of ALS. This fact combined with the ubiquitous availability of this model is the reason why we used this model and not other rodent models of ALS.

5.1.2. *Amide proton transfer (APT) imaging*

Recent work has been done to develop a novel non-invasive imaging and spectroscopy method that could be capable of detecting protein aggregation. This imaging method is based on a recently developed magnetic resonance imaging (MRI) method called amide proton transfer (APT). APT imaging is a variation of magnetization transfer imaging which can indirectly image the interaction between protons of free tissue water and the amide groups of endogenous mobile proteins and peptides. So far this imaging method has been particularly useful in sensitive detection of pH changes in strokes due to the effects of pH on proton exchange (Jokivarsi et al., 2007; Sun et al., 2007; Zhou et al., 2003a). APT has also been shown to be useful for utilising the increased concentration of mobile peptides and proteins present in brain tumours (Hobbs et al., 2003; Howe et al., 2003) to provide contrast in brain tumour imaging (Jones et al., 2006; Zhou, 2011; Zhou et al., 2003b, 2008). Despite the promising nature of the APT method in molecular MRI imaging at the protein and peptide level, the protocol is still not sensitive enough to detect cellular protein aggregation at low concentrations.

5.2.   Methods

In order to progress this technique further, we collaborated with imaging physicists Professor Xavier Golay and PhD student Marilena Rega, to improve the sensitivity of the method. They developed a new enhanced APT method to try and detect protein aggregation in the spinal cord of the SOD1 mouse model. This new APT-MRI protocol called EXPRESS consists of a 6 second sequence saturation train of 100 pulses (50ms, FA=500°, 95% duty cycle), followed by a PRESS readout. Respiration gating was used to avoid voxel movement. With this, an extra window of 0.5s of saturation was allowed until the respiration gating was triggered (Figure 27B). The output for this method was determined with a graphical projection of the APT signal against the offset frequency and APT intensity. The APT value for each data set was calculated as the integration from 2.5-4.5ppm from water, centred at 3.5ppm where the amide protons resonate. The APT intensity is calculated from the differences in the control data line (pink) and the experimental data line (blue) and calculates a value in parts per million (ppm) (Figure 27C). All this data was averaged and

normalized at 6ppm and calculated using MATLAB. The reliability and accuracy of the measurement technique was then demonstrated by the degree of fit between averaged multiple Z-spectra measurements of the control wild type and SOD1 mice measurements at 90 days. The lumbar region of the spinal cord (Figure 27A) was chosen in each of these mice as this region is the most susceptible to neurodegeneration and aggregation of SOD1. The aim of this project was to attempt to utilize this optimized APT detection method to detect any changes in protein accumulation in the lumbar spinal cord of wild type and SOD1 mice at pre and post symptomatic disease stages.

APT voxel: L3-L4 lumbar section
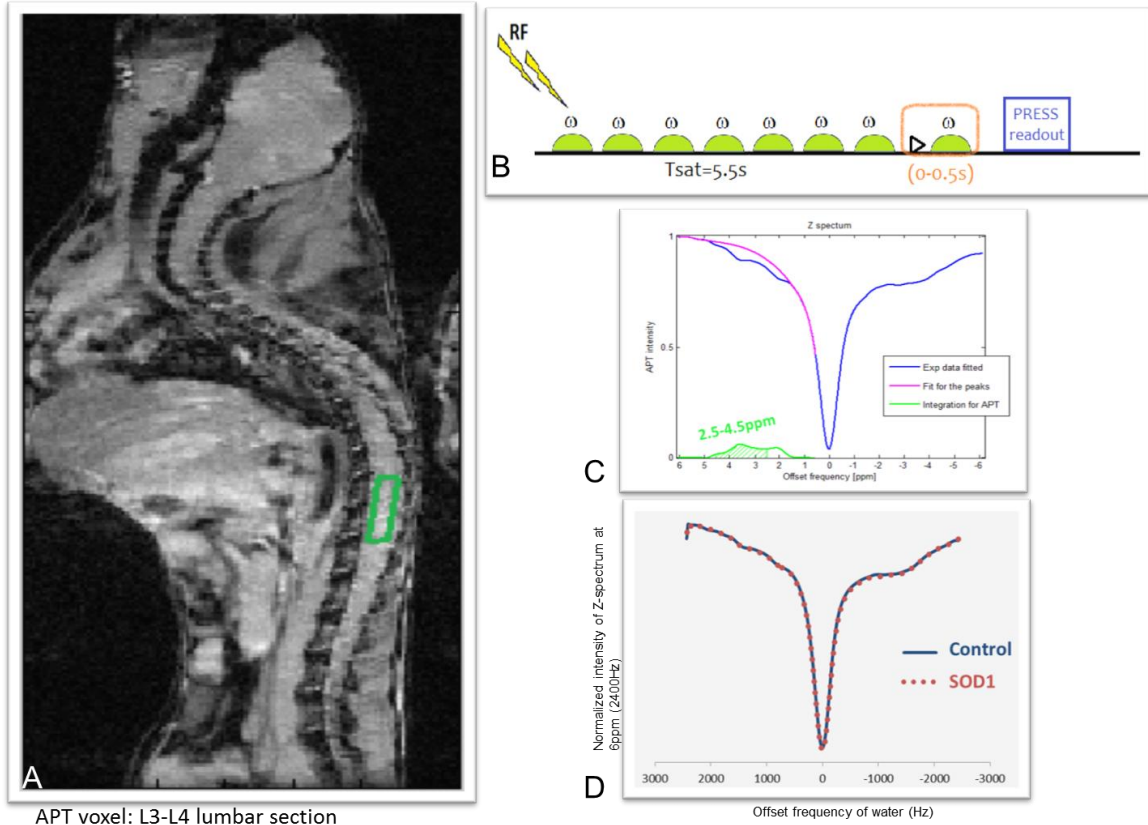
Figure 27. APT measurement method. A) MRI image of mouse spinal cord and lumbar region (L3-L4 green rectangle) for APT measurement. B) APT-MRI EXPRESS protocol: The sequence consists of a saturation train of 100 pulses (50ms, FA=500°, 95% duty cycle), followed by a PRESS readout. An extra window of 0.5s saturation was allowed until respiration gating was triggered. C) Experimental data were corrected for B=0, normalized at 6ppm and fitted to a smoothing line (blue). The positive side of the spectrum was also fitted to a power function ($y=ax^b+c$) in order to account for the amide peaks (pink). The APT signal was calculated as the area between the two curves from 2.5-4.5ppm. D) Averaged Z-spectra for all 90 day old animals indicating the accuracy and reproducibility of the APT method.

5.3. Results

We scanned groups of 7 wild type and 7 SOD1 G93A mice at the pre-symptomatic stage (90 days), and 7 wild type and 7 SOD1 G93A mice at the symptomatic stage (120 days) in a 9.4T MRI scan with the application of the exchange press APT analysis method (Figure 27 (See Methods)). To ensure the SOD1 mice were accumulating the SOD1 protein, the insoluble fraction of the spinal cord was immunoblotted for SOD1 and corrected for β-actin (Figure 28). Results demonstrated that the SOD1 protein became significantly more insoluble in the 120 day symptomatic mice compared to the presymptomatic mice at 90 days (*$p < 0.05$), indicating that SOD1 was accumulating and this accumulation correlated with disease onset.

Results showed no significant difference in measured APT signal between the wild type and SOD1 mice at either 90 days ($p = 0.71$) or 120 days ($p = 0.98$) (Figure 29A and B). Subsequent schedule 1 culling of the mice was performed followed by careful dissection of the lumbar region of the spinal cord. The lumbar regions were then analyzed and extracted in mild detergent to separate the soluble and insoluble spinal cord fractions (See methods). The APT method used here could only detect soluble protein in the spinal cord. However, when proteins aggregate they become less soluble, and therefore the analysis of the soluble fraction was used as an indirect measurement of any changes in protein concentration in the insoluble fraction. The protein from the soluble fraction of the spinal cord was then measured (mg/ml) using a standard BCA assay using bovine serum albumin as a reference protein standard. From this we demonstrated that there was no significant difference between the protein concentrations in mg/ml in the soluble fraction of the spinal cord of WT and SOD1 mice at 90 days ($p = 0.71$) and 120 days ($p = 0.71$) (Figure 29C and D).
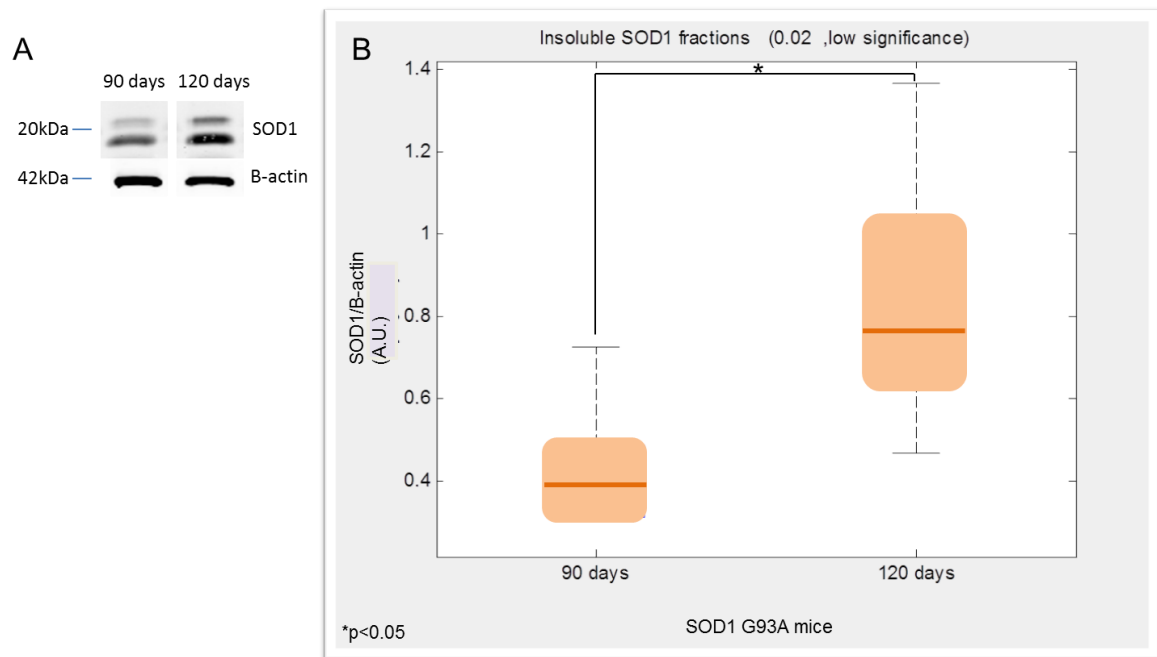
Figure 28. Levels of insoluble SOD1 protein in the lumbar spinal cord of SOD1 mice. A) Representative western blot of insoluble SOD1 protein at ~19kDa and the corresponding β-actin loading control used to calculate the levels of insoluble SOD1 protein in the lumbar spinal cord of 90 and 120 day old mice. B) Significantly Increased insoluble levels of SOD1 protein (*p<0.05) are present in 120 day compared to 90 day old mice. Significance was measured using a two tailed non paired students t-test with significance defined as *p<0.05. Error bars represent SEM and sample numbers are n=7 in each group (Graph and statistics were performed on MATLAB and are courtesy of collaborator, Marilena Rega).
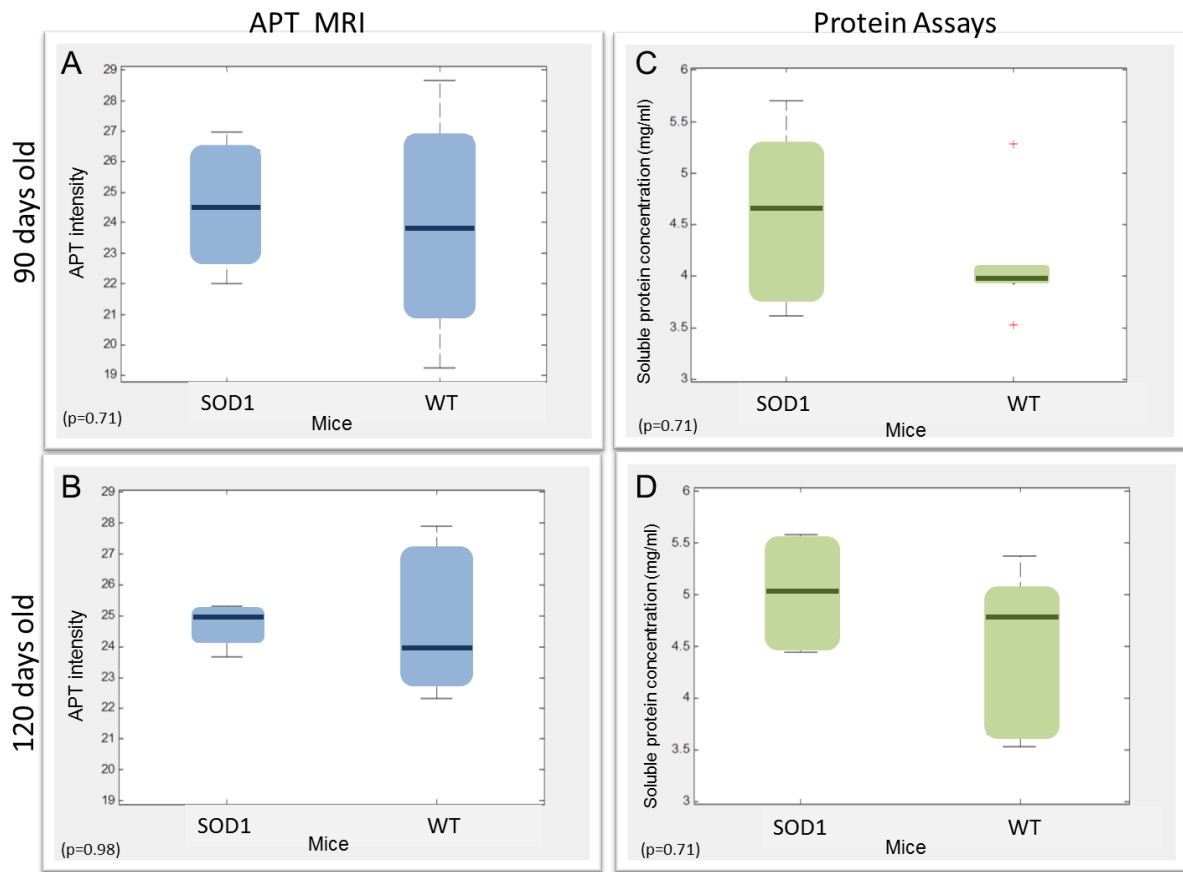
Figure 29. APT-MRI signal measurement and total soluble protein concentrations in the lumbar spinal cords of WT and SOD1 mice. There was no significant difference between SOD1 and WT mice in APT signal measurement at 90 and 120 days (A and B). Comparison of the SOD1 and wild type mice also demonstrated no significant difference at 90 and 120 days in the total soluble protein concentrations (C and D). Significance was measured using a two tailed non paired students t-test with significance defined as *p<0.05. Error bars represent SEM and sample numbers are n=7 in each group (Graph and statistics were performed on MATLAB and are courtesy of Marilena Rega).

5.4.   Discussion

The discovery of the APT imaging technique and its refinement is no doubt an important scientific progression that has been particularly useful for measuring signal contrast in gliomas and pH changes in stroke (Jokivarsi et al., 2007; Zhou et al., 2003b). However, the technique cannot currently measure APT signal from insoluble protein accumulation, which is a key pathological hallmark of many neurodegenerative diseases. These results do however highlight the fact that total soluble protein concentrations do not change significantly in SOD1 transgenic or wild type mice with age. Despite this, the only region measured here was a small region in the L3-L4 lumbar region, meaning that a broader scan covering a larger region may have revealed some other differences in protein values and APT signal. Even though the lumbar region of the spinal cord is well characterized as the main region affected by disease in this animal model, measured by motor neuron cell death, gliosis and increased microglial activation, it is known that other regions are also affected including the cervical region. Therefore this study would also benefit from scans of other spinal cord regions to assess the overall physiological protein concentrations in wild type and SOD1 mice. Previous studies suggest that the levels of soluble SOD1 protein do not change in SOD1 G93A mice (Karch et al., 2009), and although here the total protein concentration was measured, the fact that the soluble form of the toxic protein driving disease does not increase with disease progression would reflect the results obtained in our study. In support of this data, it would suggest that the insoluble rather than the soluble form is more important for neurodegeneration in this model. It is also possible that if there were any changes in protein concentration observed in our experiments, these changes could have been due to cell death and toxicity, microglial activation, increased production of cytokines and upregulation of inflammatory mediators known to be present during the disease progression.

In this study the control mice contained only the wild type mouse SOD1 protein, rather than the ideal control which would have been mice expressing the wild type human SOD1 protein at comparable levels to the mutant human SOD1 expressing mice. Indeed, over expression of the wild type SOD1 protein to the same levels of the mutant can also cause a

progressive neurodegeneration and motor phenotype (Graffmo et al., 2013) reminiscent of the ALS phenotype observed in the mutant mice. However, the lack of difference in total protein levels between our experimental and control mice suggest that these controls were sufficient for this study. For future studies, preferable controls would include wild type age matched mice in addition to transgenic mice expressing normal levels of either the human wild type or mutant SOD1 protein, and human mutant G93A SOD1 mice to compare insoluble SOD1 levels and insoluble protein concentrations between these groups. Therefore the insoluble levels of protein and toxicity could be linked specifically to SOD1 and its overexpression and/or mutation.

5.5. *Future work*

Further work on APT imaging will need to include refinement of the APT frequency detection range in order to detect insoluble, rather than soluble, protein as a marker of protein accumulation. Once this imaging technique has been refined for the measurement of insoluble protein, further work should test different age time points and larger group sizes with this mutant SOD1 mouse. An additional disease mouse model with prominent spinal pathology and no aggregation should be considered as another control, to ensure that the increases in APT signal and protein concentration are disease specific and not caused by cytokines and inflammatory mediators, microglial activation, and other secondary non-specific disease effects. Once this technique has been optimised it will be useful to adapt the protocol to scan brain regions on different mouse models of neurodegeneration with prominent protein aggregation such as Huntington's, Parkinson's and Alzheimer's disease.

5.6. Conclusion

In conclusion, our data supports previous data about the negligible effect of soluble levels of SOD1 in the spinal cord of SOD1 G93A mice (Karch et al., 2009). In addition to this, we suggest that the total levels of soluble protein in the lumbar spinal cord of SOD1 G93A mice are not significantly altered compared to wild type mice expressing no human SOD1 gene. This supports previous data that, rather than the soluble levels of SOD1, it is the insoluble levels of aggregated SOD1 protein that are more tightly linked to disease progression (Deng et al., 2006; Karch et al., 2009). This data is backed up by cellular studies where 90% of cells that contain the highest number of aggregates also had the highest levels of insoluble SOD1 and were destined for cell death. This was in contrast to 70% of cells expressing soluble mutant SOD1 which ultimately survived (Matsumoto et al., 2005). However, another study suggests that levels of SDS dissociable SOD1 monomers and SDS stable soluble SOD1 dimers were significantly elevated before the onset of motor deficits in the spinal cords of the SOD1 H46R mouse model (Koyama et al., 2006). Indeed, the misfolded soluble form of SOD1 was also found to be the toxic species in cell culture (Brotherton et al., 2012). However, the levels of these toxic soluble SOD1 species may not be raised in the mouse model used in our study, or if these toxic species were increased, then the blotting techniques used here are not sensitive or specific enough for their detection. One study was able to detect minute amounts of misfolded soluble SOD1 using a technique called hydrophobic interaction chromatography (HIC). They found that mutant forms of SOD1 from four different mutants had enriched levels of mutant soluble misfolded HIC bound SOD1 in the spinal cord. These species were present throughout the entire life of the mouse and demonstrated similar levels to aggregated insoluble SOD1 deposited at the end stage of the disease (Zetterström et al., 2007). Therefore the levels of soluble SOD1 may still be significant in accounting for toxicity in the mutant SOD1 mouse model, and therefore aggregation may be a protective factor. However from this study it is clear that an APT signal of soluble protein in a region of the spinal cord may not be sensitive or specific enough to detect disease related changes in the SOD1 mouse model.

Chapter 6

General Discussion

6. General Discussion

This thesis has explored the prion-like mechanisms of TDP-43 in ALS using human CNS tissue, cell culture and mouse models. Such prion-like features of TDP-43 included: increased levels of insoluble TDP-43 protein in different regions of the CNS, protease resistance and in vitro cellular seeding and propagation of TDP-43 directly from human ALS CNS tissue. This work should provide the foundations to explore these mechanisms in future projects. The data in this thesis along with discussion of future work will be discussed in further detail here.

6.1   Insoluble TDP-43 levels in patients with ALS

Currently little work has been done to look at the TDP-43 protein expression levels throughout the CNS. Indeed, we found that the highest levels of insoluble TDP-43 were deposited in the motor, frontal and cerebellar cortices and the pons, which were significantly higher than control patients. The increases in the frontal, motor and brainstem regions were not surprising due to their involvement in ALS. However, the increased insoluble levels of TDP-43 in the cerebellum was an intriguing discovery due to a lack of cerebellar involvement in ALS, and lack of observable TDP-43 aggregation in this region. However, our findings are reinforced by more up to date evidence about the more prominent involvement of the cerebellum in ALS (Prell and Grosskreutz, 2013). As previously mentioned, molecular, biochemical and imaging data point to a pathological changes of the cerebellum in ALS, and in particular imaging highlights the neural network connections between the cerebellum and frontal lobes. Other neurodegenerative disease related proteins such as tau and α-synuclein are thought to propagate along specific neural tracts (Liu et al., 2012; Rey et al., 2013). Therefore if similar data emerges about the propagation of ALS related proteins such as TDP-43, then these network connections could act as a trafficking system for the spread of pathology between these regions. Moreover, there is recent evidence highlighting the involvement of the cerebellum in higher cognitive functions and emotion due to connections to regions in the frontal lobes. This could suggest that the cerebellum has a role to play in the diminished cognitive faculties in some patients with ALS and patients with FTLD. Indeed, the fact that C9orf72 mutations causing ALS-FTLD produce

pathological changes in the cerebellum (Liu et al. 2013), would also suggest that the cerebellum has a potential role to play in the diminished cognitive abilities observed in these patients. The pathological spreading of pTDP-43 pathology has a proposed 4 stage model, (Brettschneider et al., 2013) and if TDP-43 pathology does indeed spread to other CNS regions such as the cerebellum, the findings observed here would support a prion-like propagation and spreading of ALS as postulated in the introduction.

Differences in phenotype here were observed with the loss of the TDP-35 isoform levels in the thoracic and lumbar spinal cord of patients with ALS compared to controls, and the lumbar spinal cord of bulbar and limb onset ALS patients. This could be due to an increased or decreased aggregation propensity of this form in specific CNS regions or the loss of this isoform from cell death. The reasons for these differences are unknown and their connection to a phenotype is tenuous without a larger cohort study. Nevertheless, these variations in TDP-35 levels warrant further study in order to pin down evidence for phenotype correlation. The difference of levels of TDP-43 deposited in the motor, frontal and cerebellar cortices in male and female patients point to a potential explanation for the higher incidence of ALS in males compared to females. However, many other co-variables in genetic and biological makeup could also account for this, hence the delineation of molecular mechanisms of sex differences and the incidence of ALS difficult to attain.

Despite the apparent propensity of TDP-43 to aggregate in ALS and FTLD, there is no proof that TDP-43 aggregation is toxic but only that TDP-43 aggregation is linked to both of these diseases. Indeed, as stated in the introduction there is a great deal of conflicting evidence regarding the toxicity of TDP-43 aggregation (Dewey et al., 2012). However, what this data does suggest is that TDP-43 is more prone to aggregation in specific regions of the CNS such as the motor, frontal and cerebellar cortices and pons. This reinforces the idea that, although ALS is thought to have multi-system involvement (Geser et al., 2008, 2009), a more regional specific toxicity may exist which may be linked to TDP-43 aggregation. This phenomenon is also observed in prion disease (Collinge et al., 1996) and, in particular, different strains differentially aggregating in different regions indicates a particular neurotropism of prion pathology. Subsequently, these results could potentially indicate a

179

neurotropism for TDP-43 aggregation in ALS, and a further more detailed analysis may reveal similar findings for FTLD.

6.2   TDP-43 protease resistance

One of the goals in this study was to assess if TDP-43 has a degree of protease resistance in order to determine if the protein is misfolded, and if the protease resistant products were indicative of strain variants. In turn, if there were any strain variants of TDP-43 then the next step was to find a correlation between these variants and the different clinical phenotype of ALS patients. Despite previous reports on the consistent protease resistance of insoluble TDP-43 in ALS and FTLD cases (Tsuji et al., 2012), we found that protease resistance was variable between ALS patients and dependent on the presence of pTDP-43 pathology beforehand. Therefore the results we obtained may be either due to technical and experimental differences compared to published reports, or that the degree of TDP-43 deposition is variable in different ALS patients and requires further investigation. Indeed, pathological studies do indicate that pathological TDP-43 deposition is variable between patients (Geser et al., 2010b). Tsuji et al made comparisons between different TDP-43 proteinopathy subtypes A-C and found specific protease resistant banding patterns to be consistent in all these subtypes. However, they made no attempt to correlate this with any of the different ALS phenotypic criteria, which was the goal of our study. Due to the observed inconsistency of protease resistance observed here, we were unable to compare the ALS phenotypic criteria with the formation of TDP-43 protease resistant bands. We have also demonstrated that TDP-43 is not resistant to proteinase K (PK) (Hasegawa et al., 2011), but partially resistant to trypsin and chymotrypsin (Hasegawa et al., 2011; Tsuji et al., 2012). As PK is a more potent enzyme that digests at more sites along the protein, it would suggest that the ability of misfolded pathological TDP-43 to survive and propagate in the CNS is not as robust as pathologically misfolded prions. This in turn may explain the facile experimental and incidental transmissible nature of prions (Brown et al., 2012) compared to other neurodegenerative disease related proteins. Indeed, there is currently no observable evidence for the human to human transmission of ALS, Alzheimer's or Parkinson's disease (Holmes and Diamond, 2012; Irwin et al., 2013), and this unique high degree of PK

resistance property may partially account for the unique infectious nature of prion disease, which is not shared with other neurodegenerative diseases demonstrating accumulation of misfolded proteins. The resistance of these protein aggregates to PK may allow the proteins to evade cellular clearance machinery and persist within the CNS as part of the disease process. Ultimately, the presence and distribution of insoluble TDP-43 protein levels throughout the CNS, and its sensitivity to proteases are key features of ALS and prion pathology which warrant further detailed future investigation.

6.3   In vitro seeding and propagation of TDP-43

Since the discovery of prion disease, and some of its subsequent pathological mechanisms involved in its propagation and toxicity, there has been significant interest in extrapolating these mechanisms to other neurodegenerative diseases. One of the initial experimental avenues for demonstrating the prion-like behaviour of a protein is to attempt to demonstrate a seeded polymerization reaction of this particular protein. This is often observed by the spatial and temporal development of the aggregated protein in cells after the introduction of a misfolded protein seed. These experiments are usually first conducted in vitro, and can be done with pure recombinant forms of the protein, or protein seeds extracted from CNS tissue of diseased patients. Another main piece of evidence for prion-like cellular mechanisms is the characteristic spreading and propagation of the particular protein. Other prion-like cellular behaviours include the demonstration of different strains of the protein, and demonstrating the neurotoxic properties of this particular protein.

Here, we demonstrated that TDP-43 can form a seeded templating polymerization reaction and can propagate from cell to cell in HEK293 cells. In addition to this, the aggregates formed were highly representative of the morphology of pathological TDP-43 aggregates seen in the pathology report of each case. Other publications have demonstrated a seeding reaction of TDP-43 from recombinant TDP-43 (Furukawa et al., 2011), and also from diseased ALS and FTLD brains (Nonaka et al., 2013). Both of these publications were in parallel to our study and support these findings. However, here we have expanded on some of these properties and examined the effects of a mutation in the prion-like domain (M337V) enhances the formation of pTDP-43 pathology in cell culture

compared to a mutation outside the prion-like domain (D169G). This suggests that this domain is important for pathological TDP-43 aggregate formation. However, as no toxicity can be observed in these cells it is still not possible to determine what effect this accelerated seeded formation of pTDP-43 pathology may have on toxicity. A non-dividing neuronal cell line may be required to ascertain toxicity and further test these differential effects. Another key finding for these prion-like mechanisms will be to elucidate the essential region of the protein responsible for this seeding reaction, and to target therapies to these regions that could eliminate or halt the spread of TDP-43 pathology. If the spread of TDP-43 pathology is indeed related to neurotoxicity then this approach may well prove fruitful as a potential therapy.

Our demonstration of propagation of pTDP-43 aggregates is supported by the Nonaka study (Nonaka et al., 2013), and provides further support for the spreading of pTDP-43 pathology as an underlying mechanism for spread in ALS (Brettschneider et al., 2013, 2014). Indeed, further studies may also link the spreading of pTDP-43 to the spreading of FTLD. Unfortunately we were not able to explore the mechanisms of pTDP-43 aggregate spread between these cells, however Nonaka and colleagues suggest that this occurs partially via exosomes (Nonaka et al., 2013). It has long been thought that ALS starts from a single focal onset at simultaneous upper and lower motor neuron levels (Ravits et al., 2007a). However, a more recent study suggests that due to the distribution of the LMN involvement, ALS has a multi focal onset with local propagation from the site of onset (Sekiguchi et al., 2014). This is in contrast to another report which report the contiguous anatomical propagation of degeneration in ALS (Fujimura-Kiyono et al., 2011). Indeed, the staging of pTDP-43 pathology progression has prompted Braaks' group to suggest that ALS has a focal onset with corticofugal pathological spread along long axonal anatomically connected regions (Braak et al., 2013). Despite this, an exosome mediated pTDP-43 spread provides support for both single or multi focal disease onset and as a mechanism for transynaptic spread between connected regions. Therefore the delineation of the exact mechanisms behind pTDP-43 spread will be important to form the basis for a therapeutic intervention to halt disease progression.

Along with TDP-43, the aggregated ALS causing protein SOD1 has now been shown to participate in a seeded templating reaction and propagation in vitro and cell culture (Chia et al., 2010; Furukawa et al., 2013; Münch et al., 2011a). This highlights the importance of these mechanisms in the disease process, and subsequent correlation of these mechanisms to neurotoxicity will demonstrate the need to target these mechanisms for future therapies. The experimental demonstration of prion-like mechanisms of a disease in cell culture offers the first step in building an effective disease model to test therapeutic targeting methods. Ultimately, the goal of much of ALS research is to build appropriate disease models for therapeutic investigation. However, most ALS models are currently designed around pathological mutations observed in various proteins, which can be useful for studying cases of fALS and sALS with gene mutations. However, our model may be more useful in studying the formation of a sporadic ALS model in the absence of pathogenic mutations. Indeed, this method of reproducing pathology may also be used to develop a cellular model of cases with and without mutations. If toxicity is indeed observed (as shown in (Nonaka et al., 2013)) to be correlated with the development of TDP-43 pathology; then this also links misfolded TDP-43 as a cause of neurotoxicity in TDP-43 proteinopathies.

6.4   TDP-43 transmission

It has now become apparent that, although there is a lack of observed infectivity in these other neurodegenerative diseases (Holmes and Diamond, 2012; Irwin et al., 2013), there is a high degree of similarity in terms of cellular and molecular mechanisms of pathogenesis between prions and other neurodegenerative disease related proteins (Frost and Diamond, 2010; Jucker and Walker, 2013; Münch and Bertolotti, 2012). One of the main ways to demonstrate the prion-like behaviour of a particular protein is to experimentally transmit this protein in vivo (usually in rodents). This was first observed from the endemic spread of kuru in the islands of Papa New Guinea (Gajdusek and Zigas, 1957) and its subsequent transmission to primates (Gajdusek et al., 1966). Since then prion disease has been experimentally transmitted a number of times in various mammalian hosts (Collinge, 2001). The transmission of a particular pathological protein accompanied with an

observable neurodegenerative phenotype provides strong support to the 'protein-only' hypothesis (Griffith, 1967).

The investigation into the prion-like cellular and molecular mechanisms of proteins involved in ALS such as SOD1 (Chia et al., 2010; Furukawa et al 2013; Münch, Brien, & Bertolotti, 2011) and TDP-43 (Furukawa et al., 2011; Nonaka et al., 2013; Tsuji et al., 2012) have been a popular line of enquiry. Indeed, here we demonstrate that TDP-43 does have prion-like cellular behaviour in vitro. In addition to this we attempted to transmit pathological TDP-43 from human ALS brain and spinal cord homogenates to wild type mice via intracerebral inoculation. Currently, after 180 days of incubation there is no observable TDP-43 pathology present in the mice injected with these ALS samples. One of the main reasons for the lack of observable TDP-43 pathology may be the limited incubation periods in these mice. Indeed, we may not expect the rapid accumulation of TDP-43 in 6 month aged mice after 180 days due to efficient cellular clearance mechanisms including UPS and autophagy. Furthermore, these mice did not overexpress a human TARDBP transgene, which is thought to act as an increased level of pathogenic substrate to enhance the seeding and aggregation process, and subsequently reduce the incubation times (Prusiner et al., 1990; Tamgüney et al., 2006). Other mouse experimentally inoculated groups of longer inoculation periods are due to be culled on 360 and 720 days, which could not be accessed in the time frame available here. Despite this, using a non-transgenic line to demonstrate the seeding and transmission of TDP-43 will be a more robust method of demonstrating seeding and propagation. This is because in most human cases of neurodegenerative disease there is not usually an overexpression of disease related proteins, and the spreading and propagation of pathology may be confounded by the anatomically restricted transgene expression in these mouse models.

The other issues have already been highlighted in chapter 4, but the other main issue may be the excessive dilution of TDP-43 seeds in a 1% brain homogenate. Indeed, this has been rectified with intracellular seeding studies in chapter 3, which we now intend to use these sarkosyl extracted seeds to inoculate into wild type mice in the recent future in order to demonstrate transmission. In the meanwhile we will be assessing this TDP-43 seeding

reaction on primary rat cortical neurons with and without a FL WT TDP-43 construct. This will aid in the assessment of whether or not this TDP-43 seeding reaction can take place in rodent cells and use murine TDP-43 as a template for seeding. Additionally, primary cortical neurons will be a more appropriate cell line to assess any toxicity and morphological and functional abnormalities.

In comparison to other neurodegenerative diseases, the facile transmission of prions may be due to their potent infectivity. For most of the other neurodegenerative diseases, there is little evidence for infectivity and transmission within the human population (Holmes and Diamond, 2012; Irwin et al., 2013). Indeed, the unusual transmission routes of prion disease seem to be responsible for the low incidence of the condition, and with preventative measures in place, the incidence of prion disease is now extremely low with about 700 cases of CJD as of 2012 (Brown et al., 2012). As of yet we do not know why some proteins can become infective and others cannot, but prions owe their infectivity in part from their remarkable durability, replication over repeated passages and the host attributes that can either facilitate or impede transmission (Prusiner, 1998). Despite the lack of evidence for infectivity observed with other neurodegenerative diseases, there is substantial evidence for a prion-like behaviour in the pathological proteins associated with these conditions. Indeed, the transmission of other ALS related proteins with observed prion-like behaviour including SOD1 and FUS to mice will provide further evidence of the protein only hypothesis and the prion-like nature of ALS. Rectifying some of the issues highlighted here including the addition of an overexpressed human TDP-43 transgene, longer incubation periods, and purification of TDP-43 in the ALS CNS tissue could potentially yield a model of pathological TDP-43 transmission in the future. These rodent disease models could then potentially be used as a standard model for TDP-43 mediated toxicity in ALS, and used to test novel therapeutic strategies.

6.5   In vivo protein aggregation imaging

The accumulation and deposition of aggregated proteins is a key feature and marker for many neurodegenerative conditions including ALS. Currently there is no method available to non-invasively image the formation of protein aggregates in vivo. The application of the APT-MRI protocol is a novel method for non-invasively measuring soluble protein levels, changes in pH, and has been useful in various other clinical applications such as contrast in brain tumours (Zhou et al., 2003b) and stroke (Jokivarsi et al., 2007). Unfortunately, it is now apparent that the APT measurement protocol cannot detect insoluble protein which is a key marker for aggregating proteins. Therefore we predicted that an aggregation of protein may be indirectly detected in the soluble fraction of the spinal cords. However, there was no observable difference between wild type and the SOD1 mice. As mentioned previously, this imaging technique will need to be refined with an extension of the APT frequency to try to include that which may detect insoluble, as well as soluble protein. However, once this issue has been rectified the APT imaging technique, this novel imaging method potentially offers a unique disease related insight into the aggregation of proteins along the course of the disease. Once this technique has been sufficiently developed, it has a huge potential clinical application for the assessment of the disease course and progression in many neurodegenerative diseases. Additionally, this measurement may provide information about the clinical onset and its correlation to protein accumulation and aggregation. Various studies so far provide conflicting evidence for the role of aggregation in cellular toxicity in neurodegeneration (Ross and Poirier, 2005), and some studies suggest that the oligomers are the toxic species (Benilova et al., 2012; Haass and Selkoe, 2007; Kalia et al., 2013; Simoneau et al., 2007; Ward et al., 2012). If the APT signal does indeed correlate both with protein accumulation and clinical disease onset, then this may provide a method to monitor the disease course, and the treatment of the removal of aggregated protein and its subsequent effects on neurodegeneration. In turn this could help answer a key question, not just in ALS but in many neurodegenerative conditions, about the toxicity of protein aggregation.

6.6   *Summary*

The role of TDP-43 in ALS and FTLD has become a major focus of research to elucidate some of the highly complex molecular and cellular mechanisms underlying these conditions. The main aim of this thesis was to investigate the prion-like mechanisms of TDP-43 pathology in ALS. Some of the criteria for prion-like behaviour of TDP-43 were identified including partial protease resistance, the formation of a templated seeding polymerization reaction of pathological TDP-43, and the propagation of TDP-43 pathology from cell to cell. Some additional prion-like features of TDP-43 were also investigated including the distribution of elevated insoluble TDP-43 levels throughout the CNS, and highlighting regional tropisms for TDP-43 aggregation in ALS. Currently there is no known molecular basis for the heterogeneity of clinical ALS phenotypes, and therefore in a similar manner to prion strain type pathology, we attempted to correlate this distributed deposition of TDP-43 with ALS clinical phenotype criteria. Despite there being no clear cut strain type pathology with ALS from the insoluble levels of TDP-43, the elevated levels in ALS patients warrants further investigation. Indeed, TDP-43 strain types for ALS may not exist at all, but instead may account for the TDP-43 proteinopathies in general and for the ALS-FTLD disease spectrum as noted in another study (Tsuji et al., 2012). It is possible that there may be no molecular basis behind phenotype variability in ALS and these phenotypes may be reflective of the unique individual complex 3D anatomy of the motor system in the brain and spinal cord. In addition it may also be due to a high degree of heterogeneity of genetic and biological differences between individuals with ALS. Indeed, as more ALS causing genes are being discovered, the apparently sporadic cases may have unknown pathogenic mutations in undiscovered ALS related genes. Despite this, a further investigation into a potential genetic and/or molecular basis behind ALS and ALS phenotype variation will be a worthwhile endeavour.

The prion-like cellular mechanisms of misfolded aggregation prone proteins in neurodegenerative diseases could provide potential explanations for the development of sporadic neurodegenerative conditions caused by a stochastic protein misfolding event. The cause of this stochastic misfolding event could have many causes including cellular stress,

defective molecular chaperones for incomplete refolding, and post translational modifications such as oxidation, phosphorylation, glycosylation, sumoylation and methylation. The reason why these proteins are susceptible to misfolding is still unknown, but like the prion protein, they may have a degree of conformational plasticity which allows the switching between conformations (Zhang et al., 1997). This means some of its inherent open domain structure may make it susceptible to misfolding from α-helices to β-sheets under the right conditions. This is thought to be the case with the prion-like domain in the C-terminal of TDP-43, which is prone to self-association and aggregation. Hence any pathological alterations or post translational modifications to this region may make the protein highly susceptible to misfolding and aggregation. The resistance of these TDP-43 aggregates to clearance by the UPS and autophagy may also be reflective of a decreased function of these protein clearance pathways, and could explain the age related incidence of ALS and other neurodegenerative diseases. A more recent hypothesis from the prion field has emerged that describes how prions can form PrP resistant forms over very long incubation periods. This is termed a 'deformed templating' mechanism whereby a recombinant PrP with a different structure to the classical PrP^{Sc} protein slowly becomes misfolded over a period of time to adopt a classical PrP^{Sc} structure, and subsequently cause prion disease (Makarava et al., 2011, 2012). This mechanism in prion disease could also be extrapolated to other neurodegenerative diseases, whereby the normal folded form of the protein gradually becomes misfolded over long periods of time. This, along with decreased efficiency of the cellular clearance mechanisms, could be responsible for the late age of onset of the condition.

In prion disease the evidence for the 'protein-only' hypothesis is now overwhelming (Acquatella-Tran Van Ba et al., 2013), with the misfolded PrP^{Sc} thought to be the toxic component driving disease. One of the key findings will be to discover if the TDP-43 protein is indeed the toxic component driving disease. Future transmission and seeding experiments with pure recombinant TDP-43 will help shed light on this matter. A number of studies of prion toxicity point to small soluble oligomeric intermediates as the toxic species. These small soluble prion oligomers are thought to form during the seeded polymerization

reaction, fibril formation and aggregation of the prion protein (Huang et al., 2013a; Silveira et al., 2005; Simoneau et al., 2007). This could also be the case for TDP-43 related toxicity, but has yet to be effectively demonstrated in vivo or in vitro. Despite mixed evidence for the toxic gain or loss of function of TDP-43, we are beginning to understand how TDP-43 aggregation can occur, and how it could spread throughout the CNS. If these prion-like mechanisms hold true and TDP-43 is indeed the toxic species in this condition, then the conformational change of normal to a misfolded form of TDP-43 could be a plausible explanation for the development of sporadic ALS. This discovery will hopefully lead to the targeting of TDP-43 for therapeutic avenues to arrest disease progression.

The data presented in this thesis provides strong support for a prion-like behaviour of the TDP-43 protein. Therefore it is of crucial importance that prion-like mechanisms of TDP-43 and other proteins involved in neurodegenerative diseases continue to be investigated. As such, further knowledge and dissection of these mechanisms in the future will aid in the discovery of therapeutic avenues for some of the most economically, physically and emotionally disabling conditions known to mankind.

Chapter 7

Methods

7. Methods

7.1.   Spinal cord extraction

Mice were euthanized with 0.1ml of pentobarbital and perfused with 0.9% saline. The spinal cord was then removed and dissected at C2 to C5 for the cervical region and L2-L6 for the lumbar region. The samples were flash frozen in liquid nitrogen and stored at -80°C for future use.

7.2.   Spinal cord fractionation

The spinal cords were separated into soluble and insoluble fractions to analyse for SOD1 levels in each mouse. To do this the spinal cords were sonicated in 1:20 (wt/vol) of TEN buffer (10mM Tris, 1mM EDTA, 100mM NaCl, pH=8.0) + 1% NP-40 and 1 x protease inhibitor at half power 10 sec 3 x with a probe sonicator (Soniprep 150, 14 Amps). The lysate was then ultracentrifuged at 100,000xg for 5 minutes and the supernatant was saved as the soluble fraction (S1). The pellet was the resuspended in 500μl of 1x TEN buffer + 1% NP-40+ 1 protease inhibitor by sonication as before then ultracentrifuged again at 100,000xg for 5 minutes. The pellet (P2) was then resuspended in equal starting volume of water and sonicated as before. The BCA assay was then performed on both S1 and P2 and 50μg of protein was loaded on to a gel for western blotting.

7.3.   CNS homogenate preparation

Human brain and spinal cord homogenates were prepared using Dulbecco's phosphate buffered saline (PBS) with no $CaCl_2$ and $MgCl_2$ (Cat no. 14190-094, Invitrogen) at 9x the wet weight of the tissue to make a 10% homogenate. Tissue was homogenised in a Duall tissue grinder (3ml grinder Cat no. K-885450-0021, Anachem) and frozen down at -80°C in 100 or 500μl aliquots. A list of all the tissues used is shown below:

Pathology Lab	Patient	Samples	Age (Years)	Sex (M/F)	Cause of Death	Post mortem delay (hours)	Disease duration (months)	ALS Phenotype Onset	Genetic Mutation
NeuroResource	J	PFC, MC, TCX, CBLM, SC Lu	72	F	MND	52	~24	Bulbar	?
NeuroResource	Q	PFC, MC, TCX, CBLM, SC Cv, SC Th, SC Lu	82	F	MND	26	6	Bulbar	?
King's	A343/10	MC, FCX, TCX, CBLM, Pons, SC Cv, SC Th, SC Lu	65	M	MND	64	90	Limb	
King's	A151/10	MC, FCX, TCX, CBLM, Pons, SC CV, SC Th, SC Lu	75	F	MND	38	36	Limb	None
King's	A251/09	MC, FCX, TCX, CBLM, Pons, SC Th, SC Lu	78	M	MND	2	60	Limb	None
King's	A148/09	MC, FCX, TCX, CBLM, Pons, SC Th, SC Lu	60	M	MND	53	24	Limb	
King's	A98/09	MC, FCX, TCX, CBLM, Pons, SC Cv, SC Th, SC Lu	72	M	MND	53	24	Bulbar	
King's	A295/08	MC, FCX, TCX, CBLM, Pons, SC Cv, SC Th, SC Lu	74	M	MND	70	24	Limb	None
King's	A257/11	MC, FCX, TCX, CBLM, Pons, SC Cv, SC Th, SC Lu	75	M	MND	38	18 months	Bulbar	
King's	A285/11	MC, FCX, TCX, CBLM, Pons, SC Cv, SC Th, SC Lu	63	F	MND	25	60	Limb	
King's	A381/11	MC, FCX, TCX, CBLM, Pons, SC Cv, SC Th,	86	F	MND	77	24	Limb	

		SC Lu							
King's	A203/11	MC, FCX, TCX, CBLM, Pons, SC Cv, SC Th, SC Lu	57	F	MND	54	24	Limb	
King's	A157/12	MC, FCX, TCX, CBLM, Pons, SC Cv, SC Th, SC Lu	66	M	MND	45	42	Bulbar	
King's	A46/12	MC, FCX, TCX, CBLM, SC Th, SC Lu	92	F	NC	N/A	N/A	N/A	N/A
King's	A136/10	MC, FCX, TCX, CBLM, Pons, SC Cv, SC Th, SC Lu	89	F	NC	N/A	N/A	N/A	N/A
King's	A63/10	MC, FCX, TCX, CBLM, Pons, SC Cv, SC Th, SC Lu	90	F	NC	N/A	N/A	N/A	N/A
King's	A130/09	MC, FCX, TCX, CBLM, Pons, SC Cv, SC Th, SC Lu	54	M	NC	N/A	N/A	N/A	N/A
King's	A48/09	MC, FCX, TCX, CBLM, Pons, SC Th	81	M	NC	N/A	N/A	N/A	N/A
King's	A265/08	MC, FCX, TCX, CBLM, Pons, SC Cv, SC Th, SC Lu	79	M	NC	N/A	N/A	N/A	N/A
King's	A49/03	MC, FCX, TCX, CBLM, Pons, SC Th, SC Lu	79	M	NC	N/A	N/A	N/A	N/A
King's	A12/12	MC, FCX, TCX, CBLM, Pons, SC Cv, SC Th, SC Lu	51	F	NC	N/A	N/A	N/A	N/A
King's	A261/12	MC, FCX, TCX, CBLM, Pons, SC Cv, SC Th, SC Lu	63	M	NC	N/A	N/A	N/A	N/A
King's	A213/12	MC, FCX, TCX, CBLM, Pons, SC Th, SC Lu	78	M	NC	N/A	N/A	N/A	N/A

Table 5. Normal control and ALS samples used in this study. These include: tissue bank supplier, patient ID, age of death, Sex, disease duration and region of disease onset. MND = motor neuron disease, NC = normal control, MC = motor cortex, FCX = frontal cortex, TCX = temporal cortex, CBLM = cerebellum, SC CV = spinal cord cervical, SC Th = spinal cord thoracic, SC Lu = spinal cord lumbar.

7.4.   *CNS tissue detergent extraction*

For the sarkosyl insoluble urea soluble fractions the CNS tissue was homogenised and then extracted as described previously (Arai et al., 2006; Hasegawa et al., 2008) but with some modifications. For each extraction we took 500µl of 10% tissue homogenate and added an equal amount of 2 x extraction buffer A (BA: 10mM Tris, 0.8M NaCl, 10% sucrose, 1mM EGTA, pH 7.5) with 2% triton X-100, 2x protease (Roche, Cat no. 05892970001) and phosphatase inhibitor cocktail tablets (Roche, Cat no. 04906837001). This was incubated for 30 minutes at 37°C and then ultracentrifuged at 100,000xg for 30 minutes at 4°C. The supernatant was removed and discarded and then briefly sonicated in the starting volume (500µl) of 1 x BA containing 1% sarkosyl (Sigma, Cat no. L9150) with 1 x protease and phosphatase inhibitors then incubated at 37°C for 30 minutes. The sample was then ultracentrifuged again at 100,000xg for 30 minutes at 23°C and the supernatant was then removed and discarded. The pellet was briefly sonicated in 200µl of 1 x BA containing 1% CHAPS (Sigma, Cat no. C9246) with protease and phosphatase inhibitors, and then ultracentrifuged for 20 minutes at 25°C. The supernatant was then removed and discarded and the pellet was either resuspended in 50µl of 8M urea (pH 7.5) for expression levels and banding ratios, 100µl of 30 mM Tris-HCl (pH 7.5) for protease digestion.

For obtaining TDP-43 seeds to introduce to cell culture, 500µl of the CNS homogenates were mixed in 2X homogenisation buffer (HB: 10 mM Tris- HCl, pH 7.5 containing 0.8M NaCl, 1mM EGTA, 1mM dithiothreitol) containing a 2% sarkosyl detergent to make a final of 1X HB with 1% sarkosyl. These samples were then sonicated briefly and heated at 37˚C for 30 minutes and then spun at 12,000xg for 10 minutes. The supernatant was taken and spun further at 100,000xg for 10 minutes. The pellet was then resuspended in 1ml of PBS to wash and spun again at 100,000xg for 20 minutes. The resultant pellet was then resuspended in

100μl of sterile PBS and BCA assay was used to assess the concentration of protein in each sample. Then 10μg of protein was then used to transfect cells.

7.5. *Immunoblotting*

Samples were measured for protein concentration using a BCA assay (Bio-Rad) and either 25, 50 or 100μg of protein was loaded on to a gel. These samples were added to an equal amount of working SDS solution with β-mercaptoethanol and boiled at 100°C for 5 minutes. The samples were then vortexed and centrifuged at 14,800 rpm for 1 minute. The appropriate protein amount from each sample was loaded on to 16% tris glycine SDS PAGE gels (Cat No. EC6498 BOX, Invitrogen) and run at 200V for 70 minutes. Gels were then blotted onto nitrocellulose membranes (Cat No. 10401196, Protran) for either 2 hours at 35V or 15V at 4°C overnight. Membranes were then blocked in 5% Milk in PBS for 1 hour then probed with either primary anti-rabbit polyclonal TDP-43 antibody (Cat no. 10782-AP, Proteintech) (1:3000), anti-mouse monoclonal TDP-43 antibody (Cat no. 60019-2-Ig, Proteintech) (1:3000), anti-rabbit polyclonal pTDP-43 (pS409/410) (Cat no. TIP-PTD-P01, Cosmo Bio co Ltd) (1:1000-1:3000), mouse monoclonal β-actin antibody Clone AC-15 (1:20,000) (Cat No. A1978, Invitrogen), anti-rabbit polyclonal SOD1 antibody (Enzo life sciences, ADI-SOD-100) in 1% non-fat milk in PBS + 0.1% tween (PBST). Blots were washed 4 times for 5 minutes each in PBST and then probed with secondary fluorescent antibodies: goat anti rabbit IgG antibody IRDye800 (Green) (Cat no. 611-132-122, Tebu-bio) (1:10,000), Alexa Fluor 700 goat anti mouse IgG (Red) (Cat no. A-21036, Invitrogen) (1:10,000) in 1% Non-fat milk in PBST. Blots were washed again 4 times for 5 minutes in PBST and washed once in PBS, then visualised with the Odyssey scanner.

7.6. Cloning

7.6.1. Constructs

The truncation 162-414 TDP-43 mutant was subcloned from the wild type TDP-43 pFLAG-CMV2 vector which was previously cloned by Burratti and Barralle. The truncation PCR products were amplified by High-fidelity Taq (Roche), and subcloned into pFLAG-CMV2 vector using HindIII and KpnI restriction sites. The following primers were used to build up the truncations:

Fwd162 ggcAAGCTT-TCACAGCGACATATGATAG (HindIII) GC% 43 (57.4C)

Rev   gctGGTACC-CTACATTCCCCAGCCAGAA (KpnI) 54.2-65C

>162-414 MSQRHMIDGRWCDCKLPNSKQSQDEPLRSRKVFVGRCTE

DMTEDELREFFSQYGDVMDVFIPKPFRAFAFVTFADDQIAQSLCGEDLII

KGISVHISNAEPKHNSNRQLERSGRFGGNPGGFGNQGGFGNSRGGGAGLG

NNQGSNMGGGMNFGAFSINPAMMAAAQAALQSSWGMMGMLASQQNQSGPS

GNNQNQGNMQREPNQAFGSGNNSYSGSNSGAAIGWGSASNAGSGSGFNGG

FGSSMDSKSSGWGM*

7.6.2. Mutagenesis

Mutagenesis was performed using the Quick Change Lightning Site Directed Mutagenesis Kit (Agilent, Cat no. 210518) according to the manufacturer's instructions. This mutagenesis was used to induce the Asp169 to Gly (D169G) and Met337 to Val (M337V) into the full length and truncated (162-414) TDP-43. The mutations were made using the following primers:

D169G-F - CGACATATGATAGGTGGACGATGGTGT

D169G-R - ACACCATCGTCCACCTATCATATGTCG

M337V-F - CAGTTGGGGTATGGTGGGCATGTTAGC

M337V-R - GCTAACATGCCCACCATACCCCAACTG

7.6.3. Propagation of plasmid constructs in E.coli

The full length wild type, truncated (162-414) wild type and truncated mutants D169G and M337V were transformed into *E.coli* to propagate the plasmid. For this about 50-100µl of High Efficiency JM109 or HB101 *E.coli* cells (thawed slowly on ice) and 5µl-10µl of ligation reaction (i.e. 10% of the cell volume) were mixed and incubated on ice for 15 minutes then "heat shocked" for 30 seconds in a 42°C heating block and returned to the ice for 10 minutes. After the addition of 500µl- 1ml of L-broth (for low or high copy number vectors respectively), the cells were incubated at 37°C for 1 hour with horizontal agitation at 150rpm. Gentle centrifugation at 3,000 x g formed a cell pellet which, after removal of the supernatant, was re-suspended in 100µl of L-broth. The full cell suspension was spread on an LB-agar plate containing an appropriate selection antibiotic and incubated overnight at 37°C.

Single, well-defined colonies were individually picked using aseptic technique and cultured in 3ml of L-broth containing the selection antibiotic. Following overnight incubation at 37°C with vigorous horizontal agitation at 250rpm, the cultured cells were harvested by centrifugation at 17,000 x g. The cloned plasmid DNA was extracted from the bacterial cells using the QIAquick Spin Miniprep kit (Cat no. 12123, QIAGEN) according to the manufacturer's protocol. For larger quantities of DNA the bacteria were grown in 250ml of LB broth and incubated overnight at 37˚C with agitation at 250rpm. After this, the QIAGEN maxi prep kit (Cat no. 12362, QIAGEN) was used to extract and purify the DNA used for transfection according to the manufacturer's protocol. Final confirmation of cloned plasmid constructs was achieved by sequencing. All DNA sequencing was outsourced to a service provider, Source BioScience Ltd.

7.7. Cell culture

HEK293T and SHSY5Y cells were grown up to 80-90% confluency in Dulbecco' Modified Eagle Medium (DMEM), containing 10% fetal bovine serum (FBS), 1% L-Glutamine and 1% penicillin and streptomycin.

7.7.1. TDP-43 seeding

For transfection, the HEK cells were grown up to 70-80% confluency in either 6 well or on 24 well plates on PDL coated coverslips. Transfection was performed with the Lipofectamine 2000 reagent (Invitrogen, Cat no. 11668-019) according to the manufacturer's protocol. Briefly, 2µl of Lipofectamine was added to 50µl of serum free DMEM for one well of a 24 well plate and 5µl of Lipofectamine was added to 200µl of serum free DMEM for one well of a 6 well plate. Then 1µg of DNA was added per 1 well of a 24 well plate and 2.5µg of DNA was added per 1 well of a 6 well plate. The mixtures were then further incubated at room temperature for 5 minutes. These mixtures were then added to the cells and left to incubate at 37˚C in 5% CO_2 for the designated time. For transfection of the TDP-43 seeds from ALS CNS tissue the transfection was done the day after with the same protocol as above with 10µg of protein from the brain lysate, and media was either changed after 4-6 hours to fresh DMEM or left to incubate with the cells. Cells were then either extracted in sarkosyl detergent for running on a western blot or fixed for immunocytochemistry. For the cell detergent extraction: cells were either collected by trypsinisation in 0.025% trypsin for 5 minutes or scraped off the plate using ice cold PBS. The cells were then centrifuged at 2000rpm for 5 minutes and resuspended in 50-100µl of TS buffer (150mM Tris HCl, 50 mM NaCl, 5mM EDTA, and 5mM EGTA) containing 1% sarkosyl and protease and phosphatase inhibitors. The samples were sonicated and incubated at 37˚C for 30 minutes. The samples were then ultra-centrifuged at 290,000 x g for 20 minutes at room temperature. The supernatant was used as the sarkosyl soluble (SS) fraction and the pellet was resuspended in 40-50µl of 8M urea. A BCA assay was performed on both fractions, and 25µg of protein was loaded on a gel for blotting.

7.7.2. TDP-43 propagation

HEK cells were grown to ~60-70% confluency in 24 well plates and either seeded with the FL WT and ALS TDP-43 seed or transfected with GFP. After 3 days of incubation both wells were trypsinised in 0.0.25% trypsin for 5 minutes and collected and spun down at 2000rpm for 5 minutes. Both populations of cells were mixed together in a 1:1 ratio and plated onto a 22mm PDL coated coverslip and incubated for a further 3 days. Cells were then fixed in 4% paraformaldehye (PFA) and for immunocytochemistry analysis.

7.7.3. Immunocytochemistry

Cells were gently washed with PBS and fixed for 15 minutes in 4% PFA then gently washed again in PBS and permeabilised with 0.5% triton X-100 in PBS for 10-15 minutes. The slides were then blocked in 5% BSA for 30 minutes and then stained with polyclonal rabbit anti-TDP-43 (1:500) (Proteintech, Cat no. 10782-2-AP), monoclonal mouse anti-TDP-43 (1:500) (Proteintech, Cat no. 60019-2-Ig), polyclonal anti-rabbit phoshpo TDP-43 (pS409/410-1) (1:500) and monoclonal mouse anti-ubiquitin (1:500) (Millipore, Cat no. MAB1510) in 5% BSA for 2 hours at room temperature. Cells were then gently washed in PBS 3 times and incubated with a fluorescent secondary anti-rabbit Alexa-Fluor 488 and anti-mouse or anti-rabbit Alexa-Fluor 568 antibodies (1:2000) (Invitrogen) in 5% BSA for 1 hour and washed again as before. They were then stained with DAPI (1:2000) in PBS for 5 minutes, washed twice with PBS, air dried and mounted onto slides with Fluoromount G (Cat No. 0100-1, Southern Biotech) and visualised with a Zeiss 700 confocal microscope.

7.8. Densitometry and statistical analysis

Densitometry analysis was performed using image J from a standard protocol and statistical analysis was done using the Prism 4 software. An unpaired two tailed student's t-test was used in all cases to generate a statistical p value. Any p value below 0.05 was considered to be statistically significant.

7.9. TDP-43 transmission

All tissue samples were supplied from London Neurodegenerative Diseases Brain Bank at the Institute of Psychiatry and have appropriate consent for this research. All inocula are 1 % w/v whole tissue homogenates in sterile D-PBS lacking calcium and magnesium ions prepared by passage through 19, 21, 23 and 25 gauge syringe needles. The following inocula were used in this study:

I16891 ALS motor cortex IoP code A257/11

I16892 ALS spinal cord (lumbar) IoP code A257/11

I16893 ALS motor cortex IoP code A381/11

I16894 ALS spinal cord (lumbar) IoP code A381/11

I16895 Normal human motor cortex IoP code A213/12

I16896 Normal human spinal cord (lumbar) IoP code A213/12

All inocula were stored at -80°C in 2ml aliquots and thawed only once to inoculate all mice in the appropriate group. 30µl of each inoculum was inoculated intracerebrally into 5 groups of 11 female C57BL/6JOlaHsd mice (stock code C57BL-6) at about 6 weeks of age. Inoculated mice were monitored for signs of neurological disease throughout the incubation periods. Inoculations and SHIRPA monitoring were conducted by Mike Brown and Anthony White at the MRC prion unit. Planned culling of groups occurred at 7, 90 and 180 days post-inoculation (follow up culls at 360 and 720 days) with collection of right half of the brain for freezing, left half to be fixed and spinal column to be fixed. Selected mice were assessed by measuring weight, grip strength and by the standard SHIRPA protocol (Licence 70/7274 19b protocol 7)(See http://empress.har.mrc.ac.uk/browser/index.html?sop_id=sop/10_002_0). Brains were collected and dissected in half sagitally. The left half was fixed in 10% buffered formal saline for immunohistochemistry and the right half was snap frozen in isopentane pre-cooled on dry ice, for detergent extraction and analysis with western blotting. The spinal column was collected and fixed in 10% buffered formal saline for a minimum of one week for immunohistochemical staining and motor neuron counting upon observation of any motor deficits.

7.10.   Histology

The buffered formal saline fixed brain samples were processed overnight through a series of alcohols, xylenes and paraffin wax and followed by paraffin wax embedding. Sections were cut at a nominal thickness of 3µm on a microtome. Post fixation, spinal columns were decalcified in 0.5M EDTA for 7 days with changes of EDTA every other day. Spinal columns were then dissected into cervical, thoracic and lumbar regions, with each region further dissected into segments of approximately 3mm thickness. Each spinal column region was then processed in its own cassette and embedded in paraffin wax as described above. Sections were cut from the lumbar region block at 3µm thick using a microtome. All cut sections were placed on slides, air dried for 2 hours and baked in the oven at 60°C overnight.

7.11.   Histochemistry and immunohistochemistry

De-waxing of the sections was achieved by placing them in a series of xylenes. The sections were re-hydrated in serial concentrations of ethanol (100%, 100%, 90% and 70%). Finally they were placed in cold running water and were ready for pre-treatment if necessary. For sample de-hydration after IHC the samples were added to increasing concentrations of ethanol (70%, 90%, 100% and 100%) and then added to a series of xylenes.

After re-hydration samples were stained with Harris' Haematoxylin (VWR Cat no 351945S) and 0.5% Eosin Y-Solution (Merck Millipore Cat no 1.09844.1000) (H&E). Slides were placed in Harris' Haematoxylin for 5 minutes, rinsed in cold running water differentiated in 1% acid alcohol for approximately 20 seconds. Slides were placed in cold running water again for 3 minutes to allow for bluing to take place. Finally, slides were placed in 0.5% Eosin for 3 minutes and rinsed in water for 20 seconds. Slides were then dehydrated as described above and mounted using the DiaPath coverslipping machine. .

All immunohistochemistry was performed on the Ventana Discovery XT automated system using the Ventana DAB-MAP kit except GFAP staining which was performed on the Ventana Benchmark XT automated system using the Ventana iView DAB kit.

The antibodies used included rabbit polyclonal anti-GFAP (Cat no. Z0334, Dako) (1:1000), rabbit polyclonal anti-pTDP-43 (pS409/410) (Cat no. TIP-PTD-P01, Cosmo-bio) (1:500), mouse monoclonal anti-ubiquitin (Sc-0817, Santa Cruz Biotechnology) (1:5000), rabbit polyclonal anti-Iba1 (019-19741, Wako) (1:250) and Guinea pig polyclonal anti-p62 (GP62-C, Progen Biotechnik) (1:400). Pre-treatment as described above was used for p62 staining only. Pre-treatment was performed using a heat and acid epitope retrieval method. Sections for all other antibodies were de-waxed, re-hydrated and pre-treated on their respective automated staining machines. Automated pre-treatments use Ventana Discovery Cell Conditioning Solution 1 (CC1) and heat. Ubiquitin pre-treatment was mild (MCC1), Iba1 was standard (SCC1) and pTDP-43 was extended (ECC1), where mild, standard and extended refer to the length of time incubated with CC1. GFAP pre-treatment was with Ventana Protease 1.

Appropriate secondary's were used (rabbit anti-mouse Dako Cat no. E0354 and swine anti-rabbit Dako Cat no. E0353) and then counter stained with the 3'3-Diaminobenzidine (DAB) within the Ventana staining kits mentioned above. Slides were then mounted with coverslips and visualised on a light microscope. All immunohistochemistry was conducted by Sarah Lyall in the MRC prion unit, and visualisation and tissue assessment was conducted by myself with co-validation from Sebastian Brandner.

Chapter 8

References

8. References

Acharya, K.K., Govind, C.K., Shore, A.N., Stoler, M.H., and Reddi, P.P. (2006). cis-requirement for the maintenance of round spermatid-specific transcription. Dev. Biol. *295*, 781–790.

Acquatella-Tran Van Ba, I., Imberdis, T., and Perrier, V. (2013). From Prion Diseases to Prion-Like Propagation Mechanisms of Neurodegenerative Diseases. Int. J. Cell Biol. *2013*, 975832.

Aguzzi, A. (2009). Cell biology: Beyond the prion principle. Nature *459*, 924–925.

Aguzzi, A., and O'Connor, T. (2010). Protein aggregation diseases: pathogenicity and therapeutic perspectives. Nat. Rev. Drug Discov. *9*, 237–248.

Aguzzi, A., and Rajendran, L. (2009). The transcellular spread of cytosolic amyloids, prions, and prionoids. Neuron *64*, 783–790.

Aguzzi, A., Heikenwalder, M., and Polymenidou, M. (2007). Insights into prion strains and neurotoxicity. Nat. Rev. Mol. Cell Biol. *8*, 552–561.

Ahmed, Z., Cooper, J., Murray, T.K., Garn, K., McNaughton, E., Clarke, H., Parhizkar, S., Ward, M. a, Cavallini, A., Jackson, S., et al. (2014). A novel in vivo model of tau propagation with rapid and progressive neurofibrillary tangle pathology: the pattern of spread is determined by connectivity, not proximity. Acta Neuropathol.

Akamatsu, M., Takuma, H., Yamashita, T., Okada, T., Keino-Masu, K., Ishii, K., Kwak, S., Masu, M., and Tamaoka, A. (2013). A unique mouse model for investigating the properties of amyotrophic lateral sclerosis-associated protein TDP-43, by in utero electroporation. Neurosci. Res.

Alami, N.H., Smith, R.B., Carrasco, M.A., Williams, L.A., Winborn, C.S., Han, S.S.W., Kiskinis, E., Winborn, B., Freibaum, B.D., Kanagaraj, A., et al. (2014). Axonal Transport of TDP-43 mRNA Granules Is Impaired by ALS-Causing Mutations. Neuron *81*, 536–543.

Alberti, S., Halfmann, R., King, O., Kapila, A., and Lindquist, S. (2009). A systematic survey identifies prions and illuminates sequence features of prionogenic proteins. Cell *137*, 146–158.

Al-Chalabi, A., and Hardiman, O. (2013). The epidemiology of ALS: a conspiracy of genes, environment and time. Nat. Rev. Neurol. 1–12.

Al-Chalabi, A., Jones, A., Troakes, C., King, A., Al-Sarraj, S., and van den Berg, L.H. (2012). The genetics and neuropathology of amyotrophic lateral sclerosis. Acta Neuropathol. *124*, 339–352.

Alexander, P.A., He, Y., Chen, Y., Orban, J., and Bryan, P.N. (2007). The design and characterization of two proteins with 88% sequence identity but different structure and function. Proc. Natl. Acad. Sci. U. S. A. *104*, 11963–11968.

Alper, T., Haig, D.A., and Clarke, M.C. (1966). The exceptionally small size of the scrapie agent. Biochem. Biophys. Res. Commun. *22*, 278–284.

Amador-Ortiz, C., Lin, W.-L., Ahmed, Z., Personett, D., Davies, P., Duara, R., Graff-Radford, N.R., Hutton, M.L., and Dickson, D.W. (2007). TDP-43 immunoreactivity in hippocampal sclerosis and Alzheimer's disease. Ann. Neurol. *61*, 435–445.

Amaral, M.D. (2004). CFTR and chaperones: processing and degradation. J. Mol. Neurosci. *23*, 41–48.

Andersen, P.M. (2006). Amyotrophic lateral sclerosis associated with mutations in the CuZn superoxide dismutase gene. Curr. Neurol. Neurosci. Rep. *6*, 37–46.

Anfinsen, C.B. (1972). The formation and stabilization of protein structure. Biochem. J. *128*, 737–749.

Arai, T., Hasegawa, M., Akiyama, H., Ikeda, K., Nonaka, T., Mori, H., Mann, D., Tsuchiya, K., Yoshida, M., Hashizume, Y., et al. (2006). TDP-43 is a component of ubiquitin-positive tau-negative inclusions in frontotemporal lobar degeneration and amyotrophic lateral sclerosis. Biochem. Biophys. Res. Commun. *351*, 602–611.

Arai, T., Hasegawa, M., Nonoka, T., Kametani, F., Yamashita, M., Hosokawa, M., Niizato, K., Tsuchiya, K., Kobayashi, Z., Ikeda, K., et al. (2010). Phosphorylated and cleaved TDP-43 in ALS, FTLD and other neurodegenerative disorders and in cellular models of TDP-43 proteinopathy. Neuropathology *30*, 170–181.

Armakola, M., Higgins, M.J., Figley, M.D., Barmada, S.J., Scarborough, E. a, Diaz, Z., Fang, X., Shorter, J., Krogan, N.J., Finkbeiner, S., et al. (2012). Inhibition of RNA lariat debranching enzyme suppresses TDP-43 toxicity in ALS disease models. Nat. Genet. *44*, 1302–1309.

Arnold, E.S., Ling, S.-C., Huelga, S.C., Lagier-Tourenne, C., Polymenidou, M., Ditsworth, D., Kordasiewicz, H.B., McAlonis-Downes, M., Platoshyn, O., Parone, P. a, et al. (2013). ALS-linked TDP-43 mutations produce aberrant RNA splicing and adult-onset motor neuron disease without aggregation or loss of nuclear TDP-43. Proc. Natl. Acad. Sci. U. S. A. 1–10.

Ash, P.E.A., Bieniek, K.F., Gendron, T.F., Caulfield, T., Lin, W.-L., DeJesus-Hernandez, M., van Blitterswijk, M.M., Jansen-West, K., Paul, J.W., Rademakers, R., et al. (2013). Unconventional Translation of C9ORF72 GGGGCC Expansion Generates Insoluble Polypeptides Specific to c9FTD/ALS. Neuron 1–8.

Ayala, Y.M., Pantano, S., D'Ambrogio, A., Buratti, E., Brindisi, A., Marchetti, C., Romano, M., and Baralle, F.E. (2005). Human, Drosophila, and C.elegans TDP43: nucleic acid binding properties and splicing regulatory function. J. Mol. Biol. *348*, 575–588.

Ayala, Y.M., Misteli, T., and Baralle, F.E. (2008a). TDP-43 regulates retinoblastoma protein phosphorylation through the repression of cyclin-dependent kinase 6 expression. Proc. Natl. Acad. Sci. U. S. A. *105*, 3785–3789.

Ayala, Y.M., Zago, P., Ambrogio, A.D., Xu, Y., Petrucelli, L., Buratti, E., and Baralle, F.E. (2008b). Structural determinants of the cellular localization and shuttling of TDP-43. J. Cell Sci. 3778–3785.

Ayala, Y.M., De Conti, L., Avendaño-Vázquez, S.E., Dhir, A., Romano, M., D'Ambrogio, A., Tollervey, J., Ule, J., Baralle, M., Buratti, E., et al. (2010). TDP-43 regulates its mRNA levels through a negative feedback loop. EMBO J.

Baker, H.F., Ridley, R.M., Duchen, L.W., Crow, T.J., and Bruton, C.J. (1994). Induction of beta (A4)-amyloid in primates by injection of Alzheimer's disease brain homogenate. Comparison with transmission of spongiform encephalopathy. Mol. Neurobiol. *8*, 25–39.

Baker, M., Mackenzie, I.R., Pickering-Brown, S.M., Gass, J., Rademakers, R., Lindholm, C., Snowden, J., Adamson, J., Sadovnick, A.D., Rollinson, S., et al. (2006). Mutations in progranulin cause tau-negative frontotemporal dementia linked to chromosome 17. Nature *442*, 916–919.

Barańczyk-Kuźma, A., Usarek, E., Kuźma-Kozakiewcz, M., Kaźmierczak, B., Gajewska, B., Schwalenstocker, B., and Ludolph, A.C. (2007). Age-related changes in tau expression in transgenic mouse model of amyotrophic lateral sclerosis. Neurochem. Res. *32*, 415–421.

Barmada, S.J., Skibinski, G., Korb, E., Rao, E.J., and Wu, J.Y. (2010). Cytoplasmic mislocalization of TDP-43 is toxic to neurons and enhanced by a mutation associated with familial ALS. Gaia Ecol. Perspect. Sci. Soc. *30*.

Barrenetxea, G. (2012). Iatrogenic prion diseases in humans: an update. Eur. J. Obstet. Gynecol. Reprod. Biol. *165*, 165–169.

Bastow, E.L., Gourlay, C.W., and Tuite, M.F. (2011). Using yeast models to probe the molecular basis of amyotrophic lateral sclerosis. Biochem. Soc. Trans. *39*, 1482–1487.

Beekes, M., and McBride, P. a (2007). The spread of prions through the body in naturally acquired transmissible spongiform encephalopathies. FEBS J. *274*, 588–605.

Bellinger-Kawahara, C.G., Kempner, E., Groth, D., Gabizon, R., and Prusiner, S.B. (1988). Scrapie prion liposomes and rods exhibit target sizes of 55,000 Da. Virology *164*, 537–541.

Benilova, I., Karran, E., and De Strooper, B. (2012). The toxic Aβ oligomer and Alzheimer's disease: an emperor in need of clothes. Nat. Neurosci. *15*, 349–357.

Berson, J.F., Theos, A.C., Harper, D.C., Tenza, D., Raposo, G., and Marks, M.S. (2003). Proprotein convertase cleavage liberates a fibrillogenic fragment of a resident glycoprotein to initiate melanosome biogenesis. J. Cell Biol. *161*, 521–533.

Bétemps, D., Verchère, J., Brot, S., Morignat, E., Bousset, L., Gaillard, D., Lakhdar, L., Melki, R., and Baron, T. (2014). Alpha-synuclein spreading in M83 mice brain revealed by detection of pathological alpha-synuclein by enhanced ELISA. Acta Neuropathol. Commun. *2*, 29.

Bigio, E.H., Wu, J.Y., Deng, H.-X., Bit-Ivan, E.N., Mao, Q., Ganti, R., Peterson, M., Siddique, N., Geula, C., Siddique, T., et al. (2013). Inclusions in frontotemporal lobar degeneration with TDP-43 proteinopathy (FTLD-TDP) and amyotrophic lateral sclerosis (ALS), but not FTLD with FUS proteinopathy (FTLD-FUS), have properties of amyloid. Acta Neuropathol. 2–4.

Bolmont, T., Clavaguera, F., Meyer-Luehmann, M., Herzig, M.C., Radde, R., Staufenbiel, M., Lewis, J., Hutton, M., Tolnay, M., and Jucker, M. (2007). Induction of tau pathology by intracerebral infusion of amyloid-beta -containing brain extract and by amyloid-beta deposition in APP x Tau transgenic mice. Am. J. Pathol. *171*, 2012–2020.

Borchelt, D.R., Guarnieri, M., Wong, P.C., Lee, M.K., Slunt, H.S., Xu, Z.S., Sisodia, S.S., Price, D.L., and Cleveland, D.W. (1995). Superoxide dismutase 1 subunits with mutations linked to familial amyotrophic lateral sclerosis do not affect wild-type subunit function. J. Biol. Chem. *270*, 3234–3238.

Bose, J.K., Hung, L., and Tarn, W. (2008). TDP-43 Overexpression Enhances Exon 7 Inclusion during the Survival of Motor Neuron Pre-mRNA Splicing *. J. Biol. Chem. *283*, 28852–28859.

Bosque, P.J., Boyer, P.J., and Mishra, P. (2013). A 43-kDa TDP-43 Species Is Present in Aggregates Associated with Frontotemporal Lobar Degeneration. PLoS One *8*, e62301.

Bousset, L., Pieri, L., Ruiz-Arlandis, G., Gath, J., Jensen, P.H., Habenstein, B., Madiona, K., Olieric, V., Böckmann, A., Meier, B.H., et al. (2013). Structural and functional characterization of two alpha-synuclein strains. Nat. Commun. *4*, 2575.

Braak, H., and Braak, E. (1991). Neuropathological stageing of Alzheimer-related changes. Acta Neuropathol. *82*, 239–259.

Braak, H., Del Tredici, K., Rüb, U., de Vos, R.A.I., Jansen Steur, E.N.H., and Braak, E. (2003). Staging of brain pathology related to sporadic Parkinson's disease. Neurobiol. Aging *24*, 197–211.

Braak, H., Brettschneider, J., Ludolph, A.C., Lee, V.M., Trojanowski, J.Q., and Del Tredici, K. (2013). Amyotrophic lateral sclerosis--a model of corticofugal axonal spread. Nat. Rev. Neurol. *9*, 708–714.

Brady, O.A., Meng, P., Zheng, Y., Mao, Y., and Hu, F. (2011). Regulation of TDP-43 aggregation by phosphorylation and p62/SQSTM1. J. Neurochem. *116*, 248–259.

Brandner, S. (2003). CNS pathogenesis of prion diseases. Br. Med. Bull. *66*, 131–139.

Brandner, S., Isenmann, S., Raeber, A., Fischer, M., Sailer, A., Kobayashi, Y., Marino, S., Weissmann, C., and Aguzzi, A. (1996). Normal host prion protein necessary for scrapie-induced neurotoxicity. Nature *379*, 339–343.

Braun, R.J., Sommer, C., Carmona-Gutierrez, D., Khoury, C.M., Ring, J., Buettner, S., and Madeo, F. (2011). Neurotoxic TDP-43 triggers mitochondrion-dependent programmed cell death in yeast. J. Biol. Chem. 1–26.

Brettschneider, J., Toledo, J.B., Van Deerlin, V.M., Elman, L., McCluskey, L., Lee, V.M.-Y., and Trojanowski, J.Q. (2012). Microglial activation correlates with disease progression and upper motor neuron clinical symptoms in amyotrophic lateral sclerosis. PLoS One *7*, e39216.

Brettschneider, J., Del Tredici, K., Toledo, J.B., Robinson, J.L., Irwin, D.J., Grossman, M., Suh, E., Van Deerlin, V.M., Wood, E.M., Baek, Y., et al. (2013). Stages of pTDP-43 pathology in amyotrophic lateral sclerosis. Ann. Neurol.

Brettschneider, J., Arai, K., Del Tredici, K., Toledo, J.B., Robinson, J.L., Lee, E.B., Kuwabara, S., Shibuya, K., Irwin, D.J., Fang, L., et al. (2014). TDP-43 pathology and neuronal loss in amyotrophic lateral sclerosis spinal cord. Acta Neuropathol.

Brooks, B.R. (1991). The role of axonal transport in neurodegenerative disease spread: a meta-analysis of experimental and clinical poliomyelitis compares with amyotrophic lateral sclerosis. Can. J. Neurol. Sci. *18*, 435–438.

Brotherton, T.E., Li, Y., and Glass, J.D. (2012). Cellular toxicity of mutant SOD1 protein is linked to an easily soluble, non-aggregated form in vitro. Neurobiol. Dis. *49C*, 49–56.

Brown, P., Gibbs, C.J., Rodgers-Johnson, P., Asher, D.M., Sulima, M.P., Bacote, A., Goldfarb, L.G., and Gajdusek, D.C. (1994). Human spongiform encephalopathy: the National Institutes of Health series of 300 cases of experimentally transmitted disease. Ann. Neurol. *35*, 513–529.

Brown, P., Brandel, J.-P., Sato, T., Nakamura, Y., MacKenzie, J., Will, R.G., Ladogana, A., Pocchiari, M., Leschek, E.W., and Schonberger, L.B. (2012). Iatrogenic Creutzfeldt-Jakob disease, final assessment. Emerg. Infect. Dis. *18*, 901–907.

Bruijn, L.I., Becher, M.W., Lee, M.K., Anderson, K.L., Jenkins, N.A., Copeland, N.G., Sisodia, S.S., Rothstein, J.D., Borchelt, D.R., Price, D.L., et al. (1997). ALS-linked SOD1 mutant G85R mediates damage to astrocytes and promotes rapidly progressive disease with SOD1-containing inclusions. Neuron *18*, 327–338.

Brundin, P., Melki, R., and Kopito, R. (2010). Prion-like transmission of protein aggregates in neurodegenerative diseases. Most *11*, 301–307.

Budini, M., and Buratti, E. (2011). TDP-43 Autoregulation: Implications for Disease. J. Mol. Neurosci.

Budini, M., Buratti, E., Stuani, C., Guarnaccia, C., Romano, V., De Conti, L., and Baralle, F.E. (2012). A cellular model of TAR DNA Binding Protein 43 (TDP-43) aggregation based on its C-terminal Q/N rich region. J. Biol. Chem. *43*.

Büeler, H., Aguzzi, A., Sailer, A., Greiner, R.A., Autenried, P., Aguet, M., and Weissmann, C. (1993). Mice devoid of PrP are resistant to scrapie. Cell *73*, 1339–1347.

Buratti, E., and Baralle, F.E. (2001). Characterization and functional implications of the RNA binding properties of nuclear factor TDP-43, a novel splicing regulator of CFTR exon 9. J. Biol. Chem. *276*, 36337–36343.

Buratti, E., and Baralle, F.E. (2011). TDP-43: New aspects of autoregulation mechanisms in RNA binding proteins and their connection with human disease. FEBS J. 0039–0040.

Buratti, E., Dörk, T., Zuccato, E., Pagani, F., Romano, M., and Baralle, F.E. (2001). Nuclear factor TDP-43 and SR proteins promote in vitro and in vivo CFTR exon 9 skipping. EMBO J. *20*, 1774–1784.

Buratti, E., Brindisi, A., Giombi, M., Tisminetzky, S., Ayala, Y.M., and Baralle, F.E. (2005). TDP-43 binds heterogeneous nuclear ribonucleoprotein A/B through its C-terminal tail: an important region for

the inhibition of cystic fibrosis transmembrane conductance regulator exon 9 splicing. J. Biol. Chem. *280*, 37572–37584.

Buratti, E., De Conti, L., Stuani, C., Romano, M., Baralle, M., and Baralle, F. (2010). Nuclear factor TDP-43 can affect selected microRNA levels. FEBS J. *277*, 2268–2281.

Burkhardt, M.F., Martinez, F.J., Wright, S., Ramos, C., Volfson, D., Mason, M., Garnes, J., Dang, V., Lievers, J., Shoukat-Mumtaz, U., et al. (2013). A cellular model for sporadic ALS using patient-derived induced pluripotent stem cells. Mol. Cell. Neurosci.

Cannon, A., Yang, B., Knight, J., Farnham, I.M., Zhang, Y., Wuertzer, C. a, D'Alton, S., Lin, W.-L., Castanedes-Casey, M., Rousseau, L., et al. (2012). Neuronal sensitivity to TDP-43 overexpression is dependent on timing of induction. Acta Neuropathol.

Di Carlo, V., Grossi, E., Laneve, P., Morlando, M., Dini Modigliani, S., Ballarino, M., Bozzoni, I., and Caffarelli, E. (2013). TDP-43 Regulates the Microprocessor Complex Activity During In Vitro Neuronal Differentiation. Mol. Neurobiol.

Casafont, I., Bengoechea, R., Tapia, O., Berciano, M.T., and Lafarga, M. (2009). TDP-43 localizes in mRNA transcription and processing sites in mammalian neurons. J. Struct. Biol. *167*, 235–241.

Chang, C.-K., Wu, T.-H., Wu, C.-Y., Chiang, M.-H., Toh, E.K.-W., Hsu, Y.-C., Lin, K.-F., Liao, Y.-H., Huang, T.-H., and Huang, J.J.-T. (2012). The N-terminus of TDP-43 promotes its oligomerization and enhances DNA binding affinity. Biochem. Biophys. Res. Commun. 1–6.

Chang, C.-K., Chiang, M.-H., Toh, E.K.-W., Chang, C.-F., and Huang, T.-H. (2013). Molecular mechanism of oxidation-induced TDP-43 RRM1 aggregation and loss of function. FEBS Lett.

Charcot, J.-M. (1874). De la sclerose laterale amyotrophique. Prog Med. *2*, 325–327, 341–342, 453–455.

Che, M.-X., Jiang, Y.-J., Xie, Y.-Y., Jiang, L.-L., and Hu, H.-Y. (2011). Aggregation of the 35-kDa fragment of TDP-43 causes formation of cytoplasmic inclusions and alteration of RNA processing. FASEB J.

Chen, A.K.-H., Lin, R.Y.-Y., Hsieh, E.Z.-J., Tu, P.-H., Chen, R.P.-Y., Liao, T.-Y., Chen, W., Wang, C.-H., and Huang, J.J.-T. (2010). Induction of amyloid fibrils by the C-terminal fragments of TDP-43 in amyotrophic lateral sclerosis. J. Am. Chem. Soc. *132*, 1186–1187.

Chia, R., Tattum, M.H., Jones, S., Collinge, J., Fisher, E.M.C., and Jackson, G.S. (2010). Superoxide dismutase 1 and tgSOD1 mouse spinal cord seed fibrils, suggesting a propagative cell death mechanism in amyotrophic lateral sclerosis. PLoS One *5*, e10627.

Chiang, P., Ling, J., Ha, Y., Price, D.L., Aja, S.M., and Wong, P.C. (2010). Deletion of TDP-43 down-regulates Tbc1d1 , a gene linked to obesity , and alters body fat metabolism. PNAS *107*, 1–5.

Chiti, F., and Dobson, C.M. (2006). Protein Misfolding, Functional Amyloid, and Human Disease. Annu. Rev. Biochem. *75*, 333–366.

Choksi, D.K., Roy, B., Chatterjee, S., Yusuff, T., Bakhoum, M.F., Sengupta, U., Ambegaokar, S., Kayed, R., and Jackson, G.R. (2013). TDP-43 Phosphorylation by Casein Kinase I{epsilon} Promotes Oligomerization and Enhances Toxicity In Vivo. Hum. Mol. Genet.

Chung, Y.H., Joo, K.M., Lim, H.C., Cho, M.H., Kim, D., Lee, W.B., and Cha, C.I. (2005). Immunohistochemical study on the distribution of phosphorylated extracellular signal-regulated kinase (ERK) in the central nervous system of SOD1G93A transgenic mice. Brain Res. *1050*, 203–209.

Citron, B.A., Arnold, P.M., Sebastian, C., Qin, F., Malladi, S., Ameenuddin, S., Landis, M.E., and Festoff, B.W. (2000). Rapid upregulation of caspase-3 in rat spinal cord after injury: mRNA, protein, and cellular localization correlates with apoptotic cell death. Exp. Neurol. *166*, 213–226.

Clavaguera, F., Bolmont, T., Crowther, R.A., Abramowski, D., Frank, S., Probst, A., Fraser, G., Stalder, A.K., Beibel, M., Staufenbiel, M., et al. (2010). Transmission and spreading of tauopathy in transgenic mouse brain. Cell *11*, 909–913.

Clavaguera, F., Akatsu, H., Fraser, G., Crowther, R. a., Frank, S., Hench, J., Probst, a., Winkler, D.T., Reichwald, J., Staufenbiel, M., et al. (2013). Brain homogenates from human tauopathies induce tau inclusions in mouse brain. Proc. Natl. Acad. Sci. 1–6.

Clippinger, A.K., D'Alton, S., Lin, W.-L., Gendron, T.F., Howard, J., Borchelt, D.R., Cannon, A., Carlomagno, Y., Chakrabarty, P., Cook, C., et al. (2013). Robust cytoplasmic accumulation of phosphorylated TDP-43 in transgenic models of tauopathy. Acta Neuropathol.

Colby, D.W., Giles, K., Legname, G., Wille, H., Baskakov, I. V, DeArmond, S.J., and Prusiner, S.B. (2009). Design and construction of diverse mammalian prion strains. Proc. Natl. Acad. Sci. U. S. A. *106*, 20417–20422.

Collinge, J. (2001). Prion diseases of humans and animals: their causes and molecular basis. Annu. Rev. Neurosci. *24*, 519–550.

Collinge, J., and Clarke, A.R. (2007). A general model of prion strains and their pathogenicity. Science *318*, 930–936.

Collinge, J., Palmer, M.S., and Dryden, A.J. (1991). Genetic predisposition to iatrogenic Creutzfeldt-Jakob disease. Lancet *337*, 1441–1442.

Collinge, J., Sidle, K.C., Meads, J., Ironside, J., and Hill, A.F. (1996). Molecular analysis of prion strain variation and the aetiology of "new variant" CJD. Nature *383*, 685–690.

Colombrita, C., Zennaro, E., Fallini, C., Weber, M., Sommacal, A., Buratti, E., Silani, V., and Ratti, A. (2009). TDP-43 is recruited to stress granules in conditions of oxidative insult. J. Neurochem. *111*, 1051–1061.

Couthouis, J., Hart, M.P., Shorter, J., Dejesus-Hernandez, M., Erion, R., Oristano, R., Liu, A.X., Ramos, D., Jethava, N., Hosangadi, D., et al. (2011). Feature Article: A yeast functional screen predicts new candidate ALS disease genes. Proc. Natl. Acad. Sci. U. S. A. 1–10.

Cozzolino, M., Pesaresi, M.G., Gerbino, V., Grosskreutz, J., and Carrì, M.T. (2012). Amyotrophic lateral sclerosis: new insights into underlying molecular mechanisms and opportunities for therapeutic intervention. Antioxid. Redox Signal. *17*, 1277–1330.

Cronier, S., Laude, H., and Peyrin, J.-M. (2004). Prions can infect primary cultured neurons and astrocytes and promote neuronal cell death. Proc. Natl. Acad. Sci. U. S. A. *101*, 12271–12276.

Cushman, M., Johnson, B.S., King, O.D., Gitler, A.D., and Shorter, J. (2010). Prion-like disorders: blurring the divide between transmissibility and infectivity. J. Cell Sci. *123*, 1191–1201.

D'Ambrogio, A., Buratti, E., Stuani, C., Guarnaccia, C., Romano, M., Ayala, Y.M., and Baralle, F.E. (2009). Functional mapping of the interaction between TDP-43 and hnRNP A2 in vivo. Nucleic Acids Res. *37*, 4116–4126.

Dahm, R., Kiebler, M., and Macchi, P. (2007). RNA localisation in the nervous system. Semin. Cell Dev. Biol. *18*, 216–223.

Dal Canto, M.C., and Gurney, M.E. (1997). A low expressor line of transgenic mice carrying a mutant human Cu,Zn superoxide dismutase (SOD1) gene develops pathological changes that most closely resemble those in human amyotrophic lateral sclerosis. Acta Neuropathol. *93*, 537–550.

Van Damme, P., and Robberecht, W. (2013). Clinical implications of recent breakthroughs in amyotrophic lateral sclerosis. Curr. Opin. Neurol. *26*, 466–472.

Van Damme, P., Martens, L., Van Damme, J., Hugelier, K., Staes, A., Vandekerckhove, J., and Gevaert, K. (2005). Caspase-specific and nonspecific in vivo protein processing during Fas-induced apoptosis. Nat. Methods *2*, 771–777.

Danzer, K.M., Krebs, S.K., Wolff, M., Birk, G., and Hengerer, B. (2009). Seeding induced by alpha-synuclein oligomers provides evidence for spreading of alpha-synuclein pathology. J. Neurochem. *111*, 192–203.

Daoud, H., Valdmanis, P.N., Kabashi, E., Dion, P., Dupre, N., Camu, W., and Meininger, V. (2009). Contribution of TARDBP mutations to sporadic amyotrophic lateral sclerosis. J. Med. Genet. 112–114.

Dayton, R.D., Gitcho, M. a, Orchard, E. a, Wilson, J.D., Wang, D.B., Cain, C.D., Johnson, J. a, Zhang, Y.-J., Petrucelli, L., Mathis, J.M., et al. (2013). Selective Forelimb Impairment in Rats Expressing a Pathological TDP-43 25 kDa C-terminal Fragment to Mimic Amyotrophic Lateral Sclerosis. Mol. Ther. 1–11.

de Calignon, A., Polydoro, M., Suárez-Calvet, M., William, C., Adamowicz, D.H., Kopeikina, K.J., Pitstick, R., Sahara, N., Ashe, K.H., Carlson, G.A., et al. (2012). Propagation of Tau Pathology in a Model of Early Alzheimer's Disease. Neuron *73*, 685–697.

DeArmond, S.J., and Prusiner, S.B. (1995). Etiology and pathogenesis of prion diseases. Am. J. Pathol. *146*, 785–811.

DeJesus-Hernandez, M., Mackenzie, I.R., Boeve, B.F., Boxer, A.L., Baker, M., Rutherford, N.J., Nicholson, A.M., Finch, N.A., Flynn, H., Adamson, J., et al. (2011). Expanded GGGGCC hexanucleotide repeat in noncoding region of C9ORF72 causes chromosome 9p-linked FTD and ALS. Neuron *72*, 245–256.

Deng, H.-X., Shi, Y., Furukawa, Y., Zhai, H., Fu, R., Liu, E., Gorrie, G.H., Khan, M.S., Hung, W.-Y., Bigio, E.H., et al. (2006). Conversion to the amyotrophic lateral sclerosis phenotype is associated with intermolecular linked insoluble aggregates of SOD1 in mitochondria. Proc. Natl. Acad. Sci. U. S. A. *103*, 7142–7147.

Deng, H.-X., Zhai, H., Bigio, E.H., Yan, J., Fecto, F., Ajroud, K., Mishra, M., Ajroud-Driss, S., Heller, S., Sufit, R., et al. (2010). FUS-immunoreactive inclusions are a common feature in sporadic and non-SOD1 familial amyotrophic lateral sclerosis. Ann. Neurol. *67*, 739–748.

Deng, H.-X., Chen, W., Hong, S.-T., Boycott, K.M., Gorrie, G.H., Siddique, N., Yang, Y., Fecto, F., Shi, Y., Zhai, H., et al. (2011). Mutations in UBQLN2 cause dominant X-linked juvenile and adult-onset ALS and ALS/dementia. Nature.

Deng, Y.P., Albin, R.L., Penney, J.B., Young, A.B., Anderson, K.D., and Reiner, A. (2004). Differential loss of striatal projection systems in Huntington's disease: a quantitative immunohistochemical study. J. Chem. Neuroanat. *27*, 143–164.

Desplats, P., Lee, H.-J., Bae, E.-J., Patrick, C., Rockenstein, E., Crews, L., Spencer, B., Masliah, E., and Lee, S.-J. (2009). Inclusion formation and neuronal cell death through neuron-to-neuron transmission of alpha-synuclein. Proc. Natl. Acad. Sci. U. S. A. *106*, 13010–13015.

Dewey, C.M., Cenik, B., Sephton, C.F., Dries, D.R., Mayer, P., Good, S.K., Johnson, B. a, Herz, J., and Yu, G. (2010). TDP-43 is directed to stress granules by sorbitol, a novel physiological osmotic and oxidative stressor. Mol. Cell. Biol.

Dewey, C.M., Cenik, B., Sephton, C.F., Johnson, B. a, Herz, J., and Yu, G. (2012). TDP-43 aggregation in neurodegeneration: Are stress granules the key? Brain Res. 1–10.

Diaper, D.C., Adachi, Y., Sutcliffe, B., Humphrey, D.M., Elliott, C.J.H., Stepto, A., Ludlow, Z.N., Vanden Broeck, L., Callaerts, P., Dermaut, B., et al. (2013). Loss and gain of Drosophila TDP-43 impair synaptic efficacy and motor control leading to age-related neurodegeneration by loss-of-function phenotypes. Hum. Mol. Genet. *22*, 1539–1557.

Dickson, D.W., Josephs, K. a, and Amador-Ortiz, C. (2007). TDP-43 in differential diagnosis of motor neuron disorders. Acta Neuropathol. *114*, 71–79.

Dinner, A.R., Sali, A., Smith, L.J., Dobson, C.M., and Karplus, M. (2000). Understanding protein folding via free-energy surfaces from theory and experiment. Trends Biochem. Sci. *25*, 331–339.

Dix, M.M., Simon, G.M., and Cravatt, B.F. (2008). Global mapping of the topography and magnitude of proteolytic events in apoptosis. Cell *134*, 679–691.

Dobson, C.M. (2003). Protein folding and misfolding. Nature *426*, 884–890.

Donaghy, C., Thurtell, M.J., Pioro, E.P., Gibson, J.M., and Leigh, R.J. (2011). Eye movements in amyotrophic lateral sclerosis and its mimics: a review with illustrative cases. J. Neurol. Neurosurg. Psychiatry *82*, 110–116.

Dormann, D., Capell, A., Carlson, A.M., Shankaran, S.S., Rodde, R., Neumann, M., Kremmer, E., Matsuwaki, T., Yamanouchi, K., Nishihara, M., et al. (2009). Proteolytic processing of TAR DNA binding protein-43 by caspases produces C-terminal fragments with disease defining properties independent of progranulin. J. Neurochem. *110*, 1082–1094.

Dreumont, N., Hardy, S., Behm-Ansmant, I., Kister, L., Branlant, C., Stévenin, J., and Bourgeois, C.F. (2010). Antagonistic factors control the unproductive splicing of SC35 terminal intron. Nucleic Acids Res. *38*, 1353–1366.

Van Eersel, J., Ke, Y.D., Gladbach, A., Bi, M., Götz, J., Kril, J.J., and Ittner, L.M. (2011). Cytoplasmic Accumulation and Aggregation of TDP-43 upon Proteasome Inhibition in Cultured Neurons. PLoS One *6*, e22850.

Eisele, Y.S., Bolmont, T., Heikenwalder, M., Langer, F., Jacobson, L.H., Yan, Z., Roth, K., Aguzzi, A., Staufenbiel, M., Walker, L.C., et al. (2009). Induction of cerebral B-amyloidosis : Intracerebral versus systemic AB inoculation. PNAS *106*, 12926–12931.

Eisele, Y.S., Obermüller, U., Heilbronner, G., Baumann, F., Kaeser, S.A., Wolburg, H., Walker, L.C., Staufenbiel, M., Heikenwalder, M., and Jucker, M. (2010). Peripherally applied Abeta-containing inoculates induce cerebral beta-amyloidosis. Science *330*, 980–982.

Ekegren, T., Grundström, E., Lindholm, D., and Aquilonius, S.M. (1999). Upregulation of Bax protein and increased DNA degradation in ALS spinal cord motor neurons. Acta Neurol. Scand. *100*, 317–321.

Elvira, G., Wasiak, S., Blandford, V., Tong, X.-K., Serrano, A., Fan, X., del Rayo Sánchez-Carbente, M., Servant, F., Bell, A.W., Boismenu, D., et al. (2006). Characterization of an RNA granule from developing brain. Mol. Cell. Proteomics *5*, 635–651.

Fallini, C., Bassell, G.J., Rossoll, W., and Biology, C. (2012). The ALS disease protein TDP-43 is actively transported in motor neuron axons and regulates axon outgrowth. Hum. Mol. Genet. 1–45.

Feiguin, F., Godena, V.K., Romano, G., D'Ambrogio, A., Klima, R., and Baralle, F.E. (2009). Depletion of TDP-43 affects Drosophila motoneurons terminal synapsis and locomotive behavior. FEBS Lett. *583*, 1586–1592.

Feneberg, E., Steinacker, P., Lehnert, S., Schneider, A., Walther, P., Thal, D.R., Linsenmeier, M., Ludolph, A.C., and Otto, M. (2014). Limited role of free TDP-43 as a diagnostic tool in neurodegenerative diseases. Amyotroph. Lateral Scler. Frontotemporal Degener. 1–6.

Fernandez-Funez, P., Zhang, Y., Casas-Tinto, S., Xiao, X., Zou, W.-Q., and Rincon-Limas, D.E. (2010). Sequence-dependent prion protein misfolding and neurotoxicity. J. Biol. Chem. 1–23.

Ferraiuolo, L., Kirby, J., Grierson, A.J., Sendtner, M., and Shaw, P.J. (2011). Molecular pathways of motor neuron injury in amyotrophic lateral sclerosis. Nat. Rev. Neurol. *7*, 616–630.

Fevrier, B., Vilette, D., Archer, F., Loew, D., Faigle, W., Vidal, M., Laude, H., and Raposo, G. (2004). Cells release prions in association with exosomes. Proc. Natl. Acad. Sci. U. S. A. *101*, 9683–9688.

Fiesel, F.C., Voigt, A., Weber, S.S., Van den Haute, C., Waldenmaier, A., Görner, K., Walter, M., Anderson, M.L., Kern, J. V, Rasse, T.M., et al. (2010). Knockdown of transactive response DNA-binding protein (TDP-43) downregulates histone deacetylase 6. EMBO J. *29*, 209–221.

Fiesel, F.C., Schurr, C., Weber, S.S., and Kahle, P.J. (2011). TDP-43 knockdown impairs neurite outgrowth dependent on its target histone deacetylase 6. Mol. Neurodegener. *6*, 64.

Filimonenko, M., Stuffers, S., Raiborg, C., Yamamoto, A., Malerød, L., Fisher, E.M.C., Isaacs, A., Brech, A., Stenmark, H., and Simonsen, A. (2007). Functional multivesicular bodies are required for autophagic clearance of protein aggregates associated with neurodegenerative disease. J. Cell Biol. *179*, 485–500.

Flynn, G.C., Pohl, J., Flocco, M.T., and Rothman, J.E. (1991). Peptide-binding specificity of the molecular chaperone BiP. Nature *353*, 726–730.

Freibaum, B.D., Chitta, R.K., High, A.A., and Taylor, J.P. (2009). Global analysis of TDP-43 interacting proteins reveals strong association with RNA splicing and translation machinery. J. Proteome Res. *9*, 1104–1120.

Frost, B., and Diamond, M.I. (2010). Prion-like mechanisms in neurodegenerative diseases. Nat. Rev. Neurosci. *11*, 155–159.

Frost, B., Jacks, R.L., and Diamond, M.I. (2009). Propagation of Tau Misfolding from the Outside to the Inside of a Cell *. J. Biol. Chem. *284*, 12845–12852.

Fuentealba, R. a, Udan, M., Bell, S., Wegorzewska, I., Shao, J., Diamond, M.I., Weihl, C.C., and Baloh, R.H. (2010). Interaction with Polyglutamine Aggregates Reveals a Q/N-rich Domain in TDP-43. J. Biol. Chem. *285*, 26304–26314.

Fujimura-Kiyono, C., Kimura, F., Ishida, S., Nakajima, H., Hosokawa, T., Sugino, M., and Hanafusa, T. (2011). Onset and spreading patterns of lower motor neuron involvements predict survival in sporadic amyotrophic lateral sclerosis. J. Neurol. Neurosurg. Psychiatry *82*, 1244–1249.

Furukawa, Y., Kaneko, K., Watanabe, S., Yamanaka, K., and Nukina, N. (2011). A seeding reaction recapitulates intracellular formation of sarkosyl-insoluble TAR DNA binding protein-43 inclusions. J. Biol. Chem.

Furukawa, Y., Kaneko, K., Watanabe, S., Yamanaka, K., and Nukina, N. (2013). Intracellular seeded aggregation of mutant Cu,Zn-superoxide dismutase associated with amyotrophic lateral sclerosis. FEBS Lett. *587*, 2500–2505.

Gajdusek, D.C., and Zigas, V. (1957). Degenerative disease of the central nervous system in New Guinea; the endemic occurrence of kuru in the native population. N. Engl. J. Med. *257*, 974–978.

Gajdusek, D.C., Gibbs, C.J., and Alpers, M. (1966). Experimental transmission of a Kuru-like syndrome to chimpanzees. Nature *209*, 794–796.

Geser, F., Brandmeir, N.J., Kwong, L.K., Martinez-Lage, M., Elman, L., McCluskey, L., Xie, S.X., Lee, V.M.-Y., and Trojanowski, J.Q. (2008). Evidence of multisystem disorder in whole-brain map of pathological TDP-43 in amyotrophic lateral sclerosis. Arch. Neurol. *65*, 636–641.

Geser, F., Martinez-Lage, M., Robinson, J., Uryu, K., Neumann, M., Brandmeir, N.J., Xie, S.X., Kwong, L.K., Elman, L., McCluskey, L., et al. (2009). Clinical and pathological continuum of multisystem TDP-43 proteinopathies. Arch. Neurol. *66*, 180–189.

Geser, F., Robinson, J.L., Malunda, J.A., Xie, S.X., Clark, C.M., Kwong, L.K., Moberg, P.J., Moore, E.M., Van Deerlin, V.M., Lee, V.M.-Y., et al. (2010a). Pathological 43-kDa transactivation response DNA-binding protein in older adults with and without severe mental illness. Arch. Neurol. *67*, 1238–1250.

Geser, F., Lee, V.M.-Y., and Trojanowski, J.Q. (2010b). Amyotrophic lateral sclerosis and frontotemporal lobar degeneration: a spectrum of TDP-43 proteinopathies. Neuropathology *30*, 103–112.

Geser, F., Stein, B., Partain, M., Elman, L.B., McCluskey, L.F., Xie, S.X., Van Deerlin, V.M., Kwong, L.K., Lee, V.M.-Y., and Trojanowski, J.Q. (2011). Motor neuron disease clinically limited to the lower motor neuron is a diffuse TDP-43 proteinopathy. Acta Neuropathol.

Gibson, S.B., and Bromberg, M.B. (2012). Amyotrophic lateral sclerosis: drug therapy from the bench to the bedside. Semin. Neurol. *32*, 173–178.

Gilks, N., Kedersha, N., Ayodele, M., Shen, L., Stoecklin, G., Dember, L.M., and Anderson, P. (2004). Stress granule assembly is mediated by prion-like aggregation of TIA-1. Mol. Biol. Cell *15*, 5383–5398.

Giordana, M.T., Piccinini, M., Grifoni, S., De Marco, G., Vercellino, M., Magistrello, M., Pellerino, A., Buccinnà, B., Lupino, E., and Rinaudo, M.T. (2010). TDP-43 redistribution is an early event in sporadic amyotrophic lateral sclerosis. Brain Pathol. *20*, 351–360.

Gitler, A.D., and Shorter, J. (2011). RNA-binding proteins with prion-like domains in ALS and FTLD-U. Prion *5*, 1–9.

Godena, V.K., Romano, G., Romano, M., Appocher, C., Klima, R., Buratti, E., Baralle, F.E., and Feiguin, F. (2011). TDP-43 Regulates Drosophila Neuromuscular Junctions Growth by Modulating Futsch/MAP1B Levels and Synaptic Microtubules Organization. PLoS One *6*, e17808.

Goedert, M., Clavaguera, F., and Tolnay, M. (2010). The propagation of prion-like protein inclusions in neurodegenerative diseases. Trends Neurosci. *33*, 317–325.

Goedert, M., Spillantini, M.G., Del Tredici, K., and Braak, H. (2013). 100 years of Lewy pathology. Nat. Rev. Neurol. *9*, 13–24.

Gousset, K., Schiff, E., Langevin, C., Marijanovic, Z., Caputo, A., Browman, D.T., Chenouard, N., de Chaumont, F., Martino, A., Enninga, J., et al. (2009). Prions hijack tunnelling nanotubes for intercellular spread. Nat. Cell Biol. *11*, 328–336.

Van der Graaff, M.M., de Jong, J.M.B. V, Baas, F., and de Visser, M. (2009). Upper motor neuron and extra-motor neuron involvement in amyotrophic lateral sclerosis: a clinical and brain imaging review. Neuromuscul. Disord. *19*, 53–58.

Grad, L.I., Guest, W.C., Yanai, a., Pokrishevsky, E., O'Neill, M. a., Gibbs, E., Semenchenko, V., Yousefi, M., Wishart, D.S., Plotkin, S.S., et al. (2011). Intermolecular transmission of superoxide dismutase 1 misfolding in living cells. Proc. Natl. Acad. Sci. *108*.

Grad, L.I., Yerbury, J.J., and Turner, B.J. (2014). Intercellular propagated misfolding of wild-type Cu/Zn superoxide dismutase occurs via exosome-dependent and -independent mechanisms.Supporting Information. 1–9.

Graffmo, K.S., Forsberg, K., Bergh, J., Birve, A., Zetterström, P., Andersen, P.M., Marklund, S.L., and Brännström, T. (2013). Expression of wild-type human superoxide dismutase-1 in mice causes amyotrophic lateral sclerosis. Hum. Mol. Genet. *22*, 51–60.

Gregory, J.M., Barros, T.P., Meehan, S., Dobson, C.M., and Luheshi, L.M. (2012). The Aggregation and Neurotoxicity of TDP-43 and Its ALS-Associated 25 kDa Fragment Are Differentially Affected by Molecular Chaperones in Drosophila. PLoS One *7*, e31899.

Gregory, R.I., Yan, K.-P., Amuthan, G., Chendrimada, T., Doratotaj, B., Cooch, N., and Shiekhattar, R. (2004). The Microprocessor complex mediates the genesis of microRNAs. Nature *432*, 235–240.

Griffith, J.S. (1967). Self-replication and scrapie. Nature *215*, 1043–1044.

Guo, J.L., and Lee, V.M.Y. (2011). Seeding of normal tau by pathological tau conformers drives pathogenesis of Alzheimer-like tangles. J. Biol. Chem.

Guo, J.L., and Lee, V.M.Y. (2014). Cell-to-cell transmission of pathogenic proteins in neurodegenerative diseases. Nat. Med. *20*, 130–138.

Guo, J.L., Covell, D.J., Daniels, J.P., Iba, M., Stieber, A., Zhang, B., Riddle, D.M., Kwong, L.K., Xu, Y., Trojanowski, J.Q., et al. (2013). Distinct α-Synuclein Strains Differentially Promote Tau Inclusions in Neurons. Cell *154*, 103–117.

Guo, W., Chen, Y., Zhou, X., Kar, A., Ray, P., Chen, X., Rao, E.J., Yang, M., Ye, H., Zhu, L., et al. (2011). An ALS-associated mutation affecting TDP-43 enhances protein aggregation, fibril formation and neurotoxicity. Supplementary information. Nat. Struct. Mol. Biol. *18*, 1–13.

Gurney, M.E., Pu, H., Chiu, A.Y., Dal Canto, M.C., Polchow, C.Y., Alexander, D.D., Caliendo, J., Hentati, A., Kwon, Y.W., and Deng, H.X. (1994). Motor neuron degeneration in mice that express a human Cu,Zn superoxide dismutase mutation. Science *264*, 1772–1775.

Haass, C., and Selkoe, D.J. (2007). Soluble protein oligomers in neurodegeneration: lessons from the Alzheimer's amyloid beta-peptide. Nat. Rev. Mol. Cell Biol. *8*, 101–112.

Hallbeck, M., Nath, S., and Marcusson, J. (2013). Neuron-to-Neuron Transmission of Neurodegenerative Pathology. Neuroscientist *19*, 560–566.

Hamaguchi, T., Eisele, Y.S., Varvel, N.H., Lamb, B.T., Walker, L.C., and Jucker, M. (2012). The presence of Aβ seeds, and not age per se, is critical to the initiation of Aβ deposition in the brain. Acta Neuropathol. *123*, 31–37.

Han, J.-H., Yu, T.-H., Ryu, H.-H., Jun, M.-H., Ban, B.-K., Jang, D.-J., and Lee, J.-A. (2013). ALS/FTLD-linked TDP-43 regulates neurite morphology and cell survival in differentiated neurons. Exp. Cell Res. 1–8.

Hansen, C., Angot, E., Bergström, A., Steiner, J.A., Pieri, L., Paul, G., Outeiro, T.F., Melki, R., Kallunki, P., and Fog, K. (2011). α-Synuclein propagates from mouse brain to grafted dopaminergic neurons and seeds aggregation in cultured human cells. Medicina (B. Aires). *121*, 715–725.

Hanson, K.A., Kim, S.H., Wassarman, D.A., and Tibbetts, R.S. (2010). Ubiquilin modifies TDP-43 toxicity in a Drosophila model of amyotrophic lateral sclerosis (ALS). J. Biol. Chem. *285*, 11068–11072.

Hardesty, B., and Kramer, G. (2001). Folding of a nascent peptide on the ribosome. Prog. Nucleic Acid Res. Mol. Biol. *66*, 41–66.

Harding, J.J. (1985). Nonenzymatic covalent posttranslational modification of proteins in vivo. Adv. Protein Chem. *37*, 247–334.

Harrison, P.M., and Gerstein, M. (2003). A method to assess compositional bias in biological sequences and its application to prion-like glutamine/asparagine-rich domains in eukaryotic proteomes. Genome Biol. *4*, R40.

Hartl, F.U., and Hayer-Hartl, M. (2002). Molecular chaperones in the cytosol: from nascent chain to folded protein. Science *295*, 1852–1858.

Hasegawa, M., Arai, T., Akiyama, H., Nonaka, T., Mori, H., Hashimoto, T., Yamazaki, M., and Oyanagi, K. (2007). TDP-43 is deposited in the Guam parkinsonism-dementia complex brains. Brain *130*, 1386–1394.

Hasegawa, M., Arai, T., Nonaka, T., Kametani, F., Yoshida, M., Hashizume, Y., Beach, T.G., Buratti, E., Baralle, F., Morita, M., et al. (2008). Phosphorylated TDP-43 in frontotemporal lobar degeneration and amyotrophic lateral sclerosis. Ann. Neurol. *64*, 60–70.

Hasegawa, M., Nonaka, T., Tsuji, H., Tamaoka, A., Yamashita, M., Kametani, F., Yoshida, M., Arai, T., and Akiyama, H. (2011). Molecular Dissection of TDP-43 Proteinopathies. J. Mol. Neurosci.

Hegde, R.S., Mastrianni, J.A., Scott, M.R., DeFea, K.A., Tremblay, P., Torchia, M., DeArmond, S.J., Prusiner, S.B., and Lingappa, V.R. (1998). A transmembrane form of the prion protein in neurodegenerative disease. Science *279*, 827–834.

Heilbronner, G., Eisele, Y.S., Langer, F., Kaeser, S.A., Novotny, R., Nagarathinam, A., Aslund, A., Hammarström, P., Nilsson, K.P.R., and Jucker, M. (2013). Seeded strain-like transmission of β-amyloid morphotypes in APP transgenic mice. EMBO Rep.

Higashi, S., Iseki, E., Yamamoto, R., Minegishi, M., Hino, H., Fujisawa, K., Togo, T., Katsuse, O., Uchikado, H., Furukawa, Y., et al. (2007). Concurrence of TDP-43, tau and alpha-synuclein pathology in brains of Alzheimer's disease and dementia with Lewy bodies. Brain Res. *1184*, 284–294.

Hill, A.F., Desbruslais, M., Joiner, S., Sidle, K.C., Gowland, I., Collinge, J., Doey, L.J., and Lantos, P. (1997). The same prion strain causes vCJD and BSE. Nature *389*, 448–450, 526.

Hobbs, S.K., Shi, G., Homer, R., Harsh, G., Atlas, S.W., and Bednarski, M.D. (2003). Magnetic resonance image-guided proteomics of human glioblastoma multiforme. J. Magn. Reson. Imaging *18*, 530–536.

Holmes, B.B., and Diamond, M.I. (2012). Amyotrophic lateral sclerosis and organ donation: Is there risk of disease transmission? Ann. Neurol. *72*, 832–836.

Holtzman, D.M., Morris, J.C., and Goate, A.M. (2011). Alzheimer's disease: the challenge of the second century. Sci. Transl. Med. *3*, 77sr1.

Howe, F.A., Barton, S.J., Cudlip, S.A., Stubbs, M., Saunders, D.E., Murphy, M., Wilkins, P., Opstad, K.S., Doyle, V.L., McLean, M.A., et al. (2003). Metabolic profiles of human brain tumors using quantitative in vivo 1H magnetic resonance spectroscopy. Magn. Reson. Med. *49*, 223–232.

Hu, X., Crick, S.L., Bu, G., Frieden, C., Pappu, R. V, and Lee, J.-M. (2009). Amyloid seeds formed by cellular uptake, concentration, and aggregation of the amyloid-beta peptide. Proc. Natl. Acad. Sci. U. S. A. *106*, 20324–20329.

Huang, P., Lian, F., Wen, Y., Guo, C., and Lin, D. (2013a). Prion protein oligomer and its neurotoxicity. Acta Biochim. Biophys. Sin. (Shanghai). *45*, 442–451.

Huang, Y.-C., Lin, K.-F., He, R.-Y., Tu, P.-H., Koubek, J., Hsu, Y.-C., and Huang, J.J.-T. (2013b). Inhibition of TDP-43 Aggregation by Nucleic Acid Binding. PLoS One *8*, e64002.

Huber, R., and Bode, W. (1978). Structural basis of the activation and action of trypsin. Acc. Chem. Res. *11*, 114–122.

Iba, M., Guo, J.L., McBride, J.D., Zhang, B., Trojanowski, J.Q., and Lee, V.M.-Y. (2013). Synthetic tau fibrils mediate transmission of neurofibrillary tangles in a transgenic mouse model of Alzheimer's-like tauopathy. J. Neurosci. *33*, 1024–1037.

Igaz, L.M., Kwong, L.K., Xu, Y., Truax, A.C., Uryu, K., Neumann, M., Clark, C.M., Elman, L.B., Miller, B.L., Grossman, M., et al. (2008). Enrichment of C-Terminal Fragments in TAR DNA-Binding Protein-

43 Cytoplasmic Inclusions in Brain but not in Spinal Cord of Frontotemporal Lobar Degeneration and Amyotrophic Lateral Sclerosis. Pathology *173*, 182–194.

Igaz, L.M., Kwong, L.K., Chen-Plotkin, A., Winton, M.J., Unger, T.L., Xu, Y., Neumann, M., Trojanowski, J.Q., and Lee, V.M.-Y. (2009). Expression of TDP-43 C-terminal Fragments in Vitro Recapitulates Pathological Features of TDP-43 Proteinopathies. J. Biol. Chem. *284*, 8516–8524.

Igaz, L.M., Kwong, L.K., Lee, E.B., Chen-Plotkin, A., Swanson, E., Unger, T., Malunda, J., Xu, Y., Winton, M.J., Trojanowski, J.Q., et al. (2011). Dysregulation of the ALS-associated gene TDP-43 leads to neuronal death and degeneration in mice. J. Clin. Invest.

Iguchi, Y., Katsuno, M., Niwa, J., Yamada, S., Sone, J., Waza, M., Adachi, H., Tanaka, F., Nagata, K., Arimura, N., et al. (2009). TDP-43 depletion induces neuronal cell damage through dysregulation of Rho family GTPases. J. Biol. Chem. *284*, 22059–22066.

Iguchi, Y., Katsuno, M., Niwa, J.-I., Takagi, S., Ishigaki, S., Ikenaka, K., Kawai, K., Watanabe, H., Yamanaka, K., Takahashi, R., et al. (2013). Loss of TDP-43 causes age-dependent progressive motor neuron degeneration. Brain.

Ihara, R., Matsukawa, K., Nagata, Y., Kunugi, H., Tsuji, S., Chihara, T., Kuranaga, E., Miura, M., Wakabayashi, T., Hashimoto, T., et al. (2013). RNA binding mediates neurotoxicity in the transgenic Drosophila model of TDP-43 proteinopathy. Hum. Mol. Genet.

Ilieva, H., Polymenidou, M., and Cleveland, D.W. (2009). Non-cell autonomous toxicity in neurodegenerative disorders: ALS and beyond. J. Cell Biol. *187*, 761–772.

Ince, P.G. (2000). Neuropathology. In Amyotrophic Lateral Sclerosis, S.M. Brown RJ, Meininger V, ed. (London: Martin Dunitz), pp. 83–112.

Ince, P.G., Highley, J.R., Kirby, J., Wharton, S.B., Takahashi, H., Strong, M.J., and Shaw, P.J. (2011). Molecular pathology and genetic advances in amyotrophic lateral sclerosis: an emerging molecular pathway and the significance of glial pathology. Acta Neuropathol.

Inukai, Y., Nonaka, T., Arai, T., Yoshida, M., Hashizume, Y., Beach, T.G., Buratti, E., Baralle, F.E., Akiyama, H., Hisanaga, S., et al. (2008). Abnormal phosphorylation of Ser409/410 of TDP-43 in FTLD-U and ALS. FEBS Lett. *582*, 2899–2904.

Irwin, D.J., Abrams, J.Y., Schonberger, L.B., Leschek, E.W., Mills, J.L., Lee, V.M.-Y., and Trojanowski, J.Q. (2013). Evaluation of Potential Infectivity of Alzheimer and Parkinson Disease Proteins in Recipients of Cadaver-Derived Human Growth Hormone. JAMA Neurol. 1–7.

Ito, M. (2008). Control of mental activities by internal models in the cerebellum. Nat. Rev. Neurosci. *9*, 304–313.

Janssens, J., and Van Broeckhoven, C. (2013). Pathological mechanisms underlying TDP-43 driven neurodegeneration in FTLD-ALS spectrum disorders. Hum. Mol. Genet. 1–11.

Janssens, J., Wils, H., Kleinberger, G., Joris, G., Cuijt, I., Ceuterick-de Groote, C., Van Broeckhoven, C., and Kumar-Singh, S. (2013). Overexpression of ALS-Associated p.M337V Human TDP-43 in Mice Worsens Disease Features Compared to Wild-type Human TDP-43 Mice. Mol. Neurobiol. *43*.

Jarrett, J.T., and Lansbury, P.T. (1993). Seeding "one-dimensional crystallization" of amyloid: a pathogenic mechanism in Alzheimer's disease and scrapie? Cell *73*, 1055–1058.

Jiang, L.-L., Che, M.-X., Zhao, J., Zhou, C.-J., Xie, M.-Y., Li, H.-Y., He, J.-H., and Hu, H.-Y. (2013). Structural Transformation of the Amyloidogenic Core Region of TAR DNA Binding Protein of 43 kDa (TDP-43) Initiates Its Aggregation and Cytoplasmic Inclusion. J. Biol. Chem.

Johnson, B.S., McCaffery, J.M., Lindquist, S., and Gitler, A.D. (2008). A yeast TDP-43 proteinopathy model: Exploring the molecular determinants of TDP-43 aggregation and cellular toxicity. Proc. Natl. Acad. Sci. U. S. A. *105*, 6439–6444.

Johnson, B.S., Snead, D., Lee, J.J., McCaffery, J.M., Shorter, J., and Gitler, A.D. (2009). TDP-43 is intrinsically aggregation-prone, and amyotrophic lateral sclerosis-linked mutations accelerate aggregation and increase toxicity. J. Biol. Chem. *284*, 20329–20339.

Johnston, J.A., Dalton, M.J., Gurney, M.E., and Kopito, R.R. (2000). Formation of high molecular weight complexes of mutant Cu, Zn-superoxide dismutase in a mouse model for familial amyotrophic lateral sclerosis. Proc. Natl. Acad. Sci. U. S. A. *97*, 12571–12576.

Jokivarsi, K.T., Gröhn, H.I., Gröhn, O.H., and Kauppinen, R.A. (2007). Proton transfer ratio, lactate, and intracellular pH in acute cerebral ischemia. Magn. Reson. Med. *57*, 647–653.

Jones, C.K., Schlosser, M.J., van Zijl, P.C.M., Pomper, M.G., Golay, X., and Zhou, J. (2006). Amide proton transfer imaging of human brain tumors at 3T. Magn. Reson. Med. *56*, 585–592.

Jucker, M., and Walker, L.C. (2011). Pathogenic protein seeding in alzheimer disease and other neurodegenerative disorders. Ann. Neurol. *70*, 532–540.

Jucker, M., and Walker, L.C. (2013). Self-propagation of pathogenic protein aggregates in neurodegenerative diseases. Nature *501*, 45–51.

Kabashi, E., Valdmanis, P.N., Dion, P., Spiegelman, D., McConkey, B.J., Vande Velde, C., Bouchard, J.-P., Lacomblez, L., Pochigaeva, K., Salachas, F., et al. (2008). TARDBP mutations in individuals with sporadic and familial amyotrophic lateral sclerosis. Nat. Genet. *40*, 572–574.

Kabashi, E., Lin, L., Tradewell, M.L., Dion, P. a, Bercier, V., Bourgouin, P., Rochefort, D., Bel Hadj, S., Durham, H.D., Vande Velde, C., et al. (2010). Gain and loss of function of ALS-related mutations of TARDBP (TDP-43) cause motor deficits in vivo. Hum. Mol. Genet. *19*, 671–683.

Kalia, L. V, Kalia, S.K., McLean, P.J., Lozano, A.M., and Lang, A.E. (2013). α-Synuclein oligomers and clinical implications for Parkinson disease. Ann. Neurol. *73*, 155–169.

Kane, M.D., Lipinski, W.J., Callahan, M.J., Bian, F., Durham, R.A., Schwarz, R.D., Roher, A.E., and Walker, L.C. (2000). Evidence for seeding of beta -amyloid by intracerebral infusion of Alzheimer brain extracts in beta -amyloid precursor protein-transgenic mice. J. Neurosci. *20*, 3606–3611.

Kanouchi, T., Ohkubo, T., and Yokota, T. (2012). Can regional spreading of amyotrophic lateral sclerosis motor symptoms be explained by prion-like propagation? J. Neurol. Neurosurg. Psychiatry.

Karch, C.M., Prudencio, M., Winkler, D.D., Hart, P.J., and Borchelt, D.R. (2009). Role of mutant SOD1 disulfide oxidation and aggregation in the pathogenesis of familial ALS. Proc. Natl. Acad. Sci. U. S. A. *106*, 7774–7779.

Kasai, T., Tokuda, T., Ishigami, N., Sasayama, H., Foulds, P., Mitchell, D.J., Mann, D.M. a, Allsop, D., and Nakagawa, M. (2009). Increased TDP-43 protein in cerebrospinal fluid of patients with amyotrophic lateral sclerosis. Acta Neuropathol. *117*, 55–62.

Kassubek, J., Muller, H.-P., Del Tredici, K., Brettschneider, J., Pinkhardt, E.H., Lule, D., Bohm, S., Braak, H., and Ludolph, a. C. (2014). Diffusion tensor imaging analysis of sequential spreading of disease in amyotrophic lateral sclerosis confirms patterns of TDP-43 pathology. Brain 1–8.

Kerman, A., Liu, H.-N., Croul, S., Bilbao, J., Rogaeva, E., Zinman, L., Robertson, J., and Chakrabartty, A. (2010). Amyotrophic lateral sclerosis is a non-amyloid disease in which extensive misfolding of SOD1 is unique to the familial form. Acta Neuropathol. *119*, 335–344.

Kfoury, N., Holmes, B.B., Jiang, H., Holtzman, D.M., and Diamond, M.I. (2012). Trans-cellular propagation of Tau aggregation by fibrillar species. J. Biol. Chem. *287*, 19440–19451.

Kim, S.H., Engelhardt, J.I., Henkel, J.S., Siklós, L., Soós, J., Goodman, C., and Appel, S.H. (2004). Widespread increased expression of the DNA repair enzyme PARP in brain in ALS. Neurology *62*, 319–322.

Kim, S.H., Shi, Y., Hanson, K. a, Williams, L.M., Sakasai, R., Bowler, M.J., and Tibbetts, R.S. (2009). Potentiation of amyotrophic lateral sclerosis (ALS)-associated TDP-43 aggregation by the proteasome-targeting factor, ubiquilin 1. J. Biol. Chem. *284*, 8083–8092.

Kim, S.H., Shanware, N., Bowler, M.J., and Tibbetts, R.S. (2010). ALS-associated proteins TDP-43 and FUS/TLS function in a common biochemical complex to coregulate HDAC6 mRNA. J. Biol. Chem.

Kim, S.H., Zhan, L., Hanson, K.A., and Tibbetts, R.S. (2012). High-content RNAi screening identifies the Type 1 inositol triphosphate receptor as a modifier of TDP-43 localization and neurotoxicity. Hum. Mol. Genet.

Kindler, S., Wang, H., Richter, D., and Tiedge, H. (2005). RNA transport and local control of translation. Annu. Rev. Cell Dev. Biol. *21*, 223–245.

King, A., Maekawa, S., Bodi, I., Troakes, C., and Al-Sarraj, S. (2010). Ubiquitinated, p62 immunopositive cerebellar cortical neuronal inclusions are evident across the spectrum of TDP-43 proteinopathies but are only rarely additionally immunopositive for phosphorylation-dependent TDP-43. Neuropathology.

Koyama, S., Arawaka, S., Chang-Hong, R., Wada, M., Kawanami, T., Kurita, K., Kato, M., Nagai, M., Aoki, M., Itoyama, Y., et al. (2006). Alteration of familial ALS-linked mutant SOD1 solubility with disease progression: its modulation by the proteasome and Hsp70. Biochem. Biophys. Res. Commun. *343*, 719–730.

Kraemer, B.C., Schuck, T., Wheeler, J.M., Robinson, L.C., Trojanowski, J.Q., Lee, V.M.Y., and Schellenberg, G.D. (2010). Loss of murine TDP-43 disrupts motor function and plays an essential role in embryogenesis. Acta Neuropathol. *119*, 409–419.

Krammer, C., Schätzl, H.M., and Vorberg, I. (2009). Prion-like propagation of cytosolic protein aggregates: insights from cell culture models. Prion *3*, 206–212.

Kreric, A., and Swanson, M. (1999). hnRNP complexes: composition, structure, and function. Curr. Opin. Cell Biol. *11*, 363–371.

Kril, J.J., and Halliday, G.M. (2011). Pathological staging of frontotemporal lobar degeneration. J. Mol. Neurosci. *45*, 379–383.

Kwiatkowski, T.J., Bosco, D.A., Leclerc, A.L., Tamrazian, E., Vanderburg, C.R., Russ, C., Davis, A., Gilchrist, J., Kasarskis, E.J., Munsat, T., et al. (2009). Mutations in the FUS/TLS gene on chromosome 16 cause familial amyotrophic lateral sclerosis. Science *323*, 1205–1208.

Kwong, L.K., Uryu, K., Trojanowski, J.Q., and Lee, V.M.-Y. (2008). TDP-43 proteinopathies: neurodegenerative protein misfolding diseases without amyloidosis. Neurosignals. *16*, 41–51.

Lalmansingh, A.S., Urekar, C.J., and Reddi, P.P. (2011). TDP-43 is a transcriptional repressor; the testis-specific mouse ACRV1 gene is a TDP-43 target in vivo. J. Biol. Chem.

Langer, F., Eisele, Y.S., Fritschi, S.K., Staufenbiel, M., Walker, L.C., and Jucker, M. (2011). Soluble Aβ seeds are potent inducers of cerebral β-amyloid deposition. J. Neurosci. *31*, 14488–14495.

Lasagna-Reeves, C. a., Castillo-Carranza, D.L., Sengupta, U., Guerrero-Munoz, M.J., Kiritoshi, T., Neugebauer, V., Jackson, G.R., and Kayed, R. (2012). Alzheimer brain-derived tau oligomers propagate pathology from endogenous tau. Sci. Rep. *2*.

Lee, V.M., Goedert, M., and Trojanowski, J.Q. (2001). Neurodegenerative tauopathies. Annu. Rev. Neurosci. *24*, 1121–1159.

Leggett, C., McGehee, D.S., Mastrianni, J., Yang, W., Bai, T., and Brorson, J.R. (2012). Tunicamycin produces TDP-43 cytoplasmic inclusions in cultured brain organotypic slices. J. Neurol. Sci.

Legname, G., Baskakov, I. V, Nguyen, H.-O.B., Riesner, D., Cohen, F.E., DeArmond, S.J., and Prusiner, S.B. (2004). Synthetic mammalian prions. Science *305*, 673–676.

Leigh, P.N., Anderton, B.H., Dodson, A., Gallo, J.M., Swash, M., and Power, D.M. (1988). Ubiquitin deposits in anterior horn cells in motor neurone disease. Neurosci. Lett. *93*, 197–203.

Leigh, P.N., Dodson, A., Swash, M., Brion, J.P., and Anderton, B.H. (1989). Cytoskeletal abnormalities in motor neuron disease. An immunocytochemical study. Brain *112 (Pt 2*, 521–535.

Li, J.-Y., Englund, E., Holton, J.L., Soulet, D., Hagell, P., Lees, A.J., Lashley, T., Quinn, N.P., Rehncrona, S., Björklund, A., et al. (2008). Lewy bodies in grafted neurons in subjects with Parkinson's disease suggest host-to-graft disease propagation. Nat. Med. *14*, 501–503.

Li, Y., Ray, P., Rao, E.J., Shi, C., Guo, W., Chen, X., Woodruff, E. a, Fushimi, K., and Wu, J.Y. (2010). A Drosophila model for TDP-43 proteinopathy. Proc. Natl. Acad. Sci. U. S. A. *107*, 3169–3174.

Liachko, N.F., Guthrie, C.R., and Kraemer, B.C. (2010). Phosphorylation promotes neurotoxicity in a Caenorhabditis elegans model of TDP-43 proteinopathy. J. Neurosci. *30*, 16208–16219.

Liachko, N.F., McMillan, P.J., Guthrie, C.R., Bird, T.D., Leverenz, J.B., and Kraemer, B.C. (2013). CDC7 inhibition blocks pathological TDP-43 phosphorylation and neurodegeneration. Ann. Neurol.

Ling, S., Albuquerque, C.P., Seok, J., Lagier-tourenne, C., and Tokunaga, S. (2010). ALS-associated mutations in TDP-43 increase its stability and promote TDP-43 complexes with FUS/TLS. Proc. Natl. Acad. Sci. *107*, 13318–13323.

Liu, G.C.-H., Chen, B.P.-W., Ye, N.T.-J., Wang, C.-H., Chen, W., Lee, H.-M., Chan, S.I., and Huang, J.J.-T. (2013a). Delineating the membrane-disrupting and seeding properties of the TDP-43 amyloidogenic core. Chem. Commun. (Camb).

Liu, L., Drouet, V., Wu, J.W., Witter, M.P., Small, S. a, Clelland, C., and Duff, K. (2012). Trans-synaptic spread of tau pathology in vivo. PLoS One *7*, e31302.

Liu, R., Yang, G., Nonaka, T., Arai, T., Jia, W., and Cynader, M.S. (2013b). Reducing TDP-43 aggregation does not prevent its cytotoxicity. Acta Neuropathol. Commun. *1*, 49.

Liu, Y., Yu, J.-T., Sun, F.-R., Ou, J.-R., Qu, S.-B., and Tan, L. (2013c). The clinical and pathological phenotypes of frontotemporal dementia with C9ORF72 mutations. J. Neurol. Sci.

Liu-Yesucevitz, L., Bilgutay, A., Zhang, Y.-J., Vanderwyde, T., Citro, A., Mehta, T., Zaarur, N., McKee, A., Bowser, R., Sherman, M., et al. (2010). Tar DNA Binding Protein-43 (TDP-43) Associates with Stress Granules: Analysis of Cultured Cells and Pathological Brain Tissue. PLoS One *5*, e13250.

Lowe, J., Lennox, G., Jefferson, D., Morrell, K., McQuire, D., Gray, T., Landon, M., Doherty, F.J., and Mayer, R.J. (1988). A filamentous inclusion body within anterior horn neurones in motor neurone disease defined by immunocytochemical localisation of ubiquitin. Neurosci. Lett. *94*, 203–210.

Lu, Y., Ferris, J., and Gao, F.-B. (2009). Frontotemporal dementia and amyotrophic lateral sclerosis-associated disease protein TDP-43 promotes dendritic branching. Mol. Brain *2*, 30.

Luk, K.C., Song, C., Brien, P.O., Stieber, A., Branch, J.R., Brunden, K.R., Trojanowski, J.Q., and Lee, V.M. (2009). Exogenous alpha-synuclein fibrils seed the formation of Lewy body-like intracellular inclusions in cultured cells. PNAS *106*, 20051–20056.

Luk, K.C., Kehm, V.M., Zhang, B., O'Brien, P., Trojanowski, J.Q., and Lee, V.M.Y. (2012a). Intracerebral inoculation of pathological -synuclein initiates a rapidly progressive neurodegenerative a-synucleinopathy in mice. J. Exp. Med.

Luk, K.C., Kehm, V., Carroll, J., Zhang, B., Brien, P.O., Trojanowski, J.Q., and Lee, V.M. (2012b). Pathological a-Synuclein Transmission in Nontransgenic Mice. Science 949–953.

Luty, A.A., Kwok, J.B.J., Dobson-Stone, C., Loy, C.T., Coupland, K.G., Karlström, H., Sobow, T., Tchorzewska, J., Maruszak, A., Barcikowska, M., et al. (2010). Sigma nonopioid intracellular receptor 1 mutations cause frontotemporal lobar degeneration-motor neuron disease. Ann. Neurol. *68*, 639–649.

Mackenzie, I.R. a, Bigio, E.H., Ince, P.G., Geser, F., Neumann, M., Cairns, N.J., Kwong, L.K., Forman, M.S., Ravits, J., Stewart, H., et al. (2007). Pathological TDP-43 distinguishes sporadic amyotrophic lateral sclerosis from amyotrophic lateral sclerosis with SOD1 mutations. Ann. Neurol. *61*, 427–434.

Mackenzie, I.R.A., Baborie, A., Pickering-Brown, S., Du Plessis, D., Jaros, E., Perry, R.H., Neary, D., Snowden, J.S., and Mann, D.M.A. (2006). Heterogeneity of ubiquitin pathology in frontotemporal lobar degeneration: classification and relation to clinical phenotype. Acta Neuropathol. *112*, 539–549.

Mackenzie, I.R.A., Neumann, M., Baborie, A., Sampathu, D.M., Du Plessis, D., Jaros, E., Perry, R.H., Trojanowski, J.Q., Mann, D.M.A., and Lee, V.M.Y. (2011). A harmonized classification system for FTLD-TDP pathology. Acta Neuropathol. *122*, 111–113.

Mahal, S.P., Browning, S., Li, J., Suponitsky-Kroyter, I., and Weissmann, C. (2010). Transfer of a prion strain to different hosts leads to emergence of strain variants. Proc. Natl. Acad. Sci. U. S. A. *2010*, 1–6.

Makarava, N., Kovacs, G.G., Savtchenko, R., Alexeeva, I., Budka, H., Rohwer, R.G., and Baskakov, I. V (2011). Genesis of mammalian prions: from non-infectious amyloid fibrils to a transmissible prion disease. PLoS Pathog. *7*, e1002419.

Makarava, N., Kovacs, G.G., Savtchenko, R., Alexeeva, I., Ostapchenko, V.G., Budka, H., Rohwer, R.G., and Baskakov, I. V (2012). A new mechanism for transmissible prion diseases. J. Neurosci. *32*, 7345–7355.

Manjaly, Z.R., Scott, K.M., Abhinav, K., Wijesekera, L., Ganesalingam, J., Goldstein, L.H., Janssen, A., Dougherty, A., Willey, E., Stanton, B.R., et al. (2010). The sex ratio in amyotrophic lateral sclerosis: A population based study. Amyotroph. Lateral Scler. *11*, 439–442.

Marsh, M. (1999). The Structural Era of Endocytosis. Science (80-.). *285*, 215–220.

Martin, L.J. (1999). Neuronal death in amyotrophic lateral sclerosis is apoptosis: possible contribution of a programmed cell death mechanism. J. Neuropathol. Exp. Neurol. *58*, 459–471.

Maruyama, H., Morino, H., Ito, H., Izumi, Y., Kato, H., Watanabe, Y., Kinoshita, Y., Kamada, M., Nodera, H., Suzuki, H., et al. (2010). Mutations of optineurin in amyotrophic lateral sclerosis. Nature *465*, 223–226.

Masuda-Suzukake, M., Nonaka, T., Hosokawa, M., Oikawa, T., Arai, T., Akiyama, H., Mann, D.M. a., and Hasegawa, M. (2013). Prion-like spreading of pathological a-synuclein in brain. Brain 1128–1138.

Matsumoto, G., Stojanovic, A., Holmberg, C.I., Kim, S., and Morimoto, R.I. (2005). Structural properties and neuronal toxicity of amyotrophic lateral sclerosis-associated Cu/Zn superoxide dismutase 1 aggregates. J. Cell Biol. *171*, 75–85.

McGoldrick, P., Joyce, P.I., Fisher, E.M.C., and Greensmith, L. (2013). Rodent models of amyotrophic lateral sclerosis. Biochim. Biophys. Acta.

McKinley, M.P., Braunfeld, M.B., Bellinger, C.G., and Prusiner, S.B. (1986). Molecular characteristics of prion rods purified from scrapie-infected hamster brains. J. Infect. Dis. *154*, 110–120.

Medina, D.X., Orr, M.E., and Oddo, S. (2013). Accumulation of C-terminal fragments of transactive response DNA-binding protein 43 leads to synaptic loss and cognitive deficits in human TDP-43 transgenic mice. Neurobiol. Aging.

Mercado, P.A., Ayala, Y.M., Romano, M., Buratti, E., and Baralle, F.E. (2005). Depletion of TDP 43 overrides the need for exonic and intronic splicing enhancers in the human apoA-II gene. Nucleic Acids Res. *33*, 6000–6010.

Meyer-Luehmann, M., Coomaraswamy, J., Bolmont, T., Kaeser, S., Schaefer, C., Kilger, E., Neuenschwander, A., Abramowski, D., Frey, P., Jaton, A.L., et al. (2006). Exogenous induction of cerebral beta-amyloidogenesis is governed by agent and host. Science *313*, 1781–1784.

Michelitsch, M.D., and Weissman, J.S. (2000). A census of glutamine/asparagine-rich regions: implications for their conserved function and the prediction of novel prions. Proc. Natl. Acad. Sci. U. S. A. *97*, 11910–11915.

Miguel, L., Frébourg, T., Campion, D., and Lecourtois, M. (2010). Both Cytoplasmic and Nuclear Accumulations of the Protein are Neurotoxic in Drosophila Models of TDP-43 Proteinopathies. Neurobiol. Dis.

Miller, R.G., Mitchell, J.D., Lyon, M., and Moore, D.H. (2002). Riluzole for amyotrophic lateral sclerosis (ALS)/motor neuron disease (MND). Cochrane Database Syst. Rev. CD001447.

Mizuno, Y., Fujita, Y., Takatama, M., and Okamoto, K. (2011). Peripherin partially localizes in Bunina bodies in amyotrophic lateral sclerosis. J. Neurol. Sci. *302*, 14–18.

Mohamed, N.-V., Herrou, T., Plouffe, V., Piperno, N., and Leclerc, N. (2013). Spreading of tau pathology in Alzheimer's disease by cell-to-cell transmission. Eur. J. Neurosci. *37*, 1939–1948.

Moisse, K., Volkening, K., Leystra-lantz, C., Welch, I., Hill, T., and Strong, M.J. (2008). Divergent patterns of cytosolic TDP-43 and neuronal progranulin expression following axotomy : Implications for TDP-43 in the physiological response to neuronal injury. Brain Res. *1249*, 202–211.

Moisse, K., Mepham, J., Volkening, K., Welch, I., Hill, T., and Strong, M.J. (2009). Cytosolic TDP-43 expression following axotomy is associated with caspase 3 activation in NFL-/- mice: support for a role for TDP-43 in the physiological response to neuronal injury. Brain Res. *1296*, 176–186.

Moore, R. a, Taubner, L.M., and Priola, S. a (2009). Prion protein misfolding and disease. Curr. Opin. Struct. Biol. *19*, 14–22.

Mori, F., Tanji, K., Tan, Y.N.C., Takahashi, H., and Wakabayashi, K. (2008). Maturation process of TDP-43-positive neuronal cytoplasmic inclusions in amyotrophic lateral sclerosis with and without dementia. Acta Neuropathol. *116*, 193–203.

Mougenot, A.-L., Nicot, S., Bencsik, A., Morignat, E., Verchère, J., Lakhdar, L., Legastelois, S., and Baron, T. (2011). Prion-like acceleration of a synucleinopathy in a transgenic mouse model. Neurobiol. Aging 7–10.

Moujalled, D., James, J.L., Parker, S.J., Lidgerwood, G.E., Duncan, C., Meyerowitz, J., Nonaka, T., Hasegawa, M., Kanninen, K.M., Grubman, A., et al. (2013). Kinase Inhibitor Screening Identifies Cyclin-Dependent Kinases and Glycogen Synthase Kinase 3 as Potential Modulators of TDP-43 Cytosolic Accumulation during Cell Stress. PLoS One *8*, e67433.

Münch, C., and Bertolotti, A. (2012). Propagation of the Prion Phenomenon: Beyond the Seeding Principle. J. Mol. Biol. 1–8.

Münch, C., Brien, J.O., and Bertolotti, A. (2011a). Prion-like propagation of mutant superoxide dismutase-1 misfolding in neuronal cells. PNAS *108*, 3548–3553.

Münch, C., O'Brien, J., and Bertolotti, A. (2011b). Prion-like propagation of mutant superoxide dismutase-1 misfolding in neuronal cells. Supporting information. Proc. Natl. Acad. Sci. U. S. A. *108*, 3548–3553.

Munsat, T.L., Andres, P.L., Finison, L., Conlon, T., and Thibodeau, L. (1988). The natural history of motoneuron loss in amyotrophic lateral sclerosis. Neurology *38*, 409–413.

Murayama, S., Mori, H., Ihara, Y., Bouldin, T.W., Suzuki, K., and Tomonaga, M. (1990). Immunocytochemical and ultrastructural studies of lower motor neurons in amyotrophic lateral sclerosis. Ann. Neurol. *27*, 137–148.

Murray, M.E., DeJesus-Hernandez, M., Rutherford, N.J., Baker, M., Duara, R., Graff-Radford, N.R., Wszolek, Z.K., Ferman, T.J., Josephs, K.A., Boylan, K.B., et al. (2011). Clinical and neuropathologic heterogeneity of c9FTD/ALS associated with hexanucleotide repeat expansion in C9ORF72. Acta Neuropathol. *122*, 673–690.

Naeem, A., and Fazili, N.A. (2011). Defective Protein Folding and Aggregation as the Basis of Neurodegenerative Diseases: The Darker Aspect of Proteins. Cell Biochem. Biophys.

Naeem, A., Khan, K.A., and Khan, R.H. (2004). Characterization of a partially folded intermediate of papain induced by fluorinated alcohols at low pH. Arch. Biochem. Biophys. *432*, 79–87.

Naeem, A., Khan, A., and Khan, R.H. (2005). Partially folded intermediate state of concanavalin A retains its carbohydrate specificity. Biochem. Biophys. Res. Commun. *331*, 1284–1294.

Nakamura, M., Kaneko, S., Ito, H., Jiang, S., Fujita, K., Wate, R., Nakano, S., Fujisawa, J.-I., and Kusaka, H. (2012). Activation of Transforming Growth Factor-β/Smad Signaling Reduces Aggregate Formation of Mislocalized TAR DNA-Binding Protein-43. Neurodegener. Dis.

Nakashima-Yasuda, H., Uryu, K., Robinson, J., Xie, S.X., Hurtig, H., Duda, J.E., Arnold, S.E., Siderowf, A., Grossman, M., Leverenz, J.B., et al. (2007). Co-morbidity of TDP-43 proteinopathy in Lewy body related diseases. Acta Neuropathol. *114*, 221–229.

Neumann, M., Sampathu, D.M., Kwong, L.K., Truax, A.C., Micsenyi, M.C., Chou, T.T., Bruce, J., Schuck, T., Grossman, M., Clark, C.M., et al. (2006). Ubiquitinated TDP-43 in frontotemporal lobar degeneration and amyotrophic lateral sclerosis. Science *314*, 130–133.

Neumann, M., Igaz, L.M., Kwong, L.K., Nakashima-Yasuda, H., Kolb, S.J., Dreyfuss, G., Kretzschmar, H. a, Trojanowski, J.Q., and Lee, V.M.-Y. (2007a). Absence of heterogeneous nuclear ribonucleoproteins and survival motor neuron protein in TDP-43 positive inclusions in frontotemporal lobar degeneration. Acta Neuropathol. *113*, 543–548.

Neumann, M., Kwong, L.K., Sampathu, D.M., Trojanowski, J.Q., and Lee, V.M.-Y. (2007b). TDP-43 proteinopathy in frontotemporal lobar degeneration and amyotrophic lateral sclerosis: protein misfolding diseases without amyloidosis. Arch. Neurol. *64*, 1388–1394.

Neumann, M., Kwong, L.K., Lee, E.B., Kremmer, E., Xu, Y., Forman, M., Troost, D., Kretzschmar, H.A., Q, J., and Lee, V.M. (2010). Phosphorylation of S409/410 of TDP-43 is a consistent feature in all sporadic and familial forms of TDP-43 proteinopathies. Acta Neuropathol. *117*, 137–149.

Nishihira, Y., Tan, C.-F., Hoshi, Y., Iwanaga, K., Yamada, M., Kawachi, I., Tsujihata, M., Hozumi, I., Morita, T., Onodera, O., et al. (2009). Sporadic amyotrophic lateral sclerosis of long duration is associated with relatively mild TDP-43 pathology. Acta Neuropathol. *117*, 45–53.

Nishimoto, Y., Ito, D., Yagi, T., Nihei, Y., Tsunoda, Y., and Suzuki, N. (2010). Characterization of alternative isoforms and inclusion body of the TAR DNA-binding protein-43. J. Biol. Chem. *285*, 608–619.

Nomura, T., Watanabe, S., Kaneko, K., Yamanaka, K., Nukina, N., and Furukawa, Y. (2014). Intranuclear Aggregation of Mutant FUS/TLS as a Molecular Pathomechanism of Amyotrophic Lateral Sclerosis. J. Biol. Chem. *289*, 1192–1202.

Nonaka, T., and Hasegawa, M. (2011). In vitro recapitulation of aberrant protein inclusions in neurodegenerative diseases: New cellular models of neurodegenerative diseases. Commun. Integr. Biol. *4*, 501–502.

Nonaka, T., Arai, T., Buratti, E., Baralle, F.E., Akiyama, H., and Hasegawa, M. (2009a). Phosphorylated and ubiquitinated TDP-43 pathological inclusions in ALS and FTLD-U are recapitulated in SH-SY5Y cells. FEBS Lett. *583*, 394–400.

Nonaka, T., Kametani, F., Arai, T., Akiyama, H., and Hasegawa, M. (2009b). Truncation and pathogenic mutations facilitate the formation of intracellular aggregates of TDP-43. Hum. Mol. Genet. *18*, 3353–3364.

Nonaka, T., Masuda-Suzukake, M., Arai, T., Hasegawa, Y., Akatsu, H., Obi, T., Yoshida, M., Murayama, S., Mann, D.M.A., Akiyama, H., et al. (2013). Prion-like Properties of Pathological TDP-43 Aggregates from Diseased Brains. Cell Rep. *4*, 124–134.

Nonoka, T., Watanabe, S.T., Iwatsubo, T., and Hasegawa, M. (2010). Seeded Aggregation and Toxicity of Alpha-Synuclein and Tau. J. Biol. Chem. *285*, 34885–34898.

Noto, Y.-I., Shibuya, K., Sato, Y., Kanai, K., Misawa, S., Sawai, S., Mori, M., Uchiyama, T., Isose, S., Nasu, S., et al. (2011). Elevated CSF TDP-43 levels in amyotrophic lateral sclerosis: specificity, sensitivity, and a possible prognostic value. Amyotroph. Lateral Scler. *12*, 140–143.

Okamoto, K., Mizuno, Y., and Fujita, Y. (2008). Bunina bodies in amyotrophic lateral sclerosis. Neuropathology *28*, 109–115.

Olney, R.K., Murphy, J., Forshew, D., Garwood, E., Miller, B.L., Langmore, S., Kohn, M.A., and Lomen-Hoerth, C. (2005). The effects of executive and behavioral dysfunction on the course of ALS. Neurology *65*, 1774–1777.

Onuchic, J.N., and Wolynes, P.G. (2004). Theory of protein folding. Curr. Opin. Struct. Biol. *14*, 70–75.

Ou, S.H., Wu, F., Harrich, D., García-Martínez, L.F., and Gaynor, R.B. (1995). Cloning and characterization of a novel cellular protein, TDP-43, that binds to human immunodeficiency virus type 1 TAR DNA sequence motifs. J. Virol. *69*, 3584–3596.

Palmer, M.S., Dryden, A.J., Hughes, J.T., and Collinge, J. (1991). Homozygous prion protein genotype predisposes to sporadic Creutzfeldt-Jakob disease. Nature *352*, 340–342.

Pamphlett, R., and Kum, S. (2008). TDP-43 inclusions do not protect motor neurons from sporadic ALS. Acta Neuropathol. *116*, 221–222.

Pan, K.M., Baldwin, M., Nguyen, J., Gasset, M., Serban, A., Groth, D., Mehlhorn, I., Huang, Z., Fletterick, R.J., and Cohen, F.E. (1993). Conversion of alpha-helices into beta-sheets features in the formation of the scrapie prion proteins. Proc. Natl. Acad. Sci. U. S. A. *90*, 10962–10966.

Pande, V.S., and Rokhsar, D.S. (1998). Is the molten globule a third phase of proteins? Proc. Natl. Acad. Sci. U. S. A. *95*, 1490–1494.

Parchi, P., Castellani, R., Capellari, S., Ghetti, B., Young, K., Chen, S.G., Farlow, M., Dickson, D.W., Sima, A.A., Trojanowski, J.Q., et al. (1996). Molecular basis of phenotypic variability in sporadic Creutzfeldt-Jakob disease. Ann. Neurol. *39*, 767–778.

Parker, S.J., Meyerowitz, J., James, J.L., Liddell, J.R., Nonaka, T., Hasegawa, M., Kanninen, K.M., Lim, S., Paterson, B.M., Donnelly, P.S., et al. (2012). Inhibition of TDP-43 Accumulation by Bis(thiosemicarbazonato)-Copper Complexes. PLoS One *7*, e42277.

Pesiridis, G.S., Tripathy, K., Tanik, S., Trojanowski, J.Q., and Lee, V.M.-Y. (2011). A "two hit" hypothesis for inclusion formation by carboxy terminal fragments of TDP-43 linked to RNA depletion and impaired microtubule dependent transport. J. Biol. Chem.

Pokrishevsky, E., Grad, L.I., Yousefi, M., Wang, J., Mackenzie, I.R., and Cashman, N.R. (2012). Aberrant Localization of FUS and TDP43 Is Associated with Misfolding of SOD1 in Amyotrophic Lateral Sclerosis. PLoS One *7*, e35050.

Polymenidou, M., and Cleveland, D.W. (2011). The Seeds of Neurodegeneration: Prion-like Spreading in ALS. Cell *147*, 498–508.

Polymenidou, M., and Cleveland, D.W. (2012). Prion-like spread of protein aggregates in neurodegeneration. J. Exp. Med. *209*, 889–893.

Polymenidou, M., Lagier-Tourenne, C., Hutt, K.R., Huelga, S.C., Moran, J., Liang, T.Y., Ling, S.-C., Sun, E., Wancewicz, E., Mazur, C., et al. (2011). Long pre-mRNA depletion and RNA missplicing contribute to neuronal vulnerability from loss of TDP-43. Nat. Neurosci.

Pradas, J., Finison, L., Andres, P.L., Thornell, B., Hollander, D., and Munsat, T.L. (1993). The natural history of amyotrophic lateral sclerosis and the use of natural history controls in therapeutic trials. Neurology *43*, 751–755.

Pradat, P.-F., Salachas, F., Lacomblez, L., Patte, N., Leforestier, N., Gaura, V., and Meininger, V. (2002). Association of chorea and motor neuron disease. Mov. Disord. *17*, 419–420.

Prell, T., and Grosskreutz, J. (2013). The involvement of the cerebellum in amyotrophic lateral sclerosis. Amyotroph. Lateral Scler. Frontotemporal Degener. 1–9.

Prudencio, M., Hart, P.J., Borchelt, D.R., and Andersen, P.M. (2009). Variation in aggregation propensities among ALS-associated variants of SOD1: correlation to human disease. Hum. Mol. Genet. *18*, 3217–3226.

Prusiner, S.B. (1982). Novel proteinaceous infectious particles cause scrapie. Science *216*, 136–144.

Prusiner, S.B. (1998). Prions. Proc. Natl. Acad. Sci. U. S. A. *95*, 13363–13383.

Prusiner, S.B., Scott, M., Foster, D., Pan, K.M., Groth, D., Mirenda, C., Torchia, M., Yang, S.L., Serban, D., and Carlson, G.A. (1990). Transgenetic studies implicate interactions between homologous PrP isoforms in scrapie prion replication. Cell *63*, 673–686.

Ramnani, N. (2012). Frontal lobe and posterior parietal contributions to the cortico-cerebellar system. Cerebellum *11*, 366–383.

Ravits, J.M., and La Spada, A.R. (2009). ALS motor phenotype heterogeneity, focality, and spread: deconstructing motor neuron degeneration. Neurology *73*, 805–811.

Ravits, J., Paul, P., and Jorg, C. (2007a). Focality of upper and lower motor neuron degeneration at the clinical onset of ALS. Neurology *68*, 1571–1575.

Ravits, J., Laurie, P., Fan, Y., and Moore, D.H. (2007b). Implications of ALS focality: rostral-caudal distribution of lower motor neuron loss postmortem. Neurology *68*, 1576–1582.

Ravits, J., Appel, S., Baloh, R.H., Barohn, R., Rix Brooks, B., Elman, L., Floeter, M.K., Henderson, C., Lomen-Hoerth, C., Macklis, J.D., et al. (2013). Deciphering amyotrophic lateral sclerosis: What phenotype, neuropathology and genetics are telling us about pathogenesis. Amyotroph. Lateral Scler. Frontotemporal Degener. *14 Suppl 1*, 5–18.

Reaume, A.G., Elliott, J.L., Hoffman, E.K., Kowall, N.W., Ferrante, R.J., Siwek, D.F., Wilcox, H.M., Flood, D.G., Beal, M.F., Brown, R.H., et al. (1996). Motor neurons in Cu/Zn superoxide dismutase-deficient mice develop normally but exhibit enhanced cell death after axonal injury. Nat. Genet. *13*, 43–47.

Ren, P., Lauckner, J.E., Kachirskaia, I., Heuser, J.E., Melki, R., and Kopito, R.R. (2009). Cytoplasmic penetration and persistent infection of mammalian cells by polyglutamine aggregates. October *11*, 219–225.

Renton, A.E., Majounie, E., Waite, A., Simón-Sánchez, J., Rollinson, S., Gibbs, J.R., Schymick, J.C., Laaksovirta, H., van Swieten, J.C., Myllykangas, L., et al. (2011). A hexanucleotide repeat expansion in C9ORF72 is the cause of chromosome 9p21-linked ALS-FTD. Neuron *72*, 257–268.

Rey, N.L., Petit, G.H., Bousset, L., Melki, R., and Brundin, P. (2013). Transfer of human α-synuclein from the olfactory bulb to interconnected brain regions in mice. Acta Neuropathol.

Ridley, R.M., Baker, H.F., Windle, C.P., and Cummings, R.M. (2006). Very long term studies of the seeding of beta-amyloidosis in primates. J. Neural Transm. *113*, 1243–1251.

Ripps, M.E., Huntley, G.W., Hof, P.R., Morrison, J.H., and Gordon, J.W. (1995). Transgenic mice expressing an altered murine superoxide dismutase gene provide an animal model of amyotrophic lateral sclerosis. Proc. Natl. Acad. Sci. U. S. A. *92*, 689–693.

Ritson, G.P., Custer, S.K., Freibaum, B.D., Guinto, J.B., Geffel, D., Moore, J., Tang, W., Winton, M.J., Neumann, M., Trojanowski, J.Q., et al. (2010). TDP-43 mediates degeneration in a novel Drosophila model of disease caused by mutations in VCP/p97. J. Neurosci. *30*, 7729–7739.

Robinson, J.L., Geser, F., Stieber, A., Umoh, M., Kwong, L.K., Van Deerlin, V.M., Lee, V.M.-Y., and Trojanowski, J.Q. (2012). TDP-43 skeins show properties of amyloid in a subset of ALS cases. Acta Neuropathol. *43*.

Rose, G.D., Fleming, P.J., Banavar, J.R., and Maritan, A. (2006). A backbone-based theory of protein folding. Proc. Natl. Acad. Sci. U. S. A. *103*, 16623–16633.

Rosen, D.R. (1993). Mutations in Cu/Zn superoxide dismutase gene are associated with familial amyotrophic lateral sclerosis. Nature *364*, 362.

Rosenbohm, A., Kassubek, J., Weydt, P., Marroquin, N., Volk, A.E., Kubisch, C., Huppertz, H.-J., Weber, M., Andersen, P.M., Weishaupt, J.H., et al. (2013). Can lesions to the motor cortex induce amyotrophic lateral sclerosis? J. Neurol.

Ross, C.A., and Poirier, M.A. (2004). Protein aggregation and neurodegenerative disease. Nat. Med. *10 Suppl*, S10–7.

Ross, C.A., and Poirier, M.A. (2005). Opinion: What is the role of protein aggregation in neurodegeneration? Nat. Rev. Mol. Cell Biol. *6*, 891–898.

Rutherford, N.J., Zhang, Y., Baker, M., Gass, J.M., Finch, N.A., Xu, Y., Stewart, H., Kelley, B.J., Kuntz, K., Crook, R.J.P., et al. (2008). Novel Mutations in TARDBP (TDP-43) in Patients with Familial Amyotrophic Lateral Sclerosis. PLoS Genet. *4*, 1–8.

Saini, A., and Chauhan, V.S. (2011). Delineation of the Core Aggregation Sequences of TDP-43 C-Terminal Fragment. Chembiochem *110067*, 1–8.

Sampathu, D.M., Neumann, M., Kwong, L.K., Chou, T.T., Micsenyi, M., Truax, A., Bruce, J., Grossman, M., Trojanowski, J.Q., and Lee, V.M.-Y. (2006). Pathological heterogeneity of frontotemporal lobar degeneration with ubiquitin-positive inclusions delineated by ubiquitin immunohistochemistry and novel monoclonal antibodies. Am. J. Pathol. *169*, 1343–1352.

Sanders, D.W., Kaufman, S.K., DeVos, S.L., Sharma, A.M., Mirbaha, H., Li, A., Barker, S.J., Foley, A.C., Thorpe, J.R., Serpell, L.C., et al. (2014). Distinct Tau Prion Strains Propagate in Cells and Mice and Define Different Tauopathies. Neuron *82*, 1–18.

Sasaki, S., and Maruyama, S. (1991). Immunocytochemical and ultrastructural studies of hyaline inclusions in sporadic motor neuron disease. Acta Neuropathol. *82*, 295–301.

Sato, T., Takeuchi, S., Saito, A., Ding, W., Bamba, H., Matsuura, H., Hisa, Y., Tooyama, I., and Urushitani, M. (2009). Axonal ligation induces transient redistribution of TDP-43 in brainstem motor neurons. Neuroscience *164*, 1565–1578.

Sawaya, M.R., Sambashivan, S., Nelson, R., Ivanova, M.I., Sievers, S.A., Apostol, M.I., Thompson, M.J., Balbirnie, M., Wiltzius, J.J.W., McFarlane, H.T., et al. (2007). Atomic structures of amyloid cross-beta spines reveal varied steric zippers. Nature *447*, 453–457.

Schiene, C., and Fischer, G. (2000). Enzymes that catalyse the restructuring of proteins. Curr. Opin. Struct. Biol. *10*, 40–45.

Schoenfeld, M.A., Tempelmann, C., Gaul, C., Kühnel, G.R., Düzel, E., Hopf, J.-M., Feistner, H., Zierz, S., Heinze, H.-J., and Vielhaber, S. (2005). Functional motor compensation in amyotrophic lateral sclerosis. J. Neurol. *252*, 944–952.

Scotter, E.L., Vance, C., Nishimura, A.L., Lee, Y.-B., Chen, H.-J., Urwin, H., Sardone, V., Mitchell, J.C., Rogelj, B., Rubinsztein, D.C., et al. (2014). Differential roles of the ubiquitin proteasome system (UPS) and autophagy in the clearance of soluble and aggregated TDP-43 species. J. Cell Sci.

Seeley, W.W., Crawford, R.K., Zhou, J., Miller, B.L., and Greicius, M.D. (2009). Neurodegenerative diseases target large-scale human brain networks. Neuron *62*, 42–52.

Sekiguchi, T., Kanouchi, T., Shibuya, K., Noto, Y., Yagi, Y., Inaba, A., Abe, K., Misawa, S., Orimo, S., Kobayashi, T., et al. (2014). Spreading of amyotrophic lateral sclerosis lesions--multifocal hits and local propagation? J. Neurol. Neurosurg. Psychiatry *85*, 85–91.

Sephton, C.F., Good, S.K., Atkin, S., Dewey, C.M., Mayer, P., Herz, J., and Yu, G. (2010a). TDP-43 is a developmentally regulated protein essential for early embryonic development. J. Biol. Chem. *285*, 6826–6834.

Sephton, C.F., Cenik, C., Kucukural, A., Dammer, E.B., Cenik, B., Han, Y.-H., Dewey, C.M., Roth, F.P., Herz, J., Peng, J., et al. (2010b). Identification of neuronal RNA targets of TDP-43-containing Ribonucleoprotein complexes. J. Biol. Chem.

Shan, X., Chiang, P.-M., Price, D.L., and Wong, P.C. (2010). Altered distributions of Gemini of coiled bodies and mitochondria in motor neurons of TDP-43 transgenic mice. Proc. Natl. Acad. Sci.

Shindo, A., Yata, K., Sasaki, R., and Tomimoto, H. (2013). Chronic cerebral ischemia induces redistribution and abnormal phosphorylation of transactivation-responsive DNA-binding protein-43 in mice. Brain Res.

Shodai, A., Ido, A., Fujiwara, N., Ayaki, T., Morimura, T., Oono, M., Uchida, T., Takahashi, R., Ito, H., and Urushitani, M. (2012). Conserved Acidic Amino Acid Residues in a Second RNA Recognition Motif Regulate Assembly and Function of TDP-43. PLoS One *7*, e52776.

Shodai, A., Morimura, T., Ido, A., Uchida, T., Ayaki, T., Takahashi, R., Kitazawa, S., Suzuki, S., Shirouzu, M., Kigawa, T., et al. (2013). Aberrant assembly of RNA-recognition motif 1 links to pathogenic conversion of TAR DNA-binding protein-43 (TDP-43). J. Biol. Chem. *43*, 1–33.

Shorter, J., and Lindquist, S. (2005). Prions as adaptive conduits of memory and inheritance. Nat. Rev. Genet. *6*, 435–450.

Sica, R.E. (2012). Is amyotrophic lateral sclerosis a primary astrocytic disease? Med. Hypotheses 8–11.

Silveira, J.R., Raymond, G.J., Hughson, A.G., Race, R.E., Sim, V.L., Hayes, S.F., and Caughey, B. (2005). The most infectious prion protein particles. Nature *437*, 257–261.

Simoneau, S., Rezaei, H., Salès, N., Kaiser-Schulz, G., Lefebvre-Roque, M., Vidal, C., Fournier, J.-G., Comte, J., Wopfner, F., Grosclaude, J., et al. (2007). In vitro and in vivo neurotoxicity of prion protein oligomers. PLoS Pathog. *3*, e125.

Skibinski, G., Parkinson, N.J., Brown, J.M., Chakrabarti, L., Lloyd, S.L., Hummerich, H., Nielsen, J.E., Hodges, J.R., Spillantini, M.G., Thusgaard, T., et al. (2005). Mutations in the endosomal ESCRTIII-complex subunit CHMP2B in frontotemporal dementia. Nat. Genet. *37*, 806–808.

Sloan, S. a, and Barres, B. a (2013). Glia as primary drivers of neuropathology in TDP-43 proteinopathies. Proc. Natl. Acad. Sci. U. S. A. 1–2.

Somerville, R.A. (2002). TSE agent strains and PrP: reconciling structure and function. Trends Biochem. Sci. *27*, 606–612.

Sorarú, G., Orsetti, V., Buratti, E., Baralle, F., Cima, V., Volpe, M., D'ascenzo, C., Palmieri, A., Koutsikos, K., Pegoraro, E., et al. (2010). TDP-43 in skeletal muscle of patients affected with amyotrophic lateral sclerosis. Amyotroph. Lateral Scler. *11*, 240–243.

Soto, C. (2003). Unfolding the role of protein misfolding in neurodegenerative diseases. Nat. Rev. Neurosci. *4*, 49–60.

Sreedharan, J., Blair, I.P., Tripathi, V.B., Hu, X., Vance, C., Rogelj, B., Ackerley, S., Durnall, J.C., Williams, K.L., Buratti, E., et al. (2008). TDP-43 mutations in familial and sporadic amyotrophic lateral sclerosis. Science *319*, 1668–1672.

Stallings, N.R., Puttaparthi, K., Luther, C.M., Burns, D.K., and Elliott, J.L. (2010). Progressive motor weakness in transgenic mice expressing human TDP-43. Neurobiol. Dis. *40*, 404–414.

Stallings, N.R., Puttaparthi, K., Dowling, K.J., Luther, C.M., Burns, D.K., Davis, K., and Elliott, J.L. (2013). TDP-43, an ALS Linked Protein, Regulates Fat Deposition and Glucose Homeostasis. PLoS One *8*, e71793.

Stohr, J., Watts, J.C., Mensinger, Z.L., Oehler, a., Grillo, S.K., DeArmond, S.J., Prusiner, S.B., and Giles, K. (2012). Purified and synthetic Alzheimer's amyloid beta (A) prions. Proc. Natl. Acad. Sci. 1–6.

Strong, M.J., and Yang, W. (2011). The Frontotemporal Syndromes of ALS. Clinicopathological Correlates. J. Mol. Neurosci.

Strong, M.J., Volkening, K., Hammond, R., Yang, W., Strong, W., Leystra-Lantz, C., and Shoesmith, C. (2007). TDP43 is a human low molecular weight neurofilament (hNFL) mRNA-binding protein. Mol. Cell. Neurosci. *35*, 320–327.

Su, A.I., Wiltshire, T., Batalov, S., Lapp, H., Ching, K.A., Block, D., Zhang, J., Soden, R., Hayakawa, M., Kreiman, G., et al. (2004). A gene atlas of the mouse and human protein-encoding transcriptomes. Proc. Natl. Acad. Sci. U. S. A. *101*, 6062–6067.

Su, J.H., Nichol, K.E., Sitch, T., Sheu, P., Chubb, C., Miller, B.L., Tomaselli, K.J., Kim, R.C., and Cotman, C.W. (2000). DNA damage and activated caspase-3 expression in neurons and astrocytes: evidence for apoptosis in frontotemporal dementia. Exp. Neurol. *163*, 9–19.

Sun, P.Z., Zhou, J., Sun, W., Huang, J., and van Zijl, P.C.M. (2007). Detection of the ischemic penumbra using pH-weighted MRI. J. Cereb. Blood Flow Metab. *27*, 1129–1136.

Suzuki, M., Mikami, H., Watanabe, T., Yamano, T., Yamazaki, T., Nomura, M., Yasui, K., Ishikawa, H., and Ono, S. (2010). Increased expression of TDP-43 in the skin of amyotrophic lateral sclerosis. Acta Neurol. Scand. *43*, 367–372.

Swarup, V., and Julien, J.-P. (2010). ALS pathogenesis: Recent insights from genetics and mouse models. Prog. Neuropsychopharmacol. Biol. Psychiatry.

Swash, M. (1980). Vulnerability of lower brachial myotomes in motor neurone disease: a clinical and single fibre EMG study. J. Neurol. Sci. *47*, 59–68.

Swash, M., Leader, M., Brown, A., and Swettenham, K.W. (1986). Focal loss of anterior horn cells in the cervical cord in motor neuron disease. Brain *109 (Pt 5*, 939–952.

Sweeney, P.J., and Walker, J.M. (1993). Pronase (EC 3.4.24.4). Methods Mol. Biol. *16*, 271–276.

Tamgüney, G., Giles, K., Bouzamondo-Bernstein, E., Bosque, P.J., Miller, M.W., Safar, J., DeArmond, S.J., and Prusiner, S.B. (2006). Transmission of elk and deer prions to transgenic mice. J. Virol. *80*, 9104–9114.

Tan, R.H., Shepherd, C.E., Kril, J.J., McCann, H., McGeachie, A., McGinley, C., Affleck, A., and Halliday, G.M. (2013). Classification of FTLD-TDP cases into pathological subtypes using antibodies against phosphorylated and non-phosphorylated TDP43. Acta Neuropathol. Commun. *1*, 33.

Tanaka, M., Collins, S.R., Toyama, B.H., and Weissman, J.S. (2006). The physical basis of how prion conformations determine strain phenotypes. Nature *442*, 585–589.

Thiede, B., Treumann, A., Kretschmer, A., Söhlke, J., and Rudel, T. (2005). Shotgun proteome analysis of protein cleavage in apoptotic cells. Proteomics *5*, 2123–2130.

Thorpe, J.R., and Cairns, N.J. (2009). Fine structural analysis of the neuronal inclusions of frontotemporal lobar degeneration with TDP-43 proteinopathy. J. Neural Transm. *115*, 1661–1671.

Thorpe, J.R., Tang, H., Atherton, J., and Cairns, N.J. (2008). Fine structural analysis of the neuronal inclusions of frontotemporal lobar degeneration with TDP-43 proteinopathy. J. Neural Transm. *115*, 1661–1671.

Tollervey, J.R., Curk, T., Rogelj, B., Briese, M., Cereda, M., Kayikci, M., König, J., Hortobágyi, T., Nishimura, A.L., Zupunski, V., et al. (2011). Characterizing the RNA targets and position-dependent splicing regulation by TDP-43. Nat. Neurosci.

Tortelli, R., Ruggieri, M., Cortese, R., D'Errico, E., Capozzo, R., Leo, A., Mastrapasqua, M., Zoccolella, S., Leante, R., Livrea, P., et al. (2012). Elevated cerebrospinal fluid neurofilament light levels in patients with amyotrophic lateral sclerosis: a possible marker of disease severity and progression. Eur. J. Neurol. *19*, 1561–1567.

Troakes, C., Maekawa, S., Wijesekera, L., Rogelj, B., Siklós, L., Bell, C., Smith, B., Newhouse, S., Vance, C., Johnson, L., et al. (2012). An MND/ALS phenotype associated with C9orf72 repeat expansion:

abundant p62-positive, TDP-43-negative inclusions in cerebral cortex, hippocampus and cerebellum but without associated cognitive decline. Neuropathology *32*, 505–514.

Tsai, K.-J., Yang, C.-H., Fang, Y.-H., Cho, K.-H., Chien, W.-L., Wang, W.-T., Wu, T.-W., Lin, C.-P., Fu, W.-M., and Shen, C.-K.J. (2010). Elevated expression of TDP-43 in the forebrain of mice is sufficient to cause neurological and pathological phenotypes mimicking FTLD-U. J. Exp. Med. *207*, 1661–1673.

Tsermentseli, S., Leigh, P.N., and Goldstein, L.H. (2011). The anatomy of cognitive impairment in amyotrophic lateral sclerosis: More than frontal lobe dysfunction. Cortex. 1–17.

Tsuiji, H., Iguchi, Y., Furuya, A., Kataoka, A., Hatsuta, H., Atsuta, N., Tanaka, F., Hashizume, Y., Akatsu, H., Murayama, S., et al. (2012). Spliceosome Integrity is Defective in the Motor Neuron Diseases ALS and SMA. EMBO J. 1–46.

Tsuji, H., Nonaka, T., Yamashita, M., Suzukake, M., Kametani, F., Akiyama, H., Mann, D.M. a, Tamaoka, A., and Hasegawa, M. (2011). Epitope mapping of antibodies against TDP-43 and detection of protease-resistant fragments of pathological TDP-43 in amyotrophic lateral sclerosis and frontotemporal lobar degeneration. Biochem. Biophys. Res. Commun. *43*, 22–27.

Tsuji, H., Arai, T., Kametani, F., Nonaka, T., Yamashita, M., Suzukake, M., Hosokawa, M., Yoshida, M., Hatsuta, H., Takao, M., et al. (2012). Molecular analysis and biochemical classification of TDP-43 proteinopathy. Brain.

Tyedmers, J., Madariaga, M.L., and Lindquist, S. (2008). Prion switching in response to environmental stress. PLoS Biol. *6*, e294.

Tyedmers, J., Mogk, A., and Bukau, B. (2010). Cellular strategies for controlling protein aggregation. Nat. Rev. Mol. Cell Biol. *11*, 777–788.

Uchida, A., Sasaguri, H., Kimura, N., Tajiri, M., Ohkubo, T., Ono, F., Sakaue, F., Kanai, K., Hirai, T., Sano, T., et al. (2012). Non-human primate model of amyotrophic lateral sclerosis with cytoplasmic mislocalization of TDP-43. Brain.

Udan, M., and Baloh, R.H. (2011). Implications of the prion-related Q/N domains in TDP-43 and FUS. Prion *5*.

Udan-johns, M., Bengoechea, R., Bell, S., Shao, J., and Diamond, M.I. (2013). Prion-like nuclear aggregation of TDP-43 during heat shock is regulated by HSP40/70 chaperones. Hum. Mol. Genet.

Ulusoy, A., Rusconi, R., Pérez-Revuelta, B.I., Musgrove, R.E., Helwig, M., Winzen-Reichert, B., and Di Monte, D.A. (2013). Caudo-rostral brain spreading of α-synuclein through vagal connections. EMBO Mol. Med. *5*, 1051–1059.

Urushitani, M., Sato, T., Bamba, H., Hisa, Y., and Tooyama, I. (2010). Synergistic effect between proteasome and autophagosome in the clearance of polyubiquitinated TDP-43. J. Neurosci. Res. *88*, 784–797.

Uryu, K., Nakashima-Yasuda, H., Forman, M.S., Kwong, L.K., Clark, C.M., Grossman, M., Miller, B.L., Kretzschmar, H.A., Lee, V.M.-Y., Trojanowski, J.Q., et al. (2008). Concomitant TAR-DNA-binding protein 43 pathology is present in Alzheimer disease and corticobasal degeneration but not in other tauopathies. J. Neuropathol. Exp. Neurol. *67*, 555–564.

Vaccaro, A., Tauffenberger, A., Aggad, D., Rouleau, G., Drapeau, P., and Parker, J.A. (2012a). Mutant TDP-43 and FUS Cause Age-Dependent Paralysis and Neurodegeneration in C. elegans. PLoS One *7*, e31321.

Vaccaro, A., Patten, S. a, Ciura, S., Maios, C., Therrien, M., Drapeau, P., Kabashi, E., and Parker, J.A. (2012b). Methylene Blue Protects against TDP-43 and FUS Neuronal Toxicity in C. elegans and D. rerio. PLoS One *7*, e42117.

Vance, C., Rogelj, B., Hortobágyi, T., De Vos, K.J., Nishimura, A.L., Sreedharan, J., Hu, X., Smith, B., Ruddy, D., Wright, P., et al. (2009). Mutations in FUS, an RNA processing protein, cause familial amyotrophic lateral sclerosis type 6. Science *323*, 1208–1211.

Verstraete, E., Veldink, J.H., Mandl, R.C.W., van den Berg, L.H., and van den Heuvel, M.P. (2011). Impaired structural motor connectome in amyotrophic lateral sclerosis. PLoS One *6*, e24239.

Voigt, A., Herholz, D., Fiesel, F.C., Kaur, K., Müller, D., Karsten, P., Weber, S.S., Kahle, P.J., Marquardt, T., and Schulz, J.B. (2010). TDP-43-Mediated Neuron Loss In Vivo Requires RNA-Binding Activity. PLoS One *5*, e12247.

Volkening, K., Leystra-Lantz, C., Yang, W., Jaffee, H., and Strong, M.J. (2009). Tar DNA binding protein of 43 kDa (TDP-43), 14-3-3 proteins and copper/zinc superoxide dismutase (SOD1) interact to modulate NFL mRNA stability. Implications for altered RNA processing in amyotrophic lateral sclerosis (ALS). Brain Res. *1305*, 168–182.

Volpicelli-Daley, L. a, Luk, K.C., Patel, T.P., Tanik, S. a, Riddle, D.M., Stieber, A., Meaney, D.F., Trojanowski, J.Q., and Lee, V.M.-Y. (2011). Exogenous α-Synuclein Fibrils Induce Lewy Body Pathology Leading to Synaptic Dysfunction and Neuron Death. Neuron *72*, 57–71.

Wadsworth, J.D. (2003). Molecular and clinical classification of human prion disease. Br. Med. Bull. *66*, 241–254.

Walker, L.C. (2012). Mechanisms of Protein Seeding in Neurodegenerative Diseases. Arch. Neurol. 1.

Walker, A.K., Soo, K.Y., Sundaramoorthy, V., Parakh, S., Ma, Y., Farg, M.A., Wallace, R.H., Crouch, P.J., Turner, B.J., Horne, M.K., et al. (2013). ALS-Associated TDP-43 Induces Endoplasmic Reticulum Stress, Which Drives Cytoplasmic TDP-43 Accumulation and Stress Granule Formation. PLoS One *8*, e81170.

Walker, L.C., Callahan, M.J., Bian, F., Durham, R.A., Roher, A.E., and Lipinski, W.J. (2002). Exogenous induction of cerebral B-amyloidosis in BAPP-transgenic mice. Microbiology *23*, 1241–1247.

Wang, F., Wang, X., Yuan, C.-G., and Ma, J. (2010a). Generating a prion with bacterially expressed recombinant prion protein. Science *327*, 1132–1135.

Wang, H.-Y., Wang, I.-F., Bose, J., and Shen, C.-K.J. (2004). Structural diversity and functional implications of the eukaryotic TDP gene family. Genomics *83*, 130–139.

Wang, I.-F., Wu, L.-S., Chang, H.-Y., and Shen, C.-K.J. (2008). TDP-43, the signature protein of FTLD-U, is a neuronal activity-responsive factor. J. Neurochem. *105*, 797–806.

Wang, I.-F., Guo, B.-S., Liu, Y.-C., Wu, C.-C., Yang, C.-H., Tsai, K.-J., and Shen, C.-K.J. (2012a). Autophagy activators rescue and alleviate pathogenesis of a mouse model with proteinopathies of the TAR DNA-binding protein 43. Proc. Natl. Acad. Sci. U. S. A. 1–6.

Wang, I.-F., Chang, H.-Y., Hou, S.-C., Liou, G.-G., Way, T.-D., and James Shen, C.-K. (2012b). The self-interaction of native TDP-43 C terminus inhibits its degradation and contributes to early proteinopathies. Nat. Commun. *3*, 766.

Wang, J., Slunt, H., Gonzales, V., Fromholt, D., Coonfield, M., Copeland, N.G., Jenkins, N.A., and Borchelt, D.R. (2003). Copper-binding-site-null SOD1 causes ALS in transgenic mice: aggregates of non-native SOD1 delineate a common feature. Hum. Mol. Genet. *12*, 2753–2764.

Wang, X., Fan, H., Ying, Z., Li, B., Wang, H., and Wang, G. (2010b). Degradation of TDP-43 and its pathogenic form by autophagy and the ubiquitin-proteasome system. Neurosci. Lett. *469*, 112–116.

Wang, Y.-T., Kuo, P.-H., Chiang, C.-H., Liang, J.-R., Chen, Y.-R., Wang, S., Shen, J.C.K., and Yuan, H.S. (2013). The truncated C-terminal RRM domain of TDP-43 plays a key role in forming proteinaceous aggregates. J. Biol. Chem. *43*, 1–16.

Ward, S.M., Himmelstein, D.S., Lancia, J.K., and Binder, L.I. (2012). Tau oligomers and tau toxicity in neurodegenerative disease. Biochem. Soc. Trans. *40*, 667–671.

Warraich, S.T., Yang, S., Nicholson, G. a, and Blair, I.P. (2010). TDP-43: A DNA and RNA binding protein with roles in neurodegenerative diseases. Int. J. Biochem. Cell Biol. *42*, 1606–1609.

Watabe, K., Akiyama, K., Kawakami, E., Ishii, T., Endo, K., Yanagisawa, H., Sango, K., and Tsukamoto, M. (2013). Adenoviral expression of TDP-43 and FUS genes and shRNAs for protein degradation pathways in rodent motoneurons in vitro and in vivo. Neuropathology.

Watanabe, S., Kaneko, K., and Yamanaka, K. (2012). Accelerated disease onset with stabilized familial Amyotrophic Lateral Sclerosis (ALS)-linked TDP-43 mutations. J. Biol. Chem.

Watts, J.C., Giles, K., Oehler, A., Middleton, L., Dexter, D.T., Gentleman, S.M., Dearmond, S.J., and Prusiner, S.B. (2013). Transmission of multiple system atrophy prions to transgenic mice. Proc. Natl. Acad. Sci. U. S. A. *110*, 19555–19560.

Wegorzewska, I., Bell, S., Cairns, N.J., Miller, T.M., and Baloh, R.H. (2009). TDP-43 mutant transgenic mice develop features of ALS and frontotemporal lobar degeneration. Proc. Natl. Acad. Sci. U. S. A. *106*, 18809–18814.

Weihl, C.C., Temiz, P., Miller, S.E., Watts, G., Smith, C., Forman, M., Hanson, P.I., Kimonis, V., and Pestronk, A. (2008). TDP-43 accumulation in inclusion body myopathy muscle suggests a common

pathogenic mechanism with frontotemporal dementia. J. Neurol. Neurosurg. Psychiatry *79*, 1186–1189.

Weill, C.O., Biri, S., Adib, A., and Erbacher, P. (2008). A practical approach for intracellular protein delivery. Cytotechnology *56*, 41–48.

Westermark, P. (2005). Aspects on human amyloid forms and their fibril polypeptides. FEBS J. *272*, 5942–5949.

Wharton S, I.P. (2003). Pathology of Motor Neurone Disorders. In Motor Neuron Disorders, pp. 17–41.

Wickner, R.B., Shewmaker, F., Kryndushkin, D., and Edskes, H.K. (2008). Protein inheritance (prions) based on parallel in-register beta-sheet amyloid structures. Bioessays *30*, 955–964.

Wider, C., Dickson, D.W., Stoessl, A.J., Tsuboi, Y., Chapon, F., Gutmann, L., Lechevalier, B., Calne, D.B., Personett, D.A., Hulihan, M., et al. (2009). Pallidonigral TDP-43 pathology in Perry syndrome. Parkinsonism Relat. Disord. *15*, 281–286.

Wijesekera, L.C., and Leigh, P.N. (2009). Amyotrophic lateral sclerosis. Orphanet J. Rare Dis. *4*, 3.

Wilcox, P. (1970). Chymotrypsinogens - chymotrypsins. Methods Enzymol. *19*, 64–108.

Williams, K.L., Warraich, S.T., Yang, S., Solski, J.A., Fernando, R., Rouleau, G.A., Nicholson, G.A., and Blair, I.P. (2012). UBQLN2/ubiquilin 2 mutation and pathology in familial amyotrophic lateral sclerosis. Neurobiol. Aging *33*, 2527.e3–10.

Wils, H., Kleinberger, G., Janssens, J., Pereson, S., Joris, G., Cuijt, I., Smits, V., Ceuterick-de Groote, C., Van Broeckhoven, C., and Kumar-Singh, S. (2010). TDP-43 transgenic mice develop spastic paralysis and neuronal inclusions characteristic of ALS and frontotemporal lobar degeneration. Proc. Natl. Acad. Sci. U. S. A. *107*, 3858–3863.

Winton, M.J., Igaz, L.M., Wong, M.M., Kwong, L.K., Trojanowski, J.Q., and Lee, V.M.-Y. (2008a). Disturbance of nuclear and cytoplasmic TAR DNA-binding protein (TDP-43) induces disease-like redistribution, sequestration, and aggregate formation. J. Biol. Chem. *283*, 13302–13309.

Winton, M.J., Deerlin, V.M. Van, Kwong, L.K., Yuan, W., Mccarty, E., Yu, C., Schellenberg, G.D., Rademakers, R., Caselli, R., Karydas, A., et al. (2008b). A90V TDP-43 variant results in the aberrant localization of TDP-43 in vitro. FEBS Lett. *582*, 2252–2256.

Wu, L.-S., Cheng, W.-C., Hou, S.-C., Yan, Y.-T., Jiang, S.-T., and Shen, C.-K.J. (2010). TDP-43, a neuro-pathosignature factor, is essential for early mouse embryogenesis. Genesis *48*, 56–62.

Wu, L.-S., Cheng, W.-C., and Shen, C.-K. (2012). Targeted Depletion of TDP-43 Expression in the Spinal Cord Motor Neurons Leads to the Development of Amyotrophic Lateral Sclerosis (ALS)-like Phenotypes in Mice. J. Biol. Chem.

Wu, L.-S., Cheng, W.-C., and Shen, C.-K.J. (2013). Similar dose-dependence of motor neuron cell death caused by wild type human TDP-43 and mutants with ALS-associated amino acid substitutions. J. Biomed. Sci. *20*, 33.

Xiao, S., Sanelli, T., Dib, S., Sheps, D., Findlater, J., Bilbao, J., Keith, J., Zinman, L., Rogaeva, E., and Robertson, J. (2011). RNA targets of TDP-43 identified by UV-CLIP are deregulated in ALS. Mol. Cell. Neurosci.

Xu, Y.-F., Gendron, T.F., Zhang, Y.-J., Lin, W.-L., D'Alton, S., Sheng, H., Casey, M.C., Tong, J., Knight, J., Yu, X., et al. (2010). Wild-Type Human TDP-43 Expression Causes TDP-43 Phosphorylation, Mitochondrial Aggregation, Motor Deficits, and Early Mortality in Transgenic Mice. J. Neurosci. *30*, 10851–10859.

Xu, Y.-F., Prudencio, M., Hubbard, J.M., Tong, J., Whitelaw, E.C., Jansen-West, K., Stetler, C., Cao, X., Song, J., and Zhang, Y.-J. (2013). The Pathological Phenotypes of Human TDP-43 Transgenic Mouse Models Are Independent of Downregulation of Mouse Tdp-43. PLoS One *8*, e69864.

Yamashita, M., Nonaka, T., Arai, T., Kametani, F., Buchman, V.L., Ninkina, N., Bachurin, S.O., Akiyama, H., Goedert, M., and Hasegawa, M. (2009). Methylene blue and dimebon inhibit aggregation of TDP-43 in cellular models. FEBS Lett. *583*, 2419–2424.

Yang, C., Tan, W., Whittle, C., Qiu, L., Cao, L., Akbarian, S., and Xu, Z. (2010). The C-Terminal TDP-43 Fragments Have a High Aggregation Propensity and Harm Neurons by a Dominant-Negative Mechanism. PLoS One *5*, e15878.

Zelphati, O., Wang, Y., Kitada, S., Reed, J.C., Felgner, P.L., and Corbeil, J. (2001). Intracellular delivery of proteins with a new lipid-mediated delivery system. J. Biol. Chem. *276*, 35103–35110.

Zetterström, P., Stewart, H.G., Bergemalm, D., Jonsson, P.A., Graffmo, K.S., Andersen, P.M., Brännström, T., Oliveberg, M., and Marklund, S.L. (2007). Soluble misfolded subfractions of mutant superoxide dismutase-1s are enriched in spinal cords throughout life in murine ALS models. Proc. Natl. Acad. Sci. U. S. A. *104*, 14157–14162.

Zhang, H., Stockel, J., Mehlhorn, I., Groth, D., Baldwin, M.A., Prusiner, S.B., James, T.L., and Cohen, F.E. (1997). Physical studies of conformational plasticity in a recombinant prion protein. Biochemistry *36*, 3543–3553.

Zhang, Y.-J., Xu, Y., Dickey, C.A., Buratti, E., Baralle, F., Bailey, R., Pickering-Brown, S., Dickson, D., and Petrucelli, L. (2007). Progranulin mediates caspase-dependent cleavage of TAR DNA binding protein-43. J. Neurosci. *27*, 10530–10534.

Zhang, Y.-J., Xu, Y.-F., Cook, C., Gendron, T.F., Roettges, P., Link, C.D., Lin, W.-L., Tong, J., Castanedes-Casey, M., Ash, P., et al. (2009). Aberrant cleavage of TDP-43 enhances aggregation and cellular toxicity. Proc. Natl. Acad. Sci. U. S. A. *106*, 7607–7612.

Zhang, Y.-J., Gendron, T.F., Xu, Y.-F., Ko, L.-W., Yen, S.-H., and Petrucelli, L. (2010). Phosphorylation regulates proteasomal-mediated degradation and solubility of TAR DNA binding protein-43 C-terminal fragments. Mol. Neurodegener. *5*, 33.

Zhang, Y.-J., Caulfield, T., Xu, Y.-F., Gendron, T.F., Hubbard, J., Stetler, C., Sasaguri, H., Whitelaw, E.C., Cai, S., Lee, W.C., et al. (2013). The dual functions of the extreme N-terminus of TDP-43 in regulating its biological activity and inclusion formation. Hum. Mol. Genet. 1–30.

Zhao, W., Beers, D.R., and Appel, S.H. (2013). Immune-mediated mechanisms in the pathoprogression of amyotrophic lateral sclerosis. J. Neuroimmune Pharmacol. *8*, 888–899.

Zhou, J. (2011). Amide proton transfer imaging of the human brain. Methods Mol. Biol. *711*, 227–237.

Zhou, J., Payen, J.-F., Wilson, D.A., Traystman, R.J., and van Zijl, P.C.M. (2003a). Using the amide proton signals of intracellular proteins and peptides to detect pH effects in MRI. Nat. Med. *9*, 1085–1090.

Zhou, J., Lal, B., Wilson, D. a, Laterra, J., and van Zijl, P.C.M. (2003b). Amide proton transfer (APT) contrast for imaging of brain tumors. Magn. Reson. Med. *50*, 1120–1126.

Zhou, J., Blakeley, J.O., Hua, J., Kim, M., Laterra, J., Pomper, M.G., and van Zijl, P.C.M. (2008). Practical data acquisition method for human brain tumor amide proton transfer (APT) imaging. Magn. Reson. Med. *60*, 842–849.

Zhou, J., Gennatas, E.D., Kramer, J.H., Miller, B.L., and Seeley, W.W. (2012). Predicting regional neurodegeneration from the healthy brain functional connectome. Neuron *73*, 1216–1227.

Zigas, V., and Gajdusek, D.C. (1957). Kuru: clinical study of a new syndrome resembling paralysis agitans in natives of the Eastern Highlands of Australian New Guinea. Med. J. Aust. *44*, 745–754.